DEPARTMENT OF ECOLOGY
State of Washington

South Puget Sound Dissolved Oxygen Study—

South and Central Puget Sound Water Circulation Model Development and Calibration

October 2009

Publication and Contact Information

South Puget Sound Dissolved Oxygen Study – South and Central Puget Sound Water Circulation Model Development and Calibration

By

Mindy Roberts, Skip Albertson,
Anise Ahmed, and Greg Pelletier

Environmental Assessment Program
Washington State Department of Ecology
Olympia, Washington 98504-7710

Waterbody Numbers: See Table 1

Table of Contents

List of Figures

List of Tables

Abstract

Portions of South Puget Sound do not meet Washington State water quality standards for dissolved oxygen. The Washington State Department of Ecology will determine whether humans are contributing to these low levels by collecting and analyzing data, developing circulation and water quality models, and assessing alternative management scenarios. This report, the second of three parts of the South Puget Sound Dissolved Oxygen Study, summarizes the calibration and confirmation of the South and Central Puget Sound circulation model.

The model's purpose is to describe how water moves around, and the model performs well. The model reproduces both water surface elevations and tidal constituents throughout the model domain. Root mean square errors (RMSEs) are <16 cm, or <5% of the tidal range, in all but Oakland Bay where the error was 10% of the tidal range. The model simulates salinity with a mean RMSE of 0.6 psu near the surface and 0.5 psu near the seafloor compared with field observations at 22 key stations. Temperature results likewise have RMSEs of 0.9°C near the surface and 0.6°C near the bottom. Current velocity measurements, both transects across inlets and time series in key locations, were also used to check the model.

We estimated flushing time in various inlets of South Puget Sound for late-summer conditions. We also simulated dye tracers from rivers and wastewater treatment plants in both Central and South Puget Sound as an initial indication of areas influenced by either. Some of the tracer from Central Puget Sound sources travels south through the Tacoma Narrows. Therefore, we cannot rule out the influence of Central Puget Sound sources on South Puget Sound water quality. However, the results are not sufficient to rule in an influence given the complexity of nutrient transport and transformation. The upcoming water quality model will address the issue.

Acknowledgements

The authors of this report would like to thank the following people and organizations for their contribution to this study:

- Curt Ebbesmeyer, Hal Mofjeld, and Bill Lavelle provided important historical insight to circulation and tidal processes in Puget Sound.

- Venkat Kollaru and ERM staff provided technical assistance and software development for the GEMSS model.

- Technical Advisory Group members provided feedback on interim model products and interpretations. In particular, Mitsuhiro Kawase (University of Washington) and Bruce Nairn (King County) provided key input and perspectives on initial calibration products.

Executive Summary

Portions of South Puget Sound do not meet Washington State water quality standards for dissolved oxygen. The Washington State Department of Ecology will determine whether humans are contributing to these low levels by collecting and analyzing data, developing circulation and water quality models, and assessing alternative management scenarios. This report, the second of three, summarizes the calibration and confirmation of the South and Central Puget Sound circulation model.

The primary area of interest is the region southwest of the Tacoma Narrows. However, one of the project questions is whether the larger rivers and population centers northeast of the Tacoma Narrows contributes to water quality problems within South Puget Sound. Therefore, the model domain includes both South and Central Puget Sound.

To describe water circulation in South and Central Puget Sound (Figure ES-1), we apply a three-dimensional model that simulates tides, water velocity, temperature, and salinity within each grid cell. The model grid cells are arranged to represent the complex morphology and bathymetry of the region, including such features as the shallow entrance sill within the Tacoma Narrows, inlets in South Puget Sound, and deeper basins in Carr Inlet and Central Puget Sound. The selected grid cell resolution (nominally 500 m by 500 m) optimizes tradeoffs between the precision required to describe circulation and the amount of time required to run the model.
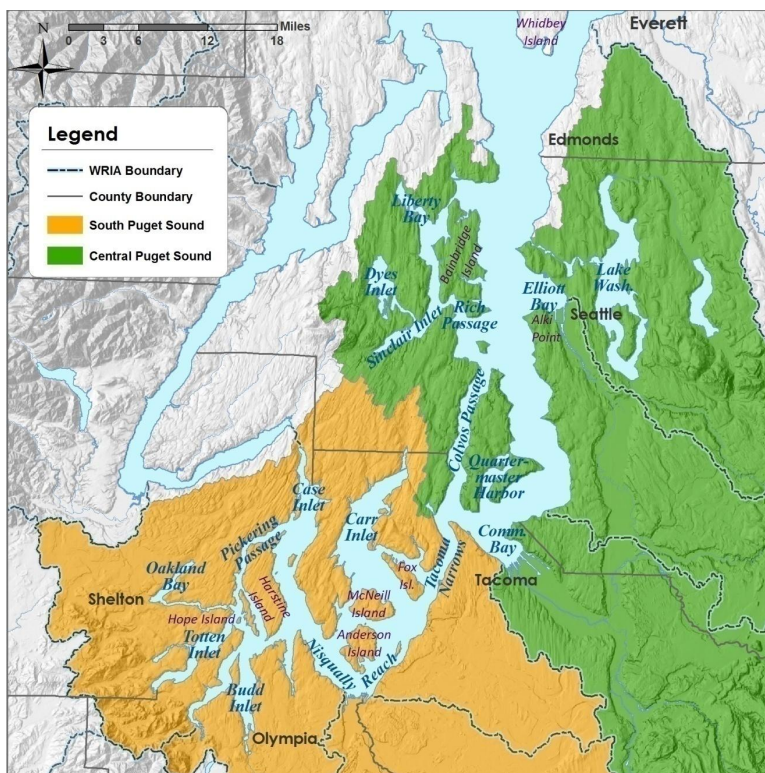
Figure ES-1. South and Central Puget Sound study area.

Circulation strongly influences dissolved oxygen levels, which will be evaluated in the subsequent water quality modeling efforts. Factors influencing circulation include the tides at the northern boundary, the physical shape of Puget Sound, meteorology including wind and air temperature, and freshwater inflows. Data collected during the first phase of the project are used as both input to the model and as output for comparison with model predictions.

The model was calibrated and confirmed using water surface elevations, tidal constituents, surface temperature and salinity spatial patterns, temperature and salinity profiles, and current velocities. Calibration refers to the iterative process of comparing model output to data and adjusting appropriate factors. The model was calibrated using data collected from July through December 2006. Once a good fit to water surface elevations, temperature, and salinity was achieved, the model was compared against a second dataset from January through October 2007 without adjusting calibrations parameters.

Overall the model performs well, the model predicts water surface elevations with a root-mean-square error (RMSE) of <10 cm throughout most of the water domain for both the calibration and confirmation time periods. Somewhat higher but still acceptable errors exist for Hammersley Inlet and Oakland Bay due to shape complexities that the model grid could not describe without significantly decreasing the model grid cell size, which would require greater computer runtime. The RMSEs are within 5% of the tidal range, which ranges from 2 m at the northern boundary to 5 m in Budd Inlet and Hammersley Inlet/Oakland Bay. Figure ES-2 presents examples from near the boundary, a typical South Sound station, and Hammersley Inlet. While the tide range in Oakland Bay matches actual tides, high and low tides precede actual tides by approximately 40 minutes because the model does not represent the two 90-degree bends in Hammersley Inlet.
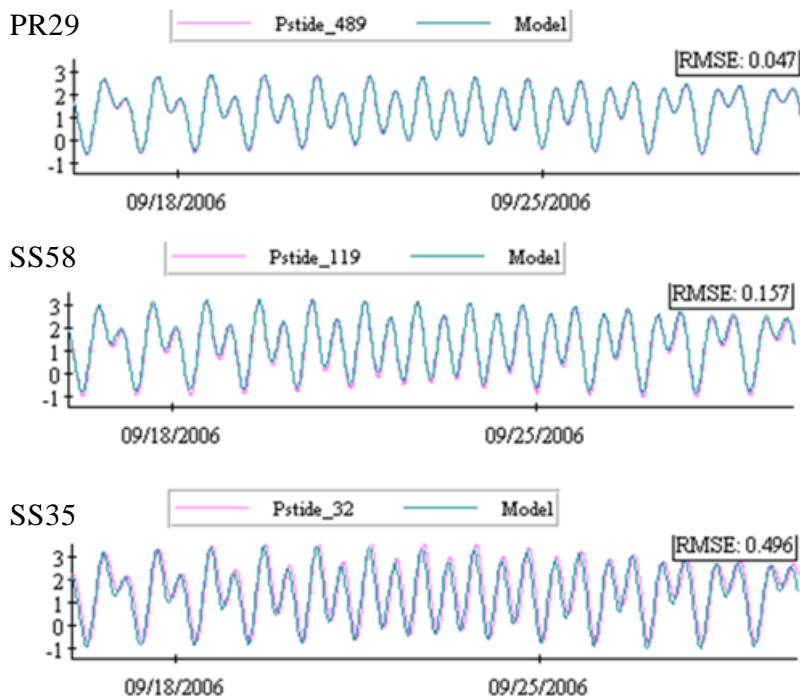
Figure ES-2. Predicted water surface elevations (meters) compared with PSTides for (a) PR29, a typical Central Puget Sound location; (b) SS58, a typical South Puget Sound location; and (c) SS35, Oakland Bay.

The complex shape and circulation patterns produce highly variable temperature and salinity patterns in Puget Sound, particularly in the surface layers that are influenced by both the meteorology and rivers. The model reproduces the spatial (Figure ES-3) and temporal (Figure ES-4) patterns in both the surface and near-bottom layers. Temperature calibration produced RMSEs of 0.9°C near the surface and 0.5°C near the bottom. For the calibration period, salinity results produced a RMSE of 0.6 psu near the surface and 0.4 psu near the bottom compared with field observations at 22 key stations. For the 2007 confirmation period, overall RMSE was 0.6 psu and 0.8°C. Water column profiles also reproduced seasonal and temporal patterns.
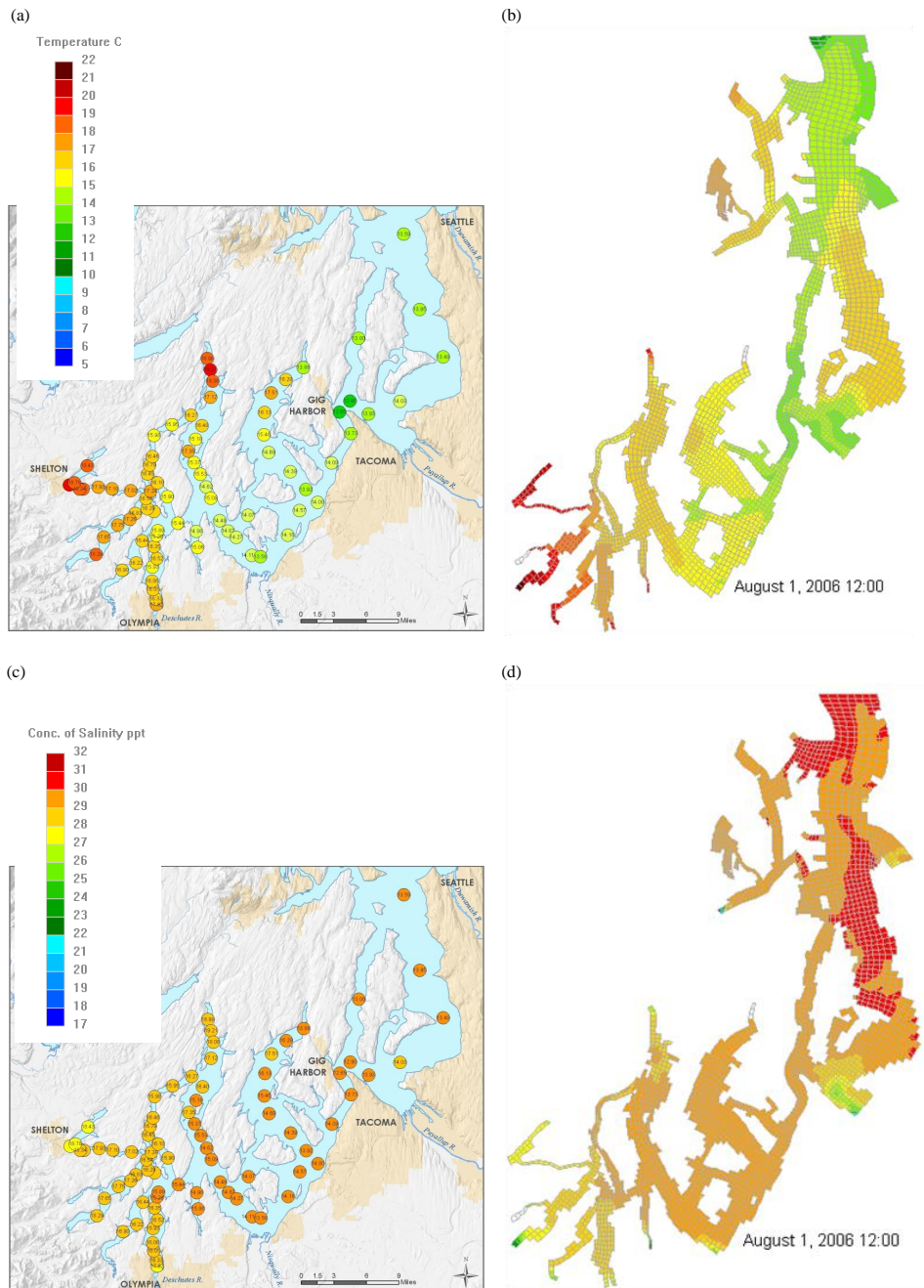
Figure ES-3. (a and c) Observed and (b and d) predicted temperature and salinity.
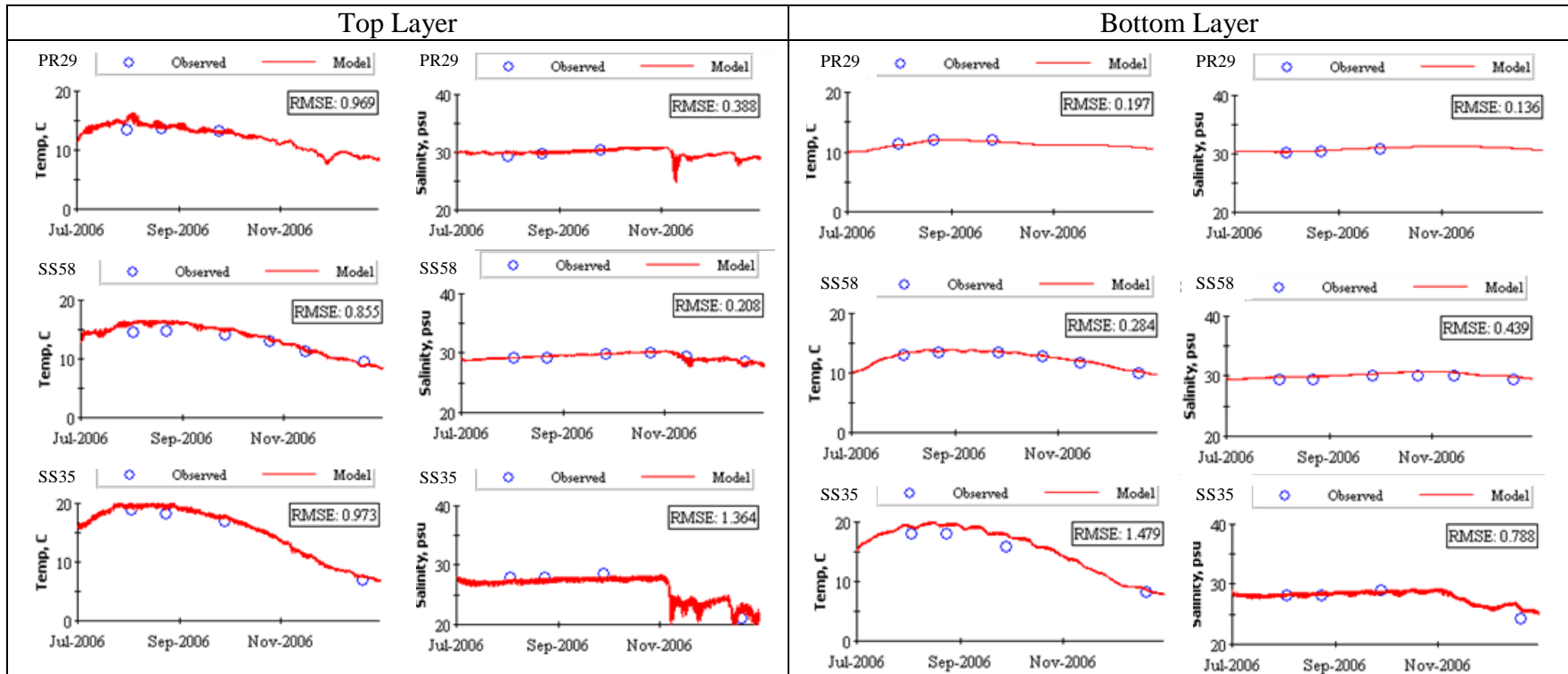
Figure ES-4. Temperature and salinity time series predictions compared with field data for September 2006 surface and near-bottom conditions for PR29, a typical Central Puget Sound location; SS58, a typical South Puget Sound locations; and SS35 Oakland Bay.

Current velocity phasing and magnitudes were confirmed with field data. Model predictions of cross-sectional averaged velocity magnitude across inlets and direction matched observed data in South Puget Sound. These comparisons focused on complex flow areas in South Puget Sound where the flood and ebb tides split around Harstine Island. The model predicts the phasing correctly in Carr, Case, and Budd Inlet, based on velocities recorded over two-week periods in 2007 (Figure ES-5), as well as the northerly and easterly components of the velocity. The surface currents predicted by the model are reasonable and match large-scale patterns (Figure ES-6).
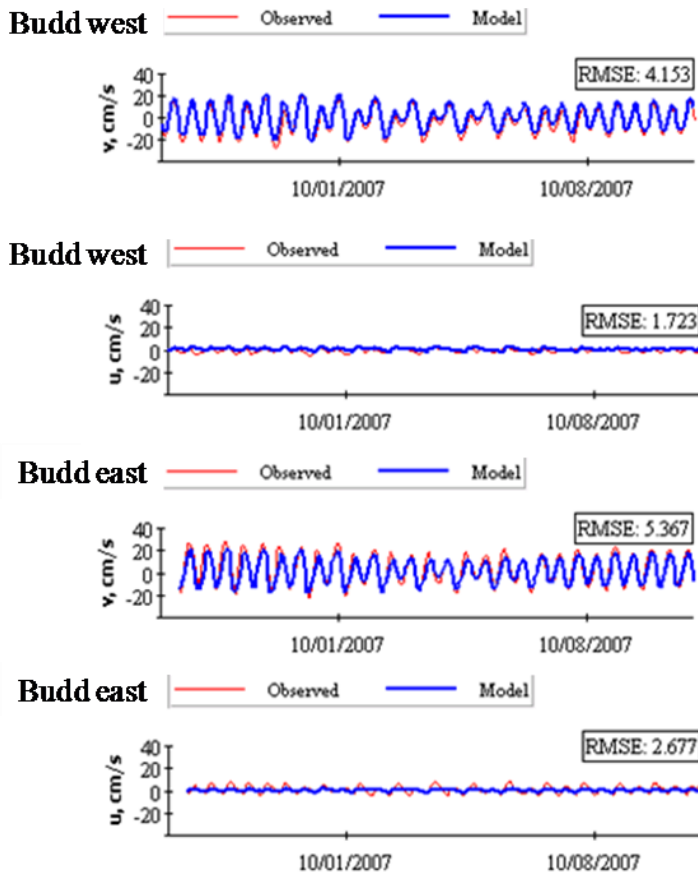
Figure ES-5. Budd Inlet surface layer velocity comparisons between the model and data for northerly (v) and easterly (u) velocity components during the confirmation period.

Using the calibrated model, we evaluated flushing time for South Puget Sound inlets. Numerous methods have been used in Puget Sound and elsewhere, and the numeric value for the flushing time strongly depends on the method used. We added a dye tracer to areas of South Puget Sound and quantified the time required to reduce the dye concentration to a percentage of the initial value within a particular grid cell. The flushing time is lowest near the Tacoma Narrows and is significantly higher toward the heads of each inlet. Flushing time varies seasonally.
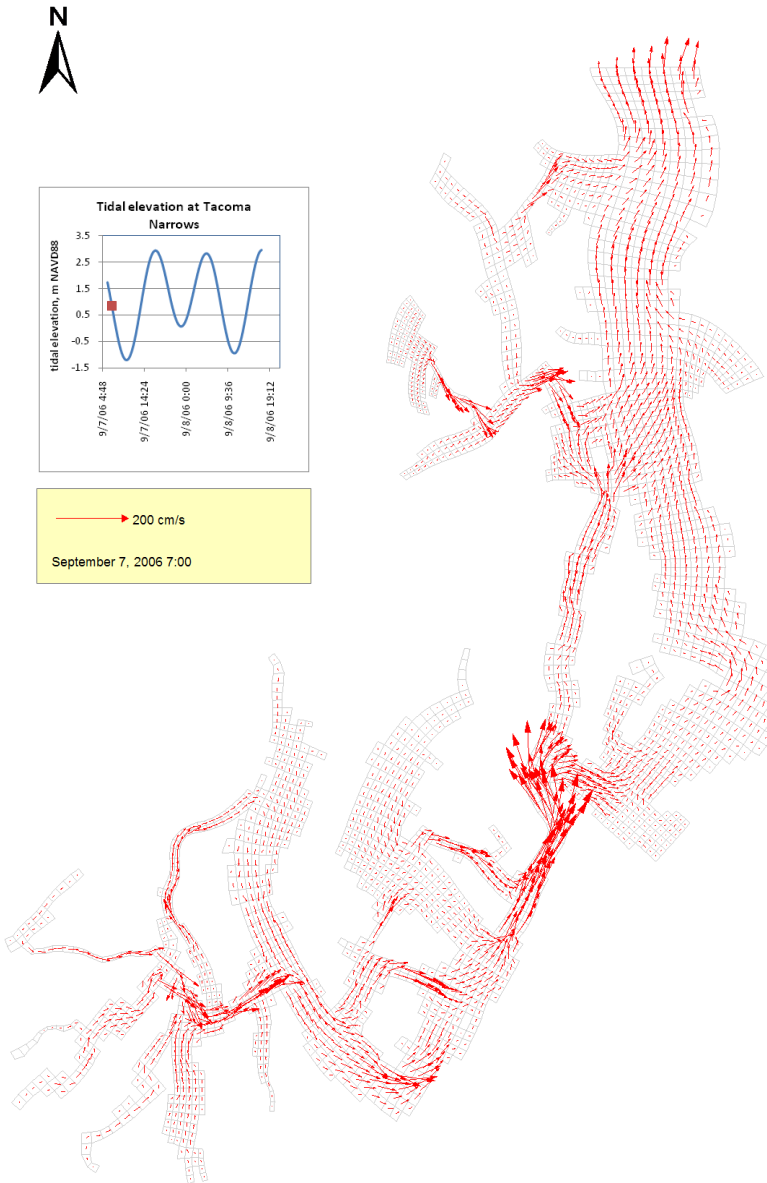
Figure ES-6. Surface currents predicted by the model during strongly ebbing tidal conditions.

The subsequent phase of model development will add water quality components to the circulation model framework. As an interim indicator of areas influenced by rivers and wastewater treatment plants, we simulated dye released from all river inflows and wastewater discharges >1 mgd. Rivers are added to the surface layer and wastewater discharges to the bottom layer in four separate runs, two each for South Puget Sound and Central Puget Sound. Dye releases began in July 2006 and slowly accumulated within the model domain through 2007.

We quantified the maximum dye concentrations that occurred anywhere in the water column. As the tide floods and ebbs, we recorded the maximum concentration at any time during September 16-30, 2007. The dilution factor for each grid cell is the ratio of the maximum concentration to the initial concentration; a dilution factor of 100 corresponds to a maximum tracer concentration of $1/100^{th}$ or 1% of the initial value.

Based on predicted dilution levels derived from water column maximum dye concentrations during September 16-30, 2007, dye from South and Central Puget Sound exchanges through the Tacoma Narrows (Figure ES-7). Therefore, we cannot rule out the influence of Central Puget Sound sources on South Puget Sound water quality. However, the results are not sufficient to rule in an influence either given the complexity of nutrient transport and transformation within marine environments. The water quality model is needed to quantify the link between sources and water quality impairments.

The next project phase is to develop the water quality components of the model. We will continue to use 2006 as the calibration time period and 2007 as the confirmation time period. All nitrogen sources will be represented as a time series of nutrients loads, including small wastewater plants that were not included in the initial tracer study.
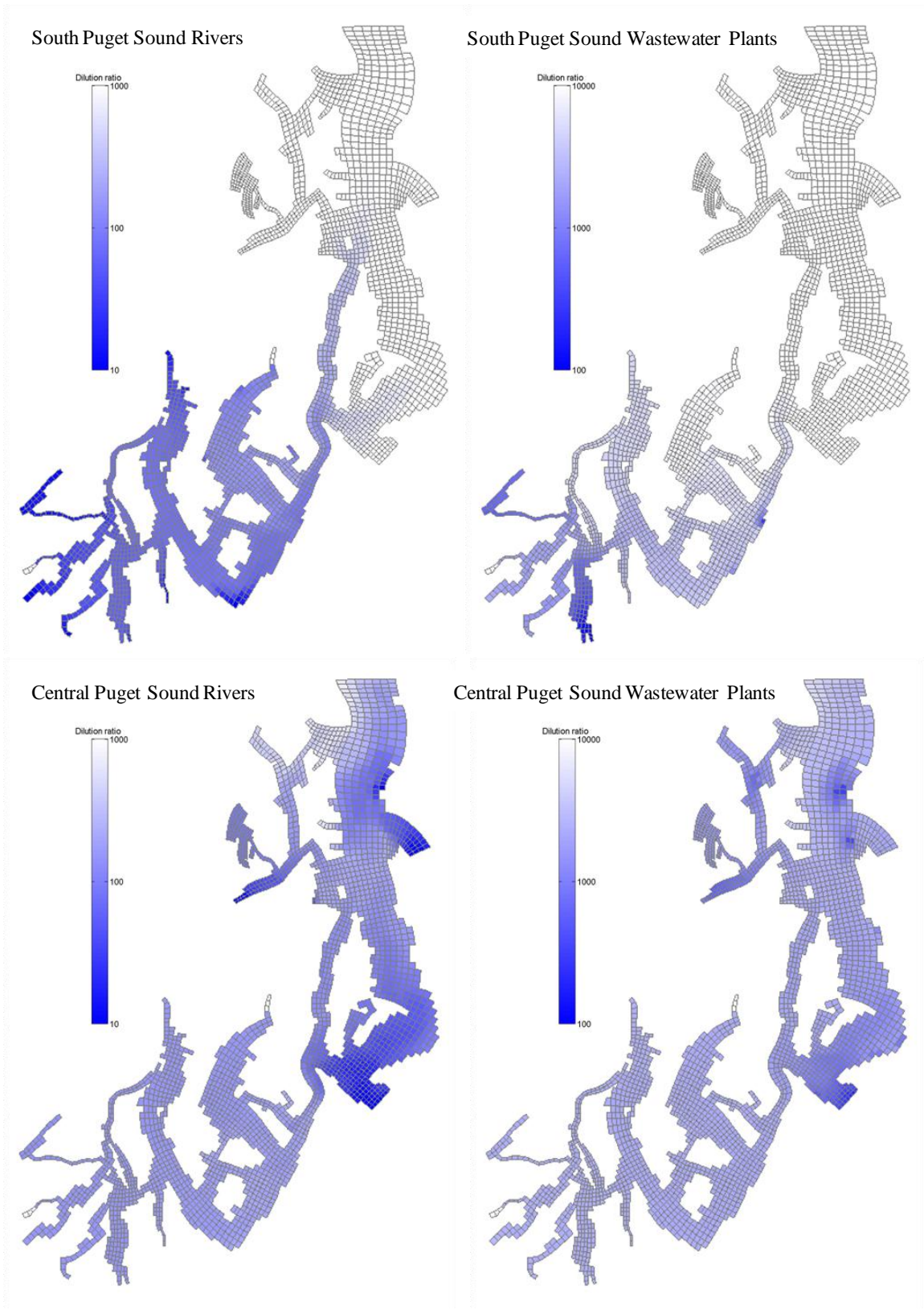
Figure ES-7. Dilution factors calculated from maximum water column dye concentrations for South and Central Puget Sound rivers and wastewater treatment plants for September 2007.

Introduction

Portions of South Puget Sound do not meet Washington State water quality standards for dissolved oxygen. The purpose of this study is to determine whether humans are contributing to low levels of dissolved oxygen in South Puget Sound. Because sources outside of South Sound could contribute to low dissolved oxygen levels within South Sound, we evaluated South and Central Puget Sound (Figure 1). Table 1 presents the waterbodies classified as Category 5 under the federal Clean Water Act §303(d) list of impaired waters. Category 5 indicates that water quality violates standards and a Total Maximum Daily Load (TMDL) study is required.
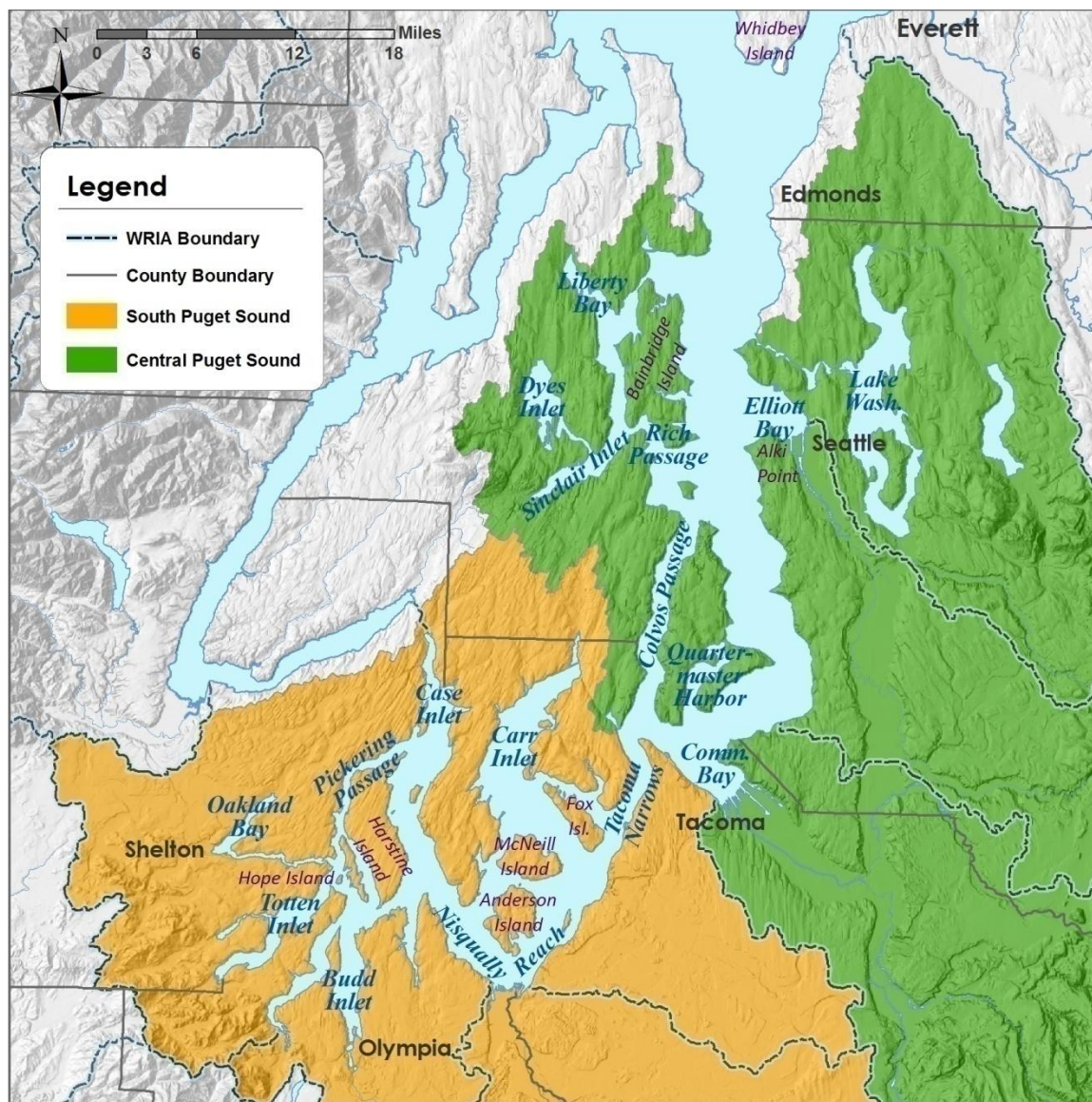
Figure 1. South and Central Puget Sound study area.

Table 1. Waterbody IDs (WBIDs) for Category 5 listings of dissolved oxygen in South and Central Puget Sound.

| Listing detail	Name	Grid Cell	LLID	WASWIS	WBID
3769	Budd Inlet (Outer)	47122B9E2	1224199478564	390KRD	WA-14-0010
3770	Squaxin, Peale, and Pickering Passages	47122B9E1	1224199478564	390KRD	
5852	Budd Inlet (Inner)	47122A9F0	1224199478564	390KRD	WA-13-0030
5853	Budd Inlet (Inner)	47122A9E0	1224199478564	390KRD	
5862	Budd Inlet (Outer)	47122A9G0	1224199478564	390KRD	
5863	Budd Inlet (Inner)	47122A8F9	1224199478564	390KRD	
5864	Budd Inlet (Inner)	47122A8G9	1224199478564	390KRD	
7582	Budd Inlet (Outer)	47122A9I0	1224199478564	390KRD	WA-13-0020
7583	Budd Inlet (Outer)	47122B9A1	1224199478564	390KRD	
7584	Budd Inlet (Outer)	47122A8J9	1224199478564	390KRD	
7585	Budd Inlet (Outer)	47122A9I1	1224199478564	390KRD	
8586	Budd Inlet (Outer)	47122B9A0	1224199478564	390KRD	
7587	Budd Inlet (Outer)	47122A0H1	1224199478564	390KRD	
10188	Budd Inlet (Outer)	47122A9J1	1224199478564	390KRD	NA
10192	Henderson Inlet	47122B8F3	1224199478564	390KRD	WA-13-0010
10229	Carr Inlet	47122C7H0	1224199478564	390KRD	WA-15-0060
10233	Case Inlet and Dana Passage	47122C8G4	1228333472646	VCNS	WA-14-0090
10244	Case Inlet and Dana Passage	47122D8F1	1224199478564	390KRD	WA-13-0090
42999	Carr Inlet	47122C6B2	1224199478564	390KRD	WA-15-0300
43000	Carr Inlet	47122C6D5	1224199478564	390KRD	WA-15-0060
43001	Carr Inlet	47122C6F9	1224199478564	390KRD	
43002	Carr Inlet	47122D7B0	1224199478564	390KRD	
43003	Carr Inlet	47122D6D9	1224199478564	390KRD	
48976	Henderson Inlet	47122B8C5	1224819475188	NA	NA
10175	Commencement Bay (Outer)	47122C4J4	1224199478564	390KRD	NA
10178	Dalco Passage/Poverty Bay	47122D4B4	1224199478564	390KRD	WA-PS-0280
12702	Duwamish Waterway	47122F3H5	1224819475188	DH90GX	WA-09-1010
12703	Duwamish Waterway	47122F3C1	1224819475188	IG58VD	
48943	Duwamish Waterway	47122F3C1	1224819475188	NA	NA
48945	Duwamish Waterway	47122F3H5	1224819475188	NA	NA
10254	Eagle Harbor	47122G5C2	1224819475188	VCAG	NA
10268	Liberty Bay	47122H6D4	1224199478564	390KRD	NA
23537	Liberty Bay	47122H6B2	1224199478564	390KRD	NA
23541	Liberty Bay	47122H6C4	1224199478564	390KRD	NA
38463	Port Orchard, Agate Passage, and Rich Passage	47122G6F1	1226207476509	674YXH	NA
38547	Port Orchard, Agate Passage, and Rich Passage	47122F6G1	1224199478564	390KRD	NA
38682	Liberty Bay	47122H6D5	1224199478564	390KRD	NA
38710	Port Madison	47122H5E5	1224199478564	390KRD	NA

Listing detail	Name	Grid Cell	LLID	WASWIS	WBID
38714	Port Madison	47122H5F5	1224199478564	390KRD	NA
38840	Puget Sound (S-Central) and East Passage	47122F5E3	1224199478564	390KRD	NA
38847	Port Orchard, Agate Passage, and Rich Passage	47122F5J4	1225364476448	VCAG	NA
38939	Puget Sound (S-Central) and East Passage	47122F5C4	1224199478564	390KRD	NA
48946	Sinclair Inlet	47122F6D7	1224819475188	NA	NA
52995	Puget Sound (S-Central) and East Passage	47122F5C1	1224819475188	NA	NA
52996	Puget Sound (S-Central) and East Passage	47122F5C3	1224819475188	NA	NA
52997	Puget Sound (S-Central) and East Passage	47122F5F3	1224819475188	NA	NA
52999	Port Orchard, Agate Passage, and Rich Passage	47122F5H9	1224819475188	NA	NA
53000	Port Orchard, Agate Passage, and Rich Passage	47122F5J7	1224819475188	NA	NA
53002	Port Orchard, Agate Passage, and Rich Passage	47122F6F0	1224819475188	NA	NA

The study includes collecting and analyzing data, developing circulation and water quality models, and assessing alternative management scenarios. Roberts et al. (2008a) summarized the data collected from June 2006 through October 2007. This report summarizes the development, calibration, and confirmation of the water circulation model of South and Central Puget Sound. A future report will present the water quality model development.

The water circulation model describes how the marine waters of South and Central Puget Sound move around. To simulate circulation, we represent South and Central Puget Sound as a series of model grid cells of varying length, width, and depth to define the complex shape of the inlets and passages. The computer model simulates water velocities, salinity, and temperature within each grid cell that result from the complex interaction of tides, bathymetry, meteorology, and freshwater inflows. The circulation model is the basis of the water quality model that will be developed next.

Physical Description

South and Central Puget Sound include a complex and interconnected system of straits and open waters in Washington State. South Puget Sound is defined traditionally by the Tacoma Narrows and an entrance sill located just to the south of the Tacoma Narrows. The sill is a shallow reach formed during the glacial epochs tens of thousands of years ago, with typical depths around 50 m. Deeper regions to the west and landward of the sill are greater than 150 m.

Central Puget Sound, also called the main basin, extends from the Tacoma Narrows to the north or seaward. Commencement Bay, Colvos Passage, Quartermaster Harbor, Sinclair and Dyes Inlets, Elliott Bay and Liberty Bay are all distinct areas within Central Puget Sound. The Puget Sound Partnership divides Central Puget Sound, which extends north to Whidbey Island, into north and

south components. Due to the complex circulation patterns near Whidbey Island, the northern model boundary was located further south, near Edmonds. This location balances the need to include Central Puget Sound water quality contributions against the circulation difficulties near Whidbey Island.

Several previous studies evaluated South and Central Puget Sound circulation and physical oceanography. Albertson et al. (2007a) described general circulation patterns and how stratification increases residence time. Previous complex and simple modeling efforts improved understanding of how water moves around in South Puget Sound, but these efforts were limited by available information (Albertson et al., 2002a and 2002b) and by coarse model scales (URS Company, 1986). Thomson (1981) and Collias et al. (1974) provide detailed summaries of the physical oceanography and chemistry of South Puget Sound inferred from data collection efforts. Seim and Gregg (1997) describe the physical processes at Tacoma Narrows. Babson et al. (2006) described seasonal and annual patterns using a two-layer box model of Puget Sound. Edwards et al. (2007) simulated circulation within Carr Inlet using a three-dimensional model.

Potential Factors Contributing to Low Dissolved Oxygen

Multiple physical, chemical, and biological processes contribute to seasonally low dissolved oxygen levels in late summer. All will be considered by the circulation and water quality models. Sunlight and nutrients may lead to algae growth. Excessive algae growth, or a bloom, produces high organic matter levels. When the algae die and sink to the bottom, bacteria decompose the organic matter and consume oxygen in the process. Lower dissolved oxygen levels occur where water stagnates, when water columns stratify, and where ample nutrients and warm temperatures occur. In addition, there are low seasonal winds and lower tidal energy near the fall equinox in September that could inhibit flushing. Typically, late summer and fall produce conditions conducive to algae growth, as noted in Bos et al. (2001) for South Puget Sound.

Factors Influencing Circulation and Flushing Time

South and Central Puget Sound experience two high and two low tides each day. The difference between high tide and low tide, or the tidal range, varies from 2 m at the northern model boundary to as much as 5 m in Olympia and Shelton. Large water surface elevation differences produce strong tidal currents (~1 m/s). Density differences produce weaker estuarine circulation currents (~0.1 m/s) that vary with depth, freshwater input, stratification, and wind. Tidal and estuarine circulation result in a net outflow of buoyant fresher water at the surface and a compensating inflow of denser saltwater from North and Central Puget Sound at depth that ultimately draws from the Pacific Ocean. Despite being much smaller in magnitude, this weaker estuarine flow can greatly influence water quality because the tidal exchanges (ebbs and floods) largely cancel each other out.

Residence time describes how long water masses persist within a particular volume. The related term flushing time refers to how quickly or slowly water flushes out of a given volume of water, such as flushing time for a specific inlet. The net circulation of water influences biological productivity because nutrients that enter Puget Sound from one watershed can affect another area

at some distance. Residence time or flushing time depends on the overall volume of water of interest and the shape of the waterbody. Because they also vary with freshwater inflows and tidal exchanges, residence time or flushing time vary by season and tidal cycle.

Report Organization

Circulation model development, calibration, and initial applications are described in five sections:

- *Model Setup* describes the capabilities of the software selected for the South and Central Puget Sound circulation model, how the model grid was developed, the boundary conditions used to force the model and the initial conditions used at the start.

- *Model Calibration and Confirmation* describes the detailed process used to calibrate the model, including what data were used to check against the model output and what parameters were varied to achieve calibration. The section also evaluates model performance against separate data sets through a process called confirmation.

- *South Puget Sound Volumes and Flushing Times* present the final model grid volumes by inlet and residence time estimates for various inlets.

- *Simulated Dye Releases* summarizes results of a virtual dye study, where the model was used to track how water from both rivers and wastewater discharges in South and Central Puget Sound move around.

- *Conclusions and Recommendations* summarize the overall performance of the model and basic capabilities. The section also documents why the northern boundary was established at Edmonds as well as recommendations for any ongoing work.

Model Setup

Model selection criteria were detailed in Albertson et al. (2007b). In summary, the circulation and associated water quality models must simulate 3-dimensional processes appropriate to estuarine areas with both tidal circulation and density-driven circulation. For potential use as a regulatory tool, the model must be peer reviewed, available in the public domain, and have thorough documentation of the theory and source code. In addition, Ecology evaluated models with past applications within Puget Sound and emphasized the quality of the graphical user interface to facilitate scenario generation. While several model frameworks provided the minimum capabilities, the Generalized Environmental Modeling System for Surface Waters (GEMSS) framework was selected (Edinger and Buchak, 1995).

This section presents the capabilities of GEMSS as well as the development of the model grid. Boundary conditions are described for the northern boundary, meteorology, and river and point source inflows. The final subsection describes how we established initial conditions within the model domain to begin the simulation.

Model Description

The GEMSS application to South and Central Puget Sound uses a curvilinear (curved) grid to represent the complex shapes. Below the intertidal zone in areas always covered with water, the layers in the model grid have fixed thicknesses that are thinner near the surface. The top three surface layers span the intertidal range, and top layer varies in thickness as water surface elevations change. The model simulates the wetting and drying of mud flats, an important process for nearshore areas. Model time steps are small enough that high gradients like acceleration through the Tacoma Narrows do not cause instabilities. GEMSS allows a variable time step. In addition, the model simulates both rivers and treatment plant outfalls.

The software was used for the Lacey Olympia Thurston Tumwater (LOTT) wastewater treatment plant (WWTP) certification study (Aura Nova et al., 1998) as well as the more recent Deschutes River, Capitol Lake, and Budd Inlet Total Maximum Daily Load study (Roberts et al., 2008b). GEMSS has a fully integrated hydrodynamic, water quality and sediment flux model embedded in a geographic information system (GIS) with environmental data tools. The graphical user interface (GUI) facilitates running scenarios.

The hydrodynamic model in GEMSS is the three-dimensional Generalized, Longitudinal-Lateral-Vertical Hydrodynamic and Transport (GLLVHT) model (Edinger and Buchak, 1980). The hydrodynamic routines extend the well known two-dimensional transport model CE-QUAL-W2 (Cole and Buchak, 1995). Kolluru et al. (1998) modified the transport scheme, added water quality modules, and incorporated supporting software, GIS, visualization tools, post-processors, and a graphical user interface. Albertson et al. (2007b) details the water quality model capabilities of the GEMSS framework.

Computational Grid Development

The current model grid was developed based on a previous model grid of South Puget Sound through Alki Point (Albertson et al., 2002). Given the potential for Central Puget Sound sources to impact South Puget Sound water quality, the model grid was extended northward to Edmonds. Each of the 2623 grid cells has a slightly different shape and surface area, but the nominal grid cell size is about 500 m x 500 m (Figure 2).
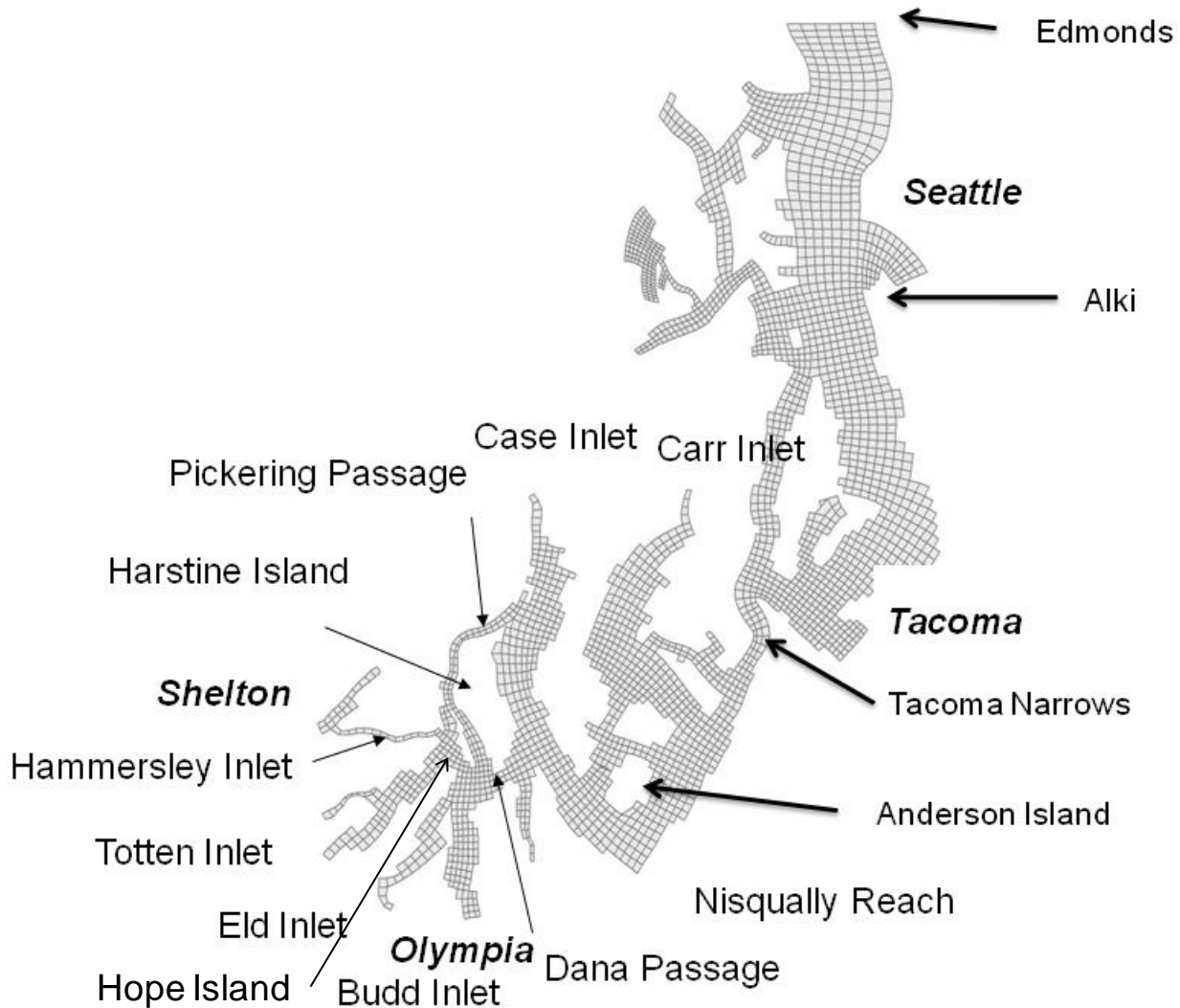
Figure 2. South and Central Puget Sound model grid.

Depths for each model grid cell were determined by sampling the Finlayson (2005) digital elevation model. Ecology reprojected the data from Washington State Plane North (feet) NAD83 to Washington State Plane South (feet) NAD83 HARN. We preserved the NAVD88 vertical datum from the original data. Using GIS, we used the model grid cell layer to define the spatial extent and averaged depth values within the 30-ft raster grid cells from the Finlayson (2003) combined bathymetry. These initial bottom elevations were smoothed once using the GEMSS Bathymetry tool. Appendix A presents the details.

Once the bottom elevations were determined, layers were assigned to fixed elevations relative to zero NAVD88. Time-varying water surface elevations show up in the top three layers to define the intertidal zone. The model uses 17 layers to represent the water column, with thicker layers lower in the water column (Figure 3). Fewer layers are used in shallower locations. To verify that this vertical resolution was appropriate, we also evaluated 35 vertical layers and tested the two during calibration.
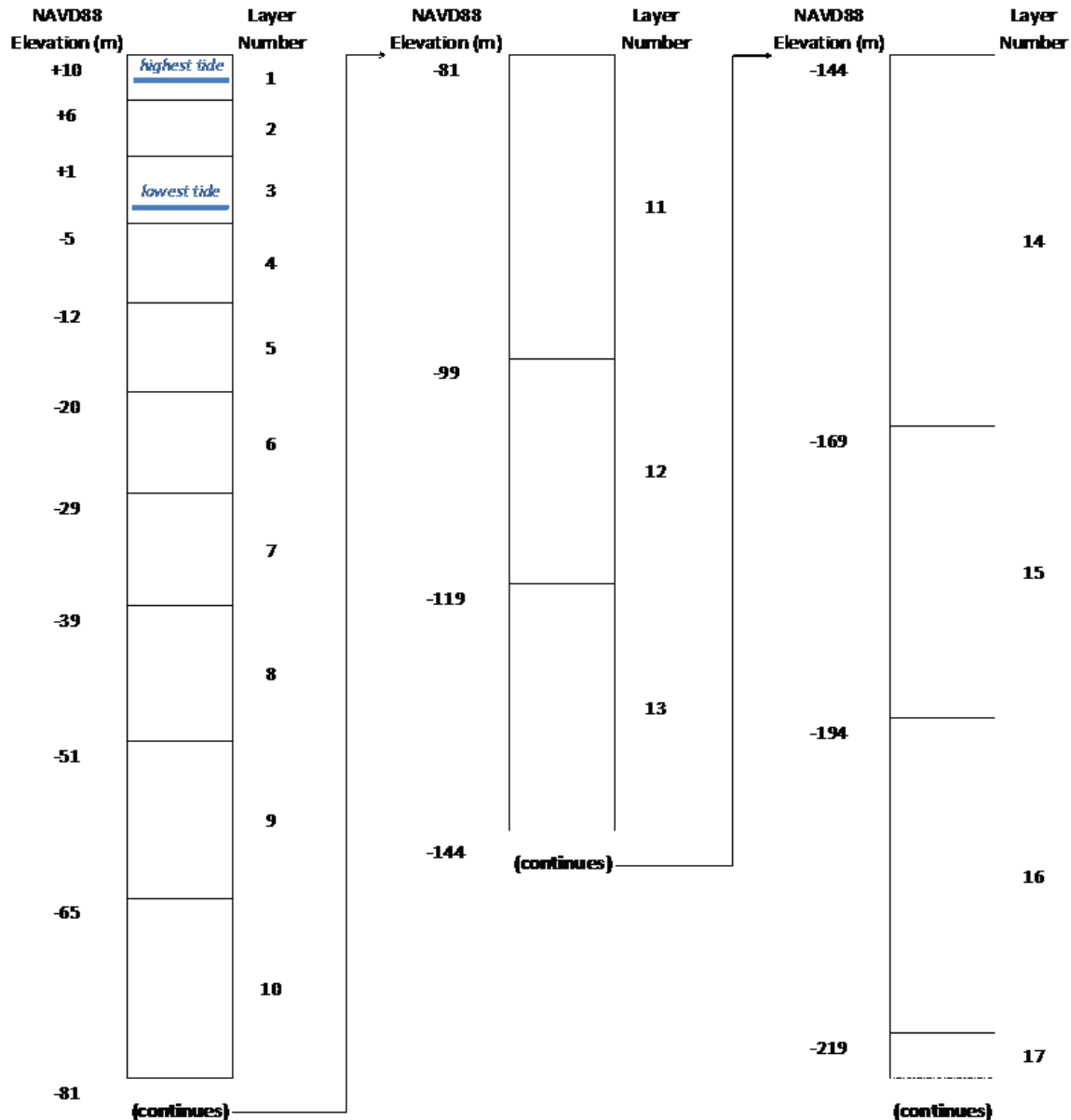
Figure 3. Elevations (m) at the top and bottom of each of the 17 model layers used in the model grid relative to the NAVD88 vertical datum.

Figure 4 presents the bathymetry used to simulate circulation in South and Central Puget Sound. The complex patterns are evident in a profile view along the deepest part (thalweg) of the channel from the northern boundary into Budd Inlet. While much of Central Puget Sound includes depths

as great as 200 to 250 m, depths decrease substantially at the Tacoma Narrows sill (50 m). Water depths are as much as 150 m east of McNeill and Anderson Islands before decreasing to 50 m around the Nisqually Reach. Depths as great as 100 m occur south of the Key Peninsula but are much lower through Dana Passage and into Budd Inlet. The quickly changing water depths produce localized bottom friction and upwelling that affect circulation and water quality.

(a)   (b)
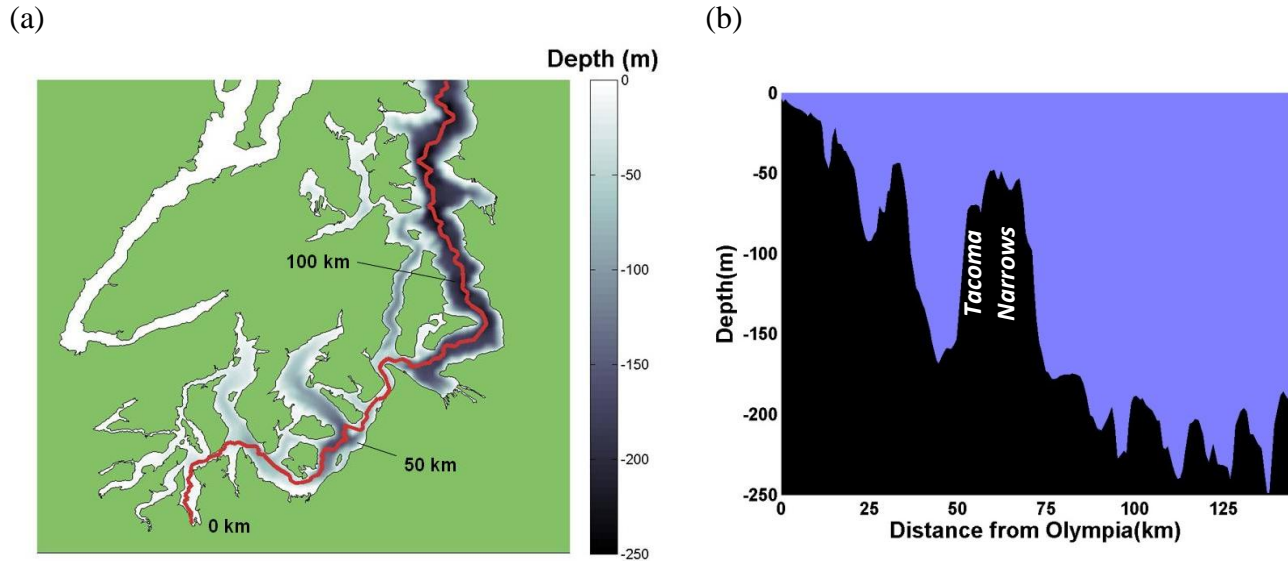

Figure 4. Bathymetry used for South and Central Puget Sound in (a) plan view, where dark color depict deeper water, and (b) as a vertical section showing depth along the thalweg with an origin in Olympia, WA.

We considered using finer grid near Hope Island and in Hammersley Inlet. However, increasing runtimes were not desirable.

Boundary Conditions

Water Surface Elevations

Water surface elevations result from the complex interaction of tidal forces from the moon and sun, the shape of marine waterbodies, wind, and freshwater inputs. Correctly predicting them is a key indicator that circulation models are calibrated correctly. Within the model domain, NOAA records and publishes water surface elevations at only two stations. However, both stations, in Elliott Bay and Commencement Bay, were too far from the Edmonds boundary to describe conditions there. To supplement these data, well established tools are available that provide detailed estimates of water surface elevations throughout the model domain.

The Puget Sound Tide Channel Model (PSTCM) predicts water surface elevations throughout Puget Sound based on the amplitude and phase of the full suite of tidal constituents (Lavelle et al., 1985; Mofjeld et al., 2002). Finlayson (2004) developed a stand-alone version of the updated PSTCM called PSTides.

Ecology used PSTides to generate tidal elevation predictions at Edmonds. Ecology converted PSTides tidal elevations, expressed relative to MLLW, to NAVD88 using NOAA's VDatum program (nauticalcharts.noaa.gov/csdl/vdatum.htm). All vertical elevations are expressed as NAVD88, Ecology's standard datum, unless otherwise specified. Positive elevations indicate locations above the datum and negative elevations below it. The water surface elevation time series at PSTides segment 388 (see *Model Calibration and Confirmation* for location) was used as the northern boundary condition. In addition, Ecology used PSTides to obtain water surface elevation for nearly every bay and channel in Puget Sound to compare with model output during model calibration and confirmation.

Temperature and Salinity Profiles

In addition to the time series of tidal elevation, the open northern boundary also requires vertical profiles of temperature and salinity gathered from monthly cruises to describe density-driven flow. Albertson et al. (2007b) describes the boundary station cruise sampling design and Roberts et al. (2008a) presents the data collected by King County Department of Natural Resources under contract to Ecology. The Edmonds east and Edmonds west vertical profiles were used as boundary conditions for the model. Table 2 lists the dates for both these boundary cruises as well as data collection at interior stations by program and vessel.

Table 2. Data collection cruise schedule by vessel for Ecology's R/V Skookum (S), University of Washington's R/V Barnes (B) and PRISM (P), and King County Department of Natural Resources' R/V Liberty (L).

Cruise	Program	Dates
P1	PRISM	6/26/06 - 6/28/06
L1	Liberty	7/26/06
B1	Barnes	7/31/06 - 8/3/06
L2	Liberty	8/16/06
S1	Skookum	8/21/06 - 8/24/06
L3	Liberty	9/20/06
B2	Barnes	9/25/06 - 9/29/06
L4	Liberty	10/18/06
S2	Skookum	10/23/06 - 10/24/06
L5	Liberty	11/8/06
S3	Skookum	11/14/06 - 11/16/06
L6	Liberty	12/6/06
B3	Barnes	12/18/06 - 12/21/06
L7	Liberty	1/10/07
L8	Liberty	2/14/07
S4	Skookum	2/26/07 - 2/27/07
L9	Liberty	3/15/07
S5	Skookum	3/26/07 - 3/27/07
S6	Skookum	4/9/07 - 4/11/07
L10	Liberty	4/11/07

B4	Barnes	4/23/07 - 4/26/07
L11	Liberty	5/9/07
S7	Skookum	5/21/07 - 5/23/07
L12	Liberty	6/13/07
B5	Barnes	6/25/07 - 6/29/07
L13	Liberty	7/11/07
S8	Skookum	7/31/07 - 8/2/07
L14	Liberty	8/8/07
S9	Skookum	8/28/07 - 8/30/07
L15	Liberty	9/5/07
B6	Barnes	9/24/07 - 9/27/07
L16	Liberty	10/3/07
S10	Skookum	10/23/07 - 10/25/07

Temperature and salinity boundary conditions are shown in Figure 5. The model implements linear interpolation between monthly cruise dates. Monthly intervals were selected to capture seasonal variability and to optimize resources available for data collection. Because monthly data could induce errors if submonthly phenomena are missed, we evaluated two supplemental sources of information for continuous temperature and salinity for northern boundary conditions: (1) the existing Princeton Ocean Model (POM) application for Puget Sound and (2) data from the nearest ORCA (Oceanic Remote Chemical Analyzer) buoy near Hood Canal.

First, we evaluated using results from POM. POM uses monthly data from a transect in the Strait of Juan de Fuca as a boundary condition. We compared POM salinity output to monthly cruise data at both the Edmonds and Alki locations for several months, including June 2007. POM surface salinity was overpredicted and near-bottom salinity was underpredicted by 0.5 to 1.5 psu by the model at the Edmonds and Alki stations compared with our measured data. POM predicts small subdaily salinity variations at Edmonds and Alki, even though the monthly boundary condition does not include submonthly forcing. POM does not simulate the heat balance or water temperature, so the model could not provide temperature profiles. For these reasons and because output was not available for the entire simulation period, Ecology determined that POM output was not a viable substitute to describe the northern boundary condition.

Second, we investigated using data collected more frequently using the nearest ORCA profiling buoy, which is near Admiralty Inlet but slightly within Hood Canal (Ruef and Devol, Hood Canal Dissolved Oxygen Program, personal communication). Comparing the monthly R/V Liberty data in Figure 5 with the buoy data confirms that monthly data do describe the overall seasonal variation well. Both time series show high-salinity water throughout the water column in October 2006 and similar conditions that are less salty in October 2007. The water column freshens in the winter with salinity decreasing to 27 psu near the surface. The ORCA buoy data show two episodes of near-bottom salinity increasing 2 psu between January and April 2007. The monthly data do capture the earlier event but not the later event. However, the event was short-lived and not coincident with the critical period.
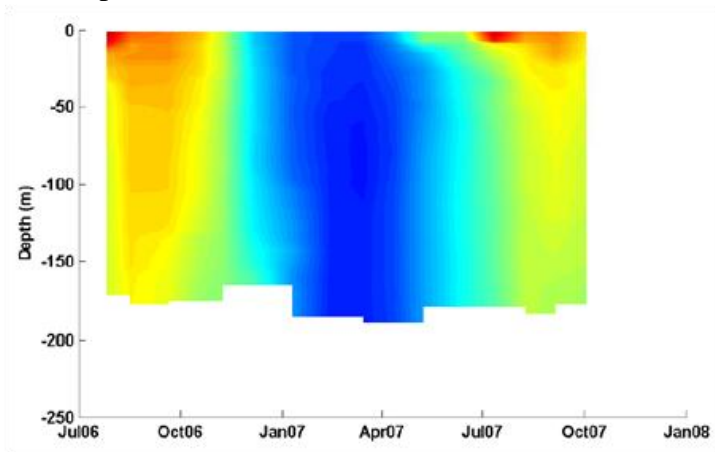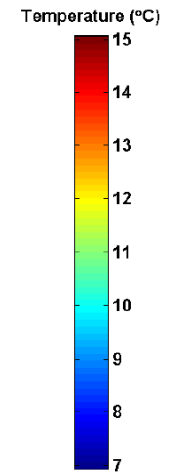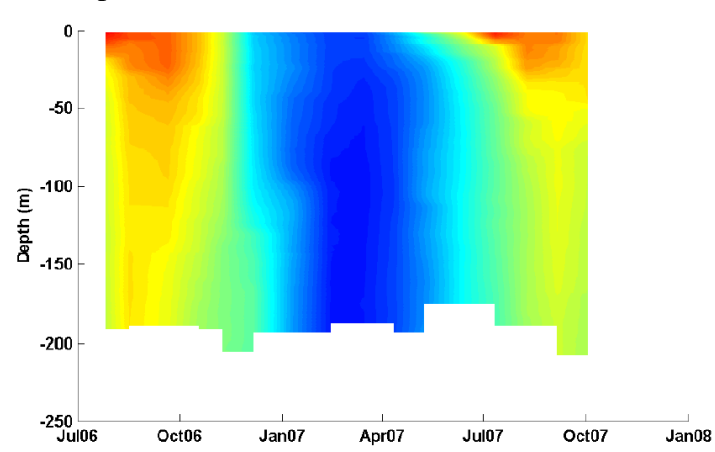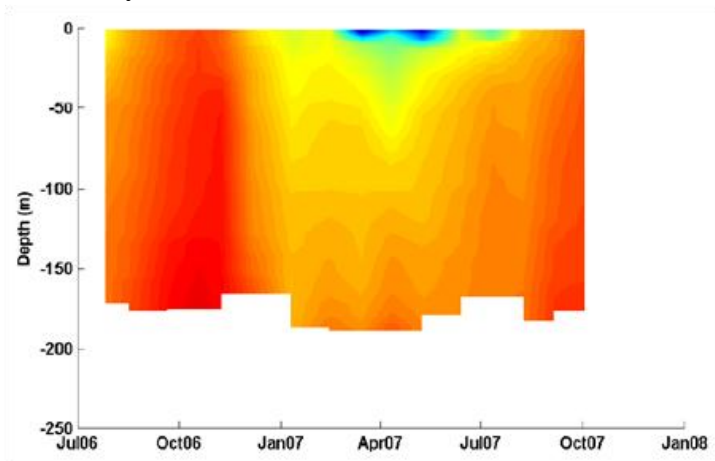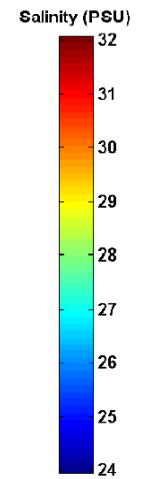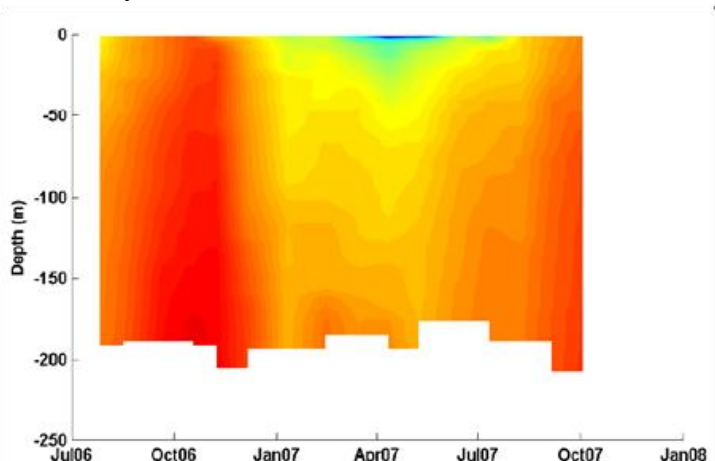
Figure 5. Temperature (a and b) and salinity (c and d) at Edmonds east and Edmonds west used as the northern boundary condition.

The ORCA buoy data provide high-resolution data useful for many purposes. For example, the salinity and temperature records do not show strong diel variations. However, the ORCA buoy is 90 km from the northern boundary and several large data gaps disrupt the time series when the equipment was either inoperable or out of calibration.

Because the monthly boundary data do appropriately capture the seasonal variability and because the other two potential sources of information were incomplete, the monthly boundary cruise data provided a better alternative for this modeling project.

Freshwater Inputs

Freshwater inflows from 66 rivers were compiled as described in Roberts et al. (2008a). Figure 6 presents the watershed definitions. Discharges were based on several USGS gaging stations within the model domain (Figure 7). Daily flows were estimated based on the ratios of watershed area and mean precipitation.

Freshwater inflows, including the shoreline areas not tributary to a major river or stream, were mapped to the surface layer of the grid cell nearest the discharge location, with the exception of Sinclair and Dyes Inlets. Roberts (2009) summarizes the inflow rate development and provides a link to an interactive tool to explore the boundary conditions.

Sinclair and Dyes Inlets are not in the primary area of interest for this modeling application. Because the waterbodies received distributed freshwater inflow from numerous small streams, watershed contributions were simplified as one composite input. All inflows are added to the western extent of Sinclair Inlet, and detailed predictions within this region will be affected. If the area influenced by this simplification extends to the primary area of interest, freshwater inflows to Sinclair and Dyes Inlets will be reevaluated.
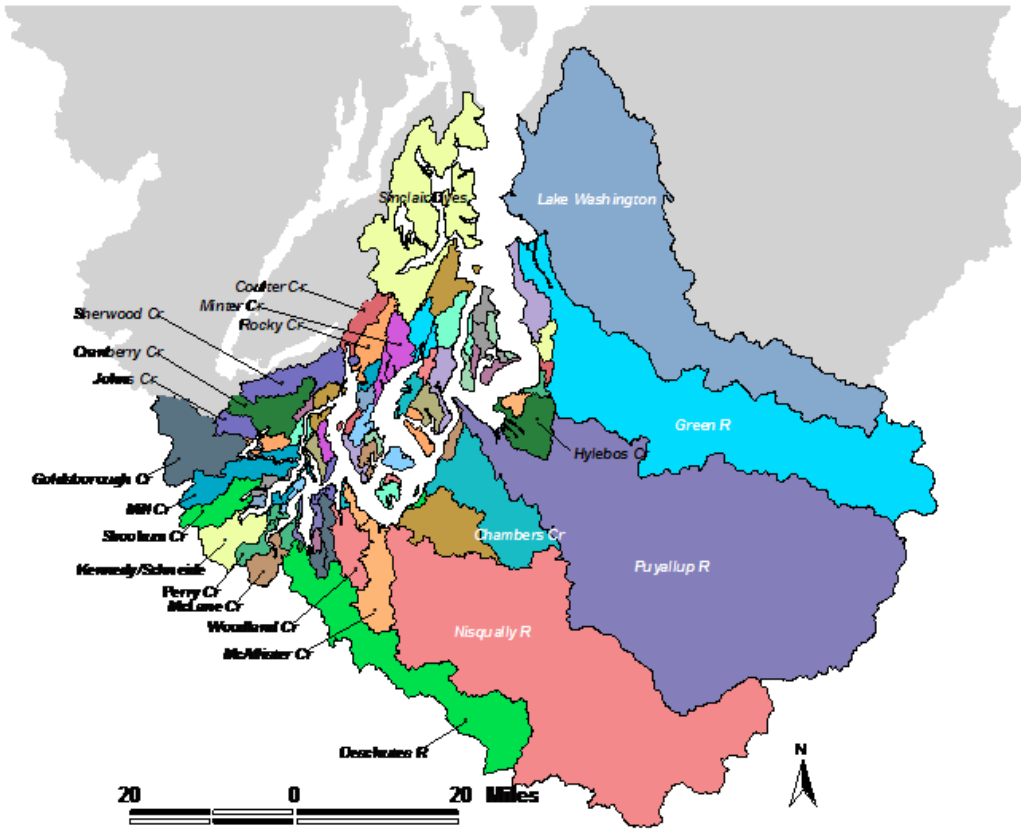
Figure 6. Watershed definitions for freshwater inflows.
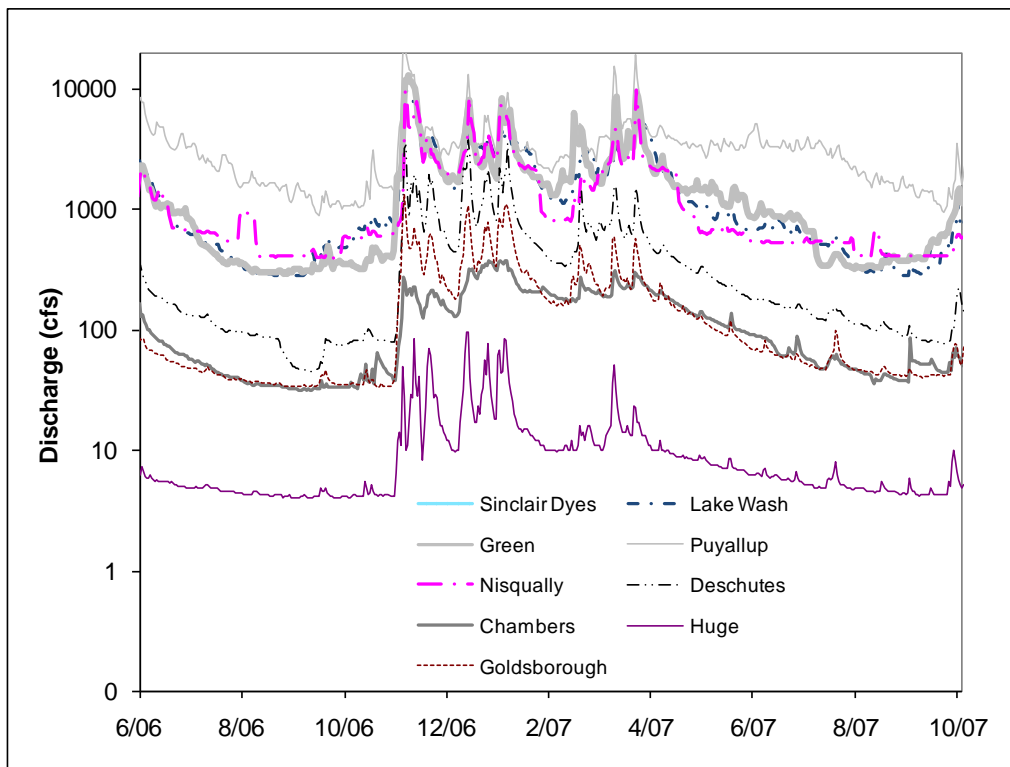
Figure 7. River, creek, and tributary discharge (cfs).

Wastewater treatment plants also discharge freshwater to South and Central Puget Sound, although they represent <5% of the total freshwater inflows. Only those >1 mgd were included (14 in Central Puget Sound and 4 in South Puget Sound) for the circulation model calibration, since the smaller plants produce insufficient volume to affect density profiles. However, wastewater treatment plant discharges will be simulated in the water quality model to be developed next.

The final source of freshwater is precipitation falling directly on the surface of South and Central Puget Sound. Figure 8 presents the precipitation volumes measured at Shelton Airport for South Puget Sound and at SeaTac Airport for Central Puget Sound. *Meteorological Forcing* describes the meteorological boundary conditions in more detail.
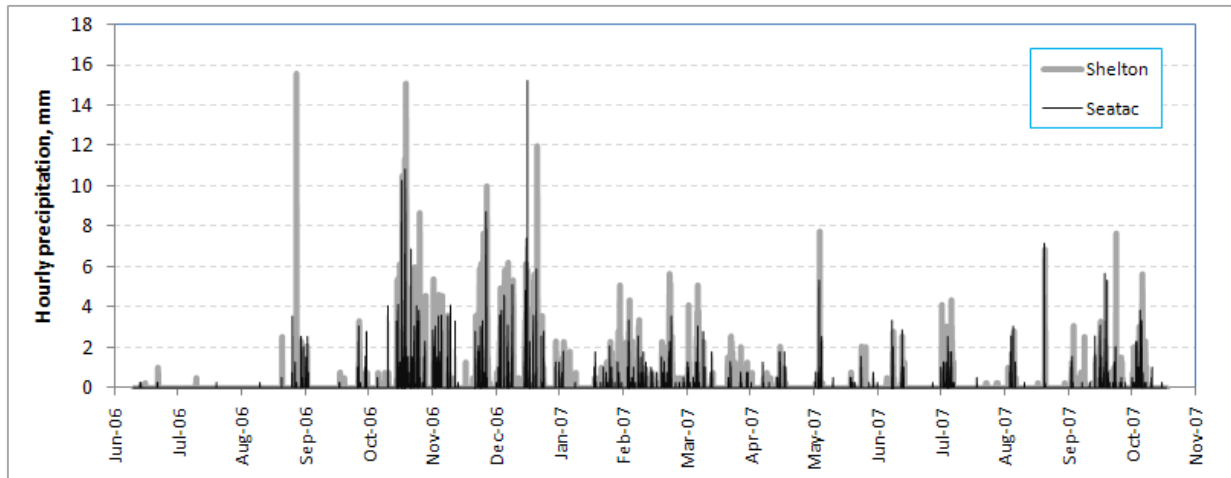

Figure 8. Precipitation measured at Shelton and SeaTac for the study period.

Continuous water temperature data are available year-round only for the Cedar River at Renton (USGS gage 12119000) (Figure 9). Continuous summer temperatures recorded at Ecology's ambient monitoring stations in the Nisqually River and Deschutes River for 2001-2006 were close to Cedar River temperatures with a mean error of +0.4 and -0.5°C, respectively. These mean errors in temperature translate to <0.1 psu density differences, which are negligible. Therefore, the water temperatures for the Cedar River were applied to all freshwater inflows. Rivers have no measurable salinity.
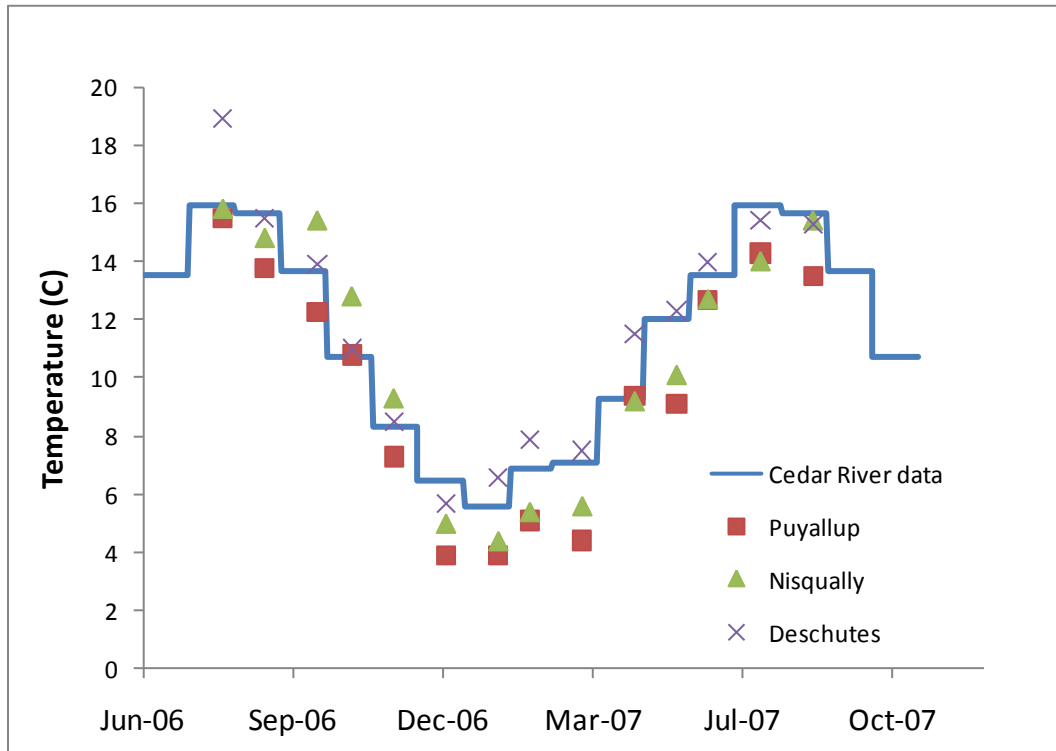
Figure 9. Cedar River mean monthly temperature (°C) compared with instantaneous monthly values recorded by Department of Ecology ambient monitoring programs.

Meteorological Forcing

In addition to precipitation, meteorology forcing functions included air and dew point temperatures, wind speed and direction, cloud cover, atmospheric pressure, relative humidity and solar radiation. Meteorological stations considered in this model are depicted in Figure 10.

GEMSS couples Puget Sound with the atmosphere through surface shear stress and heat flux. The program converts wind speed and direction, barometric pressure, precipitation, relative humidity, air temperature, cloud cover, and solar radiation into these air-sea surface terms. The solar radiation term is further split between incoming solar shortwave radiation and net outgoing longwave radiation.

Initially, meteorology data from the McChord station were used for the model domain, primarily because of its central location. During model calibration, we determined that the McChord data did not represent region-wide meteorology. The SeaTac Airport data were then used north of the Tacoma Narrows in combination with McChord data for south of Tacoma Narrows. However, McChord's warm air temperature and low cloud cover produced surface water temperatures that were too warm in southern Puget Sound. The cooler air temperatures and higher cloud cover from the Shelton Airport near Oakland Bay were more representative of marine systems. This improved model calibration.
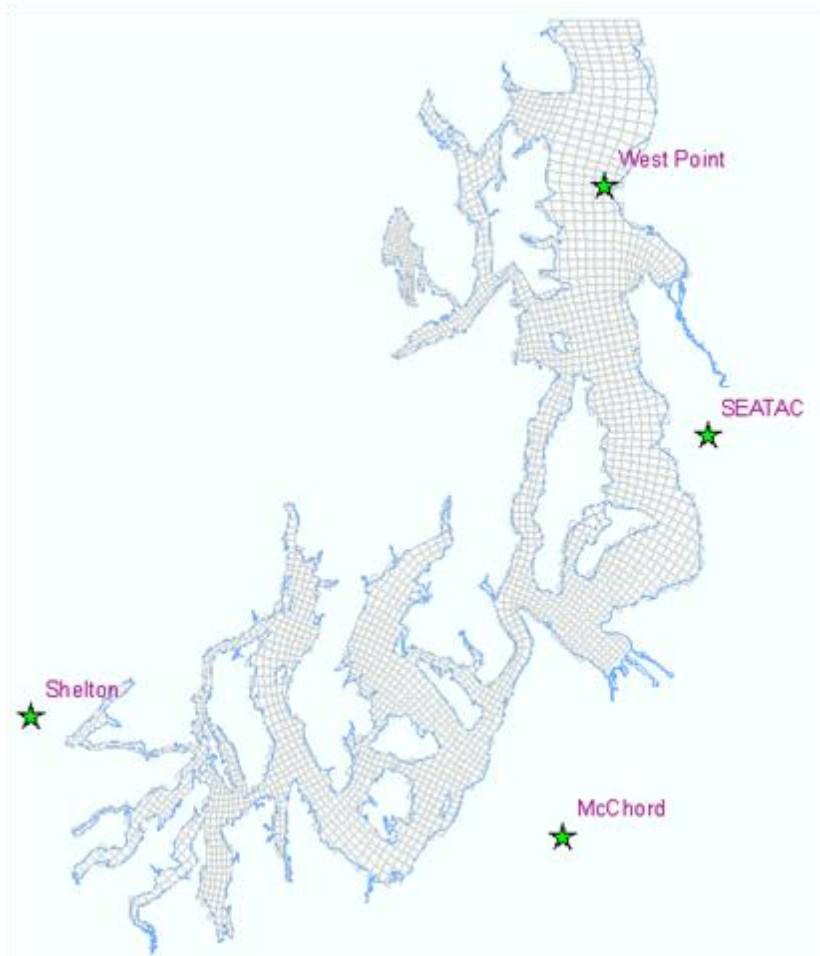
Figure 10. Location of meteorological stations considered for the model domain.

The Olympic and Cascade Mountain ranges profoundly influence wind speed and direction in Puget Sound. In South Puget Sound winds tend to be southwesterly, while in Central Puget Sound they are more southerly. Figure 11 presents the wind roses from these airport locations. Predominant wind direction at McChord was from the south and did not represent the southwesterly winds in the southern part of the model domain near Shelton. Therefore, we selected two meteorological stations, one in the south (Shelton) and the other in the north (SeaTac). The regional divide between these two stations was set immediately north of Tacoma Narrows.

Because both SeaTac and Shelton are still somewhat inland, we evaluated data from the West Point station, operated by the National Data Buoy Center (Nairn, King County, personal communication). Air temperatures at West Point were cooler than those at Shelton and SeaTac and reflected a marine influence. However, wind at West Point was still significantly different compared to Shelton although somewhat similar to SeaTac. Therefore a hybrid approach was used for meteorological forcing.

For the entire model domain, West Point station data were used for air temperature, dewpoint temperature, relative humidity, and atmospheric pressure. South of Tacoma Narrows, the Shelton station was used for wind, wind direction, cloud cover, and precipitation. North of Tacoma

Narrows, the SeaTac station was used for cloud cover and precipitation but the West Point station was used for wind and wind direction.

Cloud-free solar radiation was estimated at Shelton and SeaTac with Ecology's *Solrad* spreadsheet (http://www.ecy.wa.gov/programs/eap/models.html). We selected the Ryan/Stolzenbach solar radiation model.
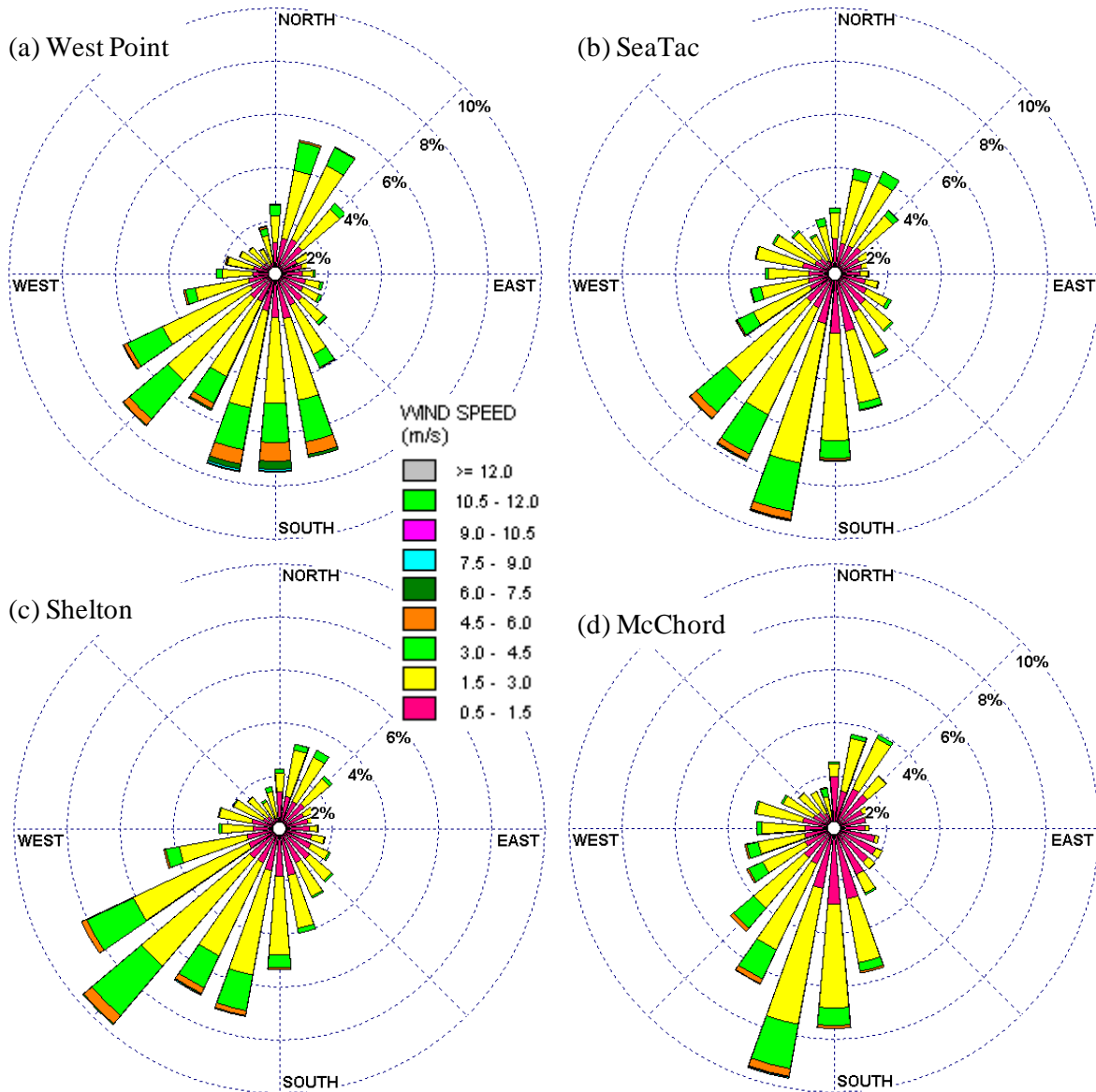

Figure 11. Wind speed, direction, and frequency plotted as wind roses at four meteorology stations in the model domain. Direction refers to where the winds originate.

Simulation Period

Data were collected between June 2006 and October 2007, as described in Roberts et al. (2008a), to provide both input to the model and output with which to compare model predictions. The simulation period was divided into separate calibration (June through December 2006) and confirmation (January through October 2007). Although 2007 had more detailed data available, the unusually cold and wet summer did not produce typical low dissolved oxygen concentrations. The calibration year (2006) represented more typical summer conditions and had enough data to calibrate the model.

Initial Conditions

The model was initialized with profiles of temperature and salinity throughout the model domain at the beginning of the simulation (July 1, 2006) collected during a late-June cruise. Several approaches were evaluated, including simulating an entire year and using the predicted July 2007 conditions as the initial July 2006 conditions. However, because 2006 and 2007 were so different in terms of meteorological boundary conditions and measured dissolved oxygen levels, we used the June 2006 cruise data as initial conditions. We divided the model domain into three zones, as shown in Figure 12, and averaged available cruise data within each zone.
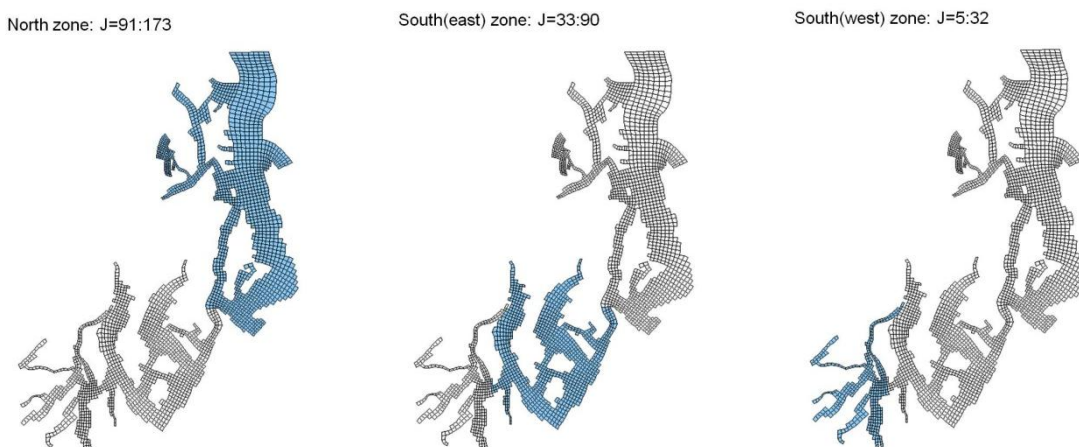

Figure 12. Three zones used to establish initial conditions for June 2006.

Model Calibration and Confirmation

Calibration refers to the iterative process of comparing model output to observed data and adjusting appropriate factors. Once a good fit is achieved, the model may be compared with an independent set of data in a process called confirmation. The ability to model circulation accurately includes well-described processes such as tidal exchanges and highly variable processes such as wind.

Marine circulation model calibration begins with comparing predicted and measured water surface elevations. Modelers adjust the grid shape, primarily depth, and the bottom friction to optimize fit. PSTides-based water surface elevations within the model domain were used to check the GEMSS model predictions. In addition, two continuous recording tide gages were used to check model predictions of water surface elevations in Commencement Bay and in Elliott Bay.

The second set of information consists of temperature and salinity values recorded during monthly cruises. To verify the model predicted spatial patterns appropriately, we compared the measured and predicted surface and near-bottom temperature and salinity time series for the simulation time period. In addition, we compared the detailed observed profiles with model output.

The third set of information used to calibrate circulation models is measured velocities. For South Puget Sound, we measured current velocities both as transects across inlets and from the bottom of several inlets. We compared both depth-averaged values between the model and the observed data as well as the tide phase (ebb and flood timing) and current velocity.

Calibration and confirmation occur sequentially. The model was calibrated using data collected from July through December 2006. Once a good fit was achieved, the model was confirmed using data for the period January through October 2007. Table 3 summarizes information sources used in the calibration and confirmation process.

Table 3. Information used to calibrate and confirm the circulation model.

Parameter	Information source	Stations
Water surface elevations	PSTides-generated water surface elevations	23 segments throughout model domain
Water surface elevations	NOAA recording tide gages measured water surface elevations	Elliott Bay (Seattle) and Commencement Bay (Tacoma)
Tidal constituent frequency and amplitude	NOAA tide gages and historical NOS stations	Elliott Bay, Commencement Bay, Budd Inlet/Boston Harbor (Olympia), and Oakland Bay (Shelton)
Surface temperature and salinity spatial patterns	Six quarterly detailed cruise data	All available stations (>70) throughout model domain
Surface and near-bottom temperature and salinity time series	All project cruise data	22 stations throughout model domain
Salinity and temperature profiles	All project cruise data	11 stations throughout model domain
Current velocities	Project current velocity data	Carr Inlet, Case Inlet, Budd Inlet, Dana Passage, Pickering Passage

Water Surface Elevations

Calibration to PSTides

Water surface elevations predicted by the model were compared with PSTides elevations for the 2006 calibration period. Comparison locations spanned the model domain, ranging from near Alki Point within Central Puget Sound to Oakland Bay in the western model domain (Figure 13). Other interim stations were used to verify circulation around complex geometry. A station within Sinclair Inlet provided a check on the circulation around Bainbridge Island. Several stations within the Tacoma Narrows were compared, since the amount of water passing over the sill influences circulation in South Puget Sound. A station in southern Budd Inlet was used because circulation influences Budd Inlet water quality (Roberts et al., 2008b). Several stations were compared near Hope Island, Hammersley Inlet, and Pickering Passage because of the complex flow patterns.

Water surface elevations predicted by the model and PSTides during a critical period of interest (September 2006) were compared throughout the model domain. Overall the model represents the time series of water surface elevations well, including both the phasing and amplitude of the tide.

Water surface elevation predictions in the northern part of the model domain (Figure 14), including Colvos Passage and stations east of Vashon Island, were very close to those predicted by PSTides. Sites nearest the northern boundary have the lowest RMSE (2.8 cm) due to proximity to the northern boundary and relatively low bathymetric complexity. The Sinclair Inlet RMSE in water surface elevation predictions (4.4 cm) is also low, and no adjustments to the local bathymetry were needed in Central Puget Sound.

To calibrate water surface elevations within South Puget Sound, the bathymetry in the Tacoma Narrows area was evaluated carefully. Initially, the grid development from the source data and smoothing steps underestimated the model grid cell depths through the Tacoma Narrows. The model grid cell widths and depths were scaled so that the grid volume within about 3 km of the Tacoma Narrows bridge matched the volume estimated from the Finlayson (2003) DEM below MLLW. Grid cells within the Tacoma Narrows were further deepened to optimize water surface elevation predictions. The final Puget Sound grid cells are within 5% of the Finlayson values. Figures 15 and 16 compare water surface elevations in the central model domain (Commencement Bay through the Tacoma Narrows) and southern model domain, respectively.
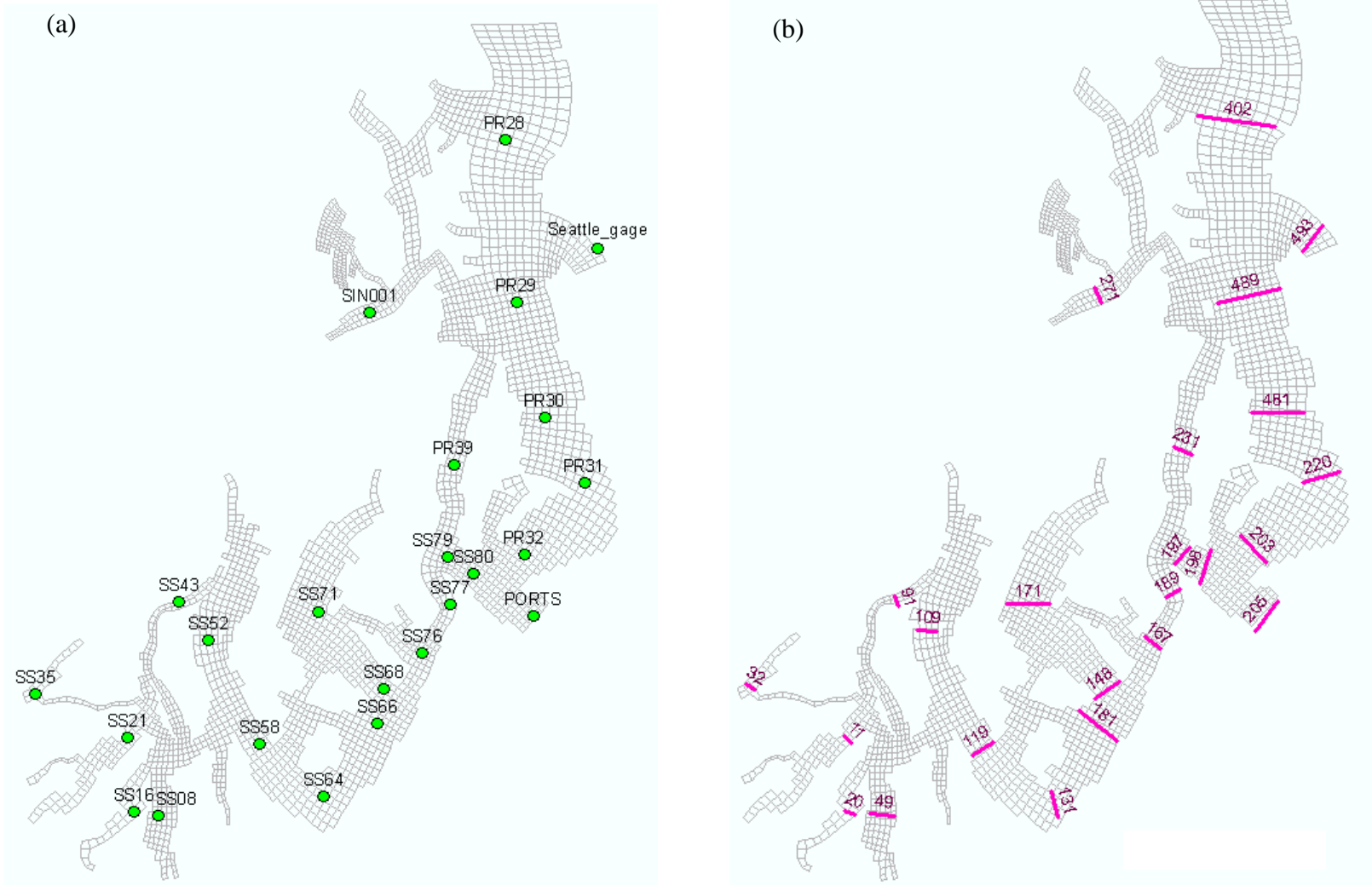
Figure 13. (a) Station locations and (b) PSTides segments used to calibrate or confirm water surface elevation predictions.
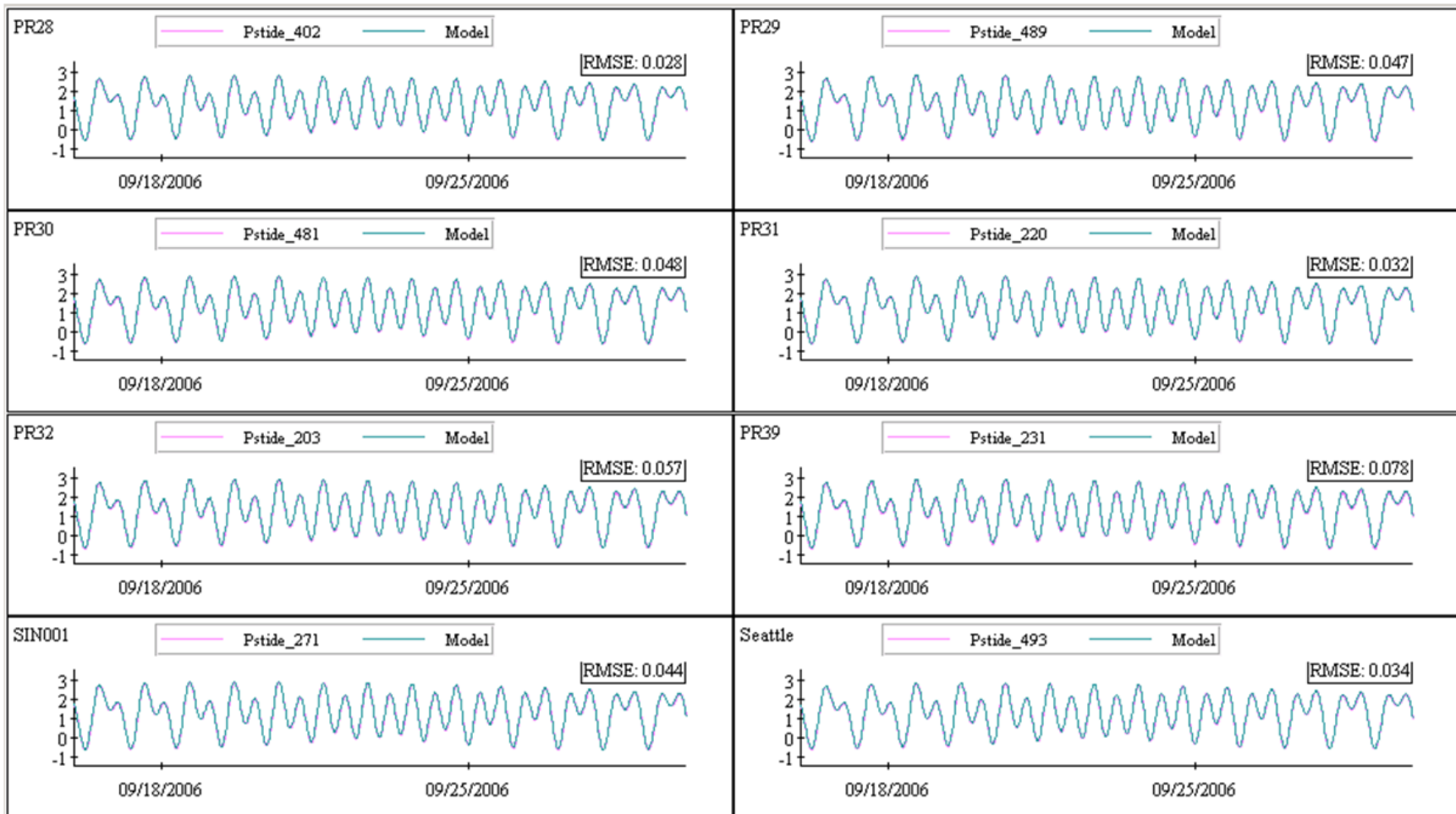
Figure 14. Predicted water surface elevations (meters) compared with PSTides for the northern model domain (south to Vashon Island) for September 2006.
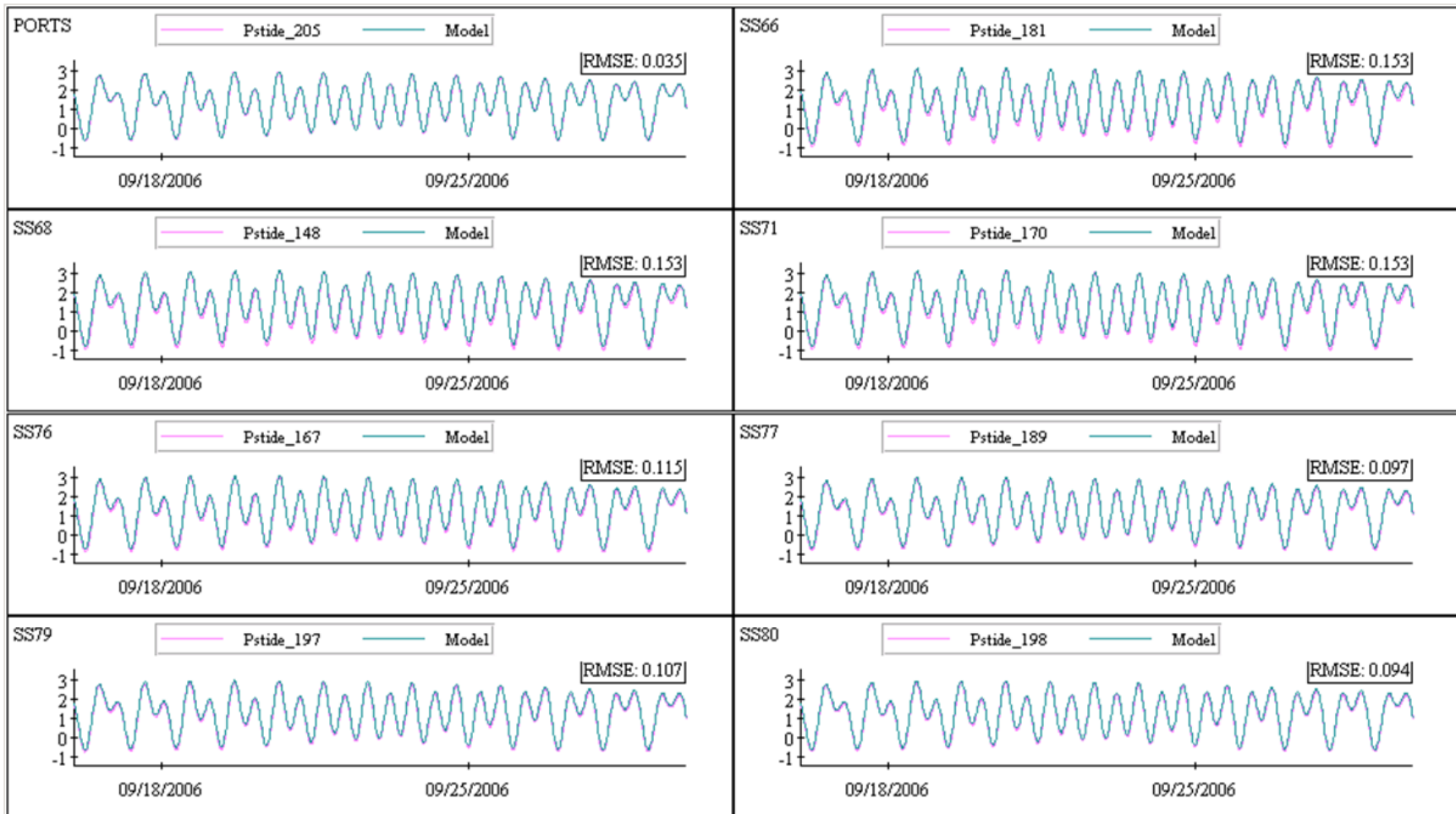
Figure 15. Predicted water surface elevations (meters) compared with PSTides for the central model domain (Commencement Bay and Tacoma Narrows) for September 2006.
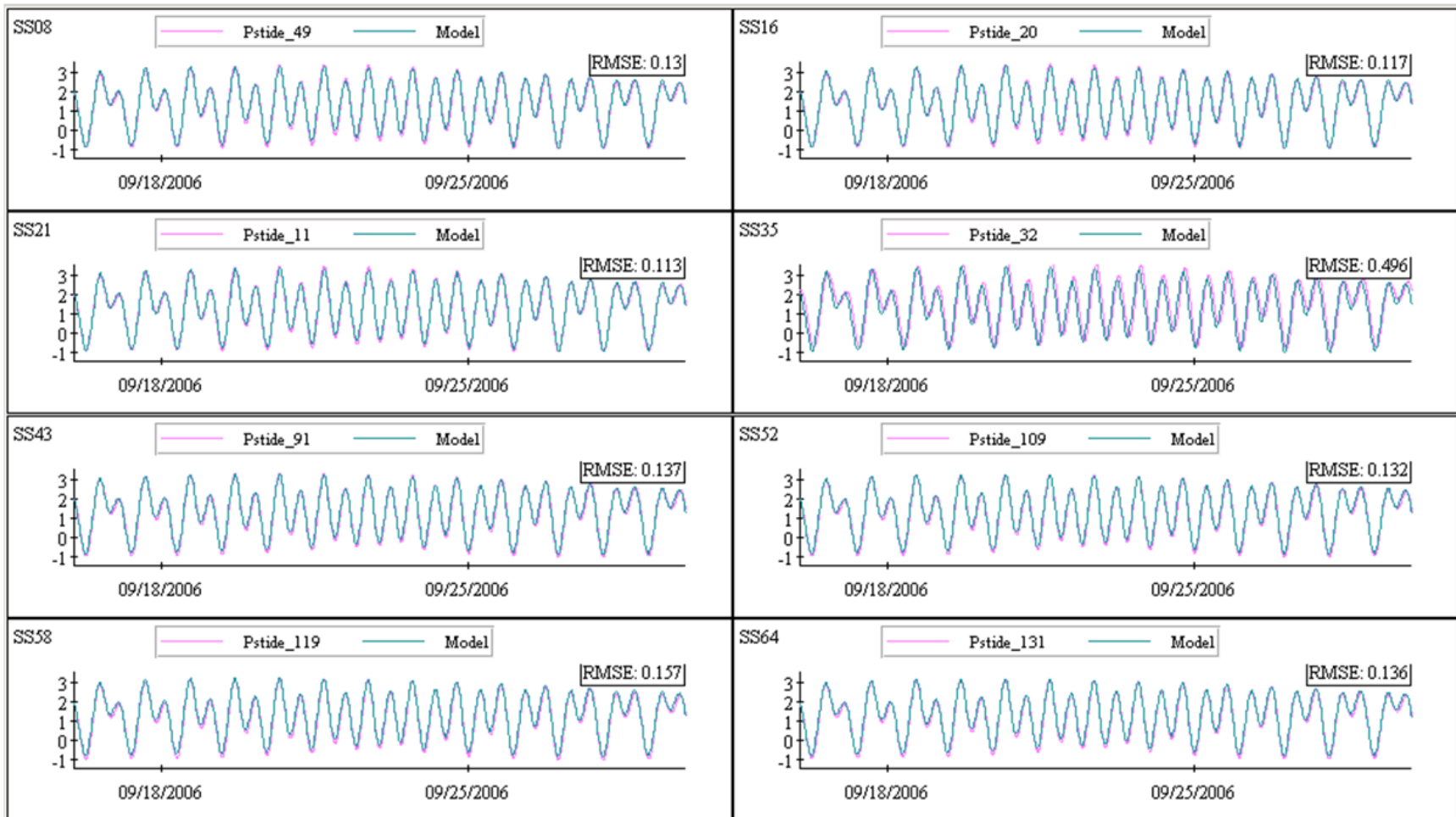
Figure 16. Predicted water surface elevations (meters) compared with PSTides for the southern model domain (west of Tacoma Narrows) for September 2006.

The original grid development and smoothing produced model grid depths that were much shallower than the deeper areas of Budd Inlet, even though the total volume error for Budd Inlet was low (3.3%). Grid cell depths in southern Budd Inlet were increased to match the Finlayson volumes for this region. Because deeper areas of Budd Inlet lie within channels, smoothing for the nominal 500-m wide grid cells averages these depths with shallower values. However, tuning the southern Budd Inlet bathymetry produced a RMSE of 13.0 cm between the model and PSTides for Budd Inlet (station SS08).

Similar to Budd Inlet, the grid development and smoothing process produced model grids for Oakland Bay, Hammersley Inlet, Pickering Passage, and Hope Island that missed key bathymetric elements. In Hammersley Inlet, the abrupt bend in the east-west arm could not be represented in the horizontal plane without causing model instabilities. Because the grid passed over land surfaces, the averaged grid cell depths were artificially shallow. The narrow channel also produced vertical constrictions that incorrectly impeded water flow into Oakland Bay and underestimated tidal exchanges. The volumes of the east-west Hammersley Inlet arm were adjusted to match the Finlayson (2003) volumes.

Pickering Passage initially was represented by shallow depths. The cross section is somewhat triangular in shape, with much deeper depths in the center of the channel than at the margins. Using two grid cells across the passage produces correct average depths but does not match the deepest depths. Therefore, widths and depths were adjusted to closer represent the shape of Pickering Passage. (See *Current Velocities* section for implications.) Peak tidal velocities through Pickering Passage, described below under *Current Velocities*, were close to those predicted by PSTides.

Hope Island influences exchanges into Hammersley and Totten Inlets. Shallow water depths both northeast and southwest of the island produce high local friction that impedes flow south of Harstine and Squaxin Islands and produces extensive tidal eddies and boils. The number of grid cells used to represent the island and the surrounding model grid cell depths were varied. Small bathymetric adjustments were made, and two inactivated model grid cells represent Hope Island.

With adjustments to Hammersley Inlet, Pickering Passage, and Hope Island, the water surface elevations predicted for South Puget Sound ranged from 15.7 cm near Nisqually Reach to 11.3 cm at the northeast end of Totten Inlet. However, Oakland Bay near Shelton still produced a RMSE of 49.6 cm when compared with PSTides. We evaluated several nearby segments in Pickering Passage and in Totten Inlet, but no other station produced such high errors as calculated for Oakland Bay. The amplitudes are reasonable, but the lack of the sharp bend in the east-west arm of Hammersley Inlet affects the phasing of tides within Oakland Bay. Our model predicts high tides and low tides approximately 40 minutes earlier than actually occurs. We accepted this model performance because the process did not influence water surface predictions in adjacent segments nor did it affect the overall amplitude of the tide.

Calibration to NOAA Recording Tide Stations

No continuously recording tide gages exist within South Puget Sound, which would have included the effect of wind. Therefore, the South Puget Sound water surface elevations cannot be compared with actual measured data. However, we compared predicted tidal elevations with those recorded at the NOAA continuously recording tide stations in Elliott Bay and Commencement Bay.

The model predicts Commencement Bay and Elliott Bay water surface elevations well, with RMSEs of 12.5 cm and 12.1 cm, respectively, for September 2006 (Figure 17). Model predictions are closer to PSTides-generated water surface elevations, partly because PSTides data were used to force the model and partly because the comparison was conducted with the wind turned off. Variability in wind magnitude and direction over the water likely contributes to the differences, but model predictions are still appropriate and acceptable. Strong wind events, as occurred later in December 2006, may produce bigger differences in water surface elevations (>50 cm) over those predicted by PSTides, but these events generally do not occur during critical conditions for low dissolved oxygen. They may affect circulation during less critical times of year.

Water Surface Elevation Confirmation

The period January through October 2007 was used as the model confirmation period with no further adjustments to the grid or bottom friction factors. Compared with PSTides or the NOAA recording tide stations described above, the model produced water surface elevation RMSEs ranging from 2.6 cm near the northern model boundary to 15.5 cm in Case Inlet. Oakland Bay continued to have the highest errors (51.1 cm) due to the phase advance in the model. Figures 18 through 20 compare water surface elevations in the north, central, and southern model domain areas, respectively, during September 2007. Overall the circulation model performs well and matches the water surface elevations throughout the model domain for the confirmation time period.
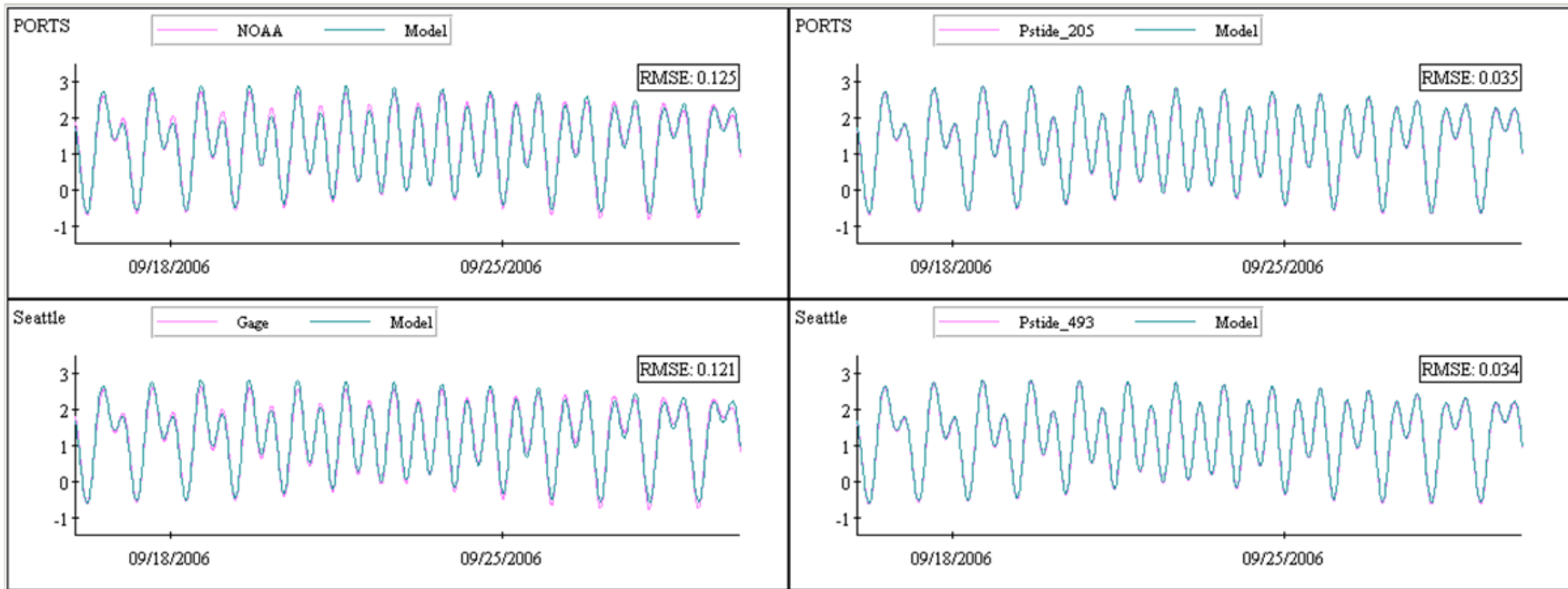
Figure 17. Predicted water surface elevations (meters) compared with NOAA recording stations (left) and PSTides (right) in Commencement Bay (top) and Elliott Bay (bottom) for September 2006.
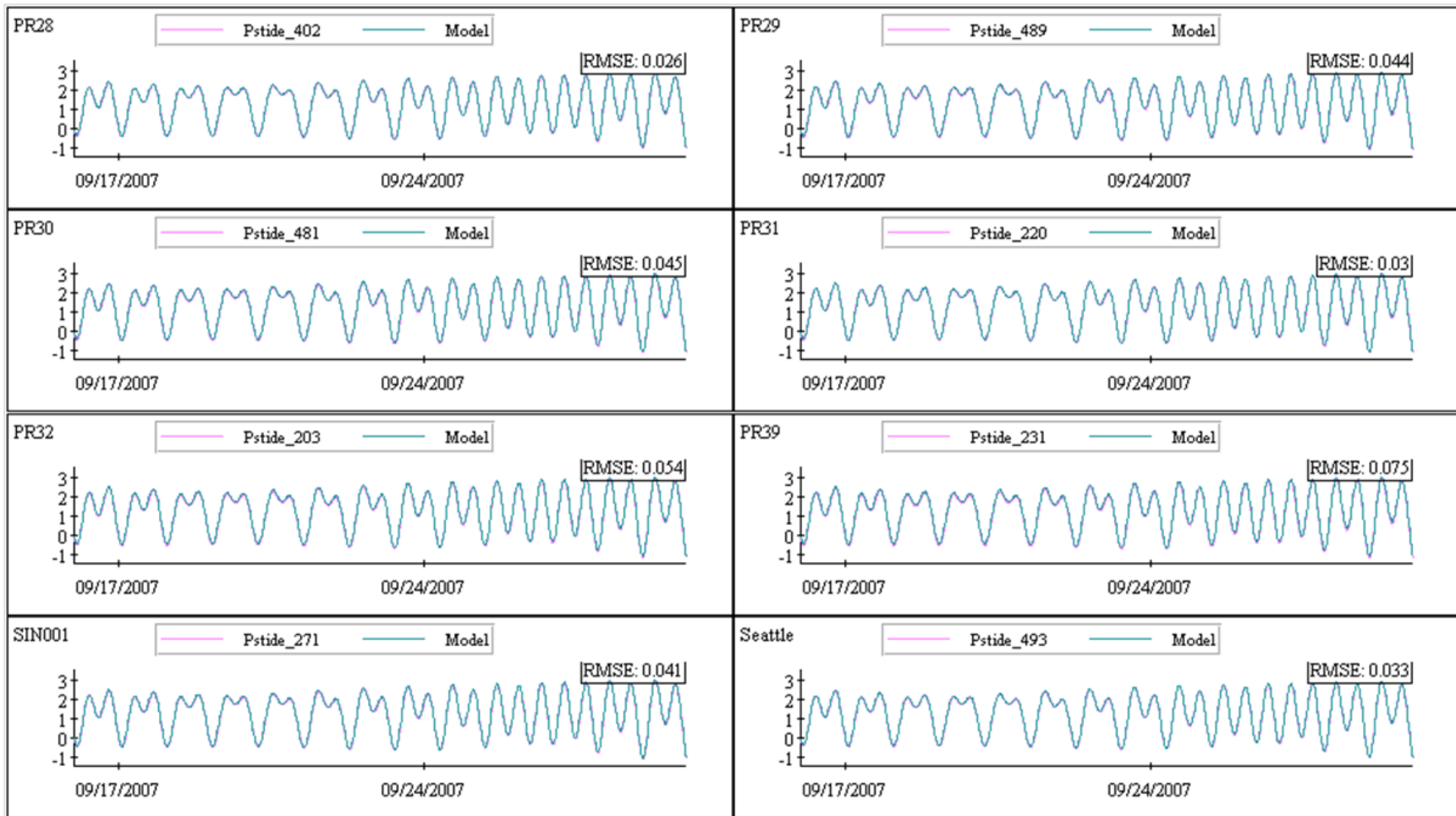
Figure 18. Predicted water surface elevations (meters) compared with PSTides for the northern model domain (south to Vashon Island) for September 2007.
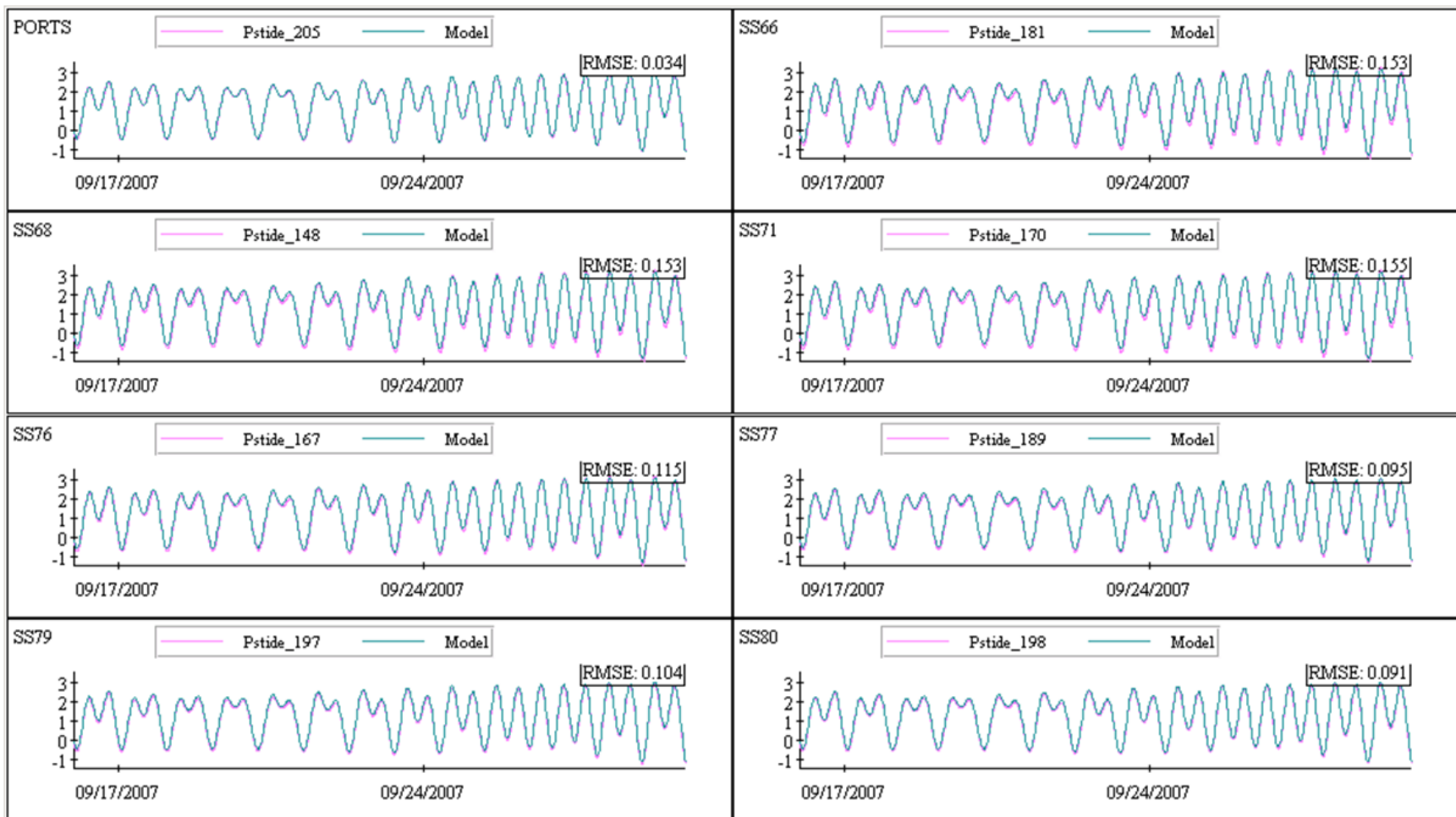
Figure 19. Predicted water surface elevations (meters) compared with PSTides for the central model domain (Commencement Bay and Tacoma Narrows) for September 2007.
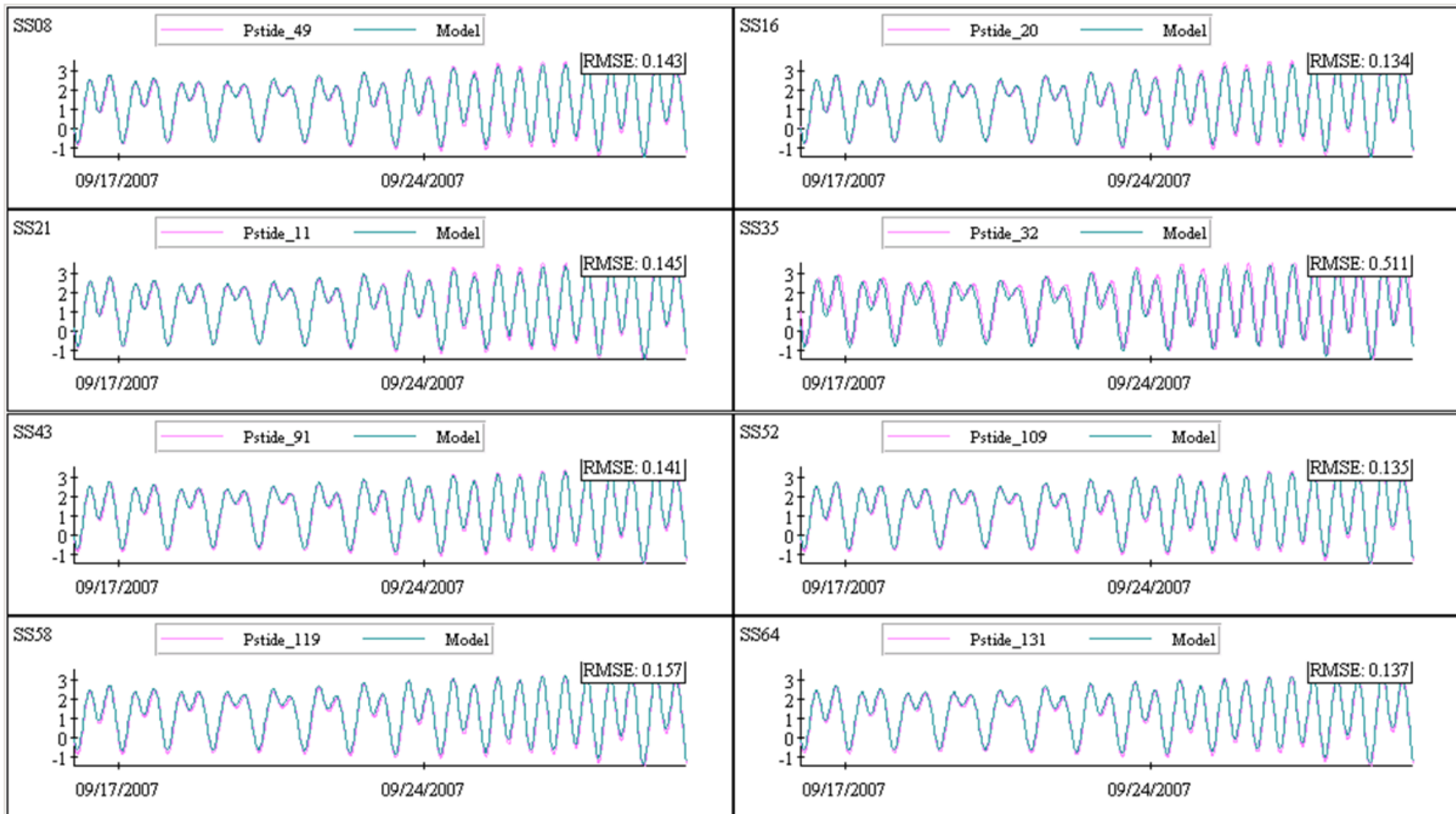
Figure 20. Predicted water surface elevations (meters) compared with PSTides for the southern model domain (west of Tacoma Narrows) for September 2007.

Tidal Constituents Comparison

In addition to the time series plots above, where we compared the amplitude and timing of the predicted and PSTides-generated water surface elevations, we compared predictions in the frequency domain. Water surface elevations result from the superposition of multiple tidal constituents, or harmonics (Hicks, 2006), each represented with an amplitude in meters and phase in degrees relative to Greenwich Mean Time. These constituents represent the separate effects of solar and lunar gravitational pull, the tilt of the Earth, and the orbits of the moon around the Earth and the Earth around the sun.

We compared the five dominant harmonics, including M2, K1, S2, N2, and O1 (see *Glossary*). The principal component is the M2 tide, or the half lunar day. Fourier transforms were used to calculate the harmonic phase and amplitude for the predicted model water surface elevations to compare with values from the two measured tide gages and other historical monitoring stations for which the tidal constituents are available. Table 4 summarizes the amplitude and phase for the model run, literature values, and PSTides for the four comparison locations, and measured data for the two available sites for September 2006 during the calibration period.

The model describes the amplitudes and phases of the various tidal constituents well compared with literature values (Lavelle et al., 1988), PSTides, and measured data. GEMSS predictions are within 5 cm and 2 degrees of each tidal constituent in the measured data in Elliott Bay and Commencement Bay for September 2006.

GEMSS tidal constituent predictions are within 10 cm of the published literature values for all four stations, including Oakland Bay. Phases are generally within 5 degrees of the published literature values, except for the S2 component in Budd Inlet and the M2 component in Oakland Bay.

GEMSS predictions also compare well with PSTides. All amplitudes are within 10 cm, including Oakland Bay. However, Oakland Bay phases are off compared with PSTides.

Budd Inlet reflects the accumulation of constituent amplitude and phase errors through South Sound and generally exhibits greater errors than the two Central Puget Sound stations compared with either PSTides or literature values. As described above, the model cannot simulate the lag associated with the sharp bend in the east-west arm, and Oakland Bay predictions have the largest error due to the geometry. The effect is limited to Hammersley Inlet and Oakland Bay.

In addition, we compared tidal constituents for the 2007 confirmation period for both March (Table 5) and September (Table 6). We found that the September 2007 tidal constituents were comparable to September 2006. The March 2007 comparison shows somewhat higher differences compared with the measured data. The model was run without wind for these comparisons, and the differences in this spring period could be due in part to the effect of wind. However, the GEMSS predictions compared well with the literature, PSTides, and measured data throughout 2007.

Table 4. Tidal harmonics (H, amplitude and Ω, phase relative to Greenwich Mean Time) predicted by GEMSS for September 2006.

Station/ Constituent	GEMSS		Lavelle et al. (1988)		GEMSS vs. literature			PSTides		GEMSS vs. PSTides			NOAA (measured)		GEMSS vs. measured		
	H (m)	Ω (deg)	H (m)	Ω (deg)	H (%)	dH (cm)	dΩ (deg)	H (m)	Ω (deg)	H (%)	dH (cm)	dΩ (deg)	H (m)	W (deg)	H (%)	dH (cm)	dΩ (deg)
Elliott Bay (ALKE)																	
O1	0.476	255.0	0.458	255.4	104%	1.78	-0.5	0.474	255.5	100%	0.16	-0.5	0.491	254.0	97%	1.53	1.0
K1	0.824	280.6	0.831	277.3	99%	0.67	3.3	0.843	280.6	98%	1.82	-0.1	0.866	281.6	95%	4.16	-1.1
N2	0.245	343.5	0.212	340.3	115%	3.25	3.2	0.247	344.6	99%	0.21	-1.1	0.263	343.3	93%	1.82	0.2
M2	1.060	11.9	1.070	11.5	99%	1.02	0.4	1.062	11.5	100%	0.23	0.4	1.074	10.5	99%	1.41	1.4
S2	0.257	30.0	0.258	37.9	100%	0.12	-7.9	0.264	29.3	97%	0.73	0.7	0.278	30.0	92%	2.17	-0.1
Commencement Bay (SS80)																	
O1	0.479	255.2	0.465	254.8	103%	1.35	0.4	0.479	255.7	100%	0.09	-0.5	0.496	253.7	96%	1.77	1.5
K1	0.833	280.8	0.834	278.0	100%	0.14	2.8	0.854	280.9	97%	2.15	0.0	0.872	281.2	95%	3.98	-0.4
N2	0.257	345.2	0.236	343.0	109%	2.08	2.2	0.260	345.5	99%	0.30	-0.3	0.280	343.9	92%	2.33	1.3
M2	1.123	13.1	1.133	13.0	99%	1.02	0.1	1.123	12.5	100%	0.00	0.6	1.145	11.3	98%	2.22	1.8
S2	0.274	31.4	0.273	38.6	100%	0.07	-7.2	0.279	30.4	98%	0.57	1.0	0.296	31.5	93%	2.19	-0.1
Budd Inlet/Boston Harbor (SS13)																	
O1	0.514	262.4	0.483	259.1	106%	3.07	3.3	0.507	262.6	101%	0.63	-0.2					
K1	0.903	288.9	0.945	287.7	96%	4.21	1.2	0.915	288.6	99%	1.23	0.3					
N2	0.305	3.0	0.262	0.8	116%	4.32	2.2	0.335	2.1	91%	2.93	0.9					
M2	1.361	28.2	1.440	32.2	95%	7.92	-4.0	1.459	29.5	93%	9.85	-1.3					
S2	0.330	49.7	0.354	61.5	93%	2.36	-11.8	0.372	48.3	89%	4.12	1.5					
Oakland Bay (SS35)																	
O1	0.515	265.8						0.512	275.8	100%	0.23	-10.0					
K1	0.914	293.0						0.925	303.2	99%	1.03	-10.2					
N2	0.316	11.4						0.339	32.2	93%	2.30	-20.8					
M2	1.415	35.3	1.490	58.0	95%	7.53	-22.7	1.502	57.8	94%	8.71	-22.5					
S2	0.341	58.5						0.385	77.9	89%	4.39	-19.4					

Table 5. Tidal harmonics (H, amplitude and Ω, phase relative to Greenwich Mean Time) predicted by GEMSS for March 2007.

Station/ Constituent	GEMSS		Lavelle et al. (1988)		GEMSS vs. literature			PSTides		GEMSS vs. PSTides			NOAA (measured)		GEMSS vs. measured		
	H (m)	Ω (deg)	H (m)	Ω (deg)	H (%)	dH (cm)	dΩ (deg)	H (m)	Ω (deg)	H (%)	dH (cm)	dΩ (deg)	H (m)	W (deg)	H (%)	dH (cm)	dΩ (deg)
Elliott Bay (ALKE)																	
O1	0.465	253.2	0.458	255.4	102%	0.72	-2.2	0.461	253.2	101%	0.45	-0.1	0.469	247.8	99%	0.36	5.4
K1	0.895	280.9	0.831	277.3	108%	6.44	3.6	0.889	280.6	101%	0.60	0.2	0.906	278.1	99%	1.08	2.7
N2	0.230	351.7	0.212	340.3	109%	1.83	11.4	0.231	350.4	100%	0.09	1.3	0.240	348.6	96%	0.98	3.1
M2	1.065	12.0	1.070	11.5	100%	0.51	0.5	1.067	11.7	100%	0.23	0.3	1.046	11.3	102%	1.92	0.7
S2	0.269	34.4	0.258	37.9	104%	1.12	-3.5	0.271	33.8	99%	0.16	0.5	0.286	34.0	94%	1.68	0.3
Commencement Bay (SS80)																	
O1	0.457	254.3	0.465	254.8	98%	0.76	-0.5	0.466	253.4	98%	0.81	0.9	0.476	248.1	96%	1.84	6.3
K1	0.885	281.8	0.834	278.0	106%	5.05	3.8	0.901	280.9	98%	1.63	0.9	0.921	278.5	96%	3.62	3.4
N2	0.240	352.3	0.236	343.0	102%	0.42	9.3	0.243	351.4	99%	0.33	0.9	0.257	350.1	93%	1.67	2.2
M2	1.126	13.0	1.133	13.0	99%	0.69	0.0	1.128	12.7	100%	0.20	0.3	1.117	12.7	101%	0.89	0.3
S2	0.290	35.2	0.273	38.6	106%	1.69	-3.4	0.287	34.9	101%	0.34	0.2	0.305	36.0	95%	1.50	-0.8
Budd Inlet/Boston Harbor (SS13)																	
O1	0.507	260.2	0.483	259.1	105%	2.38	1.1	0.493	260.3	103%	1.41	-0.1					
K1	0.975	289.0	0.945	287.7	103%	3.02	1.3	0.962	288.2	101%	1.30	0.9					
N2	0.292	11.5	0.262	0.8	112%	3.03	10.7	0.313	8.0	93%	2.07	3.5					
M2	1.365	28.1	1.440	32.2	95%	7.48	-4.1	1.466	29.7	93%	10.10	-1.6					
S2	0.351	55.0	0.354	61.5	99%	0.28	-6.5	0.381	52.8	92%	2.97	2.2					
Oakland Bay (SS35)																	
O1	0.508	263.6						0.498	273.5	102%	0.99	-10.0					
K1	0.988	293.2						0.971	302.1	102%	1.76	-8.9					
N2	0.306	20.5						0.317	37.0	97%	1.08	-16.5					
M2	1.418	35.3	1.490	58.0	95%	7.22	-22.7	1.514	58.1	94%	9.59	-22.8					
S2	0.362	63.9						0.393	82.2	92%	3.04	-18.3					

Table 6. Tidal harmonics (H, amplitude and Ω, phase relative to Greenwich Mean Time) predicted by GEMSS for September 2007.

Station/ Constituent	GEMSS		Lavelle et al. (1988)		GEMSS vs. literature			PSTides		GEMSS vs. PSTides			NOAA (measured)		GEMSS vs. measured		
	H (m)	Ω (deg)	H (m)	Ω (deg)	H (%)	dH (cm)	dΩ (deg)	H (m)	Ω (deg)	H (%)	dH (cm)	dΩ (deg)	H (m)	W (deg)	H (%)	dH (cm)	dΩ (deg)
Elliott Bay (ALKE)																	
O1	0.455	257.0	0.458	255.4	99%	0.32	1.6	0.455	256.2	100%	0.05	0.8	0.475	255.7	96%	2.00	1.3
K1	0.847	280.9	0.831	277.3	102%	1.64	3.6	0.840	280.5	101%	0.72	0.4	0.846	282.2	100%	0.18	-1.3
N2	0.208	349.8	0.212	340.3	98%	0.45	9.5	0.204	350.3	101%	0.31	-0.5	0.205	348.7	101%	0.22	1.1
M2	1.070	10.5	1.070	11.5	100%	0.03	-1.0	1.072	10.5	100%	0.15	0.1	1.091	9.1	98%	2.11	1.4
S2	0.260	31.1	0.258	37.9	101%	0.19	-6.8	0.260	30.2	100%	0.06	0.9	0.274	28.4	95%	1.43	2.7
Commencement Bay (SS80)																	
O1	0.457	257.0	0.465	254.8	98%	0.79	2.2	0.460	256.4	99%	0.31	0.7	0.480	256.1	95%	2.24	1.0
K1	0.855	281.0	0.834	278.0	103%	2.13	3.0	0.852	280.8	100%	0.36	0.3	0.854	282.6	100%	0.12	-1.6
N2	0.218	351.5	0.236	343.0	92%	1.79	8.5	0.215	351.3	101%	0.29	0.2	0.209	350.0	104%	0.89	1.5
M2	1.133	11.8	1.133	13.0	100%	0.03	-1.2	1.133	11.5	100%	0.04	0.3	1.161	10.9	98%	2.74	0.8
S2	0.277	32.9	0.273	38.6	102%	0.44	-5.7	0.276	31.3	101%	0.18	1.5	0.292	30.8	95%	1.43	2.0
Budd Inlet/Boston Harbor (SS13)																	
O1	0.493	263.6	0.483	259.1	102%	0.96	4.5	0.487	263.3	101%	0.55	0.4					
K1	0.925	289.2	0.945	287.7	98%	1.97	1.5	0.912	288.4	101%	1.29	0.8					
N2	0.259	11.6	0.262	0.8	99%	0.30	10.8	0.277	7.7	93%	1.83	3.8					
M2	1.375	26.8	1.440	32.2	95%	6.54	-5.4	1.473	28.4	93%	9.86	-1.7					
S2	0.335	51.3	0.354	61.5	95%	1.92	-10.2	0.367	49.1	91%	3.18	2.2					
Oakland Bay (SS35)																	
O1	0.493	267.0						0.492	276.5	100%	0.04	-9.5					
K1	0.937	293.3						0.923	303.2	102%	1.47	-9.9					
N2	0.270	21.2						0.279	34.6	97%	0.92	-13.4					
M2	1.428	33.9	1.490	58.0	96%	6.19	-24.1	1.522	56.9	94%	9.37	-23.0					
S2	0.347	59.9						0.378	78.8	92%	3.10	-18.9					

Effect of Bottom Friction

In addition to varying the bathymetry to achieve calibration, we adjusted the bottom friction to enhance or reduce tidal exchanges. We varied bottom friction within a typical range of 20 to 50 (unitless Chezy friction coefficient) in multiple model runs, but the effect on water surface elevations was much lower than refining the model bathymetry. Overall, a bottom friction of 40 provided the best fit between water surface elevations predicted between the model and both PSTides and the measured tide stations.

Effect of Model Layering

We evaluated multiple vertical layering thicknesses during the calibration process. Initially we developed a 35-layer model. However, even with a powerful computer[1], the 35-layer run required 9 days to simulate 17 months. Initial runs with the 35-layer model produced slightly lower RMSEs in water surface elevations compared with the selected 17-layer model. Because the water quality model will need to evaluate multiple scenarios in a reasonable time period, the slow run times far outweighed the slight improvement in water surface elevations. The 17-layer version was a reasonable compromise between providing good vertical structure in density stratification and available computational speed.

We also evaluated increased spatial detail near the surface in case that is needed to describe the complex biogeochemical processes and spatial scales in the upcoming water quality model. Layer thicknesses of 3 m or less led to model instabilities and could not be used. Maintaining 4-m layer thicknesses near the surface was possible, but the additional layering increased model run times substantially. The increased surface detail did not significantly improve temperature and salinity profiles, described below. If the detail is warranted during water quality model development, we will investigate detailed surface layering further. However, the current layering reproduces vertical profiles and is sufficient for calibration.

---

[1] 2.66-GHz CPU with 8 GB of RAM under a Windows server 64-bit operating system

Surface Temperature and Salinity Spatial and Temporal Patterns

Model output was compared with cruise data to confirm spatial patterns in temperature and salinity predicted by the model during the calibration and confirmation time periods. We compare near-surface patterns because they are influenced by river and meteorology boundary conditions and generally show more variability than near-bottom conditions. We present near-bottom results in the *Salinity and Temperature Profiles* section.

Cruise data were collected over multiple days and at different times of day. However, differences in cloud cover, tidal phase, and diel variations contribute to variability during the multi-day data collection period. We compare model results from noon in the middle of the cruise window as a snapshot of conditions as a synoptic proxy for cruise conditions.

Calibration to 2006 Data

Predicted surface temperatures for both summer 2006 cruises reflect available data (Figures 21 and 22). Cruise tracks did not reach the shallow terminus of each inlet to verify these spatial patterns, but the model predicts high temperatures consistent with the shallow water depths. Warm water temperatures within Sinclair and Dyes Inlets, Liberty Bay, and Quartermaster Harbor are reasonable, but no data were collected within these regions of Central Puget Sound. Outside of these shallow bays, Central Puget Sound surface temperatures were cooler than those in South Puget Sound in both the model predictions and measured data, and overall magnitudes and spatial patterns are appropriate. Overall cooler summer temperatures near the Tacoma Narrows reflect intense mixing with cooler bottom waters.

Winter surface temperatures are more uniform than summer throughout the domain in both the model predictions and data (Figure 23), with the coldest temperatures in the shallow waters of western inlets.

Salinity has a stronger effect on density than does temperature. The summer 2006 model output and cruise data show good agreement throughout the model domain (Figures 24 and 25). Lowest surface salinities occur nearest river inputs, but few data were available from these shallow waters to corroborate. The plumes from the Puyallup and Nisqually Rivers are evident, as are smaller river inputs to more quiescent regions in the model. Surface salinities reached seasonal maxima in September 2006, coincident with low river inputs. The December 2006 cruise data confirm the wide range of surface salinities predicted by the model (from <20 psu to nearly 30 psu) due to the increase in river inflows (Figure 26).
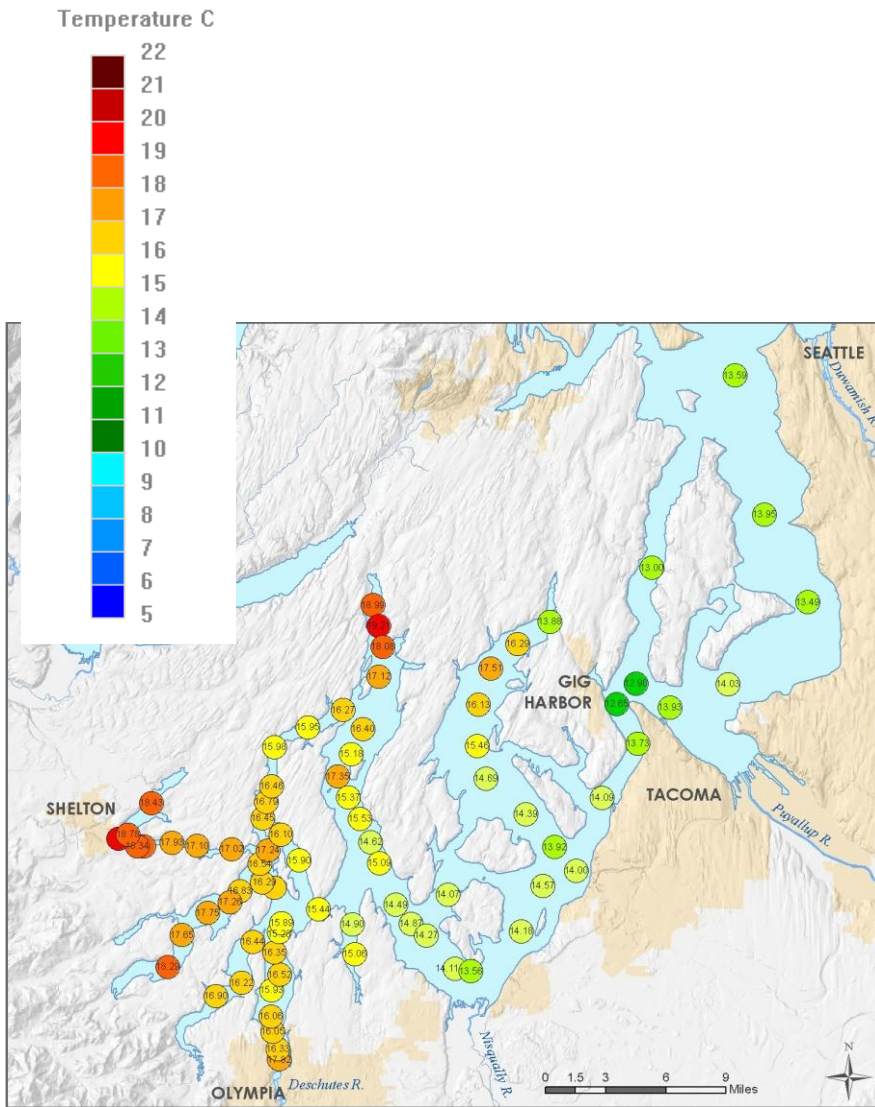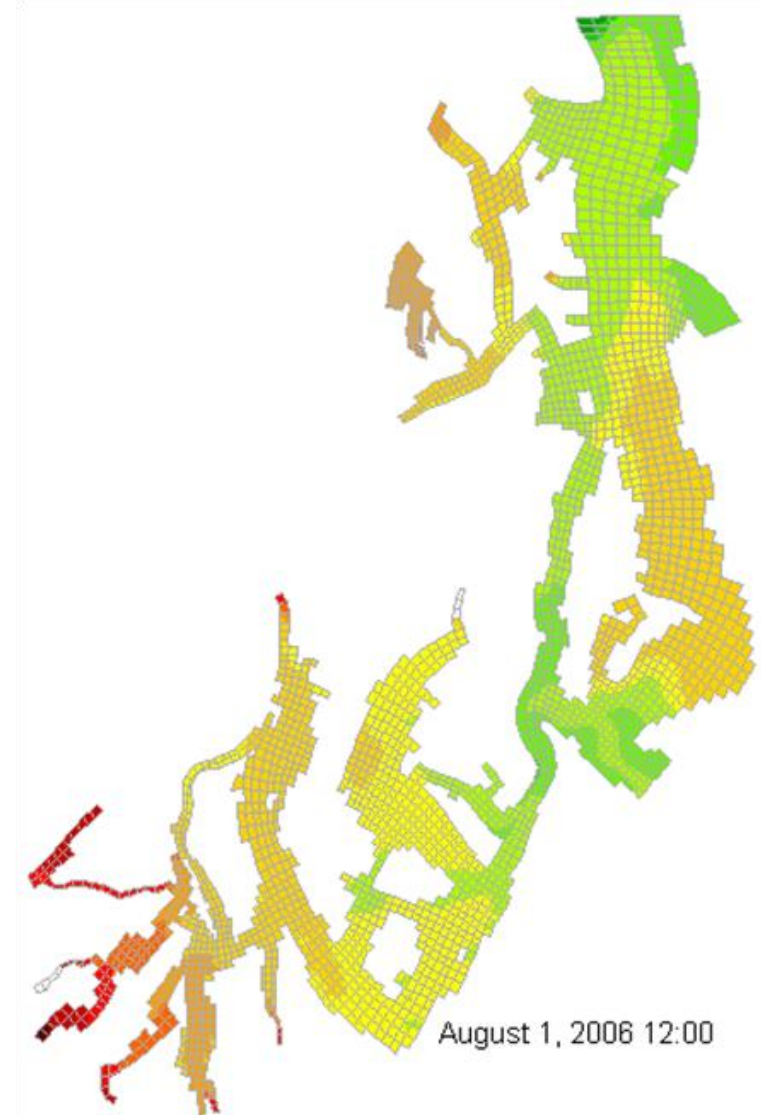
Figure 21. (a) Field observations (July 31 – August 3, 2006) of near-surface temperature (°C) compared with (b) model output (August 1, 2006).
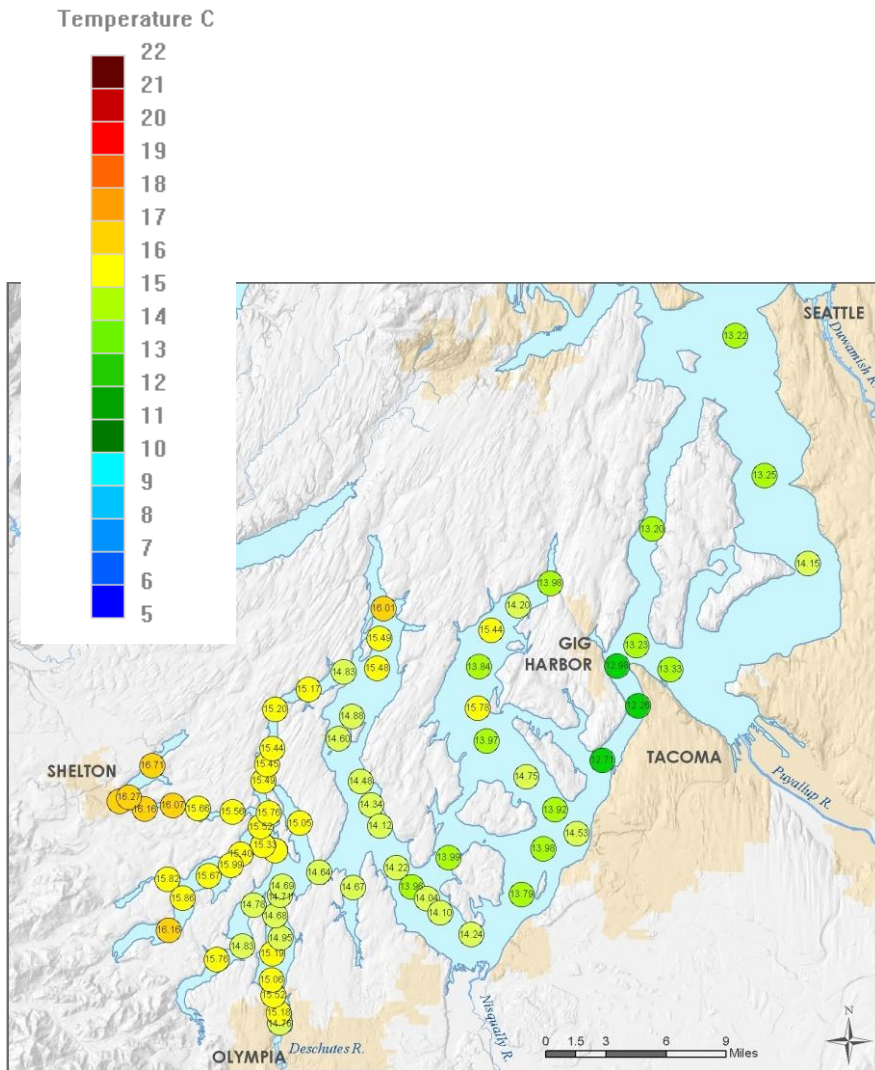
Figure 22. (a) Field observations (September 25-29, 2006) of near-surface temperature (°C) compared with (b) model output (September 27, 2006).
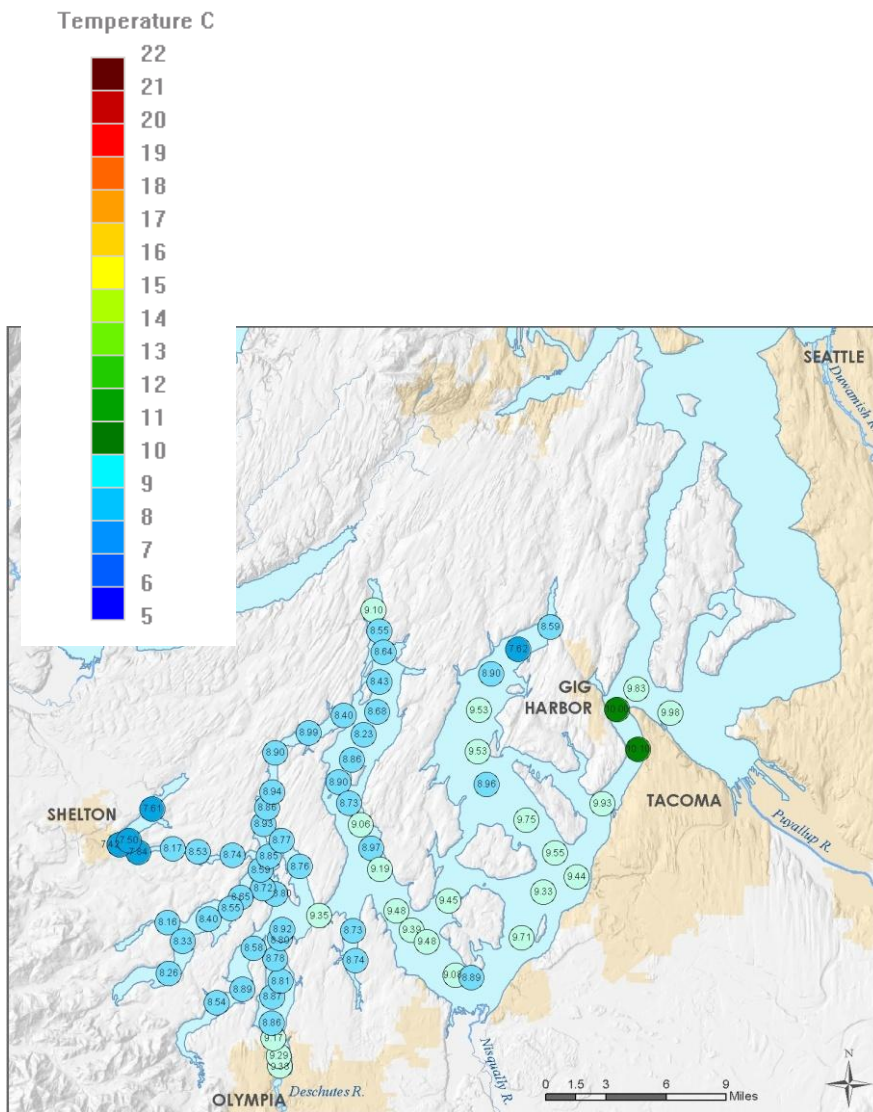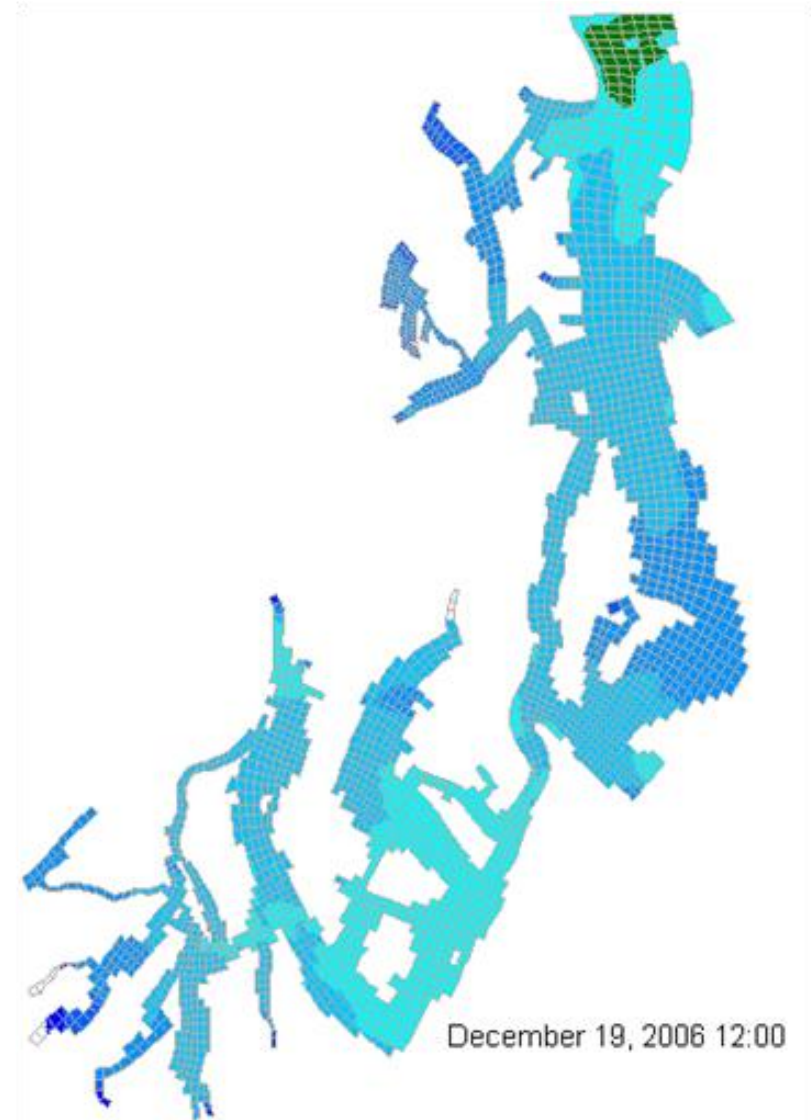
Figure 23. (a) Field observations (December 18-21, 2006) of near-surface temperature (°C) compared with (b) model output (December 19, 2006).
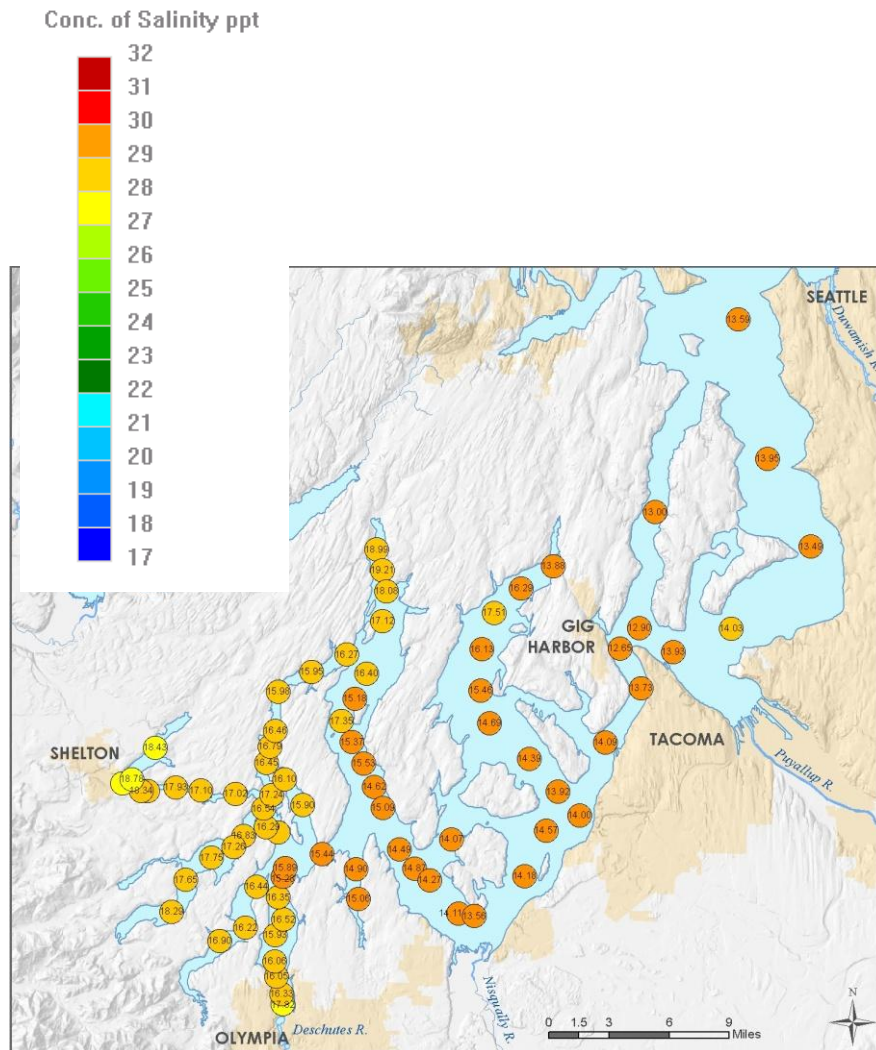
Figure 24. (a) Field observations (July 31 – August 3, 2006) of near-surface salinity (PSU) compared with (b) model output (August 1, 2006).
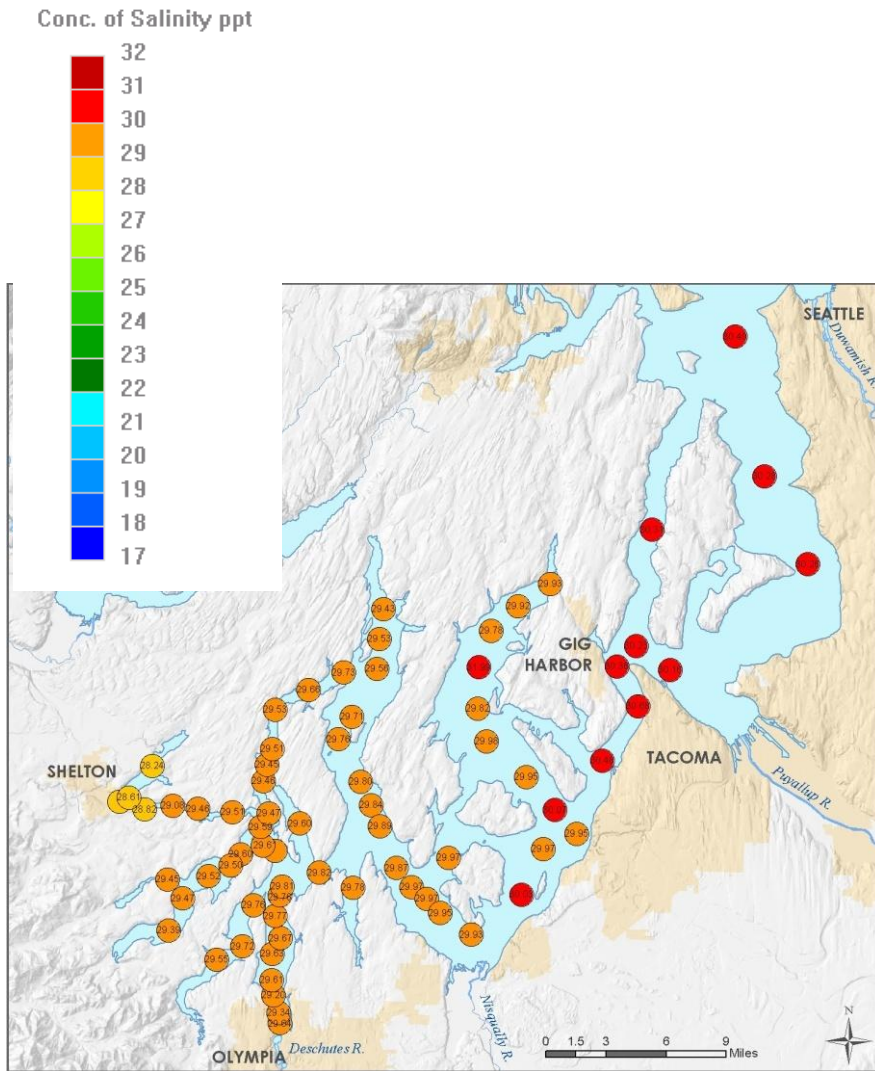
Figure 25. (a) Field observations (September 25-29, 2006) of near-surface salinity (PSU) compared with (b) model output (September 27, 2006).
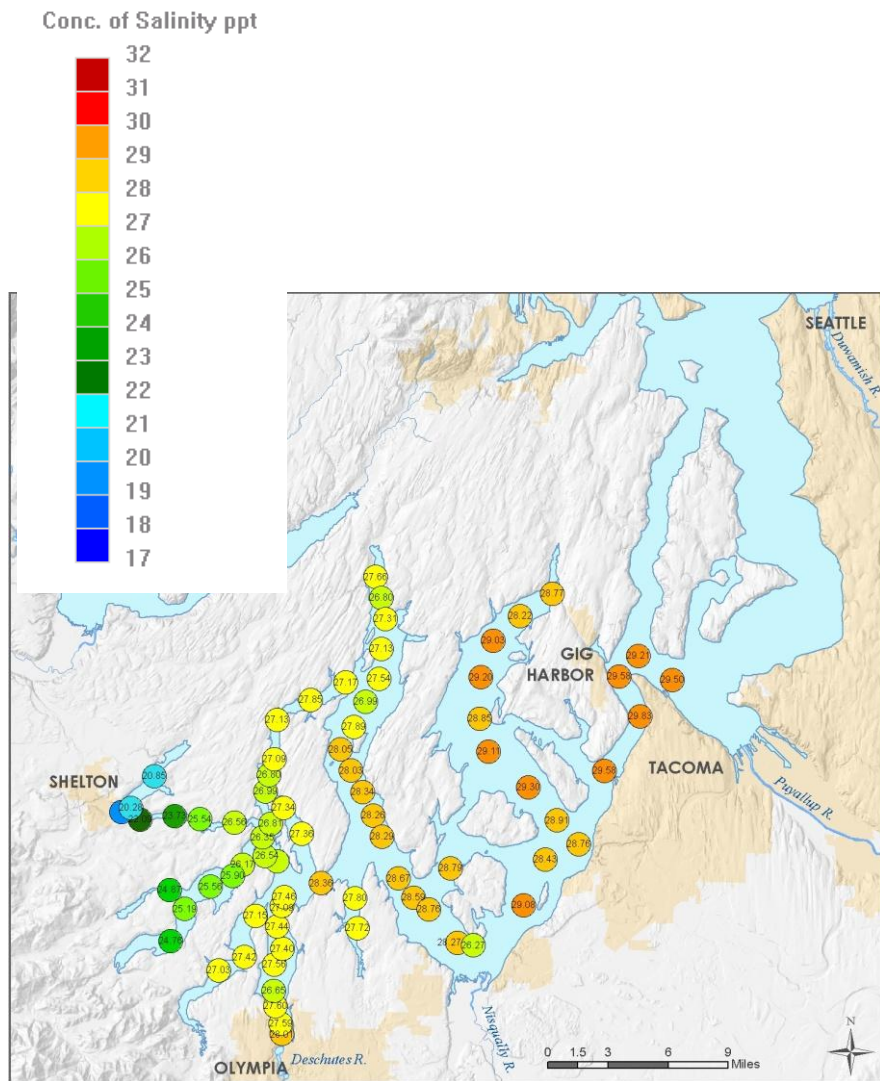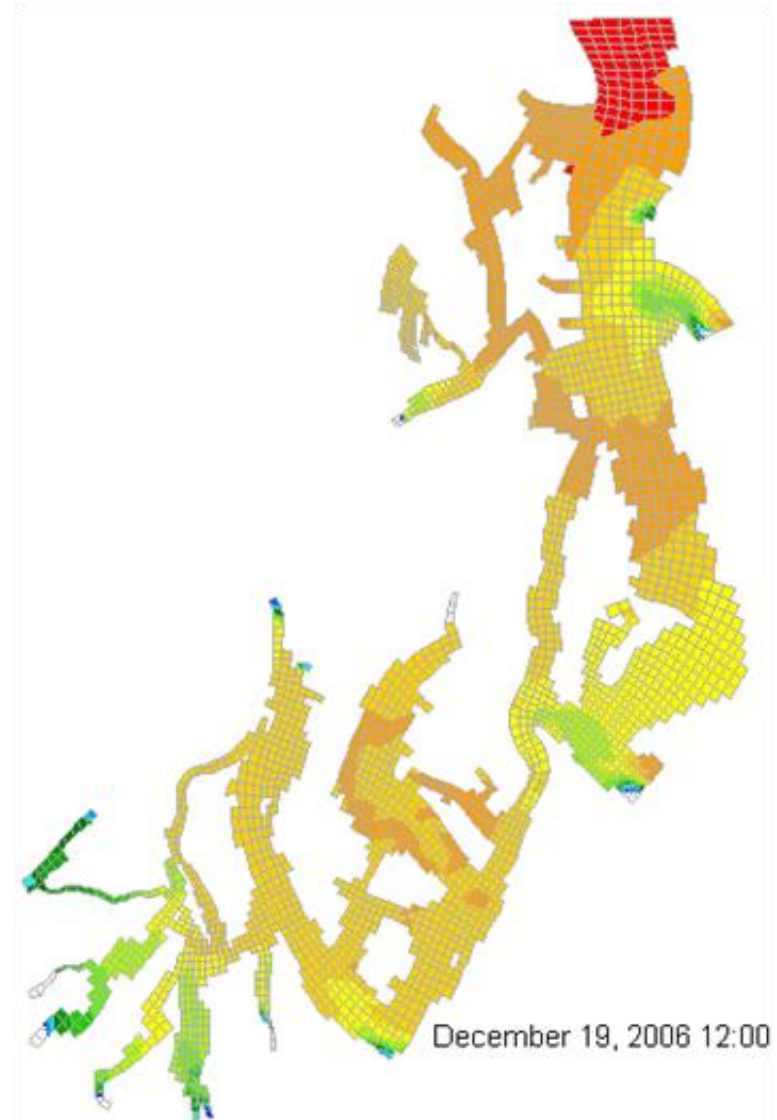
Figure 26. (a) Field observations (December 18-21, 2006) of near-surface salinity (PSU) compared with (b) model output (December 19, 2006).

Confirmation with 2007 Data

Three detailed cruises during the confirmation period represent spring, early summer, and late-summer 2007 conditions. April 2007 surface temperatures in Figure 27 remain cool throughout the model domain. The shallow western inlets were warmer than other areas, and the coolest waters were around the Tacoma Narrows and northern boundary. By June 2007, significant heating contributed to warm temperatures in the shallow western inlets in particular (Figure 28). Cool and wet summer conditions decreased surface temperatures by September 20077 (Figure 29). The model captures the temperature patterns and magnitudes.

The model also predicts surface salinity patterns and magnitudes well for the confirmation period. The April 2007 predictions and data in Figure 30 show continuing freshened conditions, particularly near freshwater sources. Similarly, the June 2007 cruise data and model predictions both show similar patterns, with surface salinities (Figure 31) generally dominated by freshwater inflows with continued high discharge rates. By September 2007, cruise data and model predictions show higher and more uniform values than in June throughout South and Central Puget Sound except for limited areas near freshwater inflows where no cruise data are available to corroborate. Overall patterns and magnitudes are reasonable. The model predicts 1 to 3 psu fresher conditions than in the data for the surface layer, partly because the cruises did not include shallow areas nearest the freshwater inflows.

In summary, cruise data corroborate the predicted surface temperatures and salinities within South and Central Puget Sound. The surface values are more difficult to simulate than near-bottom values because they reflect meteorology and river inflow boundary conditions that change significantly over time. The seasonal shifts are appropriately represented by the model, and the spatial patterns are well characterized.
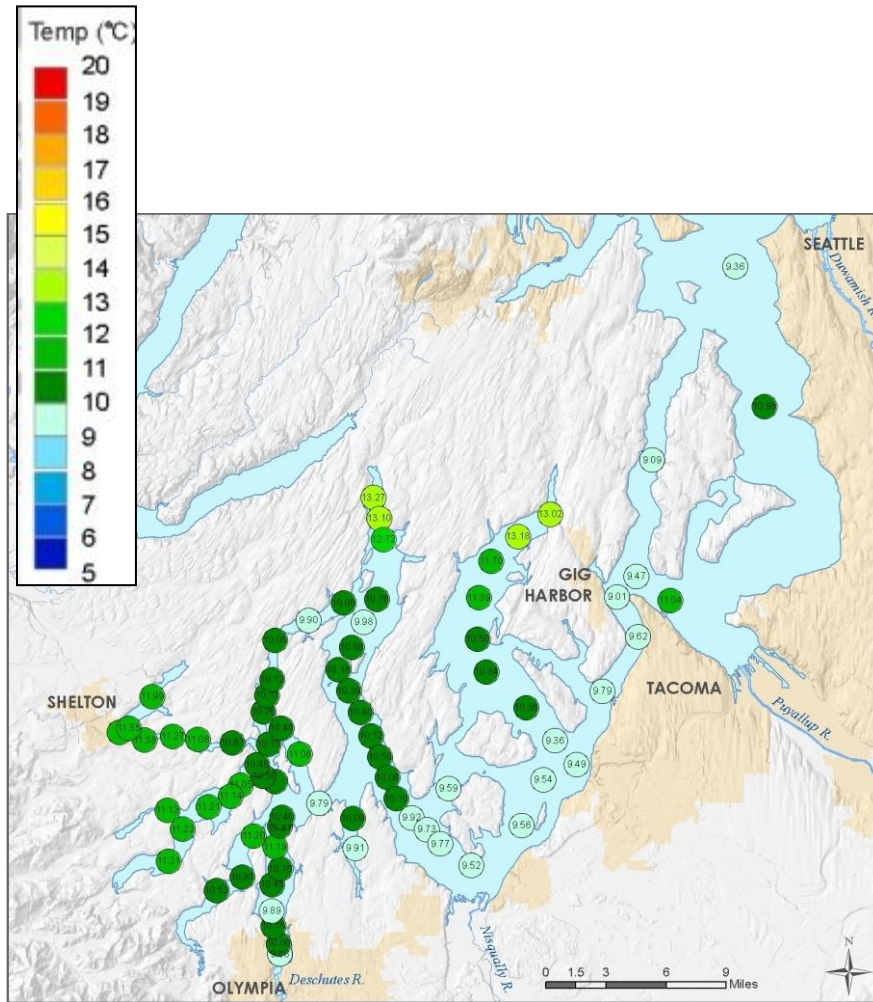
Figure 27. (a) Field observations (April 23-26, 2007) of near-surface temperature (°C) compared with (b) model output (April 24, 2007).
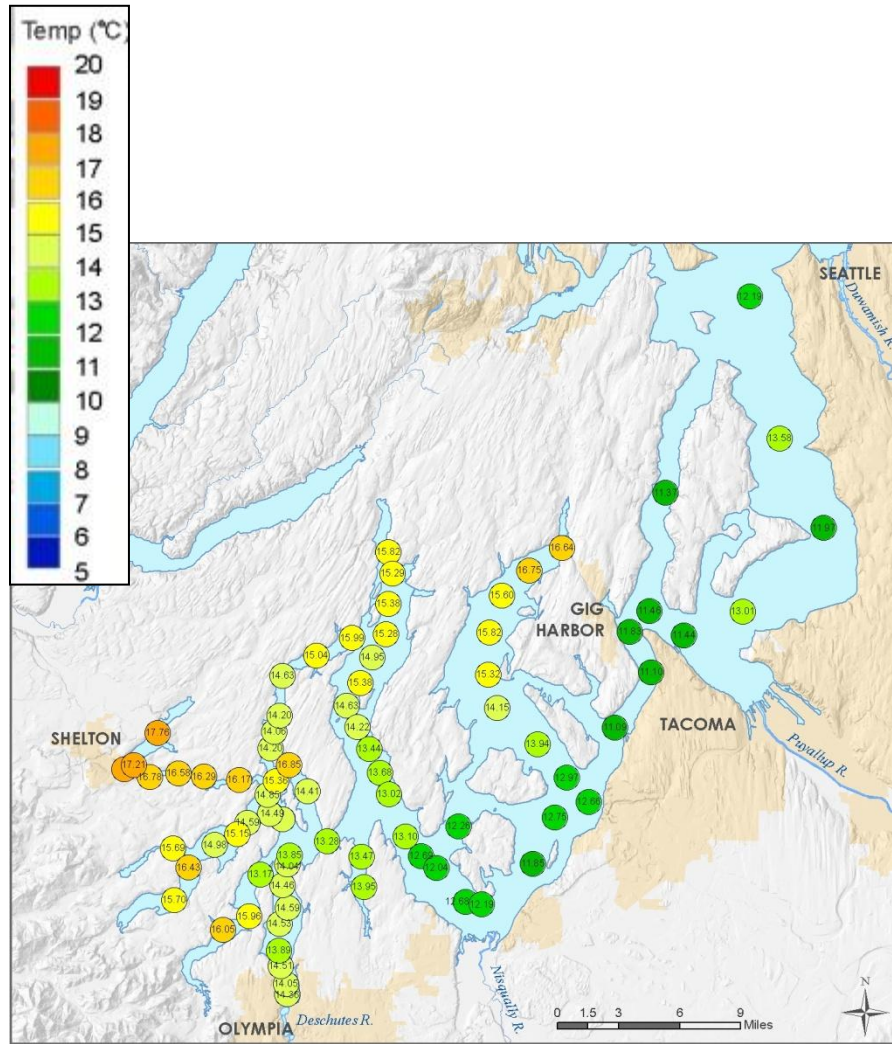
Figure 28. (a) Field observations (June 25-29, 2007) of near-surface temperature (°C) compared with (b) model output (June 27, 2007).

Figure 29. (a) Field observations (September 24-27, 2007) of near-surface temperature (°C) compared with (b) model output (September 25, 2007).
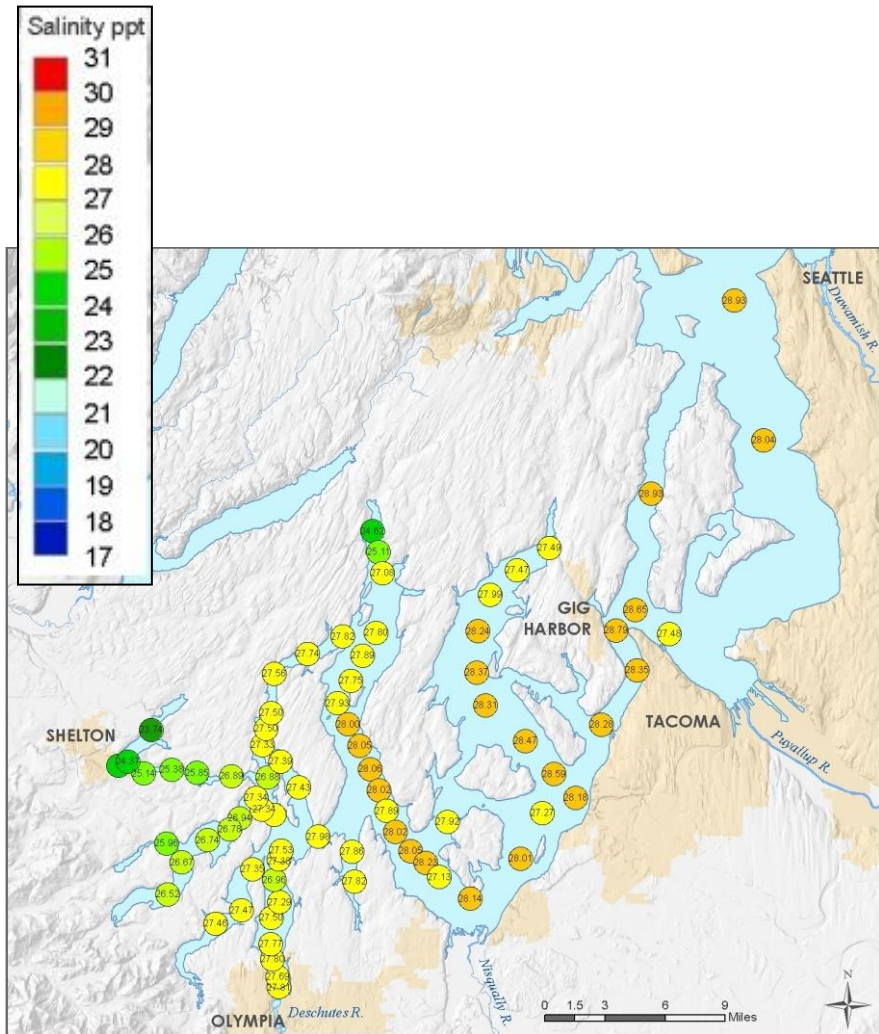
Figure 30. (a) Field observations (April 23-26, 2007) of near-surface salinity (PSU) compared with (b) model output (April 24, 2007).
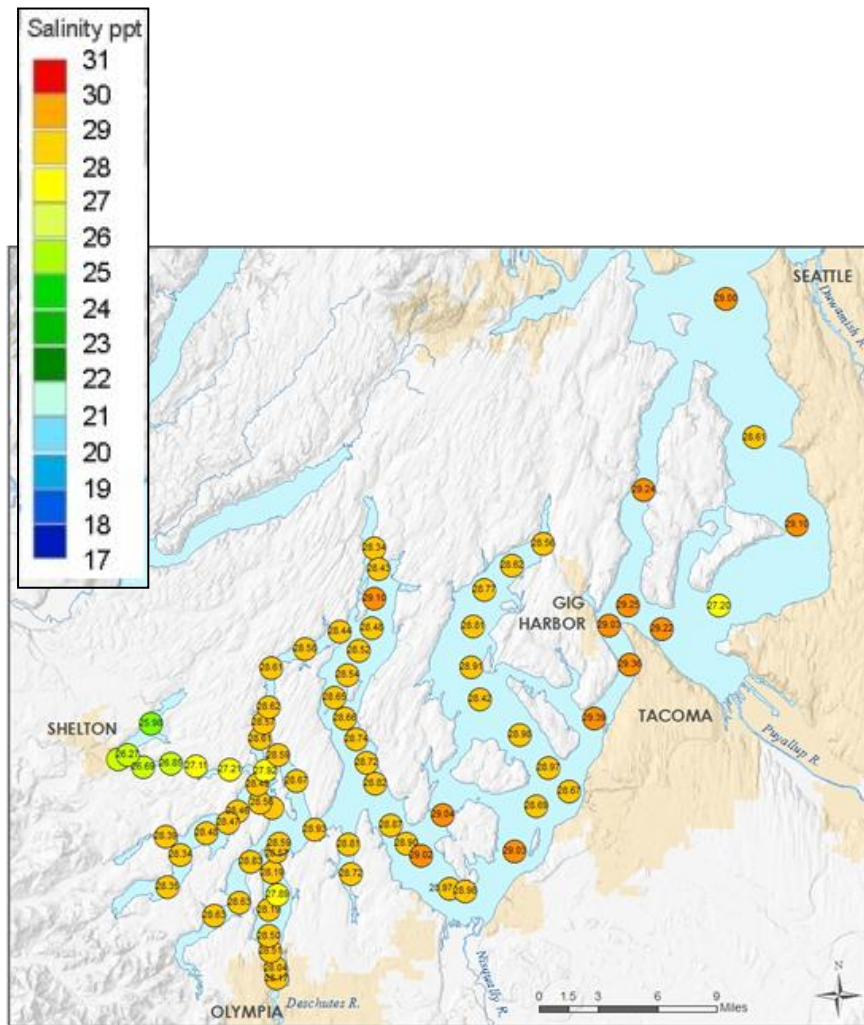
Figure 31. (a) Field observations (June 25-29, 2007) of near-surface salinity (PSU) compared with (b) model output (June 27, 2007).
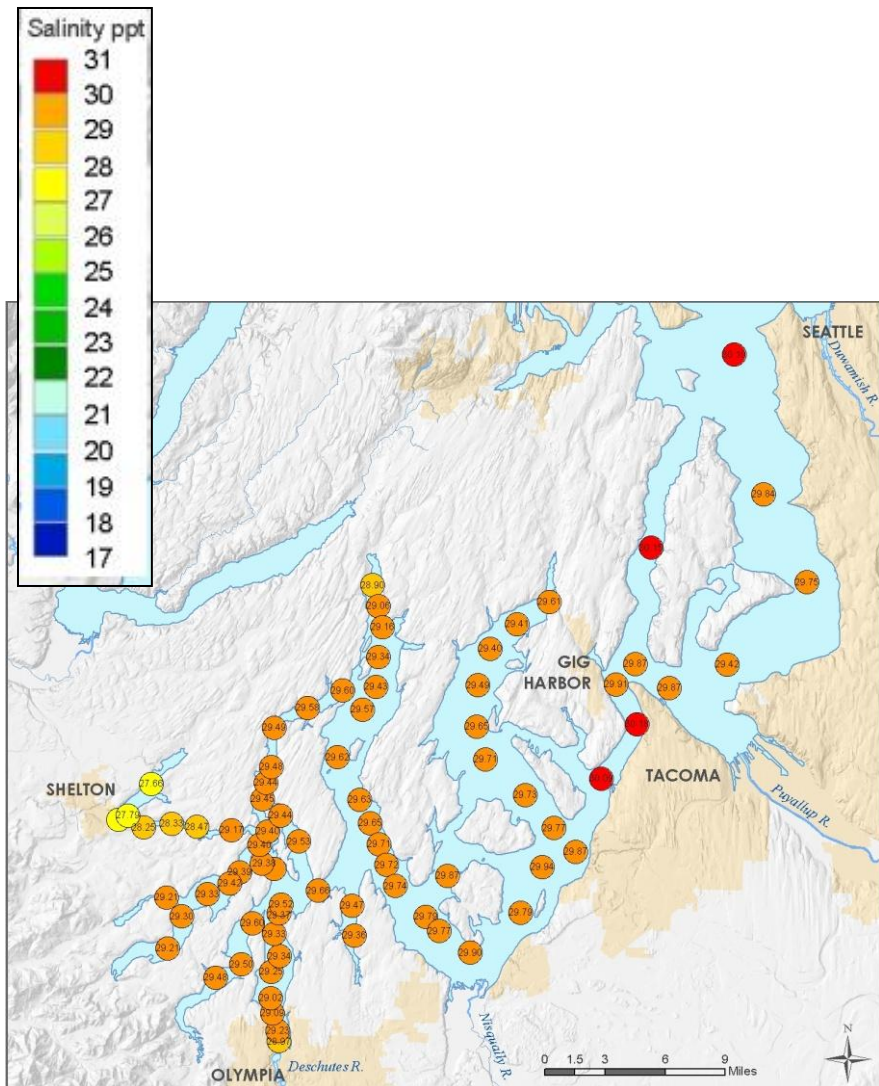
Figure 32. (a) Field observations (September 24-27, 2007) of near-surface salinity (PSU) compared with (b) model output (September 25, 2007).

Time Series for Surface and Near Bottom Temperature and Salinity

In addition to the spatial patterns in surface temperature and salinity, we also compared surface and near-bottom temperature and salinity time series at 22 stations (Figure 33).
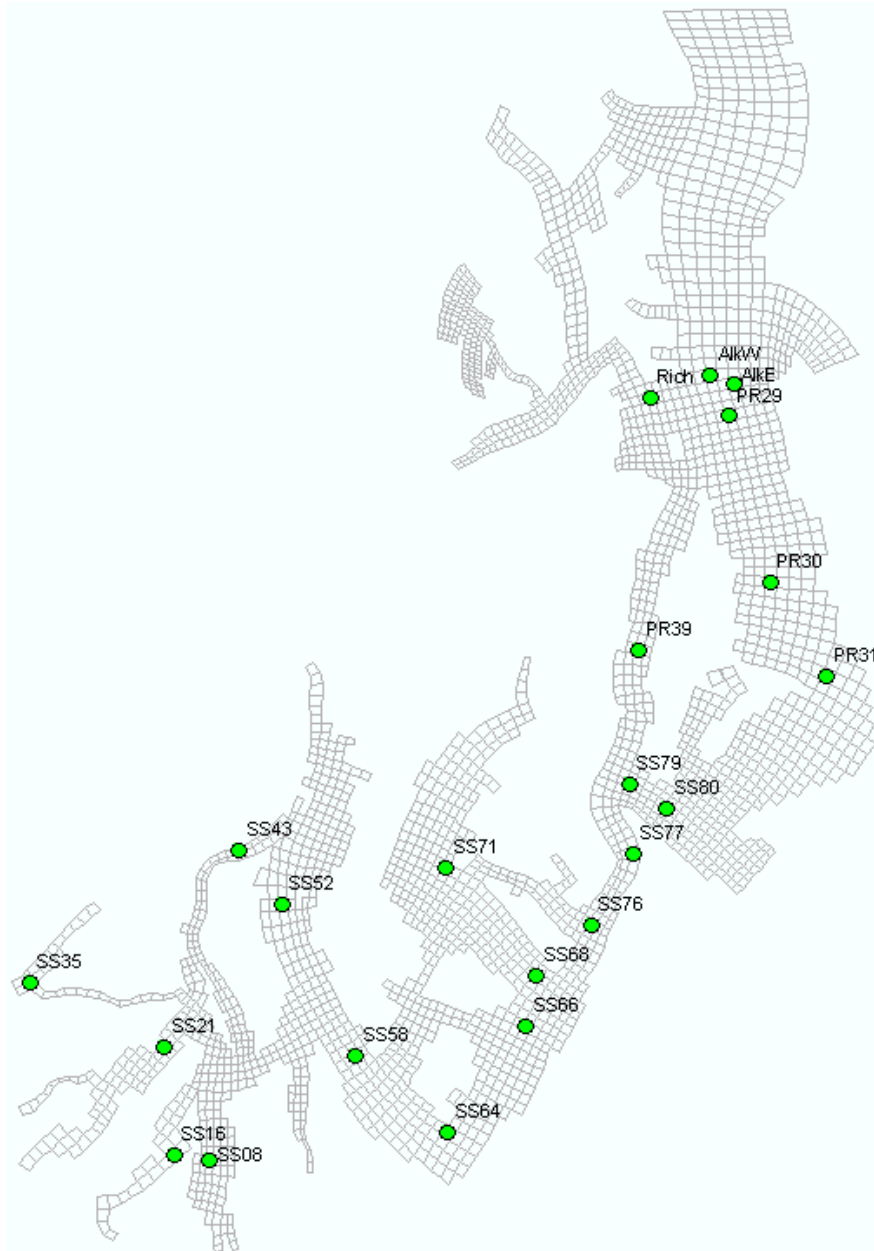
Figure 33. Stations used to compare salinity and temperature between the model and measured data.

Calibration to 2006 Data

To confirm that the model captures temporal patterns in both temperature and salinity, we compared model predictions to measured values throughout the calibration period. The surface values exhibit much greater variability than the near-bottom values, but both are important to describing the density structure.

Temperatures predicted for the northern region exhibit the seasonal patterns of warming through summer and cooling into the winter months (Figure 34). The near-bottom conditions do not vary as much as the surface waters. Surface temperature RMSEs range from 0.8°C to 1.8°C, with warmer peak temperatures predicted. Salinity values generally rise in the summer months before exhibiting episodic freshening of the surface waters with fall storm events (Figure 35). The Alki East and PR29 stations in particular show significant freshwater influences in November and December, associated with large rain events. Near-bottom salinity gradually rises through September and gradually declines with fall storms. The model produces salinity RMSEs of <0.6 psu at all but Alki West, which had RMSEs of 0.9 psu near the surface and 0.2 psu near the bottom.

The central model domain, including the area within and adjacent to the Tacoma Narrows, also exhibits typical seasonal warming and cooling (Figure 36). RMSEs in the near-surface values are comparable to those in the northern part of the model domain, and only Carr Inlet had a RMSE >1°C. The highest temperatures measured at SS71 in central Case Inlet were underpredicted by the model; measured temperatures at nearby stations were not as high. Surface temperatures predicted at stations within the Tacoma Narrows (SS76, SS77, and SS79) exhibit much greater subdaily variability than at other stations within the model domain and likely reflect lateral and vertical mixing phenomenon within the Narrows.

Salinity in the central domain surface layer also reflects increased freshwater discharges in the fall and winter months (Figure 37). Puyallup River water decreases surface salinity at stations SS80 and SS79, but other central domain stations also show decreased surface salinity. Near-bottom salinity values are more constant than surface values but do reflect seasonal freshening.

South of the Tacoma Narrows, the model predictions for surface and near-bottom track the seasonal variability in temperature (Figure 38) and salinity (Figure 39) well. Due to the shallow water depths, the summer temperatures are warmer and winter temperatures cooler at these stations than further north in the model domain. Near-bottom salinities had RMSEs <0.6 psu, but surface salinities in Budd Inlet were higher as the model predicted lower salinity than measured. From previous modeling efforts (Roberts et al., 2008), the plume from the Deschutes River and Capitol Lake travels northward on the east side of the inlet due in part to the Budd Inlet gyre, but surface salinity (Figure 26) suggests it spreads out across the inlet in this model. The grid scale may not resolve this feature, and the model predicts that Deschutes River/Capitol Lake influences surface salinity at station SS08.

During the 2006 calibration period, temperature RMSEs averaged 0.7°C, with lower RMSEs near the bottom (0.5°C) and near the Tacoma Narrows (0.6°C). Salinity RMSEs averaged 0.5 psu, with lowest values near the bottom (0.4 psu) and near the northern boundary (0.3 psu).
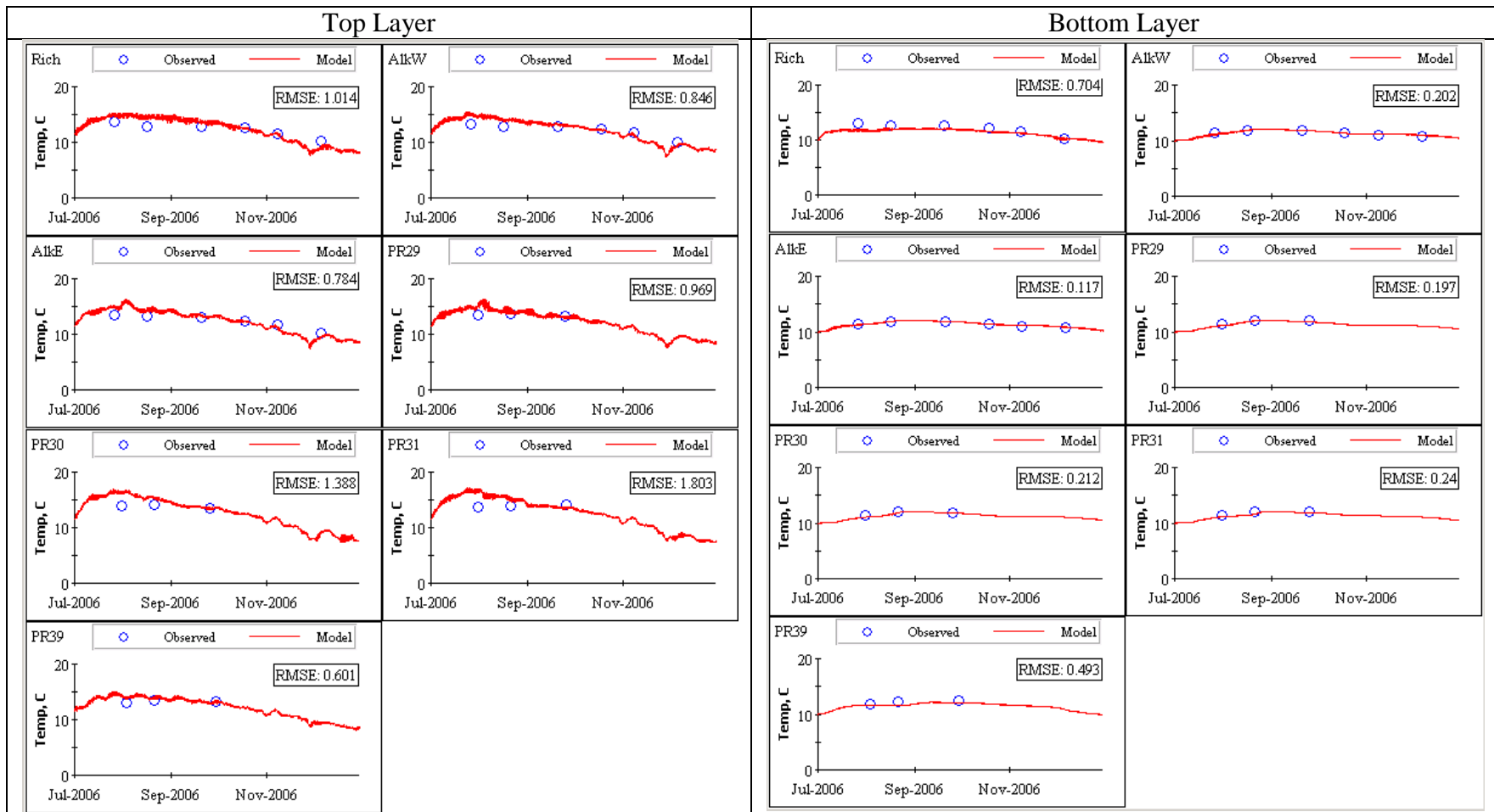
Figure 34. Observed and predicted temperature in the northern model domain (north of Vashon Island) during the 2006 calibration period.
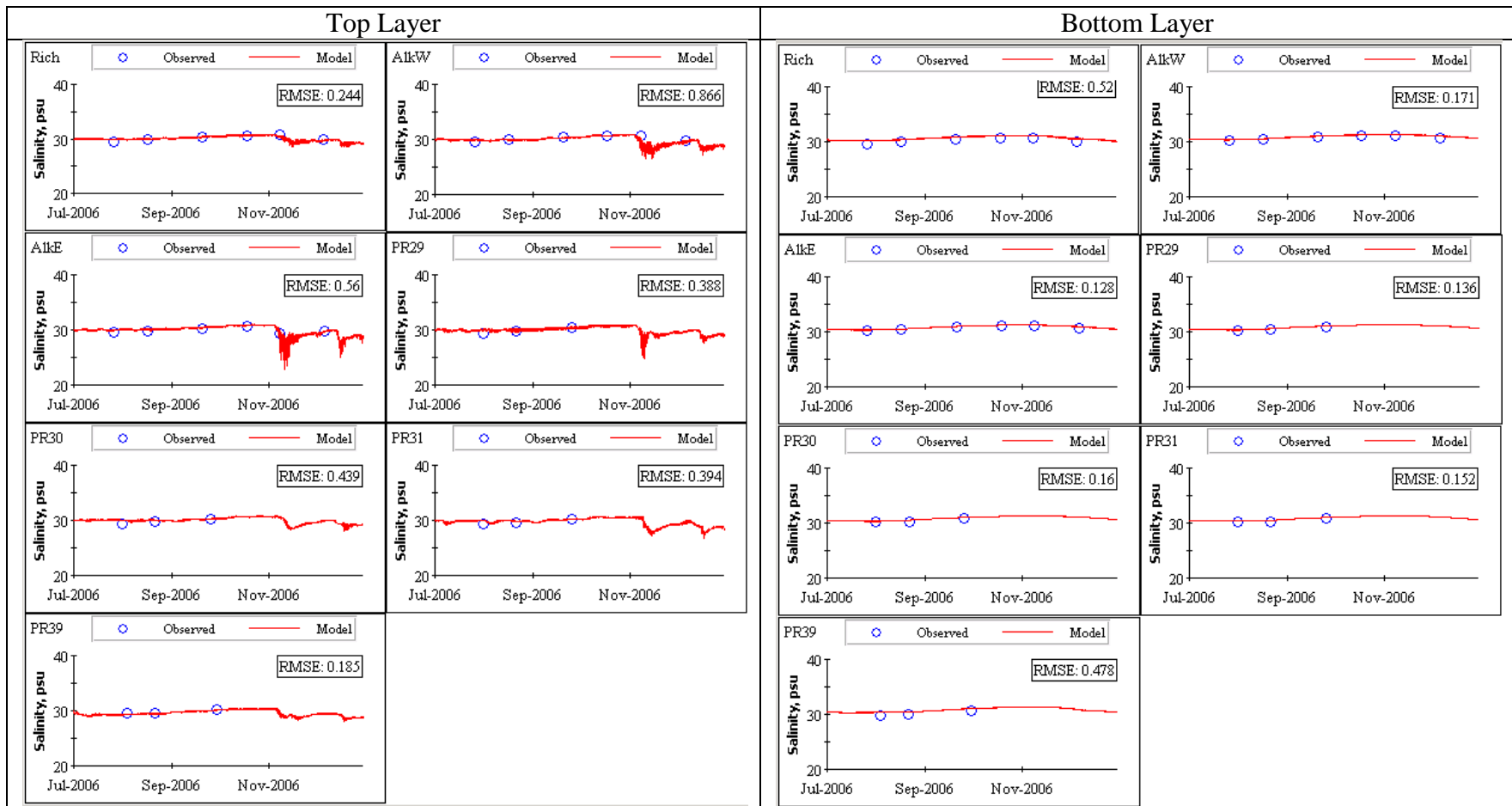
Figure 35. Observed and predicted salinity in the northern model domain (north of Vashon Island) during the 2006 calibration period.
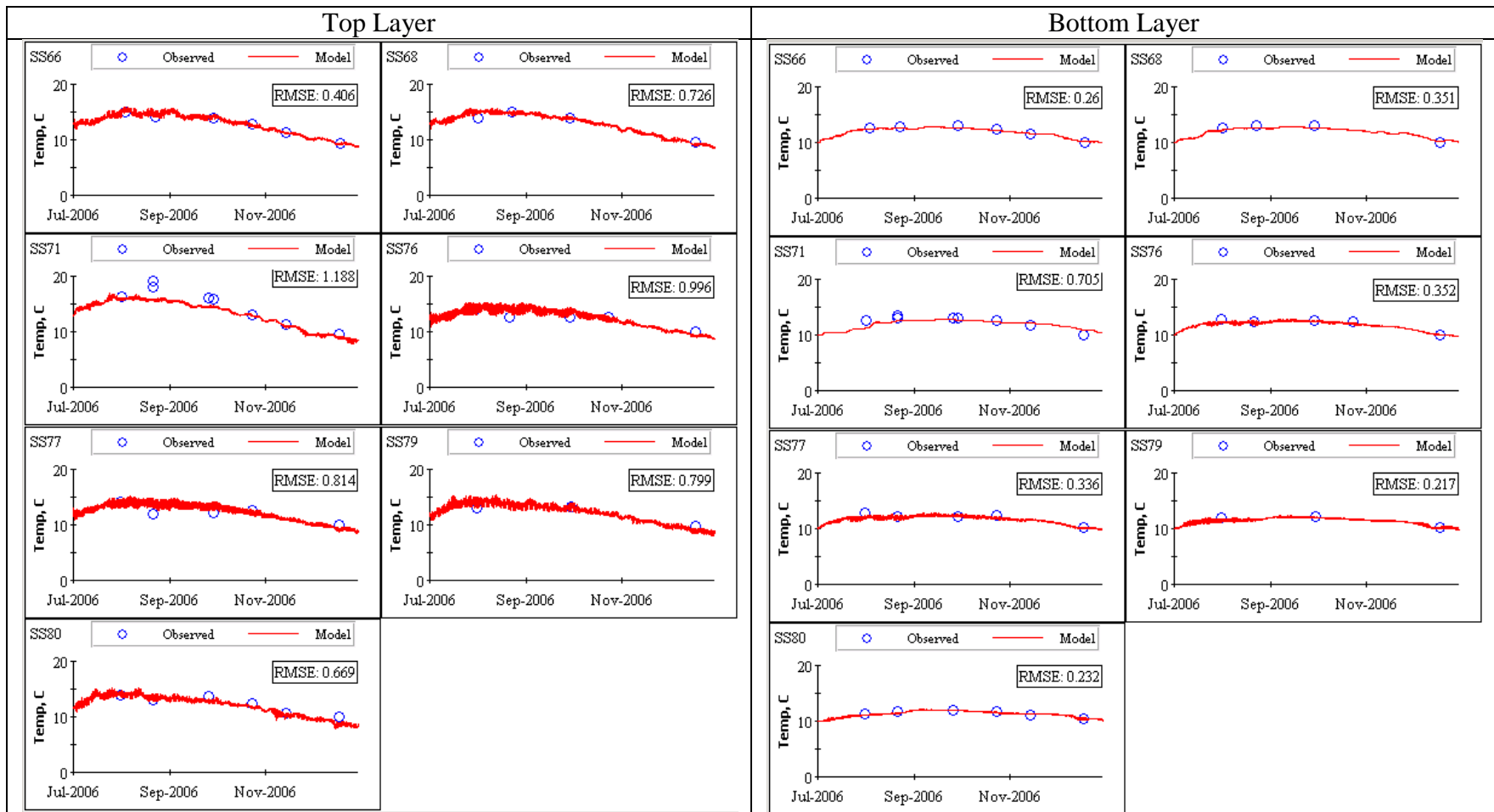
Figure 36. Observed and predicted temperature in the central model domain (Commencement Bay and Tacoma Narrows) during the 2006 calibration period.
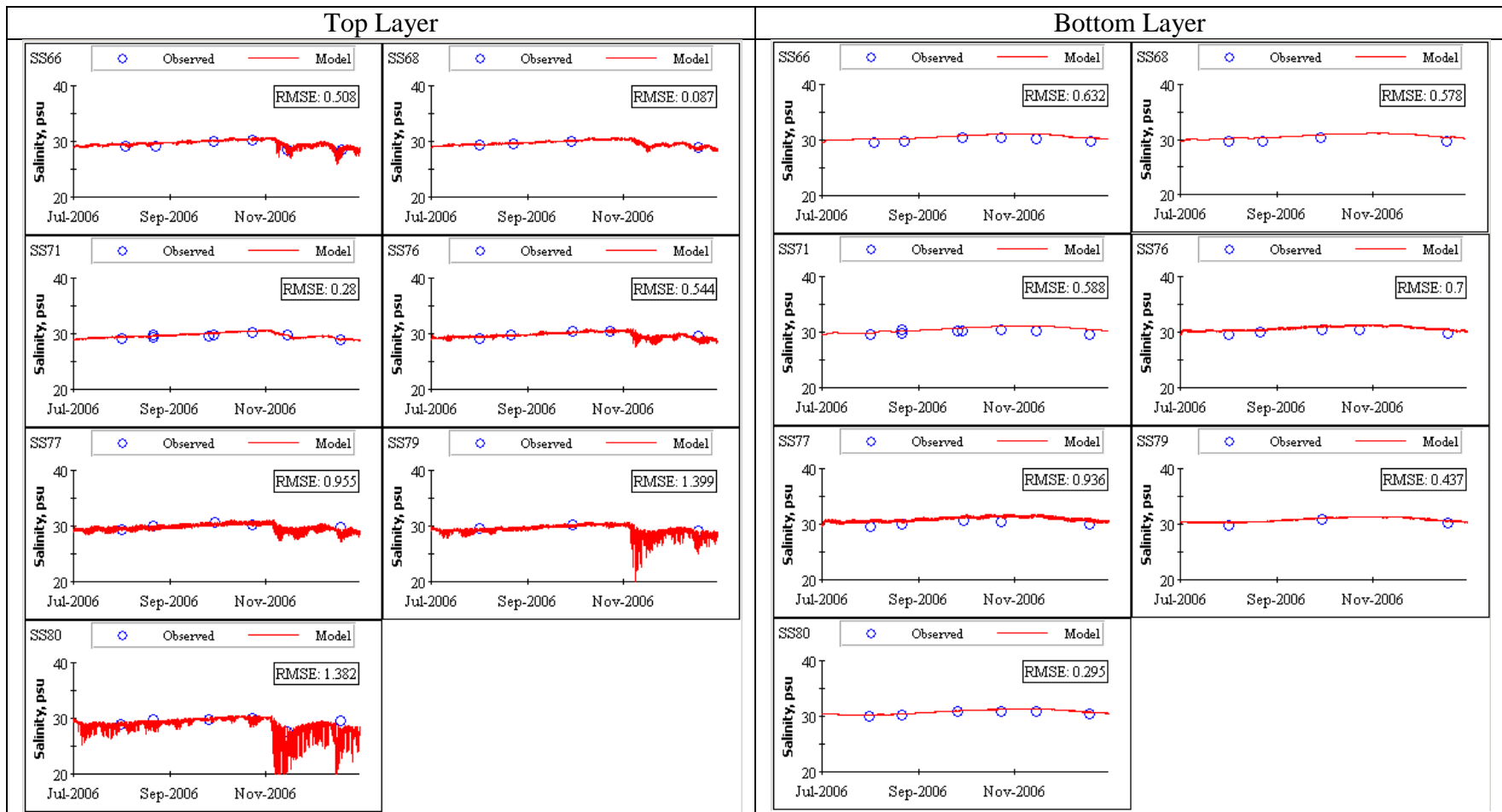
Figure 37. Observed and predicted salinity in the central model domain (Commencement Bay and Tacoma Narrows) during the 2006 calibration period.
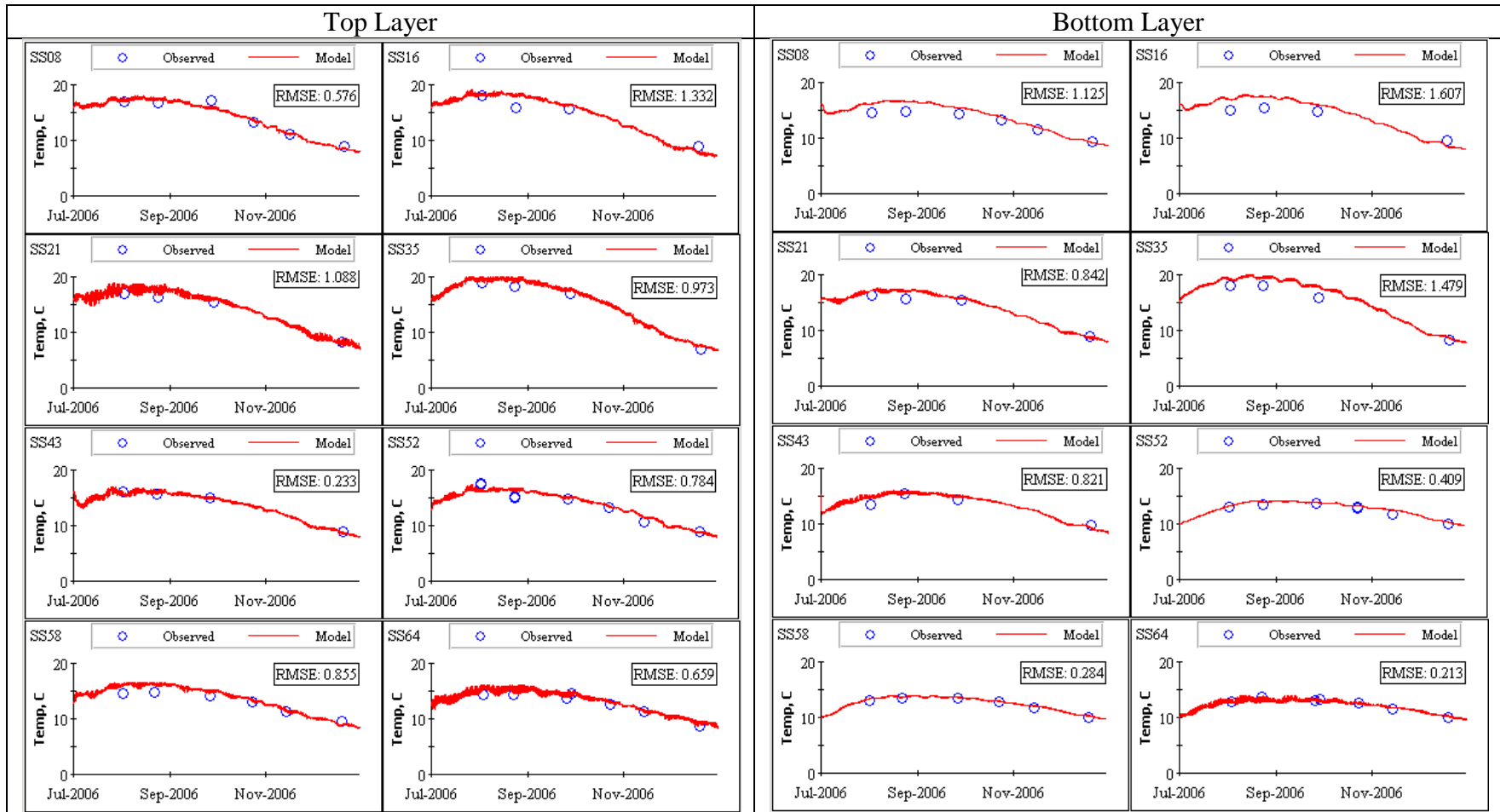
Figure 38. Observed and predicted temperature in the southern model domain (west of Tacoma Narrows) during the 2006 calibration period.
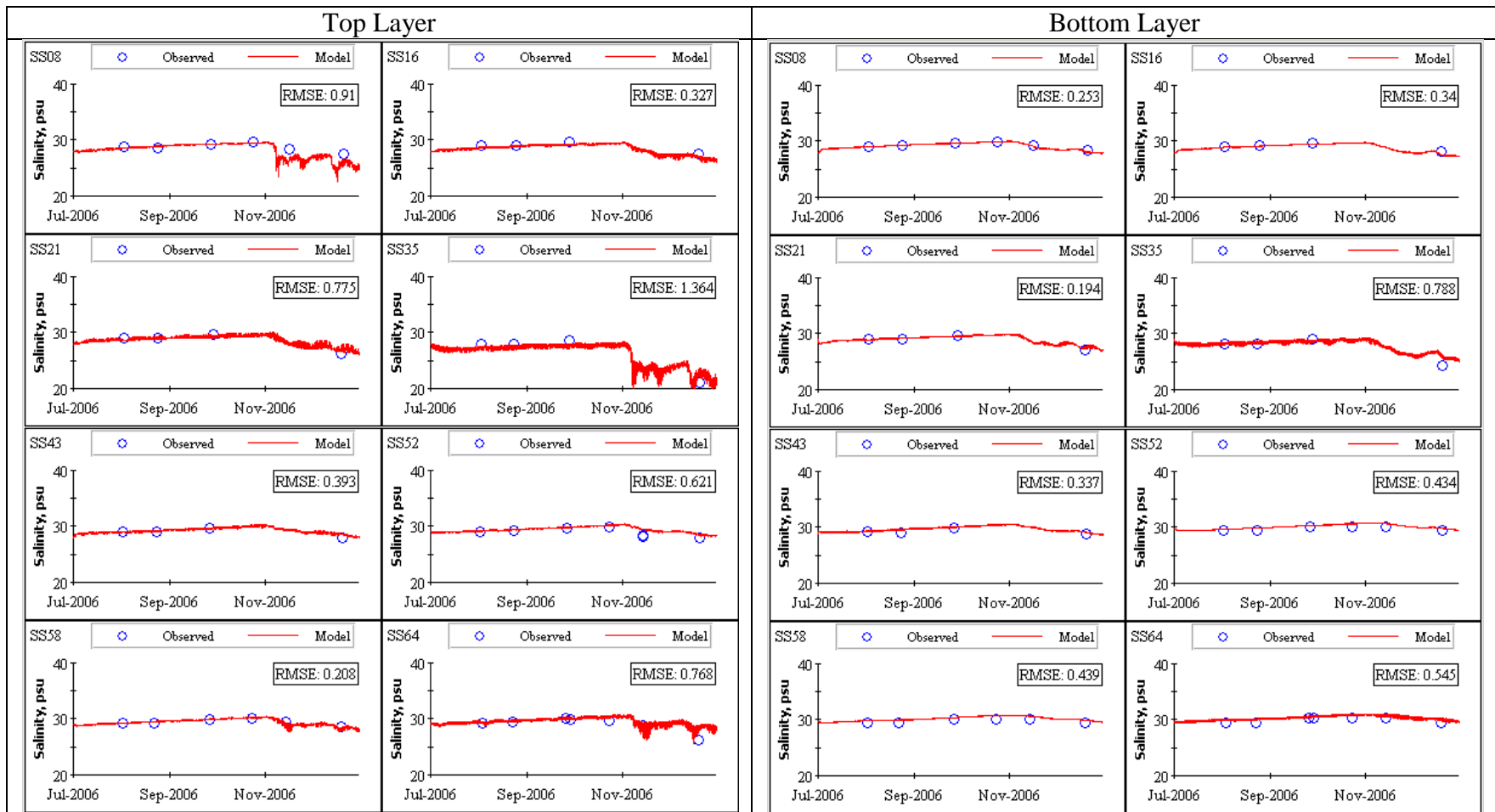
Figure 39. Observed and predicted salinity in the southern model domain (west of Tacoma Narrows) during the 2006 calibration period.

Confirmation with 2007 Data

Similar to the calibration results, the confirmation results illustrate that the model appropriately represents seasonal temperature and salinity variations throughout the model domain (Figures 40 through 45). Near-bottom conditions show less variability and RMSEs are generally lower than surface waters (0.6°C vs. 0.9°C and 0.5 psu vs. 0.6 psu, respectively). Confirmation RMSEs are similar to calibration values, and the same sites produce the highest errors (Oakland Bay, Budd Inlet, and SS71 in Case Inlet).

In summary, surface and near-bottom temperature and salinity time series are well represented by the model throughout Central Puget Sound and in the major inlets and open waters of South Puget Sound. The western inlets had greater differences between modeled and measured values, but the model appropriately captures the seasonal variation in temperature and salinity and values recorded during data collection.
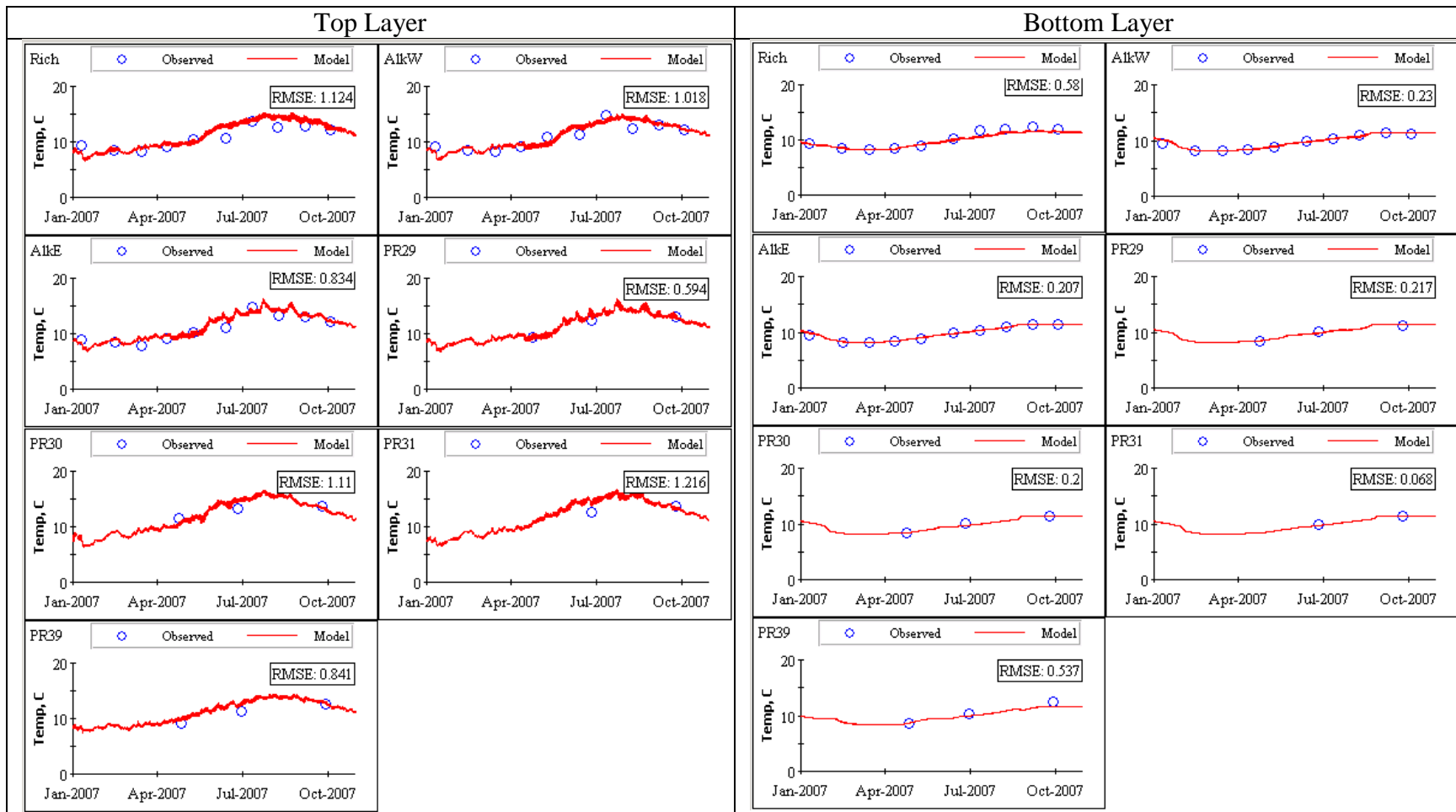
Figure 40. Observed and predicted continuous temperatures in the northern model domain (north of Vashon Island) during the 2006 calibration period.
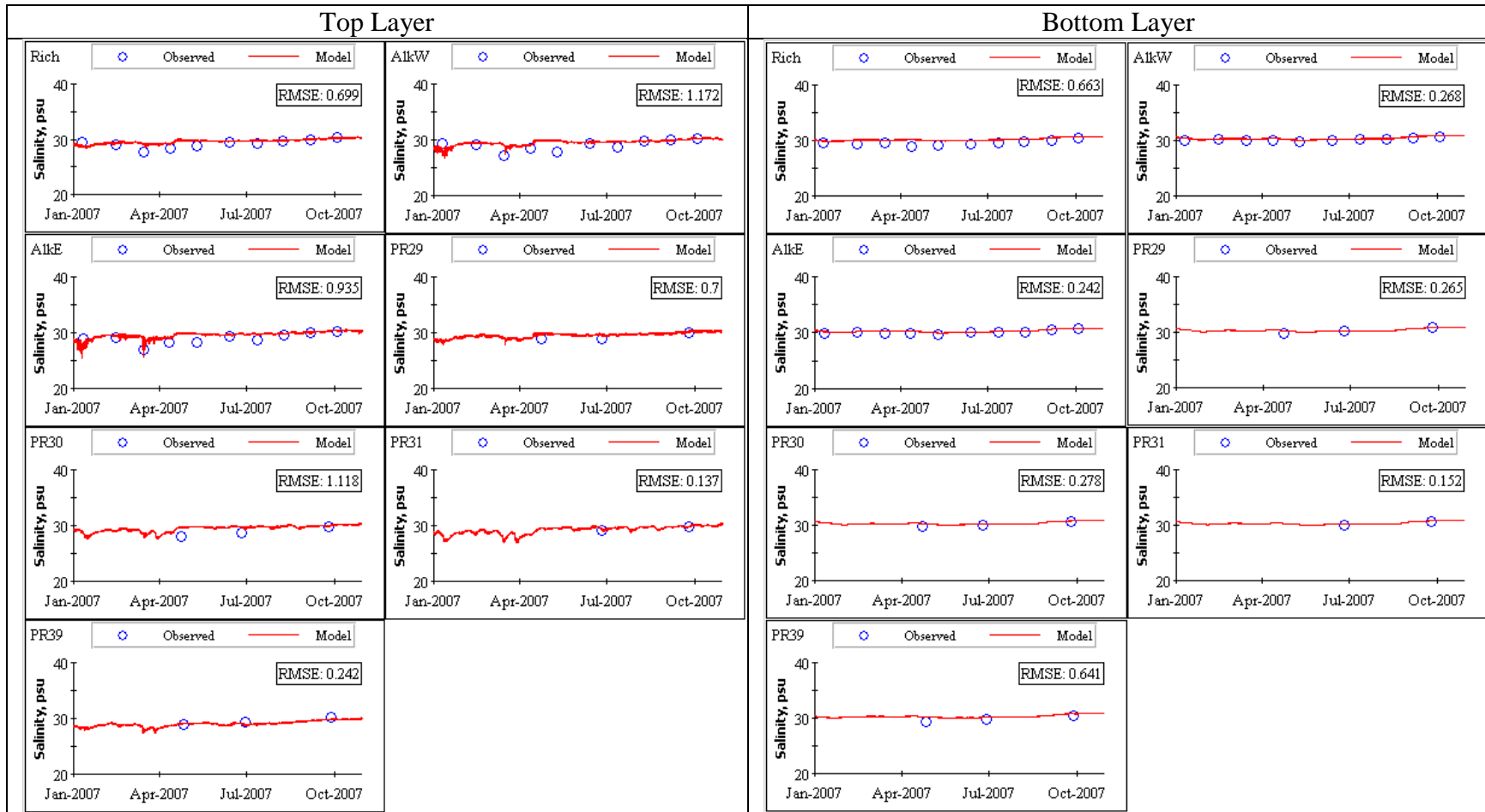
Figure 41. Observed and predicted continuous salinity in the northern model domain (north of Vashon Island) during the 2006 calibration period.
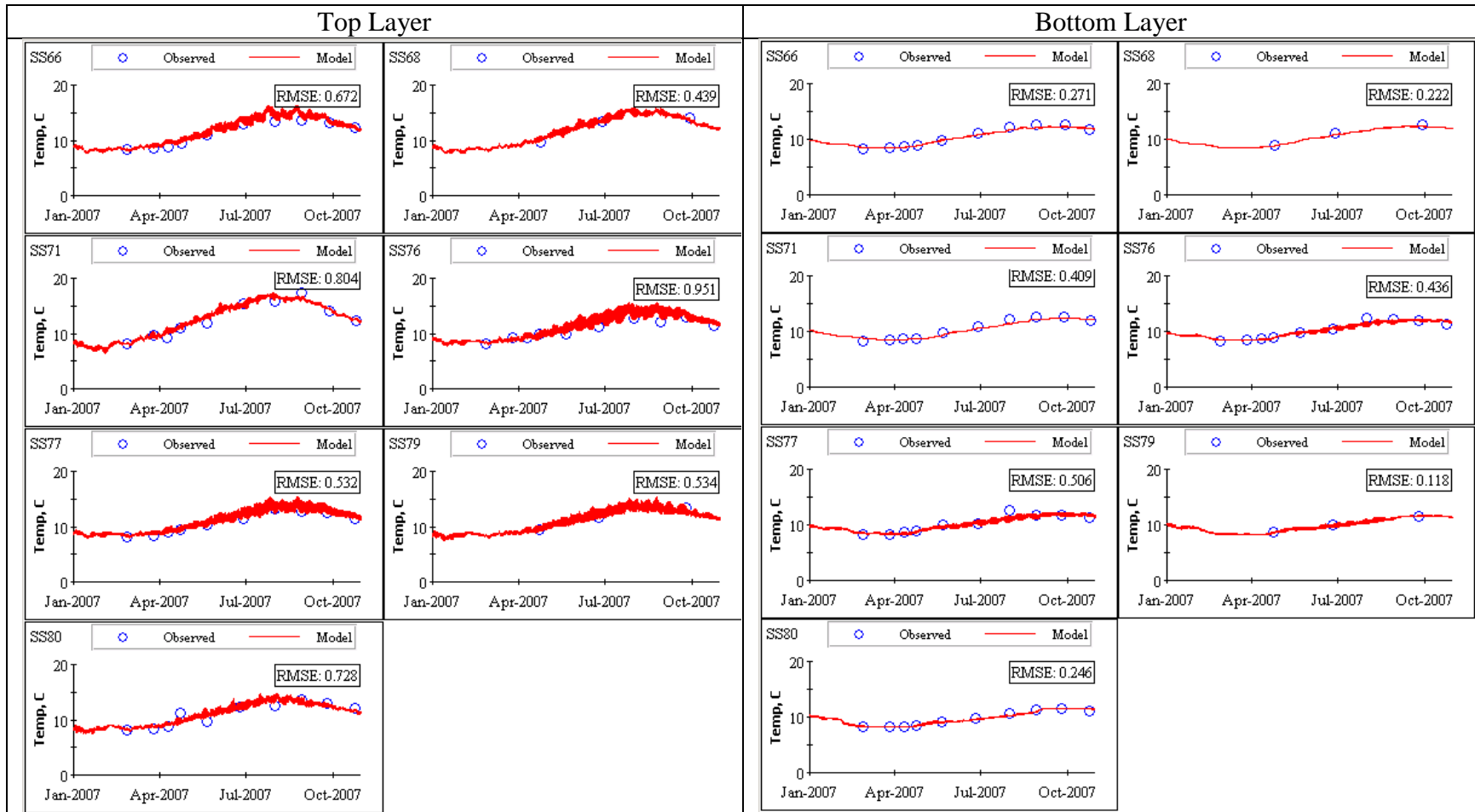
Figure 42. Observed and predicted continuous temperatures in the central model domain (Commencement Bay and Tacoma Narrows) during the 2006 calibration period.
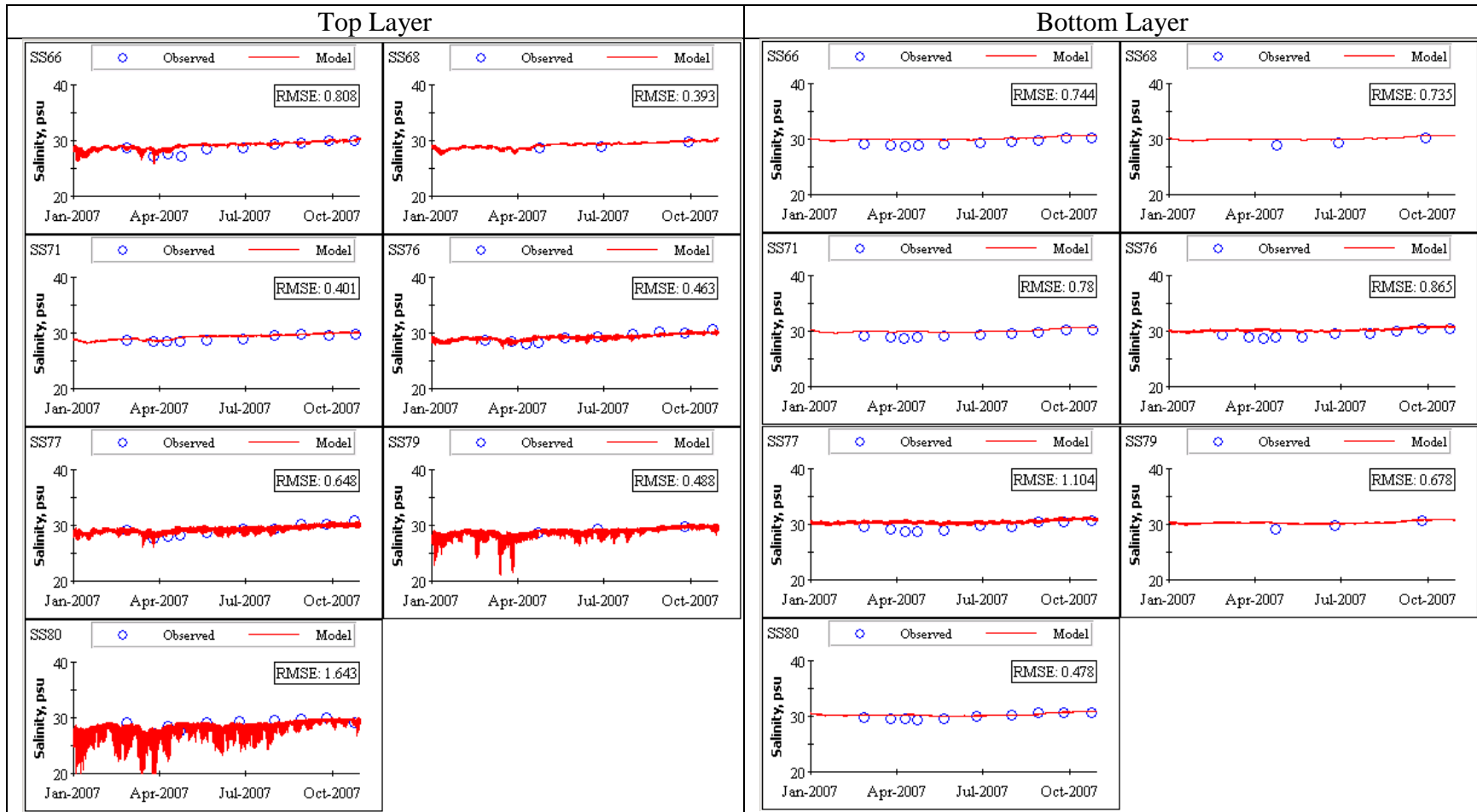
Figure 43. Observed and predicted continuous salinity in the central model domain (Commencement Bay and Tacoma Narrows) during the 2006 calibration period.
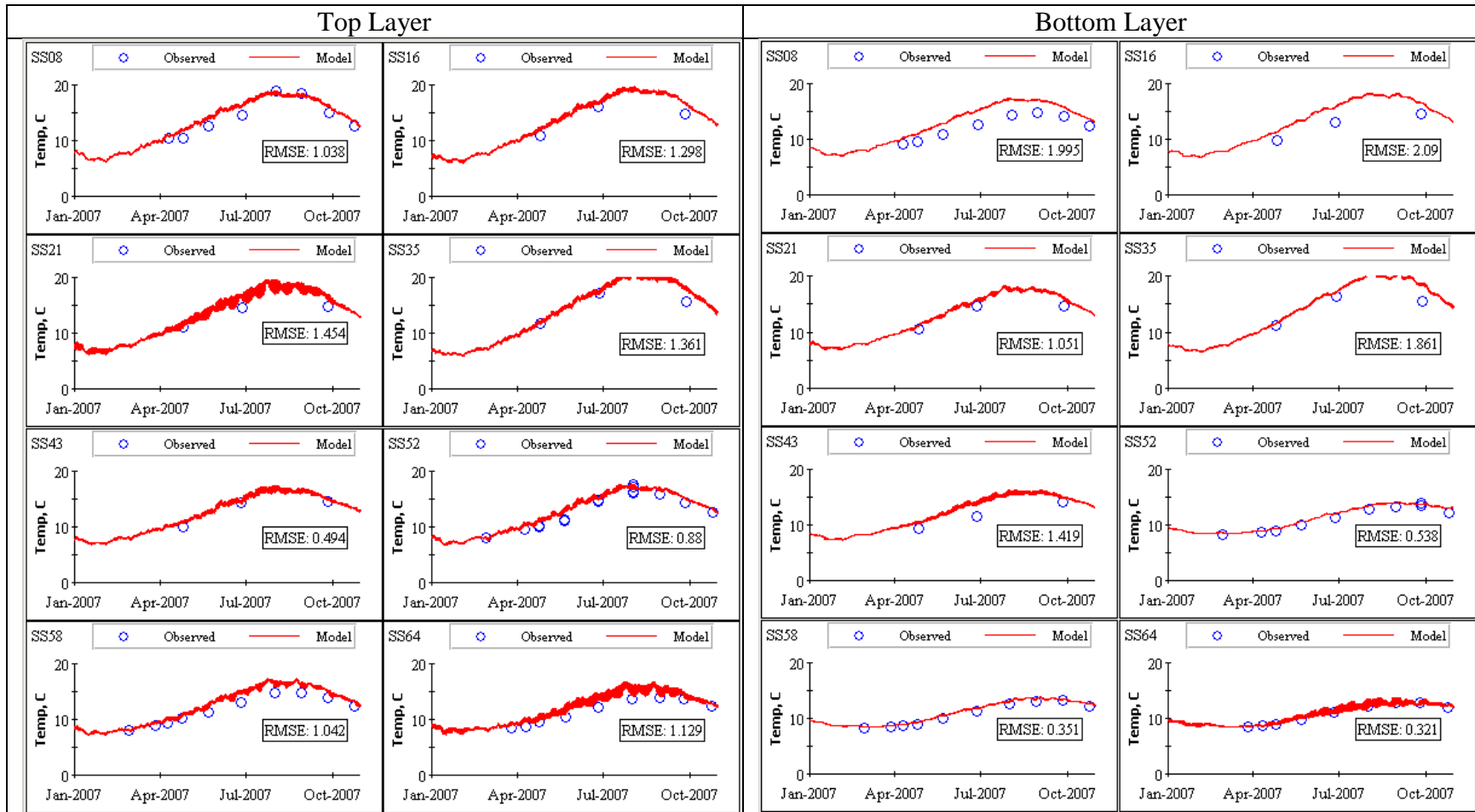
Figure 44. Observed and predicted continuous temperatures in the southern model domain (west of Tacoma Narrows) during the 2006 calibration period.
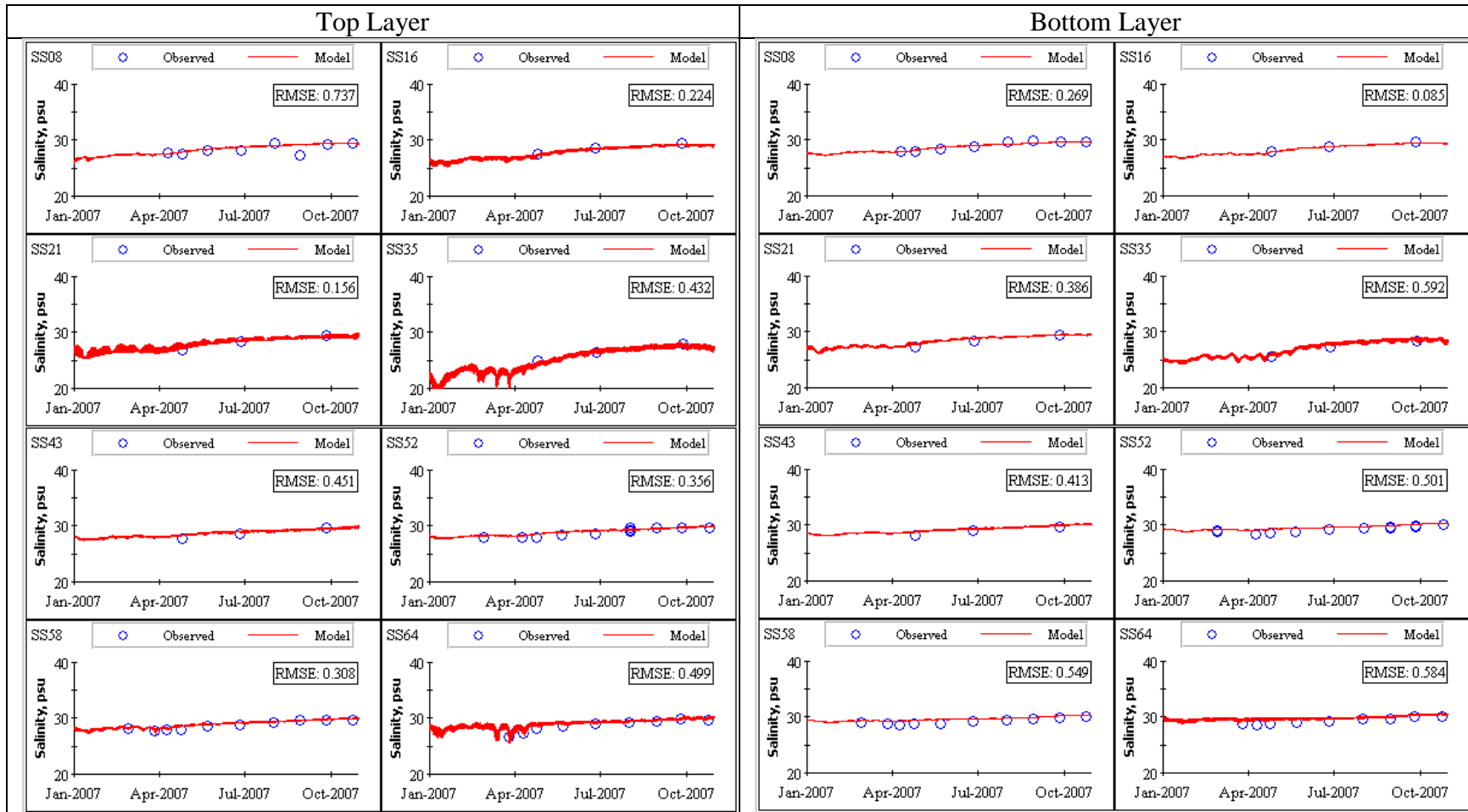
Figure 45. Observed and predicted continuous salinity in the southern model domain (west of Tacoma Narrows) during the 2006 calibration period.

Salinity and Temperature Profiles

Vertical profiles predicted by the model were compared with data collected during cruises. Details in vertical profiles indicate fine-scale stratification structures often difficult to reproduce when modeling estuarine conditions. Figure 46 identifies the profile locations used for calibration and confirmation.
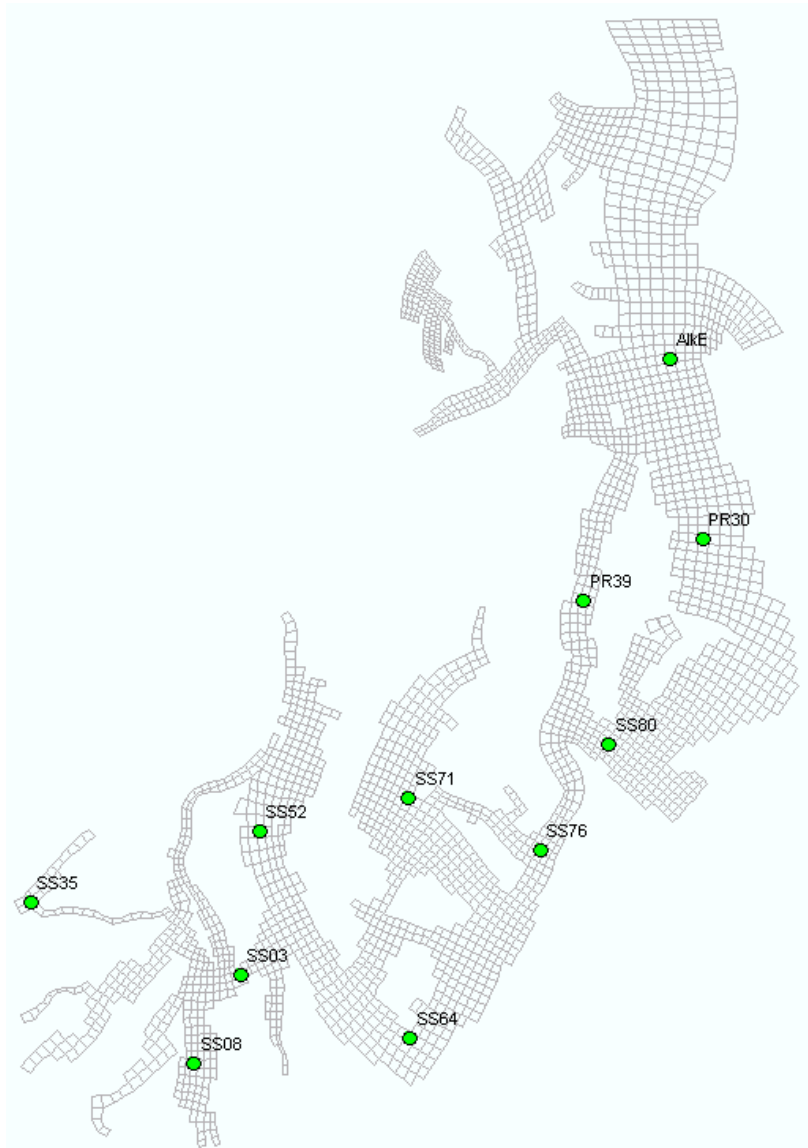
Figure 46. Locations for salinity and temperature profile comparisons between model predictions and data.

Calibration to 2006 Data

Figures 47 through 55 present temperature and salinity profiles from Central and South Puget Sound during the calibration period. RMSEs averaged 0.5°C and 0.4 psu, with lowest errors in the summer and fall and in the area nearest the northern boundary.

The Central Puget Sound profiles (Figures 47 and 48) reflect the data structure throughout the water column, including near-surface warming and freshening. However, the model is limited by the layer thickness whereas the data are recorded and reported at 0.5-m intervals. Around the Tacoma Narrows, the model predicts more freshening within 20 meters of the surface, whereas the data indicate freshening is limited to nearer the surface (November 14, 2006 in Figure 49) or little at all. The model predicts limited salinity-induced stratification at SS76 (Figure 50) until fall storms began, but data indicate a nearly uniform profile.

In South Puget Sound, the model predicts surface, water column, and near-bottom patterns and magnitudes well overall. Sharp surface temperature gradients between July and September available from the 0.5-m interval data could not be reproduced with these model layers. Near-bottom salinity was overpredicted in late fall in Carr Inlet (SS71, Figure 51). In the Nisqually Reach, summer salinity was well described through late summer and into the winter months (Figure 52). Model predicted salinity profiles in Case Inlet were good, but temperatures were over predicted throughout the water column in August (Figure 53). Oakland Bay salinity was reasonable, although temperatures were overpredicted by 1-2°C. Budd Inlet temperature profiles were the most different between model and data, but salinity profiles were reasonable through late summer. In the winter months, the model underpredicts the salinity due to the river plume.
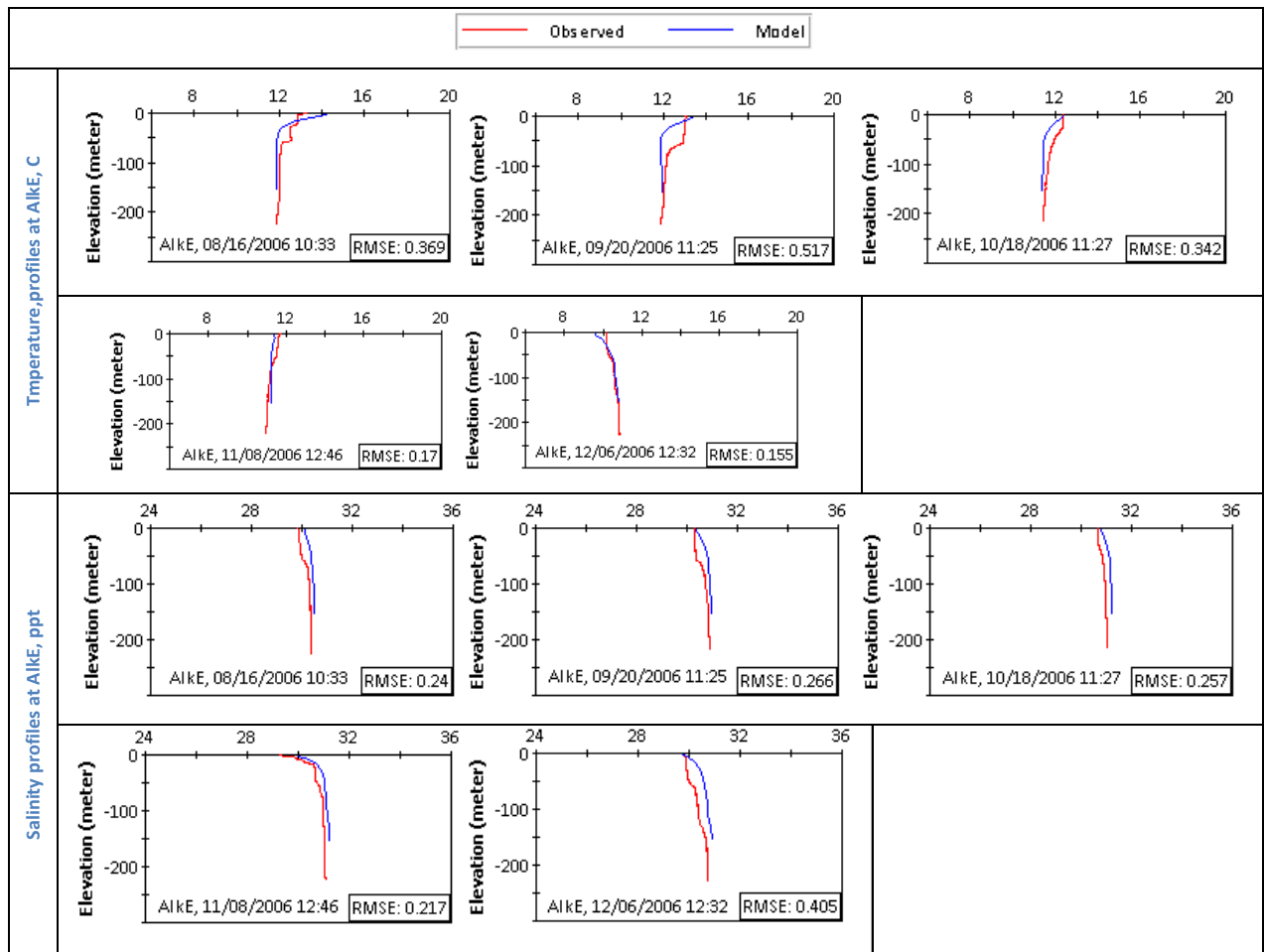
Figure 47. Temperature and salinity profile comparison at Alki East.
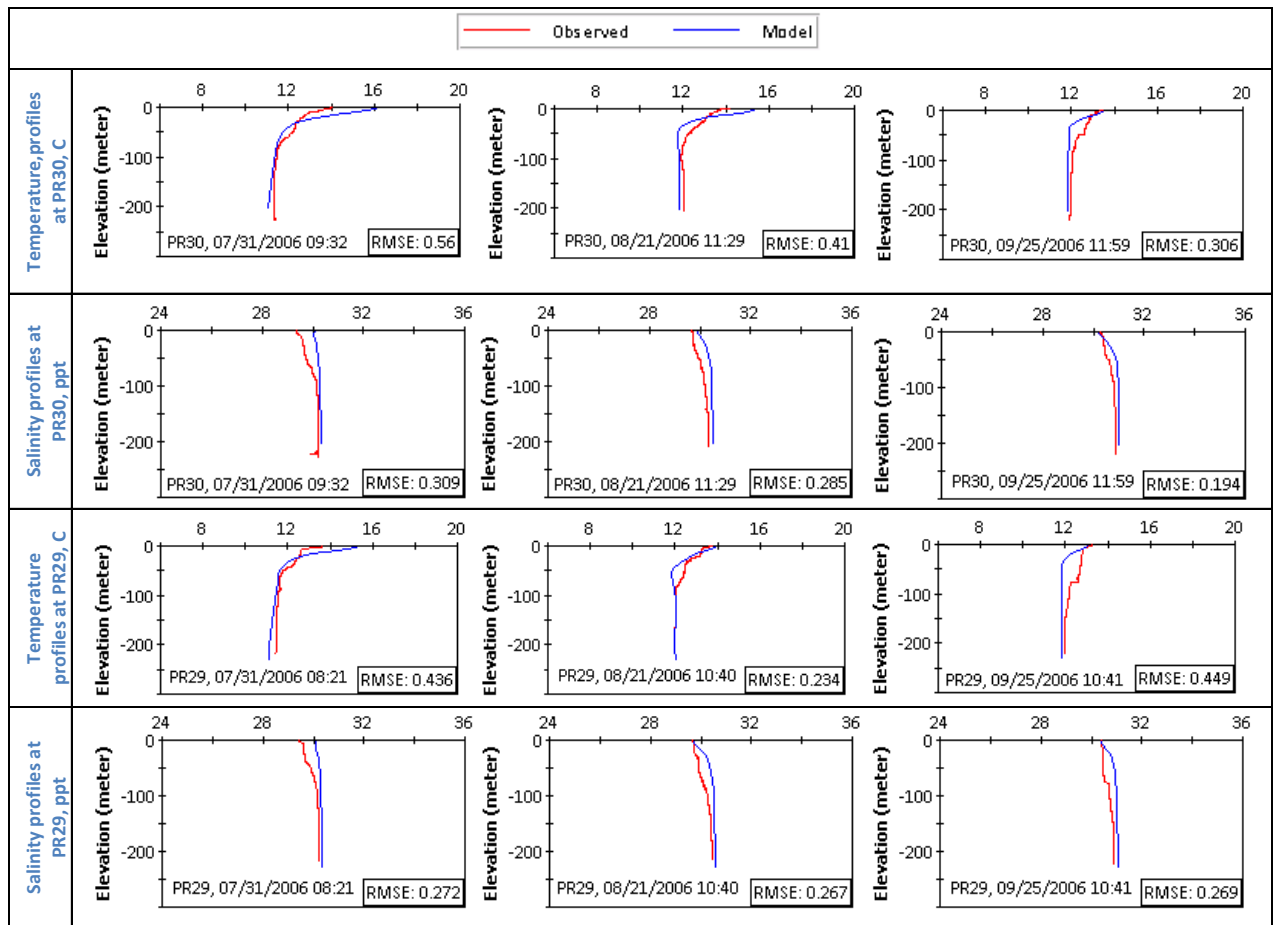
Figure 48. Temperature and salinity profile calibration in Central Puget Sound (PR29 and PR30).
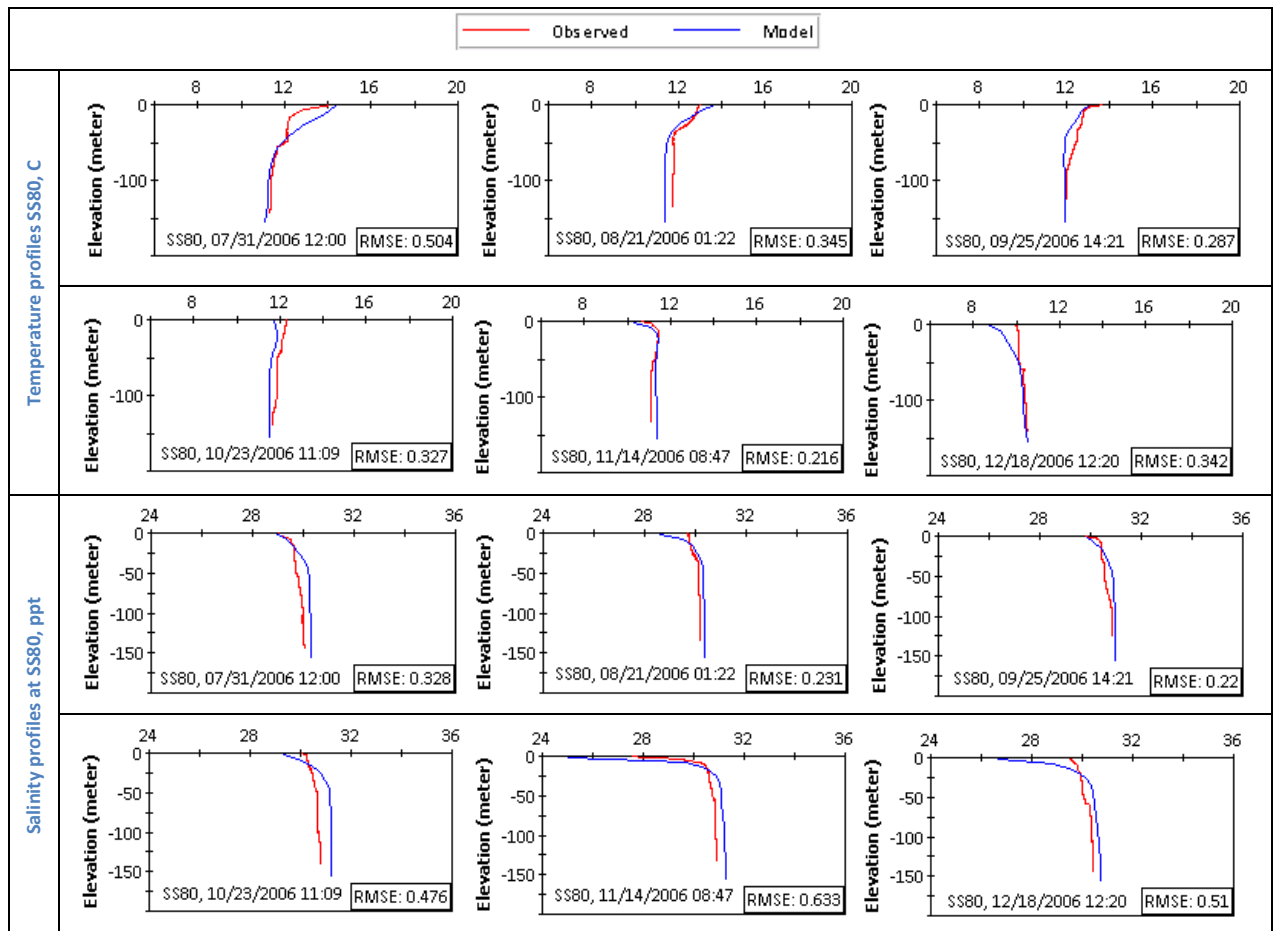
Figure 49. Temperature and salinity profile calibration at northeast of the Tacoma Narrows (SS80).
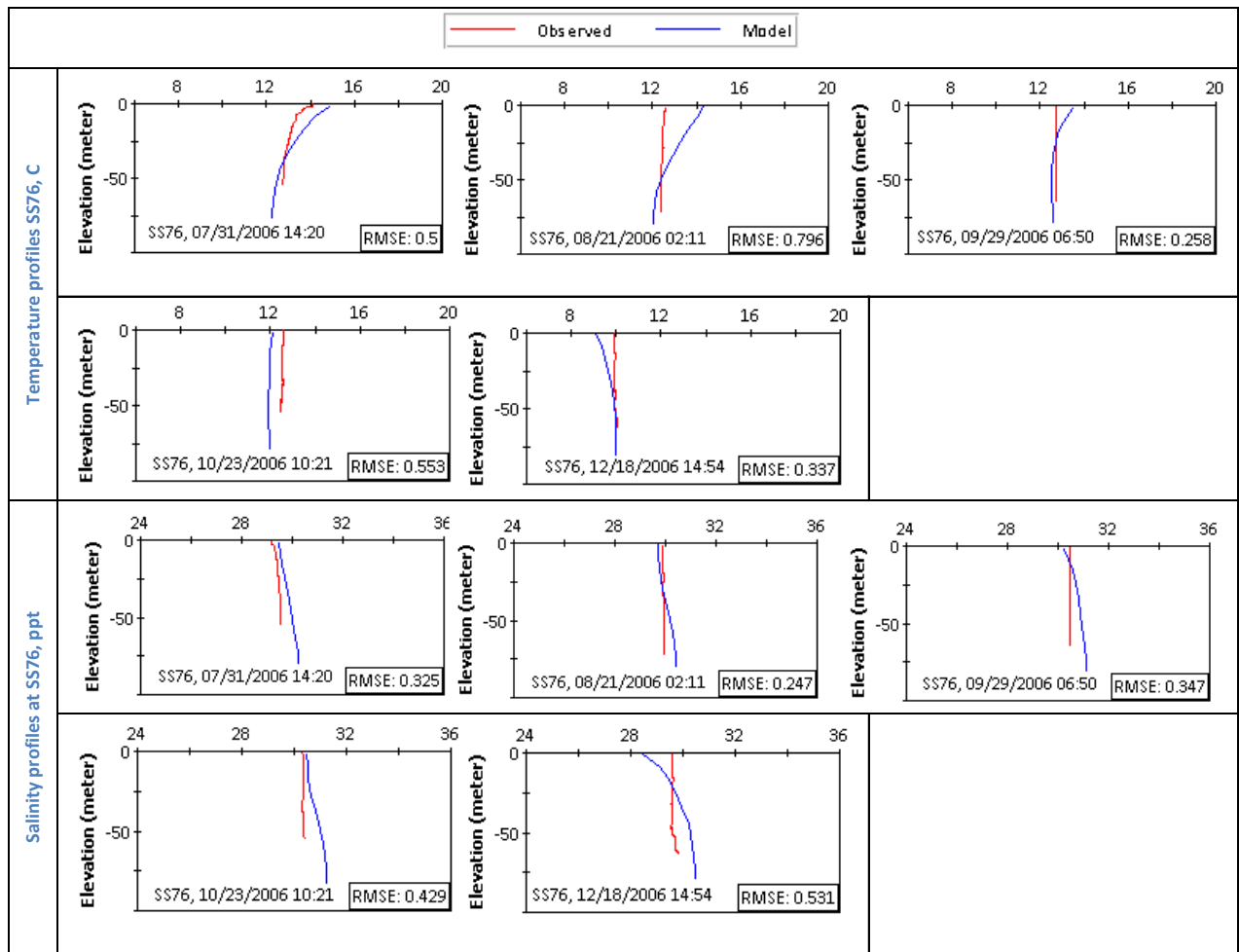
Figure 50. Temperature and salinity profile calibration at Tacoma Narrows (SS76).
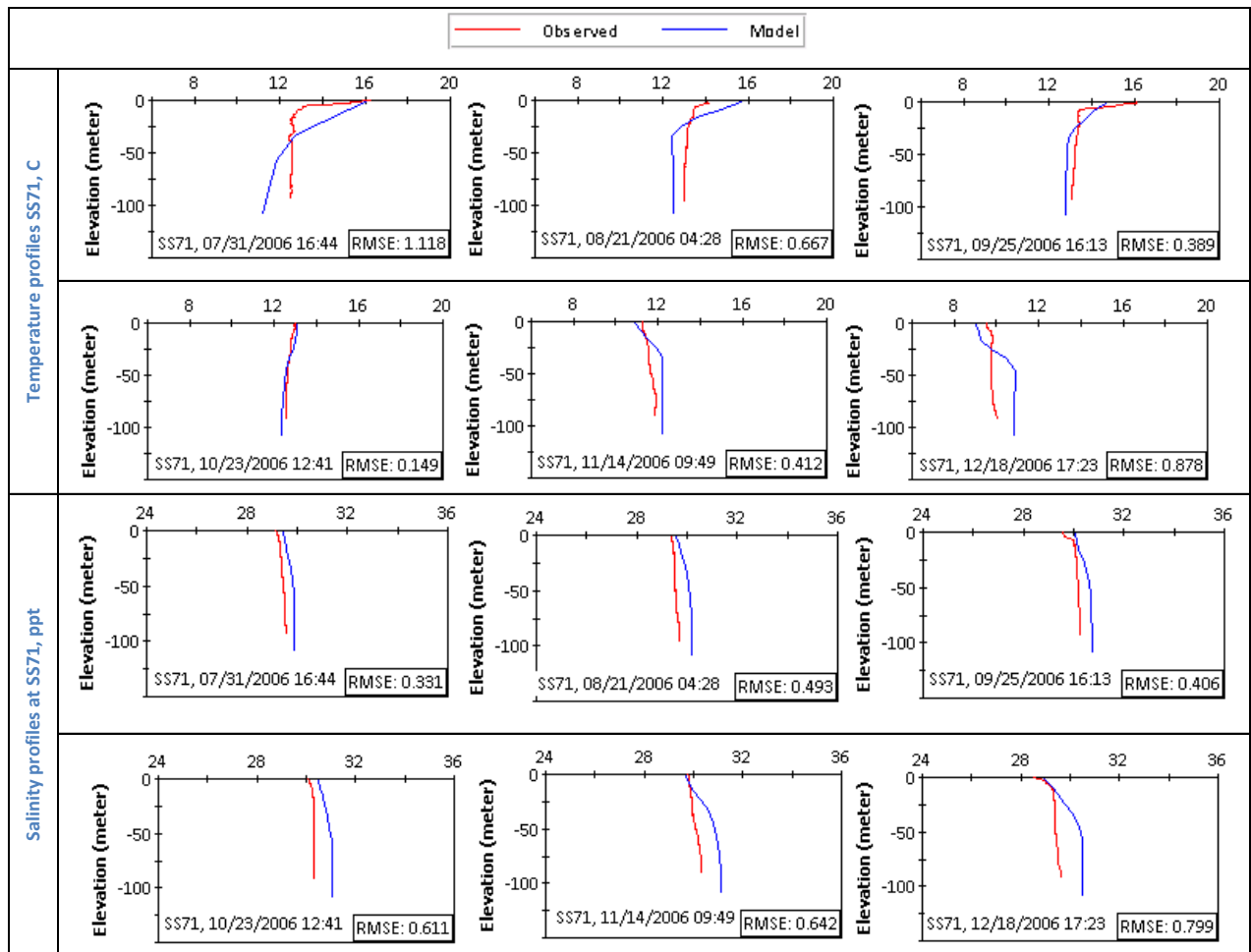
Figure 51. Temperature and salinity profile calibration at Carr Inlet (SS71).
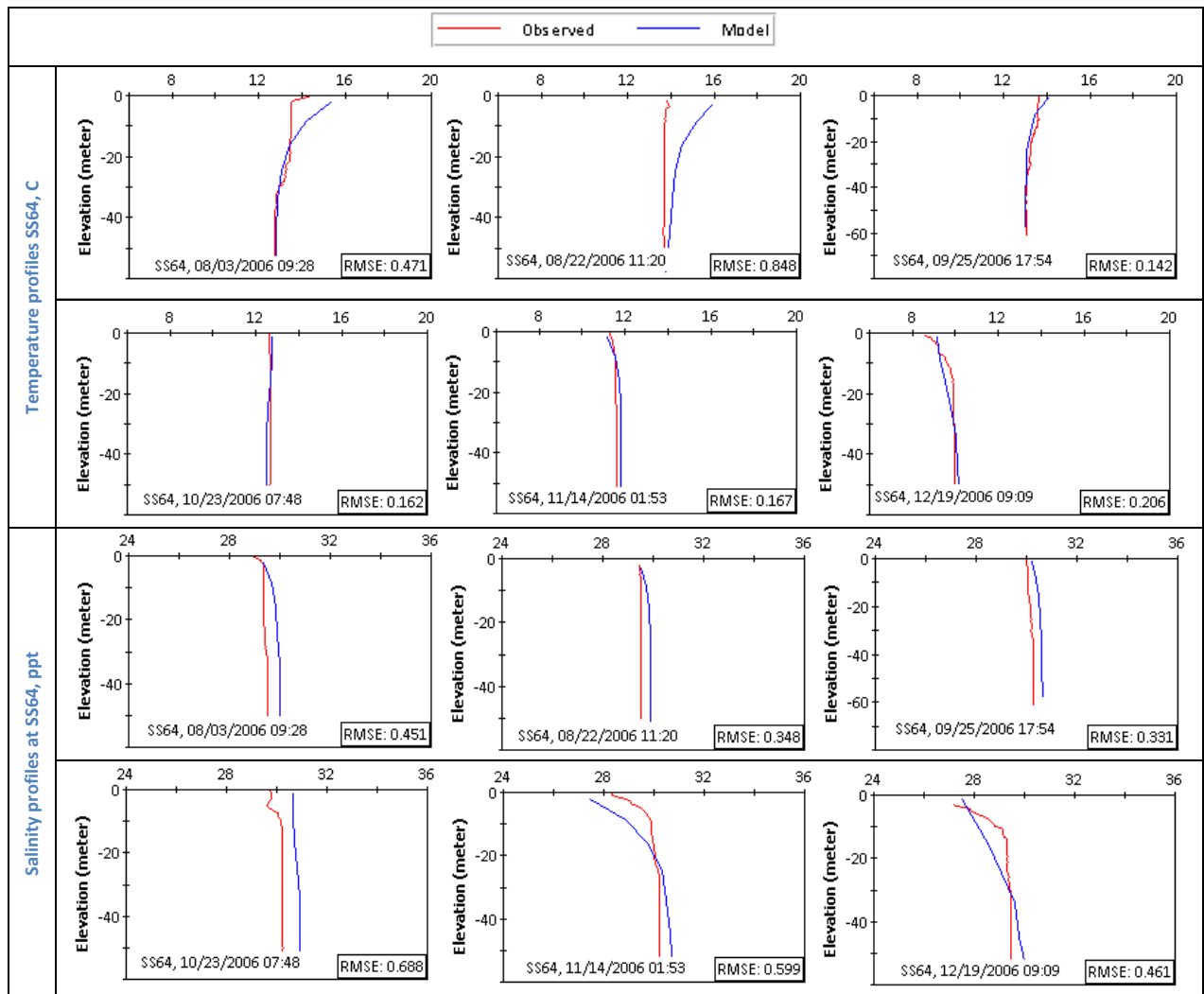
Figure 52. Temperature and salinity profile calibration near Nisqually (SS64).
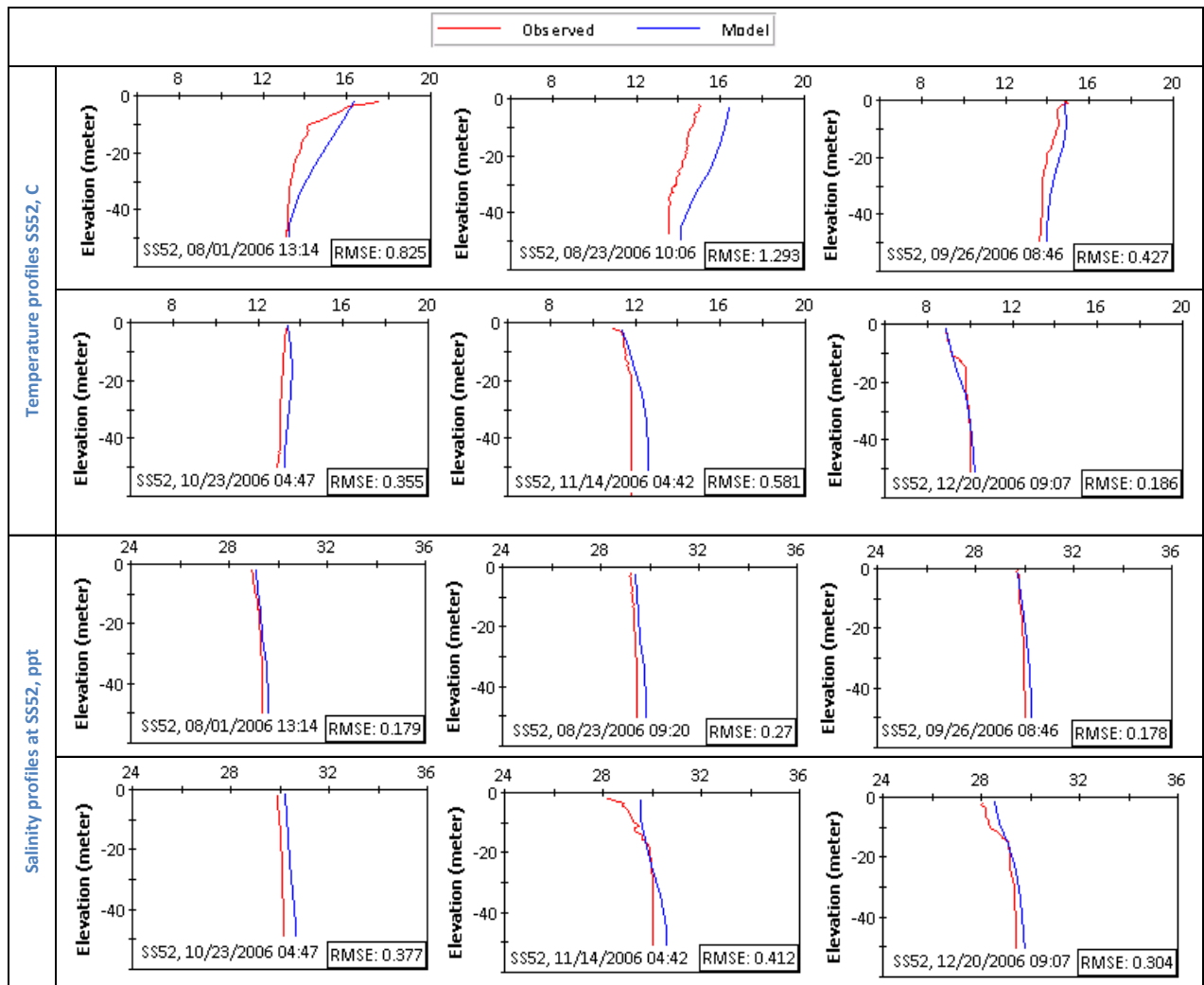
Figure 53. Temperature and salinity profile calibration at Case Inlet (SS52).
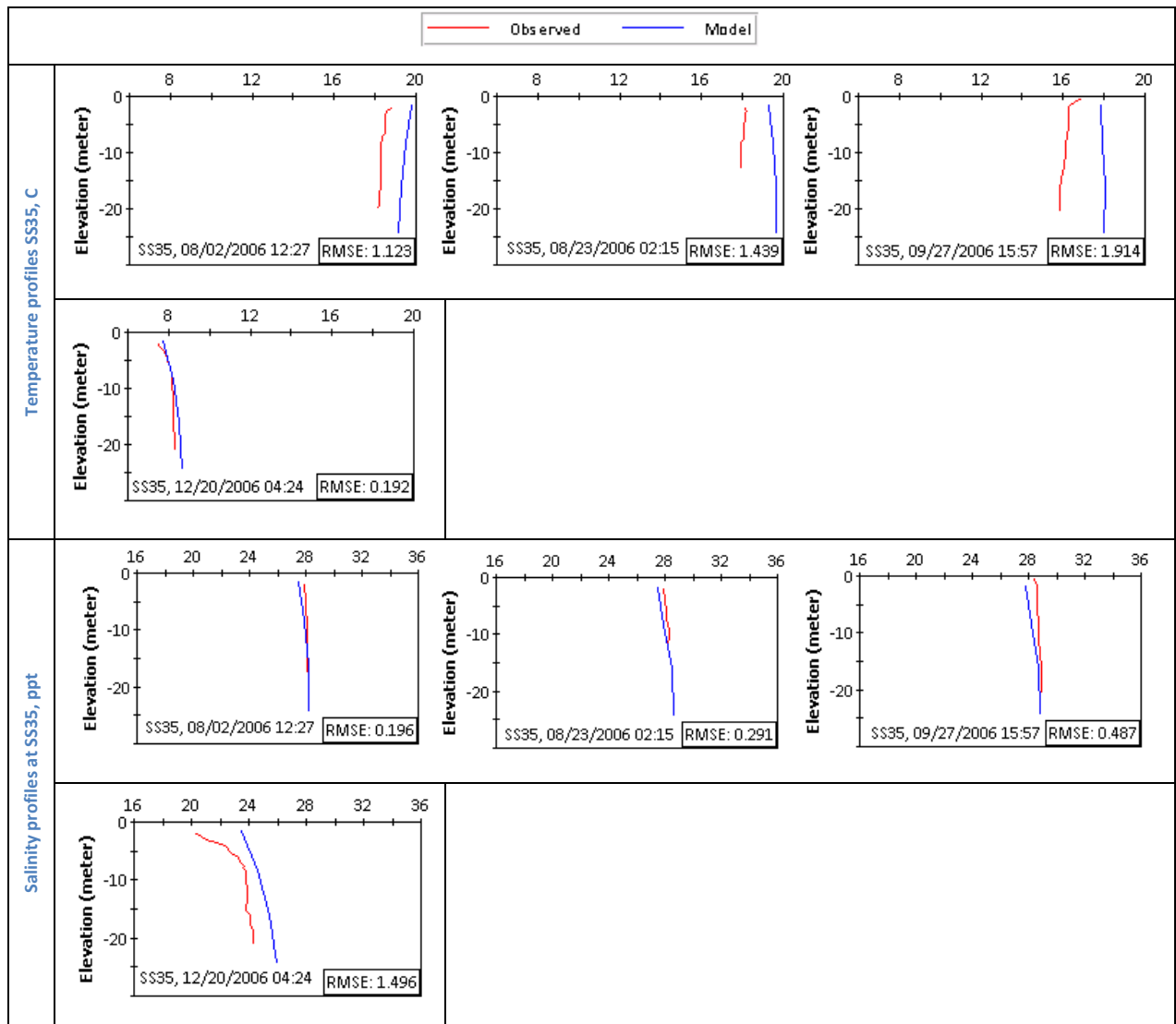
Figure 54. Temperature and salinity profile calibration at Oakland Bay (SS35).
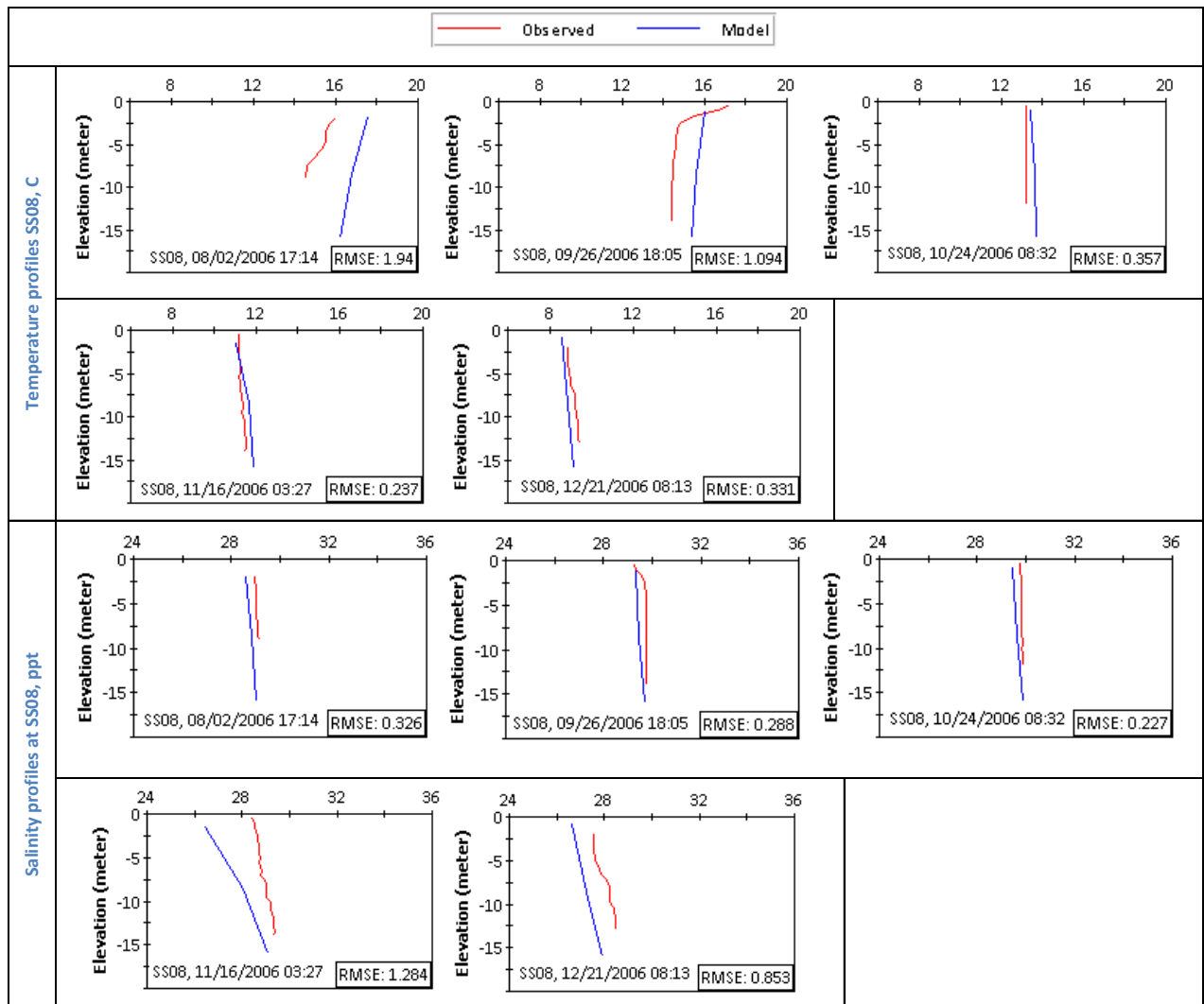
Figure 55. Temperature and salinity profile calibration at Budd Inlet (SS08).

Confirmation with 2007 Data

During the 2007 confirmation period, data and model comparisons were similar to 2006, with the lowest RMSEs closest to the northern boundary (Figures 56 through 64). Model-predicted temperatures were warmer than measured temperatures in the western inlets (Figures 62 through 64), especially near the surface (Figure 59) or in early summer (Figure 61). Temperature RMSEs averaged 0.7°C.

Salinity profile RMSEs averaged 0.4 psu, with similar errors throughout the model domain and lowest errors during the summer and fall months (0.3 psu). The model tended to predict higher salinity levels in the spring (Figures 58, 60, 61, and 62). The Budd Inlet salinity was well predicted throughout 2007.
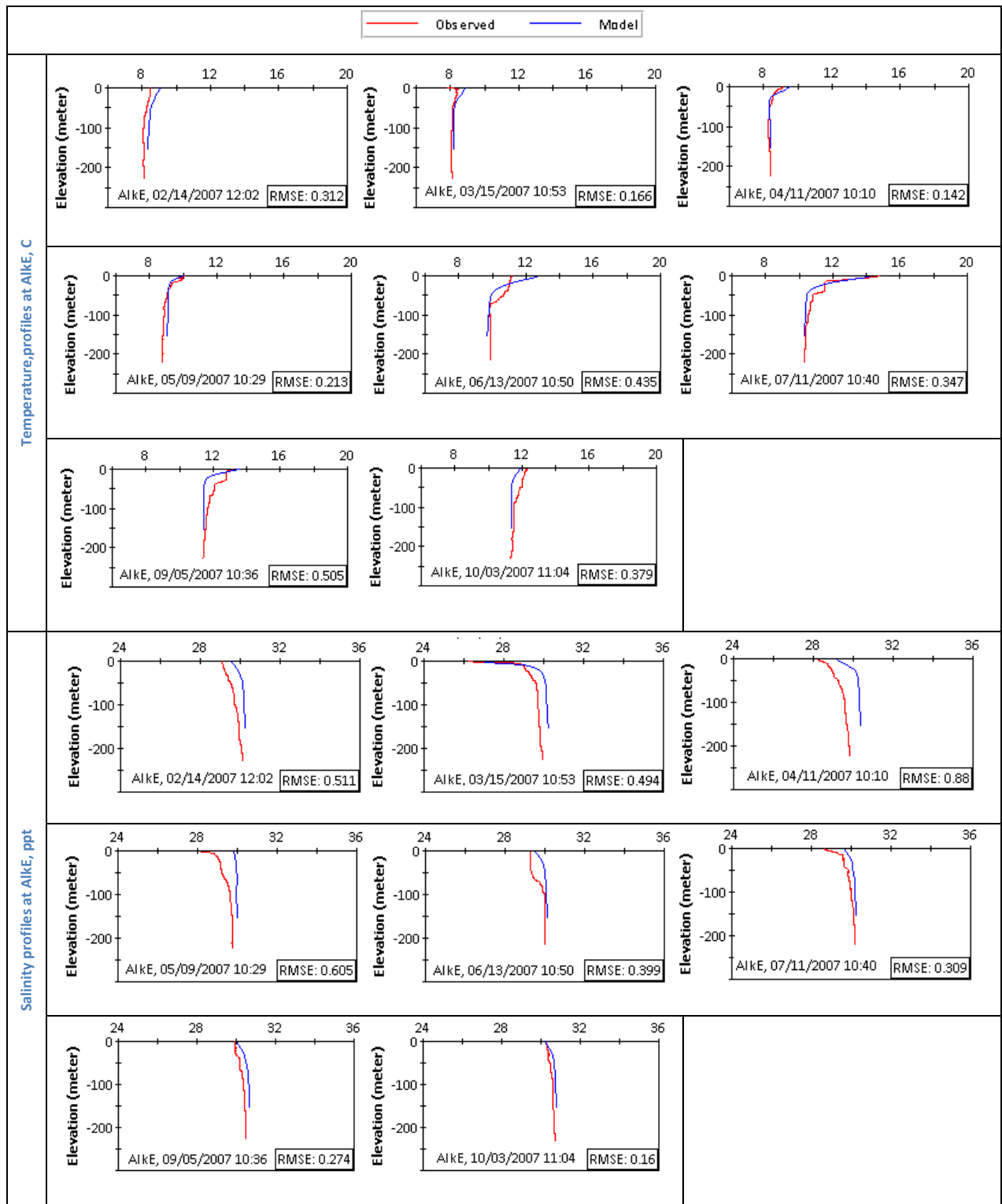
Figure 56. Temperature and salinity profile confirmation at Alki East.
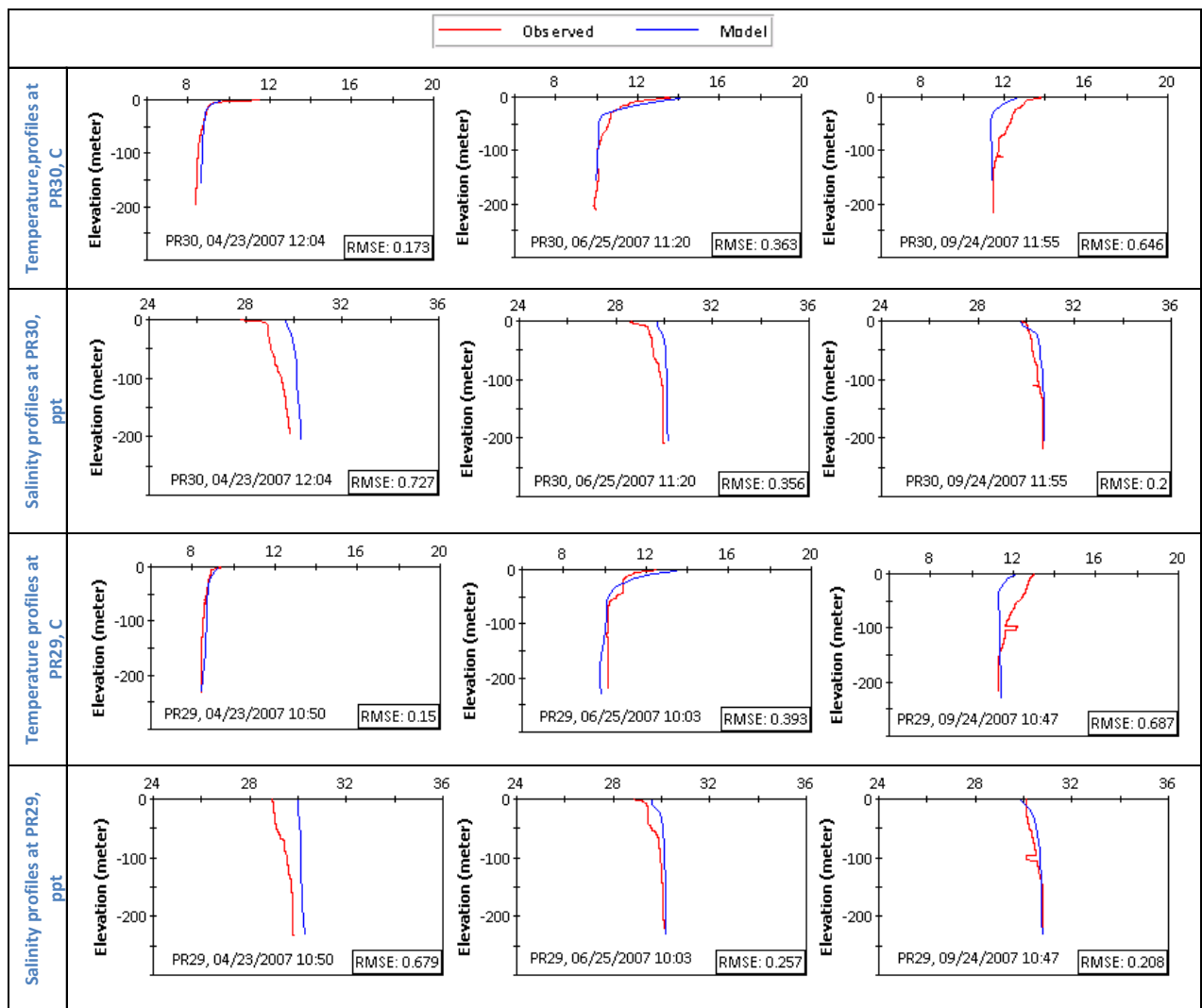
Figure 57. Temperature and salinity profile confirmation in Central Puget Sound (PR29 and PR30).
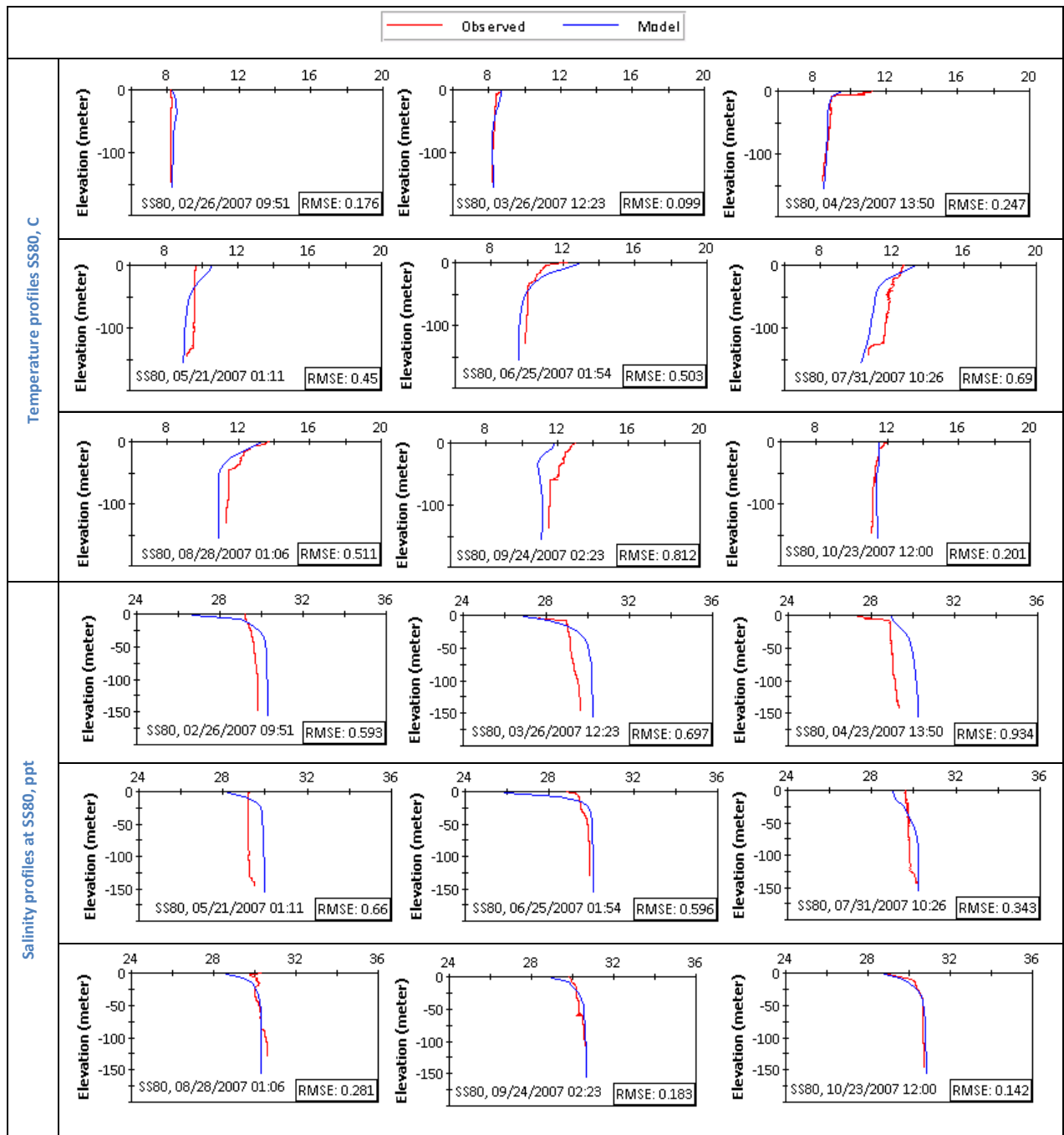
Figure 58. Temperature and salinity profile calibration south of Vashon Island (SS80).
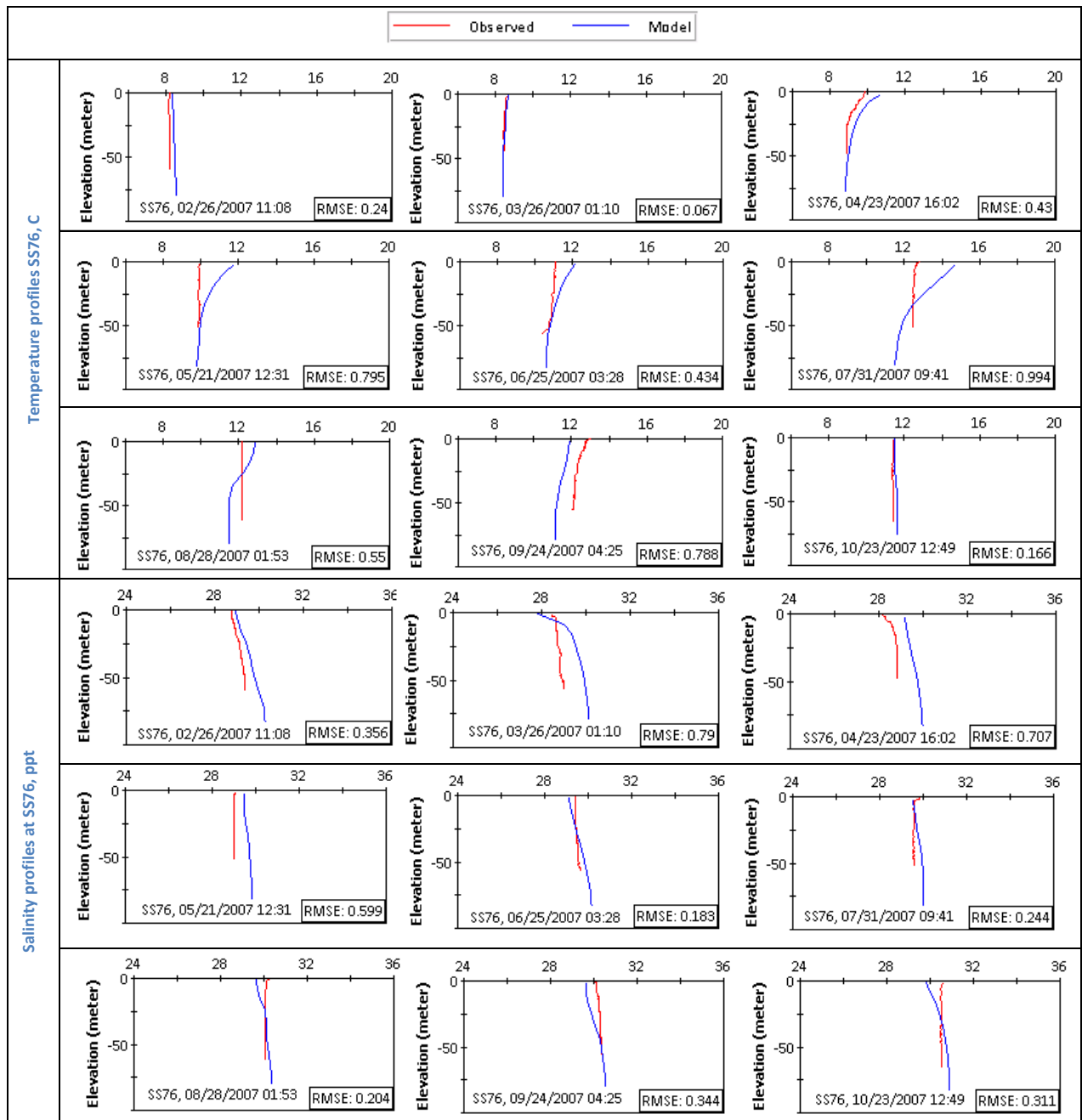
Figure 59. Temperature and salinity profile confirmation at Tacoma Narrows (SS76).
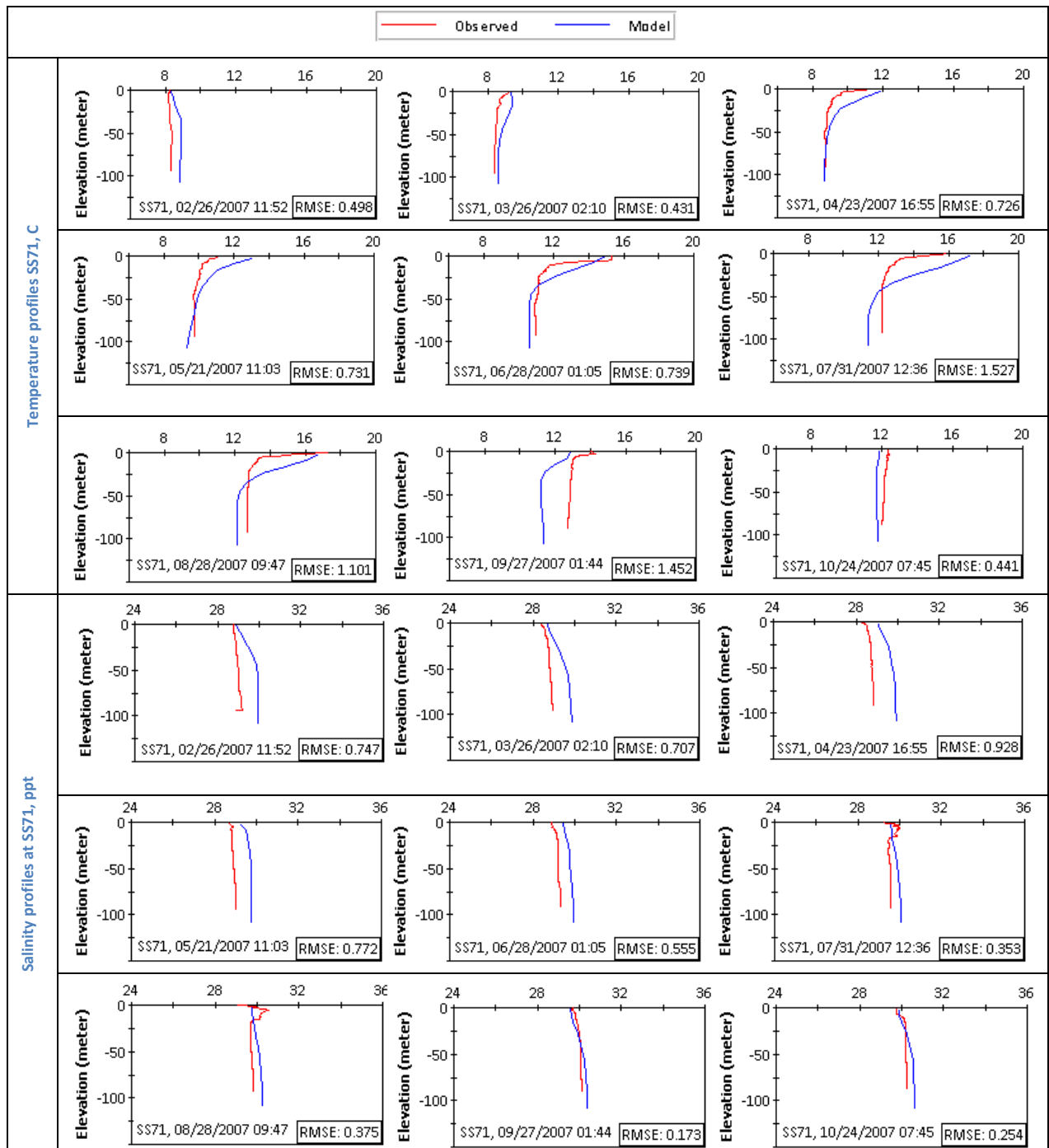
Figure 60. Temperature and salinity profile confirmation at Carr Inlet (SS71).
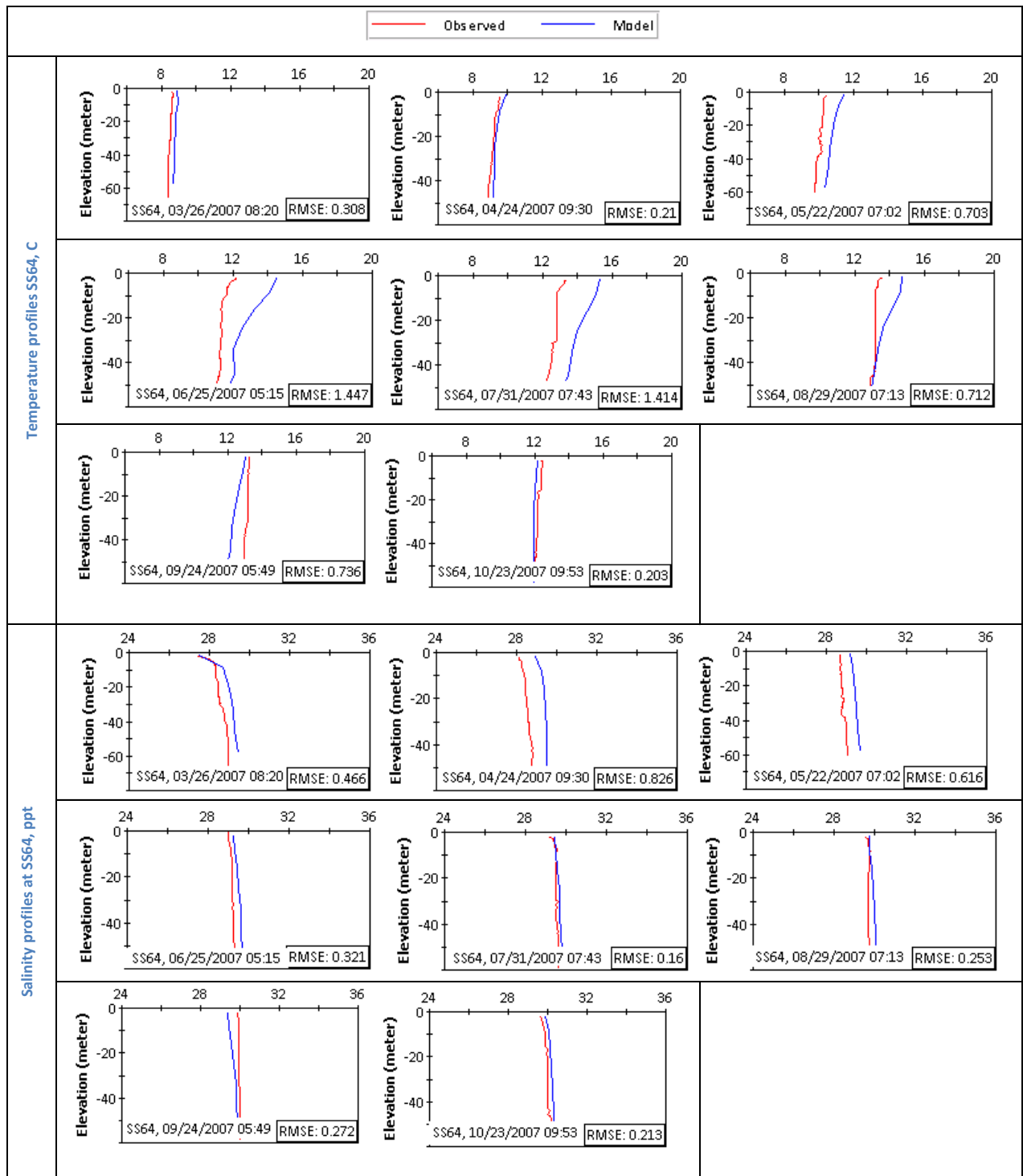
Figure 61. Temperature and salinity profile confirmation near Nisqually (SS64).
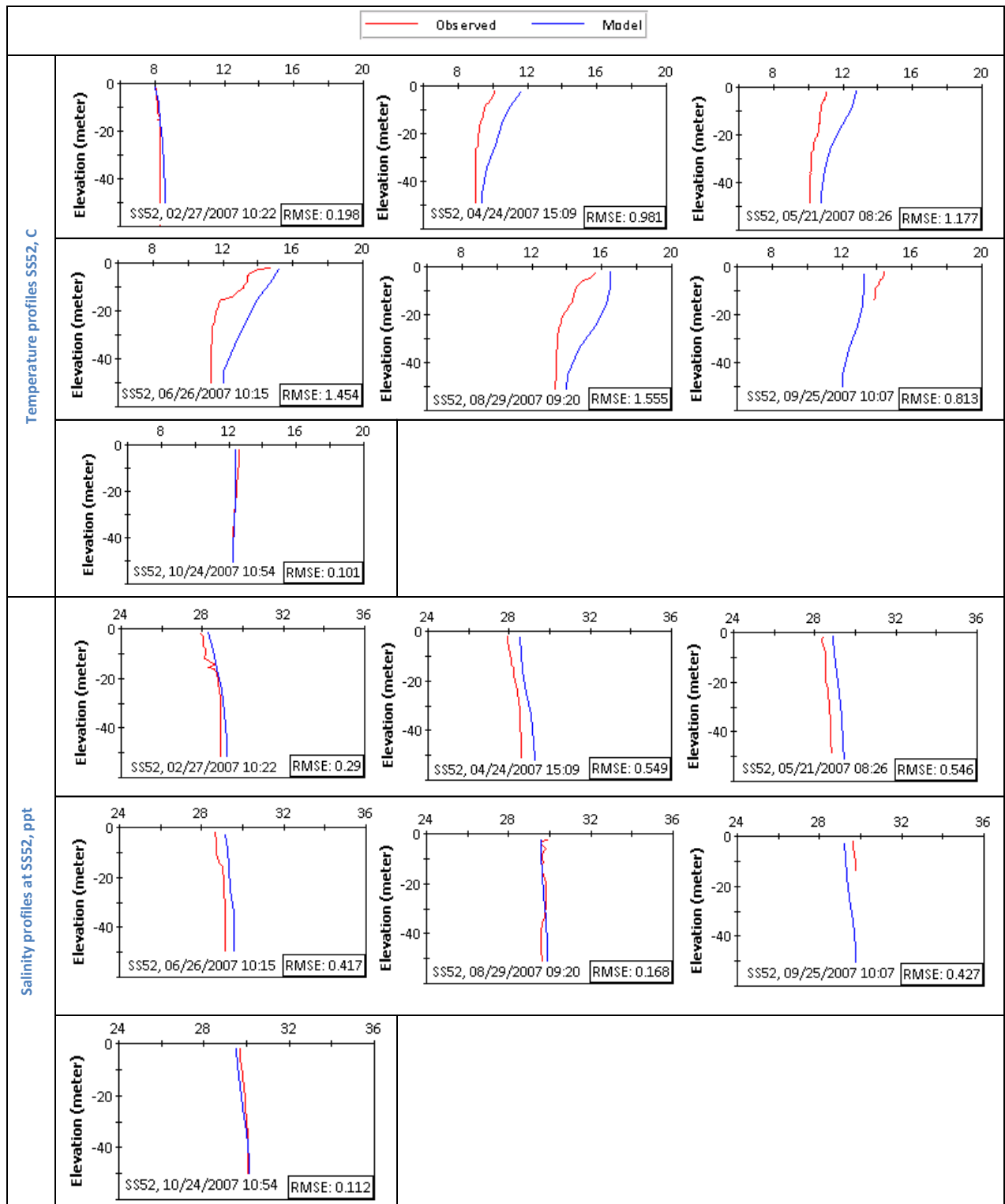
Figure 62. Temperature and salinity profile confirmation at Case Inlet (SS52).
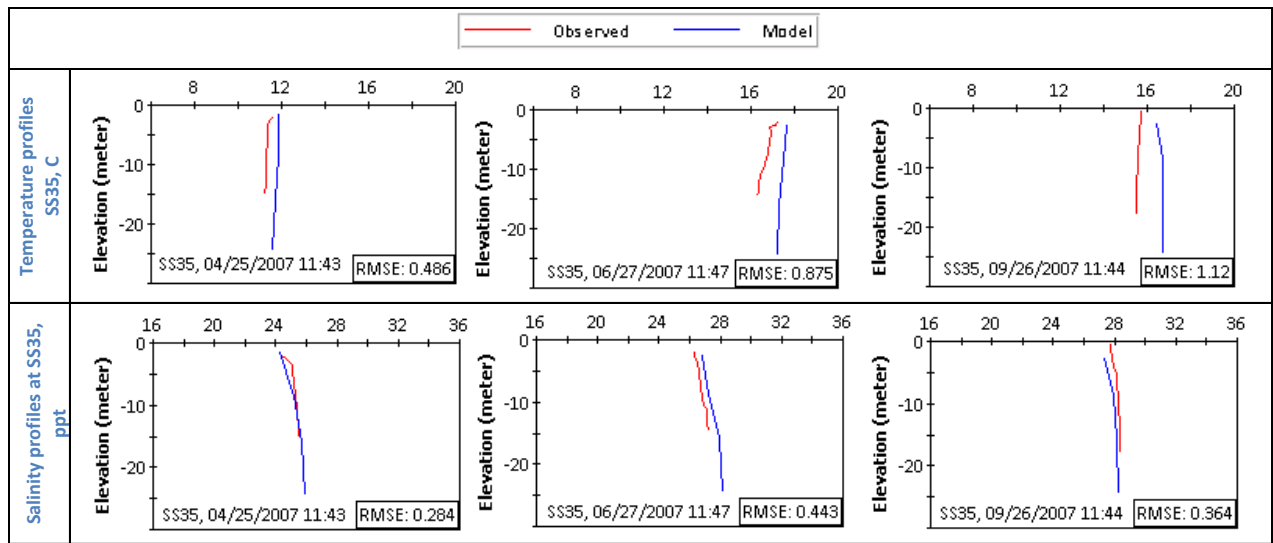
Figure 63. Temperature and salinity profile confirmation at Oakland Bay (SS35).
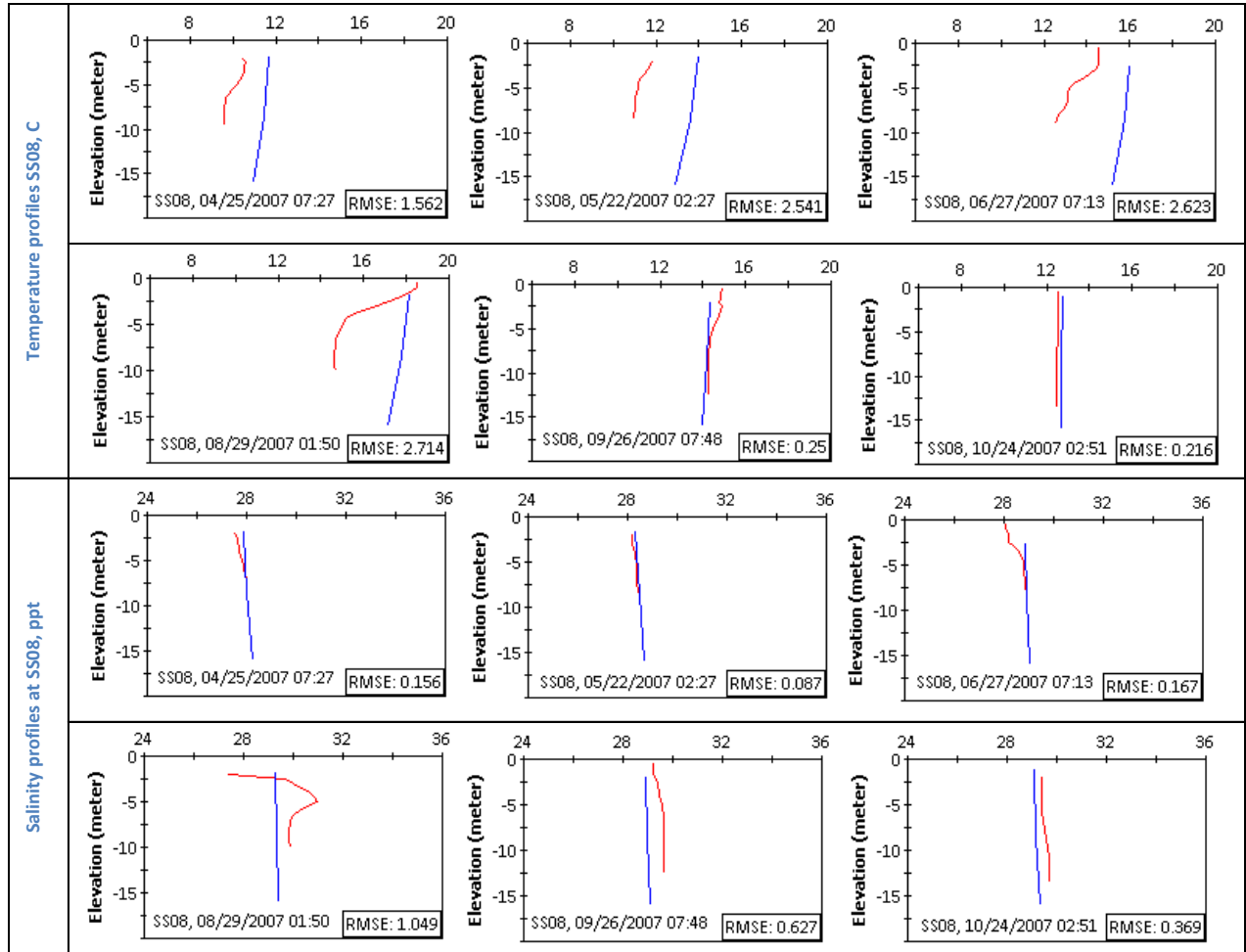
Figure 64. Temperature and salinity profile confirmation at Budd Inlet (SS08).

Brunt-Väisälä Buoyancy Frequency

The Brunt-Väisälä buoyancy frequency is a measure of the stability of the water column or stratification calculated from water density and the rate of change of density with depth. The value includes the effects of both temperature and salinity and provides a numeric corollary to the profile plots presented above. The buoyancy frequency (N) is calculated as

$$N = \sqrt{-\frac{g}{\rho}\frac{\partial \rho}{\partial z}}$$

Where g is gravitational acceleration, ρ is density, and $\partial \rho / \partial z$ is the density gradient, either between adjacent data bins or model layers. The buoyancy frequency, expressed as Hertz (Hz), increases as the density gradient increases and typically reaches a maximum value at the depth of the pycnocline. The square of the buoyancy frequency was calculated for both the calibration and confirmation time periods, and no other adjustments to the model were made to improve fit. Figure 65 identifies the comparison locations for both calibration and confirmation. Figures 66 through 68 present 2006 comparisons and Figures 69 through 72 present 2007 comparisons.

The buoyancy frequency squared generally decreases with depth in both the data and model predictions. Data and model predictions are of comparable magnitude at most stations and generally higher in the western inlets.
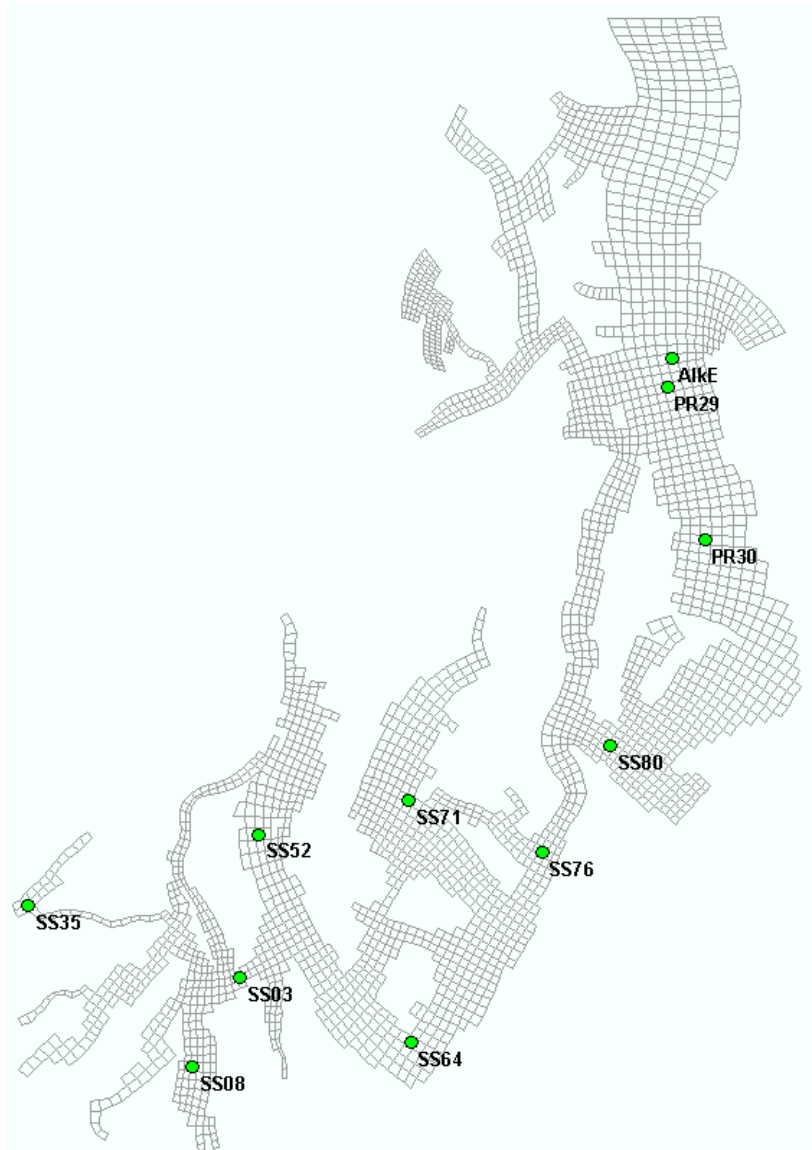
Figure 65. Locations for comparing model and data Brunt-Väisälä buoyancy frequency.
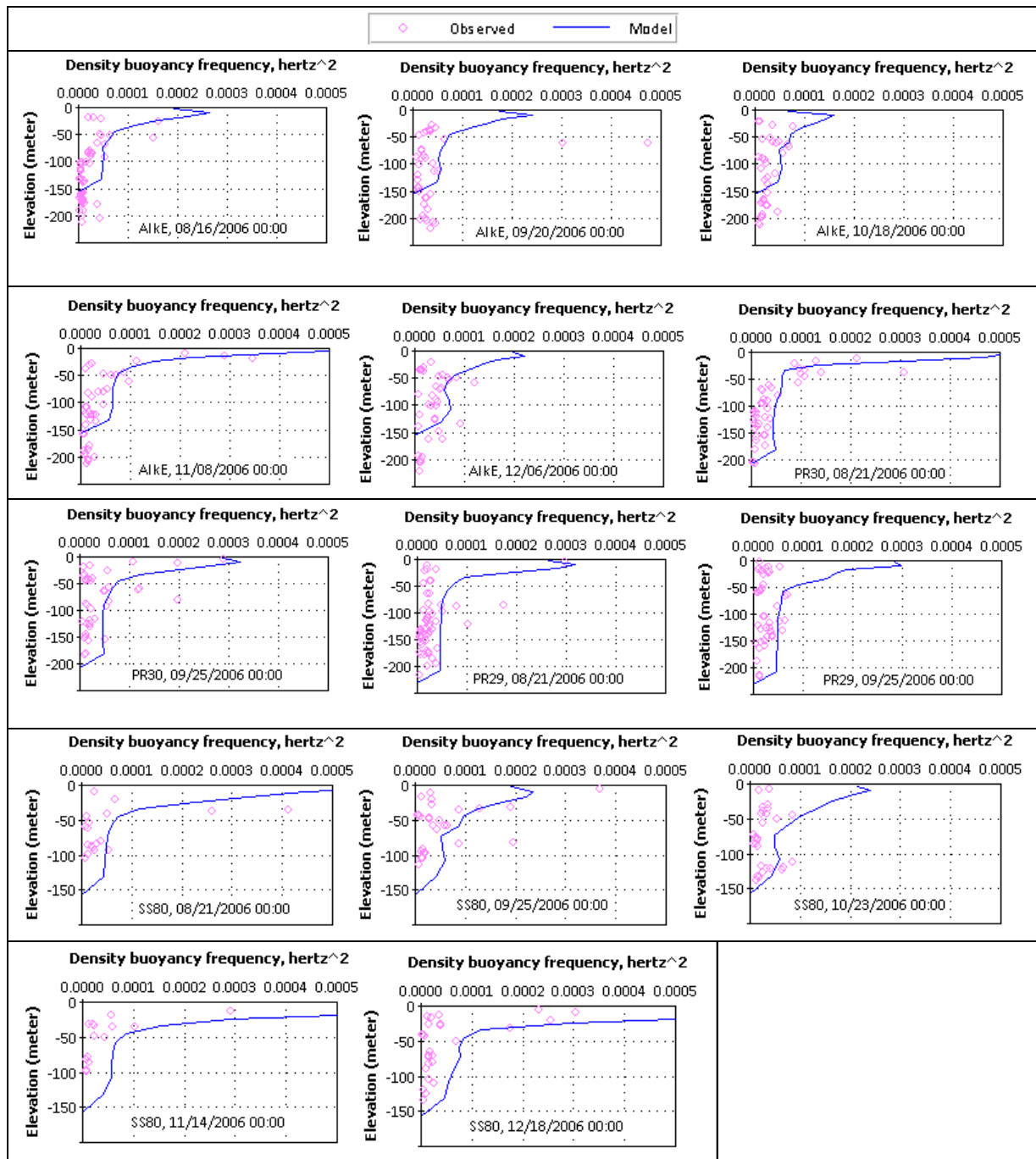
Figure 66. Density buoyancy frequency profiles at stations north of Tacoma Narrows (ALKE, PR30, PR29, and SS80) for the 2006 calibration period.
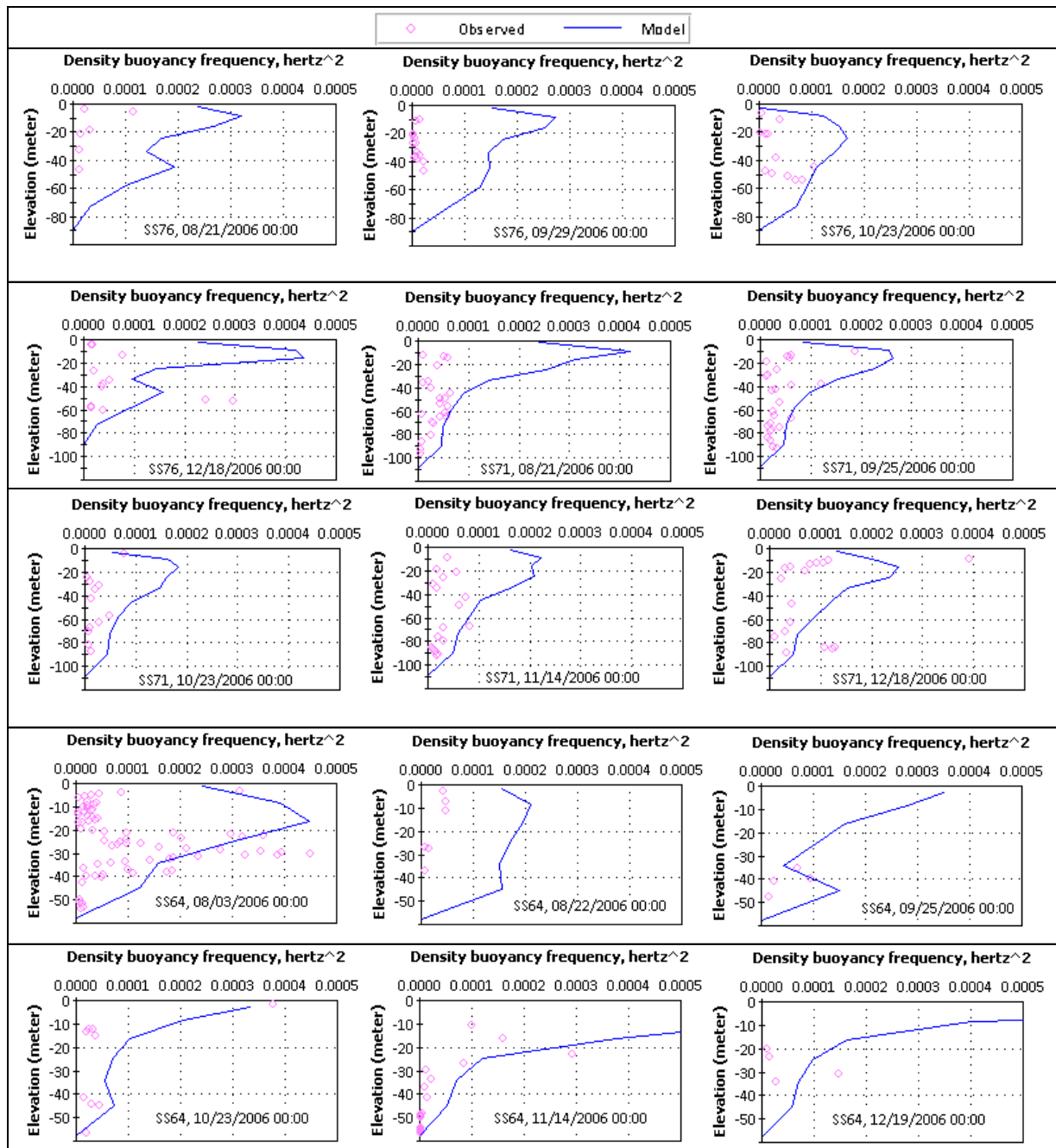
Figure 67. Density buoyancy frequency profiles at stations in the Tacoma Narrows (SS76), Carr Inlet (SS71), and Nisqually Reach (SS64) for the 2006 calibration period.
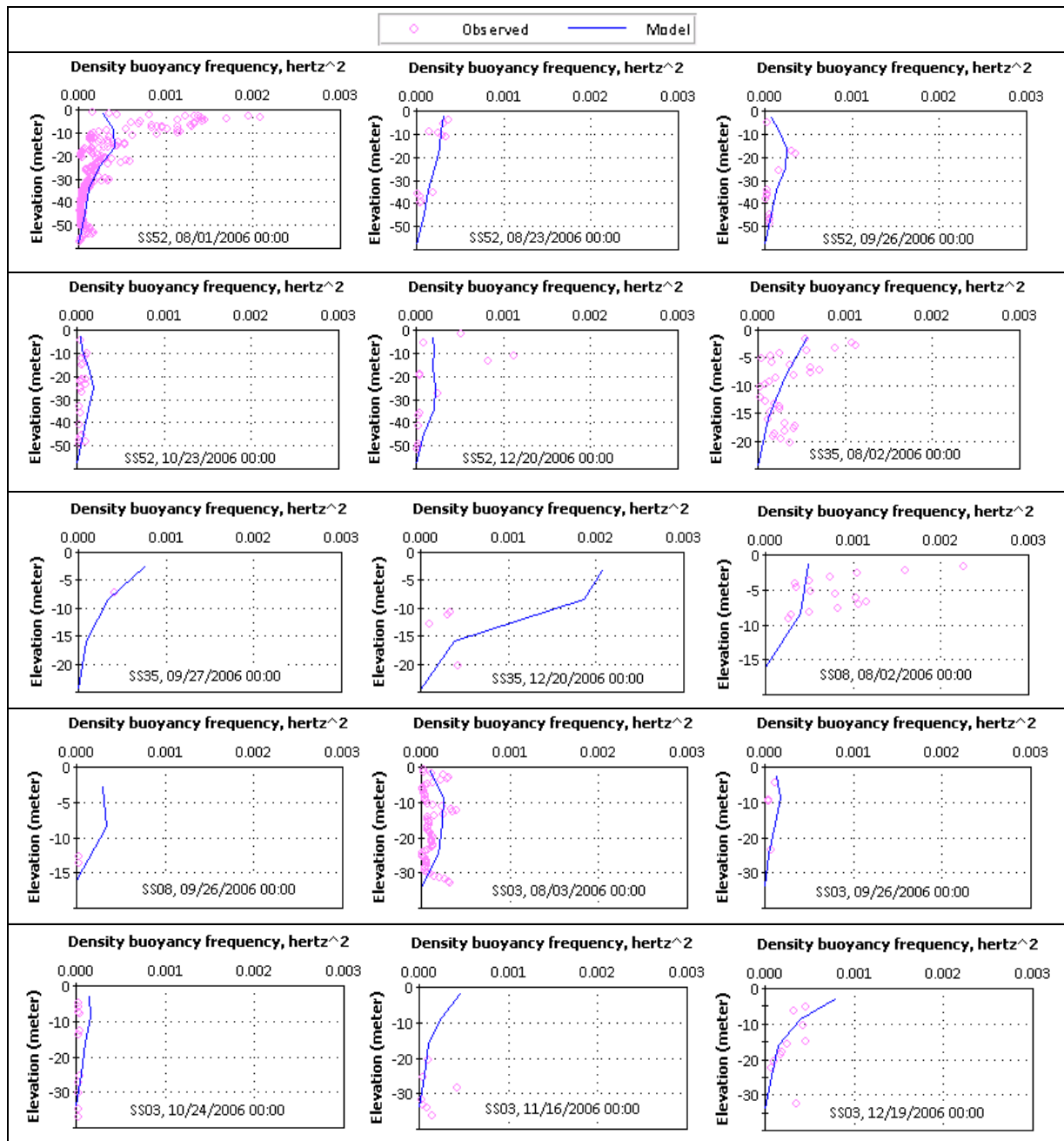
Figure 68. Density buoyancy frequency profiles at stations in Case Inlet (SS52), Oakland Bay (SS35), Dana Passage (SS03), and Budd Inlet (SS08) for the 2006 calibration period.
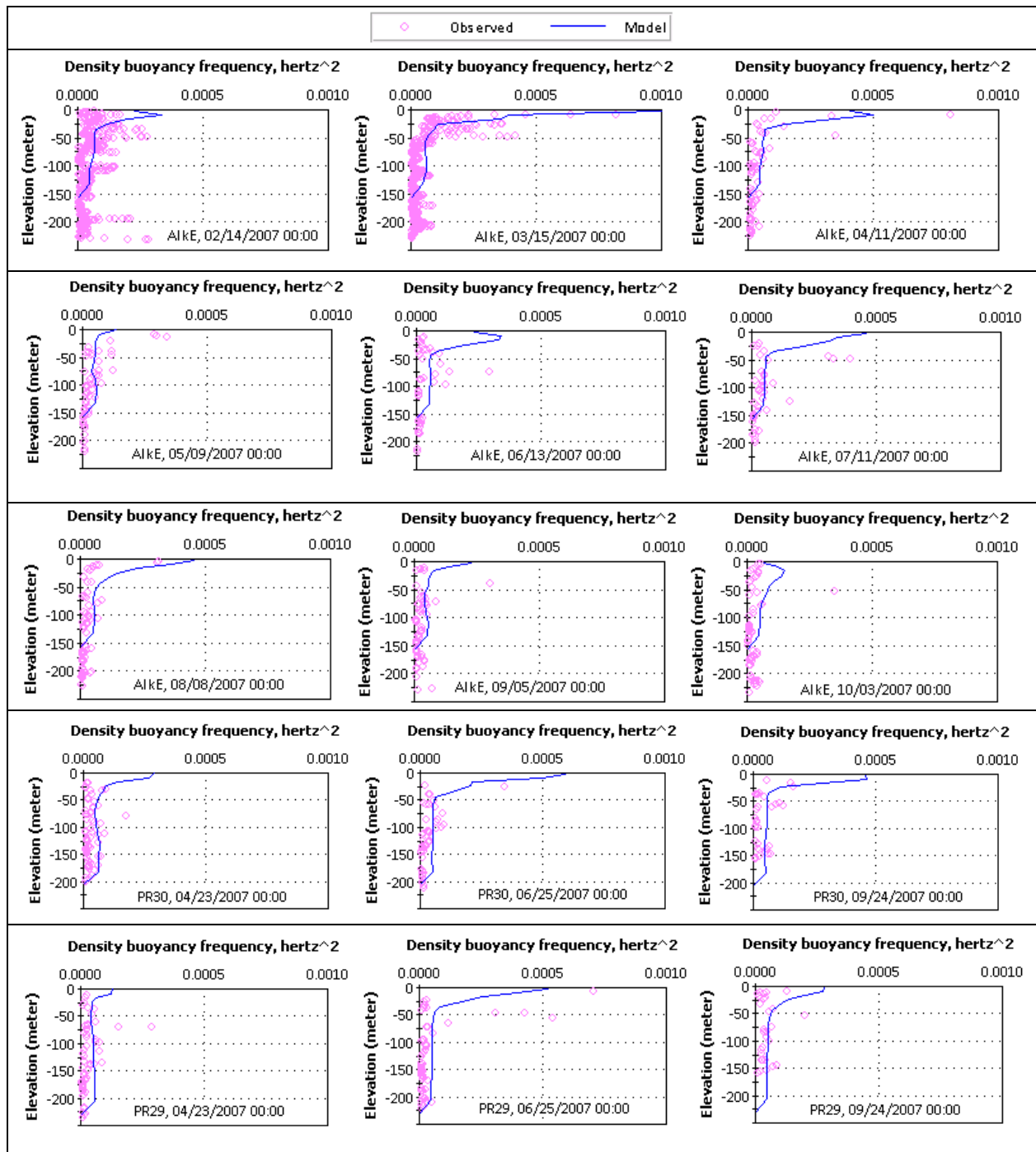
Figure 69. Density buoyancy frequency profiles at stations north of Tacoma Narrows (ALKE, PR30, and PR29) for the 2007 confirmation period.
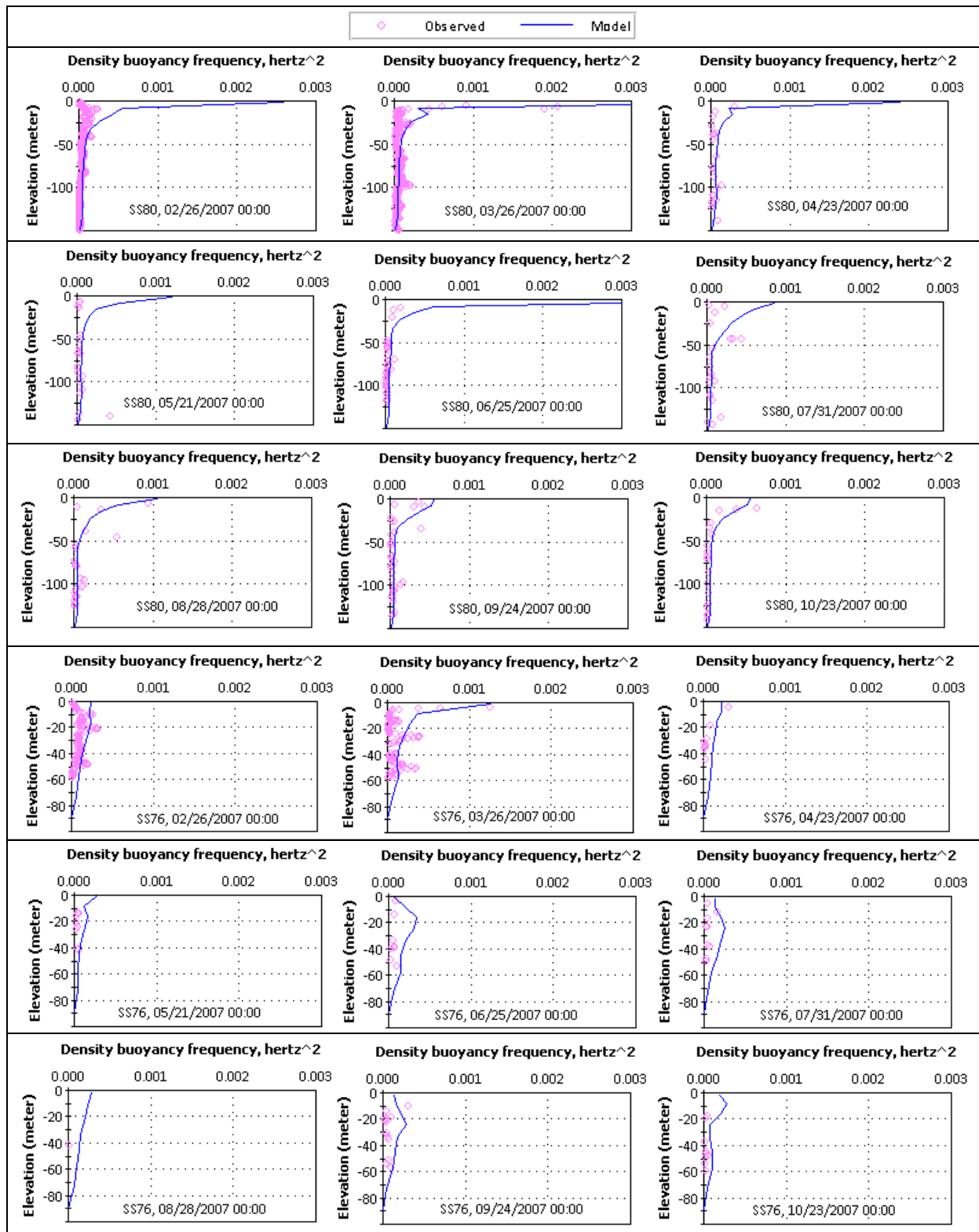
Figure 70. Density buoyancy frequency profiles north of Tacoma Narrows (SS80) and south of Tacoma Narrows (SS76) for the 2007 confirmation period.
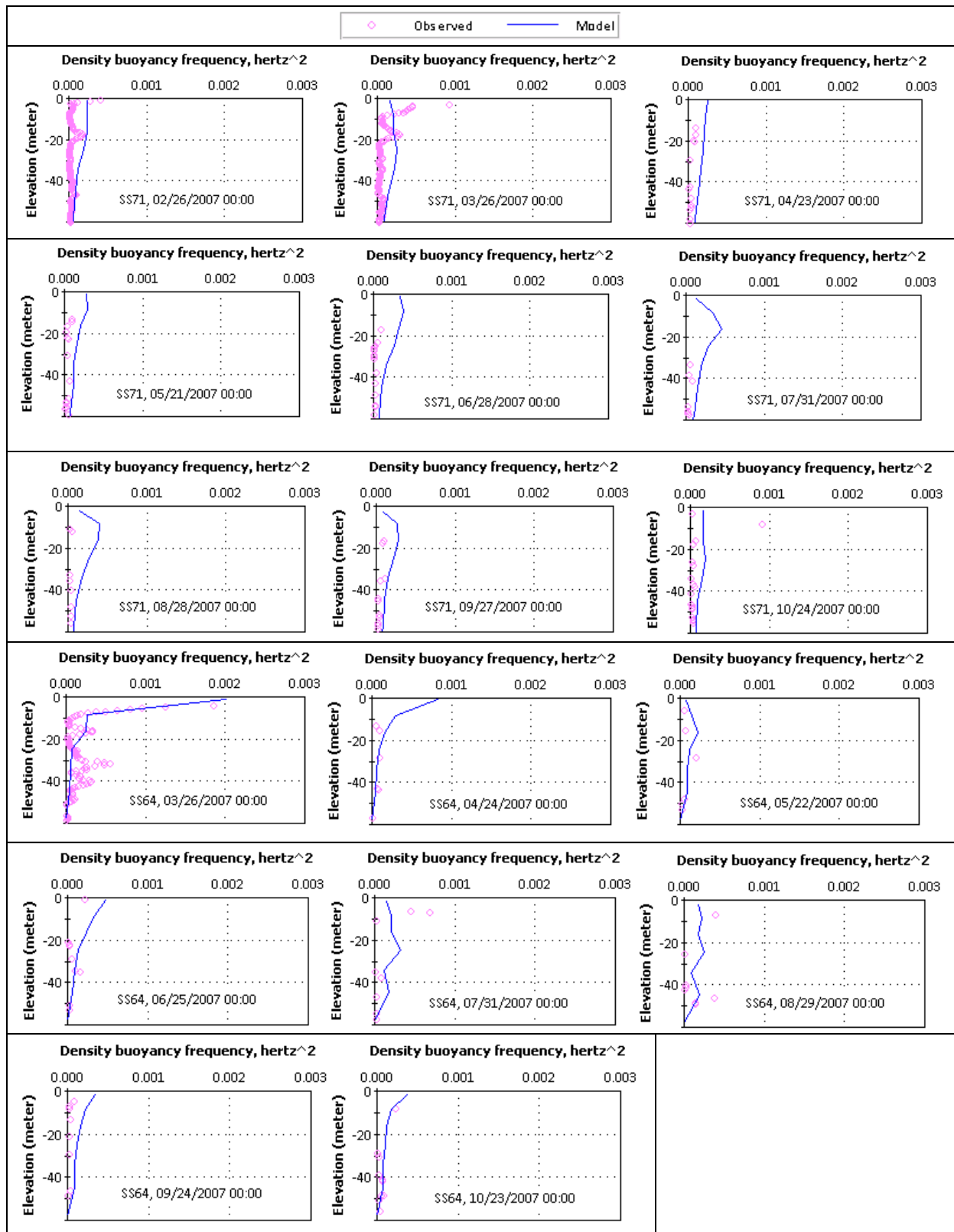
Figure 71. Density buoyancy frequency profiles in Carr Inlet (SS71) and Nisqually Reach (SS64) for the 2007 confirmation period.
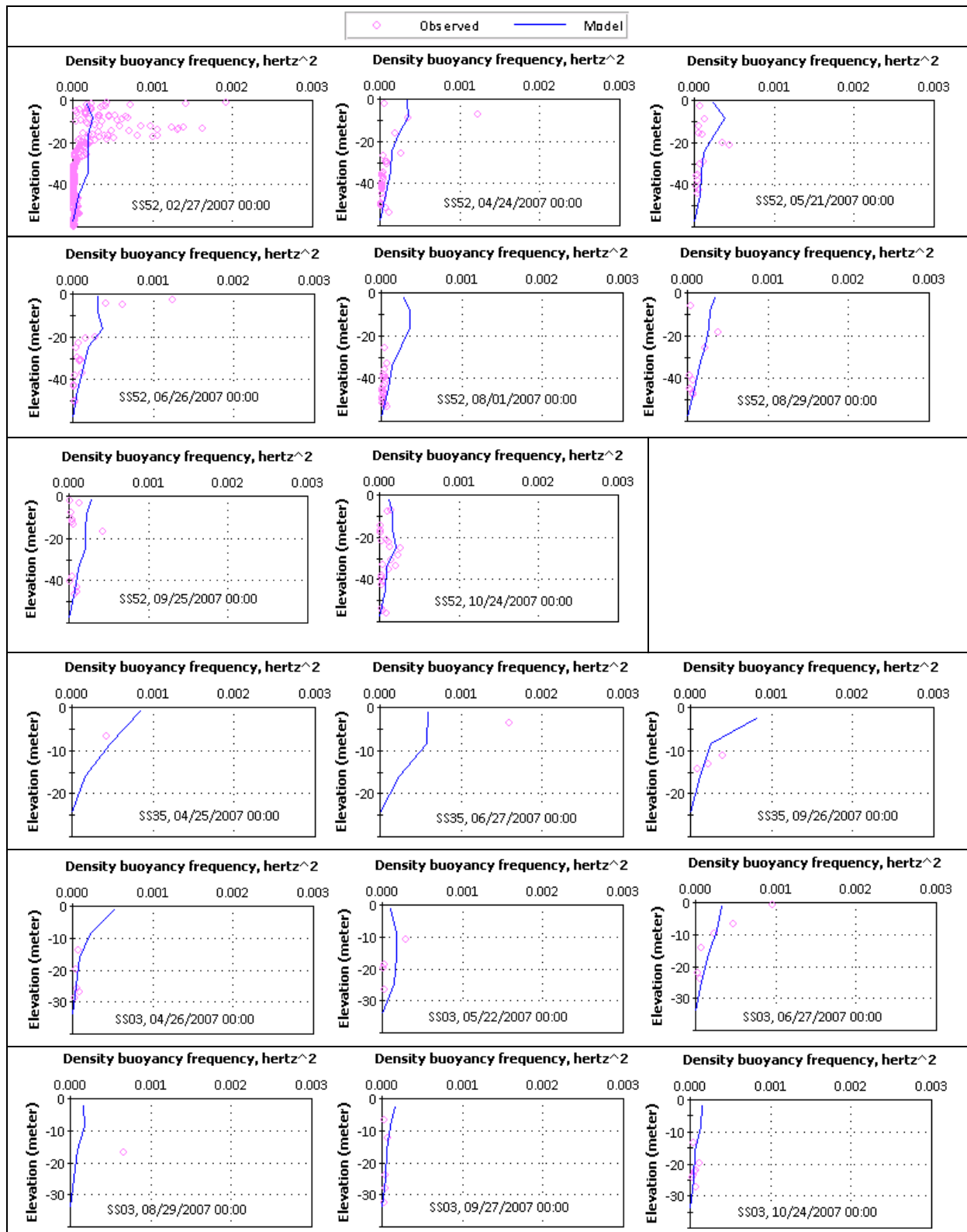
Figure 72. Density buoyancy frequency profiles in Case Inlet (SS52), Oakland Bay (SS35), and Dana Passage (SS03) for the 2007 confirmation period.

Current Velocities

The current velocity data were used as a general comparison during calibration and confirmation to verify that the phasing and magnitude are correct. Field programs were developed to investigate current directions within complex passages and inlets and to evaluate inlet-to-inlet differences. Because the model simplifies the vertical structure into layers and averages bathymetry over model grid cells on the order of 500 m, the model does not capture finer-resolution features that may be evident in the observed current data. However, observed current data are useful to confirm large-scale patterns.

Both surface-mounted transects and bottom deployments characterized currents in key locations within South Puget Sound. Roberts et al. (2008a) summarizes current data recorded using acoustic Doppler current profilers (ADCPs) during the 2007 confirmation period based on the deployment plan described in Addendum 1 to the QA Project Plan (Albertson et al. 2007b). Additional bottom-mounted deployments in Dana and Pickering Passages were part of a separate project that coincided with the 2006 calibration period.

All measurements were recorded with a 300-kHz Workhorse Sentinel ADCP from Teledyne-RD Instruments. The instrument sends a ping and records scattering over a broadband spectrum. The frequency is related to the velocity of the water masses encountered. Due to interference and equipment limitations near the water surface and the sediment surface, data cannot be recorded close to either boundary, typically within a few meters. In addition, the unit cannot record velocities at water depths below 100 m, and no data are returned. While the recorded velocity data are highly precise, field factors such as boat tracks not perpendicular to shore or lack of data near the surface or bottom may increase the uncertainty in derived parameters such as water flux and average velocity.

Surface-mounted Transects

During July and September 2007, Ecology conducted transects with the ADCP mounted to a boat (Figures 73 and 74, respectively). The resulting profiles provide both the cross-sectional area of the transect and the detailed velocity distribution through the transect. Data were recorded in 1-m bins, a finer scale than can be resolved with the layering of the model. The field data were mapped to model layers to facilitate comparisons. The data collection program was designed to estimate instantaneous velocities on flooding and ebbing tides. Detailed results were presented in Appendix E of Roberts et al. (2008). Transects were recorded during different tide stages and were not coincident in time. Boat passes across the inlet required 10 to 20 minutes to complete.

Table 7 compares instantaneous cross-sectional area (m^2) and average velocity (m/s) with those predicted by the model. While the model operates on a fine time scale, output data are saved at hourly intervals. These hourly values were linearly interpolated to the time that the transect was conducted. Model cross-sectional areas and velocities are similar to those recorded during the ADCP transects. Differences in transect aspect and model grid cell orientation likely contribute to some differences, particularly at transect T5, but overall the velocities predicted by the model reasonably describe those derived from field data.

Figure 73. July 2007 surface-mounted ADCP transect locations.

Figure 74. September 2007 surface-mounted ADCP transect locations.

Table 7. Summary of surface-mounted ADCP-measured tidal fluxes versus model results from July and September 2007. Positive values are flood tide directions and negative values are ebbs.

Transect	Date/Time	Area (m^2)		Mean Velocity (m/s)	
		ADCP	Model	ADCP	Model
BTE1 - Mouth of Totten	7/10/07 09:27	14,327	20,094	0.10	0.08
BTE4 - Mouth of Eld	7/10/07 10:05	10,300	8,254	0.26	0.16
BTE5 - Mouth of Budd	7/10/07 10:25	22,663	22,601	0.20	0.14
BTE3a - S. of Hope Island	7/10/07 11:01	3,452	3,650	0.91	0.86
BTE3b - Replicate	7/10/07 11:10	3,509	3,650	0.90	0.86
BTE6 - Central Budd	7/10/07 11:57	25,869	25,141	0.13	0.06
CARR4 - Allen Pt.	7/11/07 13:29	44,986	62,140	0.11	0.02
CASE1a - S. of McMicken	7/11/07 14:56	96,638	100,767	0.14	0.15
CASE1b - Replicate	7/11/07 15:28	97,170	100,767	0.12	0.15
CASE3 - N. of Harstine	7/12/07 13:20	24,672	25,928	0.31	0.22
CASE4 - E. of Stretch Island	7/12/07 13:48	44,986	51,424	0.11	0.06
T1 - Harstine bridge (ebb)	9/26/07 08:00	7,258	7,158	-0.55	-0.29
T3 – N. Squaxin Peale (ebb)	9/26/07 08:43	1,458	1,506	-0.36	-0.76
T5 - Hammersley Inlet (ebb) *	9/26/07 09:28	2,657	6,438	-1.19	-0.14
T8 - S. Squaxin (flood) *	9/26/07 13:13	12,039	9,568	0.41	0.53
T7 – Totten (flood)	9/26/07 14:46	11,538	9,696	0.64	0.27
T6 - Potlatch Pt. (flood) *	9/26/07 15:09	10,177	12,106	0.25	0.46
T5 - Hammersley Inlet (flood)	9/26/07 15:31	3,316	7,081	0.93	0.13
T1 - Harstine bridge (flood)	9/26/07 16:37	7,609	8,280	0.72	0.37

* Indicates transect and model grid cell orientation are very different, and some error may be due to this.

Bottom-mounted Deployments

Bottom-mounted ADCPs were deployed at paired locations shown in Figure 75 over at least one full neap-spring cycle of the moon (~14 days). The instruments recorded the three components of water velocity (longitudinal, lateral, and vertical) at 90-second intervals that were averaged over 6 minutes in 1-m layers or bins. Results were post-processed into time series of depth-averaged velocities and the net velocity over the full deployment was calculated. Comparing results for the two paired instruments indicates cross-inlet variability if present. Figure 93 from Roberts et al. (2008) presented both the average of the paired deployments for Budd, Carr, and Case Inlets as well as the difference.

We placed the bottom-mounted ADCPs in the deepest part of any channels present. The model grid cells were assigned represent depths that represent the average of all actual depths within the horizontal extent of that grid cell. Where the bottom depth changes quickly toward land, such as the channels of Budd Inlet and Pickering Passage, the average depths of the model are shallower than the depth of the ADCP deployment. The water column velocity structure could be much different than that determined from field data. Also, the field data did not capture the velocity structure nearest the surface and nearest the bottom. We selected the field data that correspond to specific model layers that were not affected by these data limitations. Figure 76 identifies the portions of the water column that we used to compare between field data and model predictions. We distinguished between the north-south (v) components and the east-west (u) components.

Dana Passage (Figure 77) has a stronger east-west (u) component than north-south (v) in both the field data and model predictions, consistent with its physical orientation. Predicted phasing agrees well with field data. However, the model overpredicts the smaller northerly velocity components compared with the observed data. Pickering Passage (Figure 78) also has a stronger east-west component in both the field data and model predictions.

Carr Inlet velocities (Figure 79) low velocities overall but also reflect significant east-west components compared with the north-south in both the model and the data. However, the model generally overestimates the northerly velocities. Case Inlet (Figure 80) exhibits a lower east-west component in the field data and model compared with Carr Inlet, and the model reproduces the overall low velocities.

In Budd Inlet, nearly all of the energy is in the northerly velocity components (Figure 81). The Budd West east-west (u) components are underpredicted in the model, likely because the model does not reproduce the fine-scale phenomenon indicated in Budd Inlet (Roberts et al., 2008b).

The observed velocities confirm the overall phasing of the tide and relative cross-inlet components. The model cannot resolve the fine-scale complexities captured in the ADCP measurements because each layer is thicker than 1 m and horizontal grid cell dimensions are nominally 500 m. However, ADCP data binned at the same resolution as the model grid cells provide data for quantitative comparisons, and the model performs well. The detailed ADCP data also provide a qualitative sense of the vertical and temporal complexity at the deployment locations.
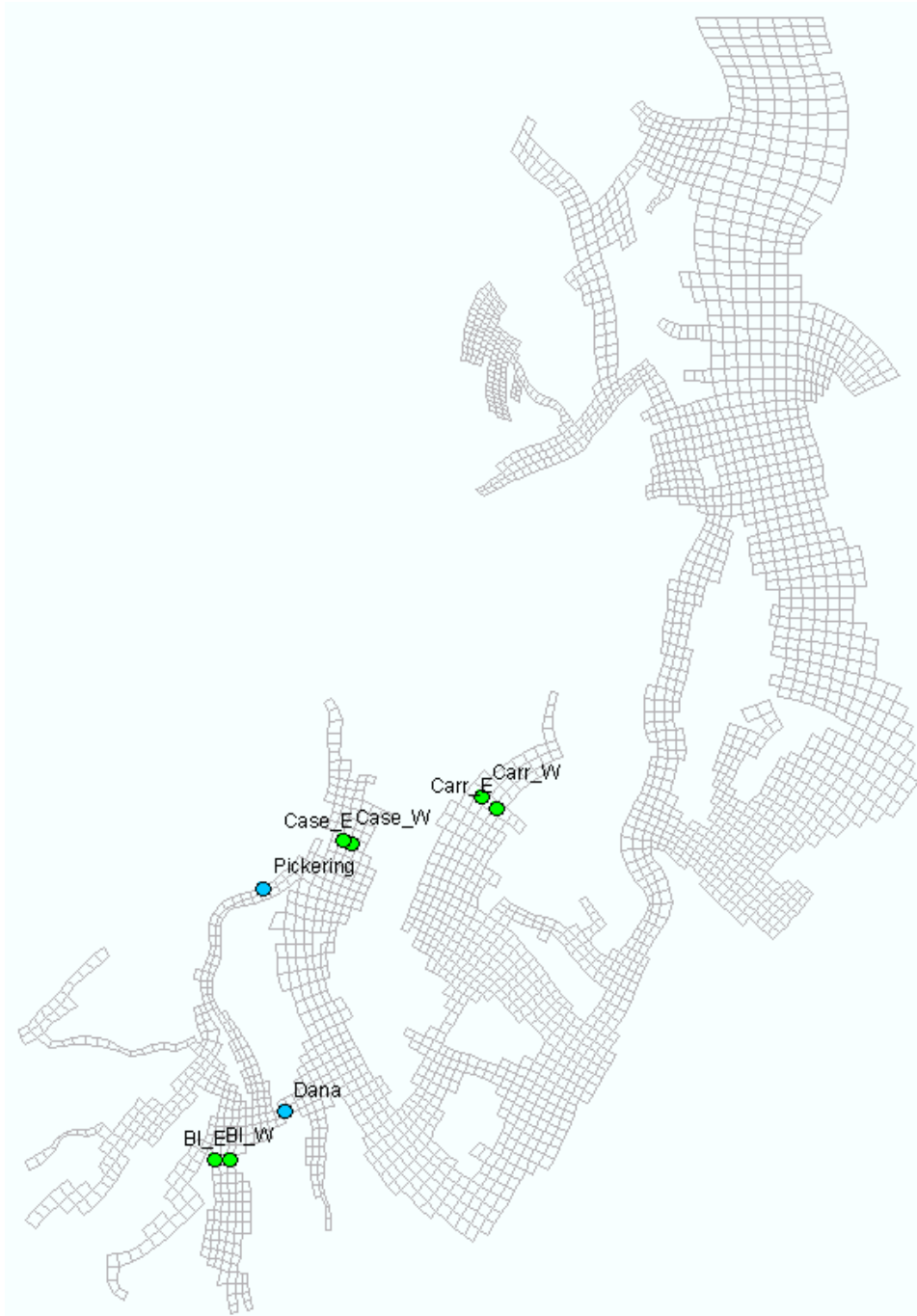
Figure 75. Locations for comparisons between model output and measured current velocities from bottom-mounted ADCP deployments during both calibration and confirmation.
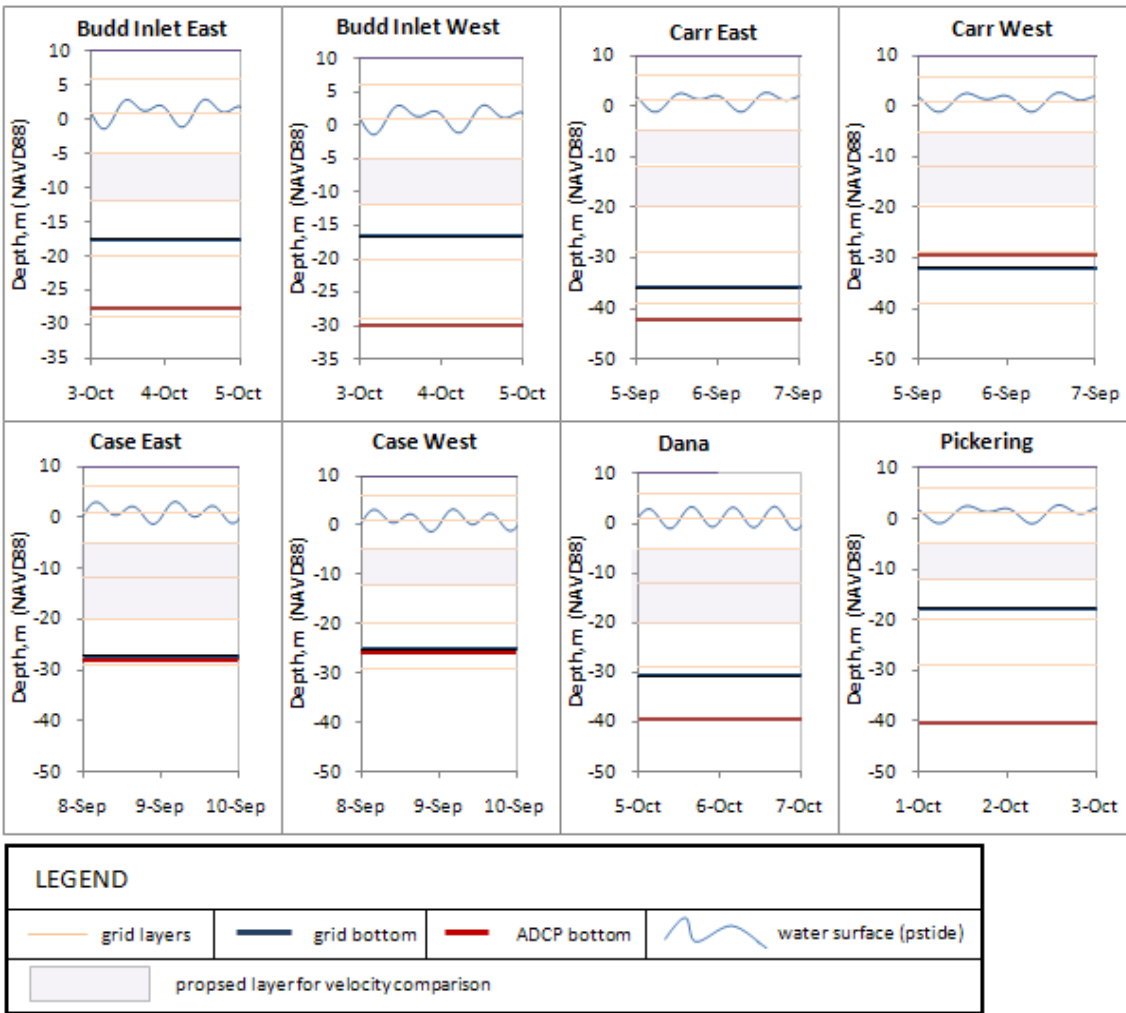
Figure 76. Actual (at ADCP location) and model (layer average) water column depths and selection of layer for current velocity comparisons.
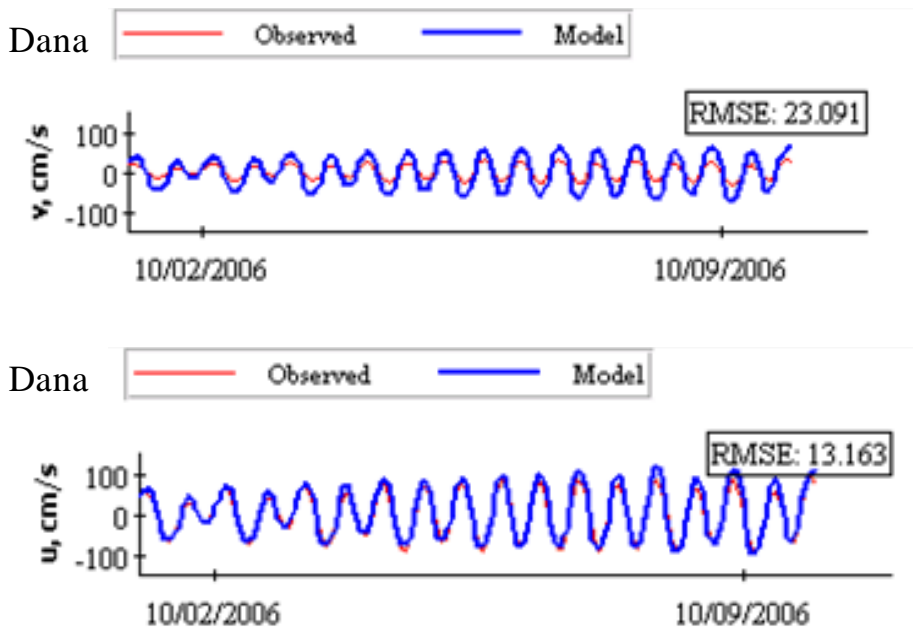
Figure 77. Dana Passage surface layer velocity comparison between the model and data for the northerly (v) and easterly (u) velocity components during the calibration period.
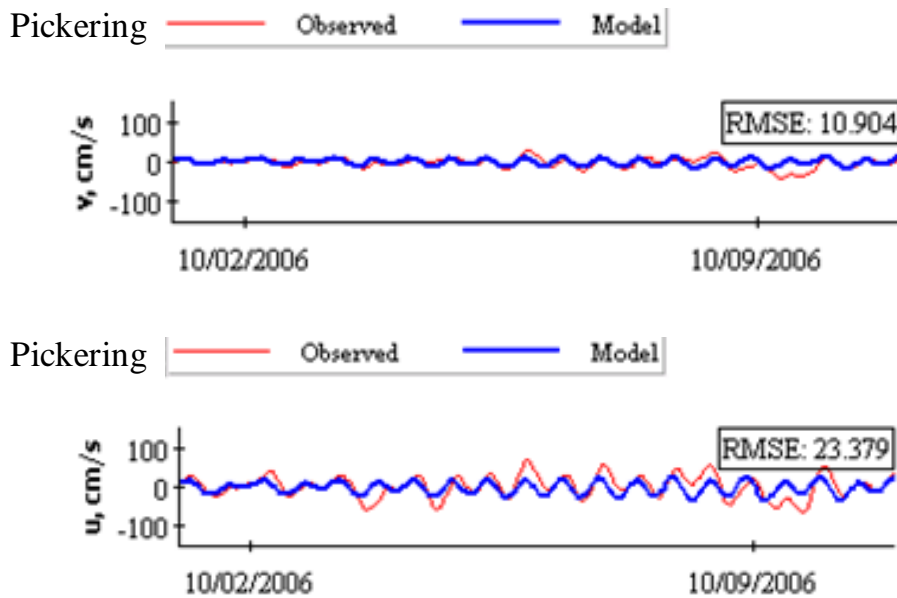
Figure 78. Pickering Passage surface layer velocity comparison between the model and data for the northerly (v) and easterly (u) velocity components during the calibration period.
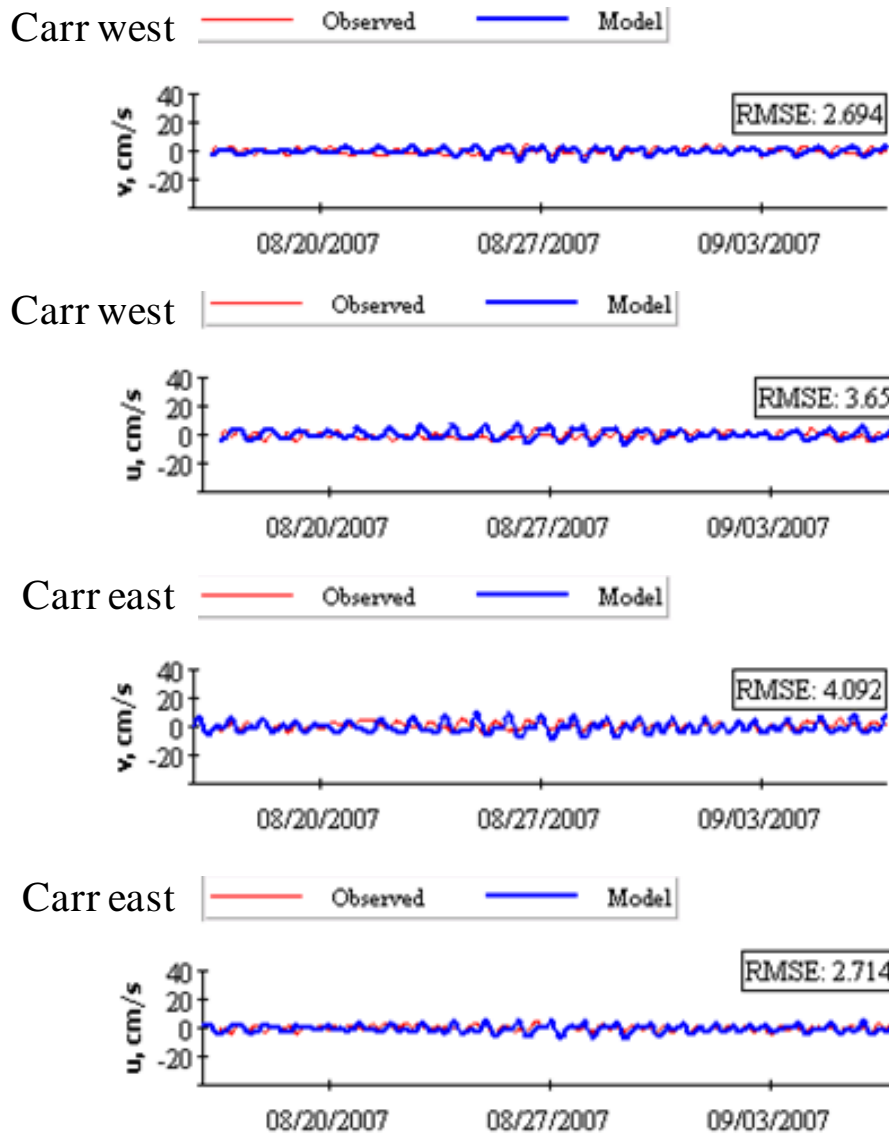
Figure 79. Carr Inlet west and east surface layer velocity comparison between the model and data for the northerly (v) and easterly (u) velocity components for the confirmation period.
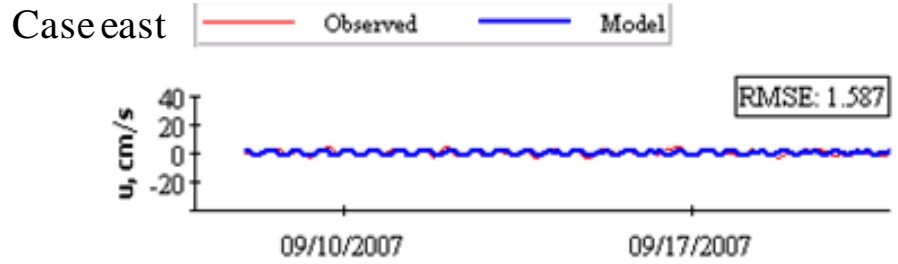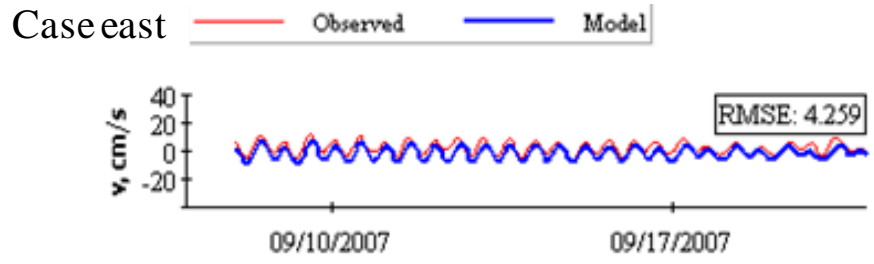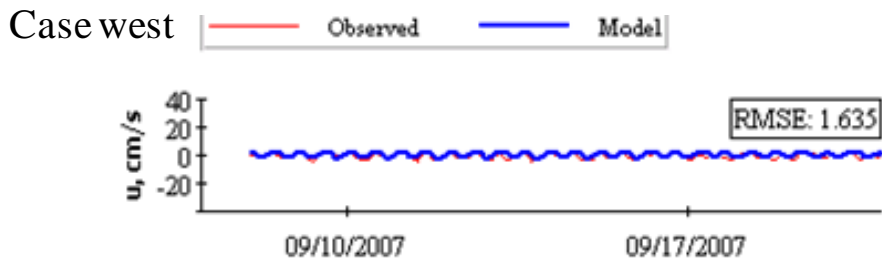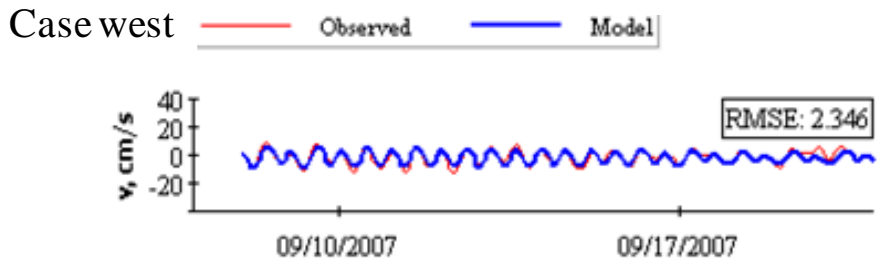
Figure 80. Case Inlet west and east surface layer velocity comparison between the model and data for the northerly (v) and easterly (u) velocity components for the confirmation period.

Budd west

Budd west
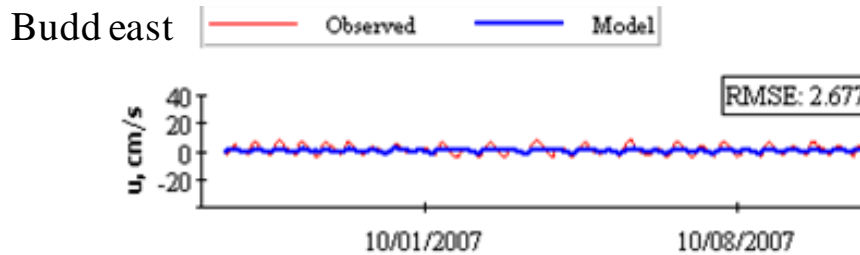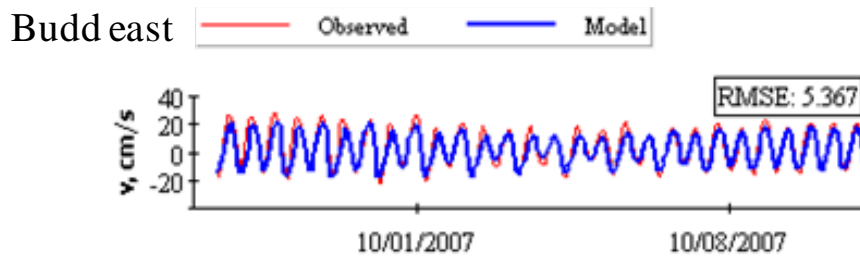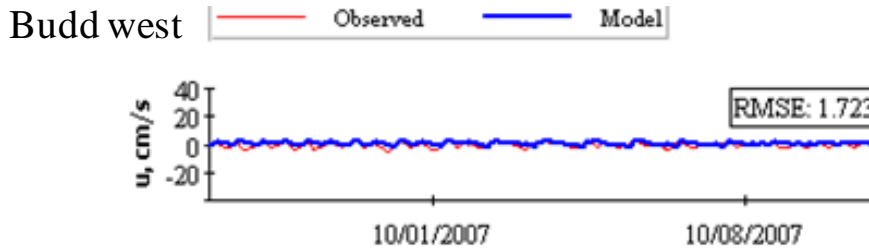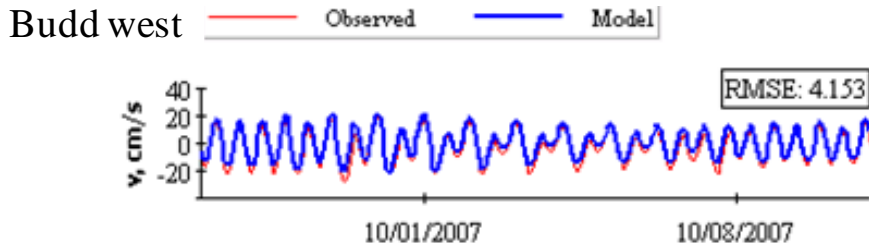
Budd east

Budd east

Figure 81. Budd Inlet west and east surface layer velocity comparison between the model and data for the northerly (v) and easterly (u) velocity components for the confirmation period.

Surface Currents

Once the model was compared with observed velocity data, we evaluated surface currents during strong and weak ebb and flood tides. We compared the results with surface current patterns developed with Tide Prints (McGary and Lincoln, 1977). Tide Prints was developed with the physical Puget Sound model using time-lapse photos of floating beads. The 2-dimensional figures represent typical strong and weak ebb- and flood-tide conditions. We compared model output for a strong and weak ebb- and flood-tide condition in September 2006.

On a strong ebbing tide (Figure 82), Central Puget Sound surface currents in the main basin reflect northerly currents, with more quiescent waters in Elliott Bay, Sinclair and Dyes Inlets, quartermaster Harbor, and Commencement Bay. Strong surface currents are evident in the narrow passages of the Agate Passage, Port Washington Narrows, Rich Passage, and Colvos Passage. In South Puget Sound, the strong currents in Tacoma Narrows, Hale Passage, north and south of Anderson Island, Dana Passage, Hammersley Inlet, and Pickering Passage are well represented. The model also reproduces the quiescent waters of northern Carr and Case Inlets, Oakland Bay, and the southern ends of Totten, Eld, and Budd Inlets.

Strong flood tides (Figure 83) produce similar patterns of varying quiescent and strong currents as well as the zones of convergence and divergence from Tide Prints. The model predicts that Colvos Passage floods to the south under this particularly strong event.

Under weak ebb (Figure 84) and flood (Figure 85) tidal exchanges, velocities are much lower in both Tide Prints and as predicted by the model. Quiescent waters extend further from land in the inlets of South Puget Sound. While diminished, surface currents through the narrow inlets are larger than those in the more quiescent bays. Under a weak flood tide, Colvos Passage floods to the north.

The model predicts the overall surface current patterns, including relative magnitude and direction, well.
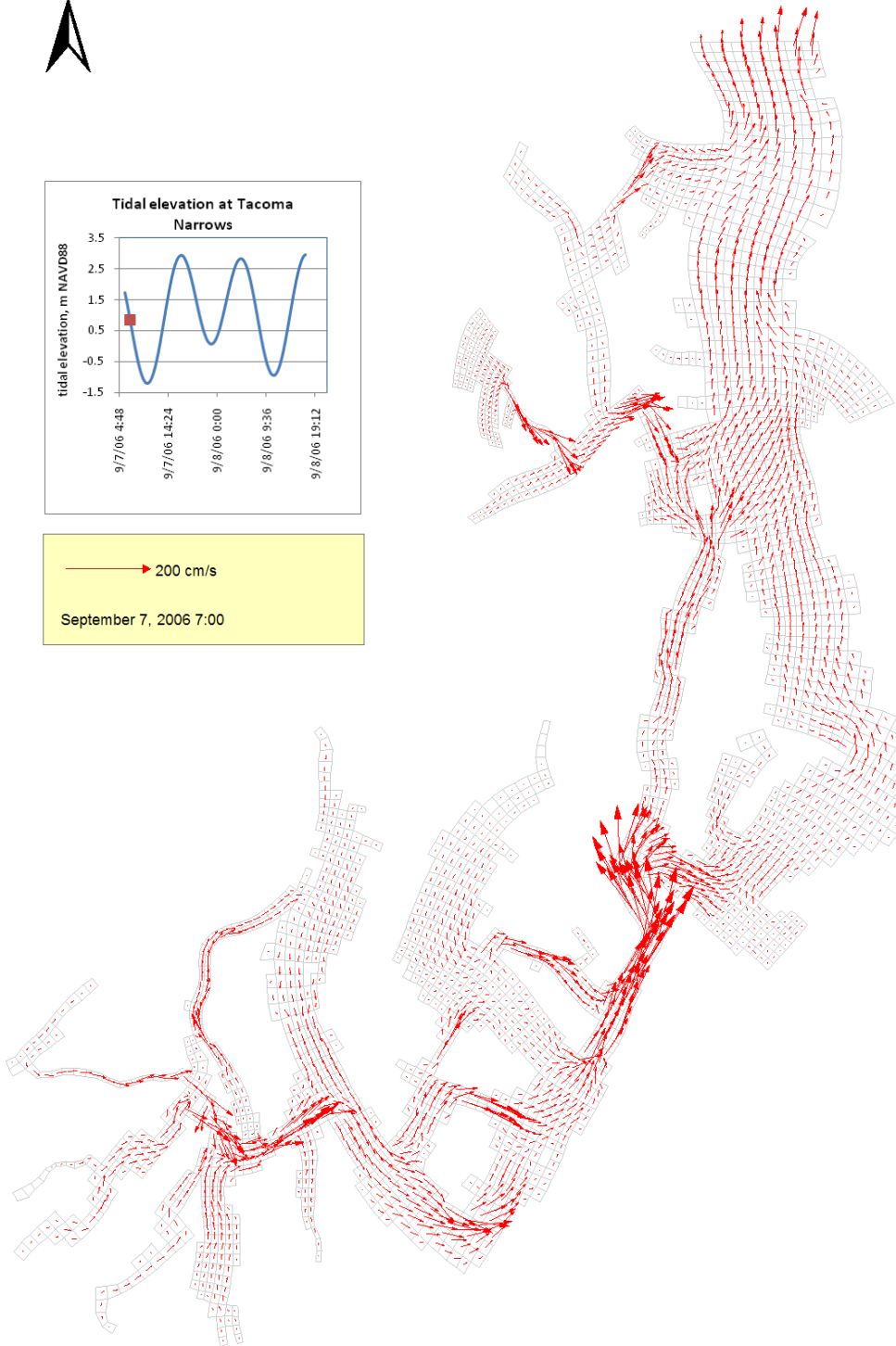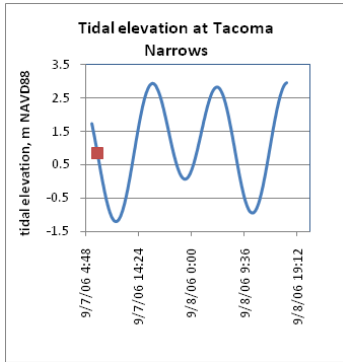
Figure 82. Surface current patterns during a strong ebb tide.
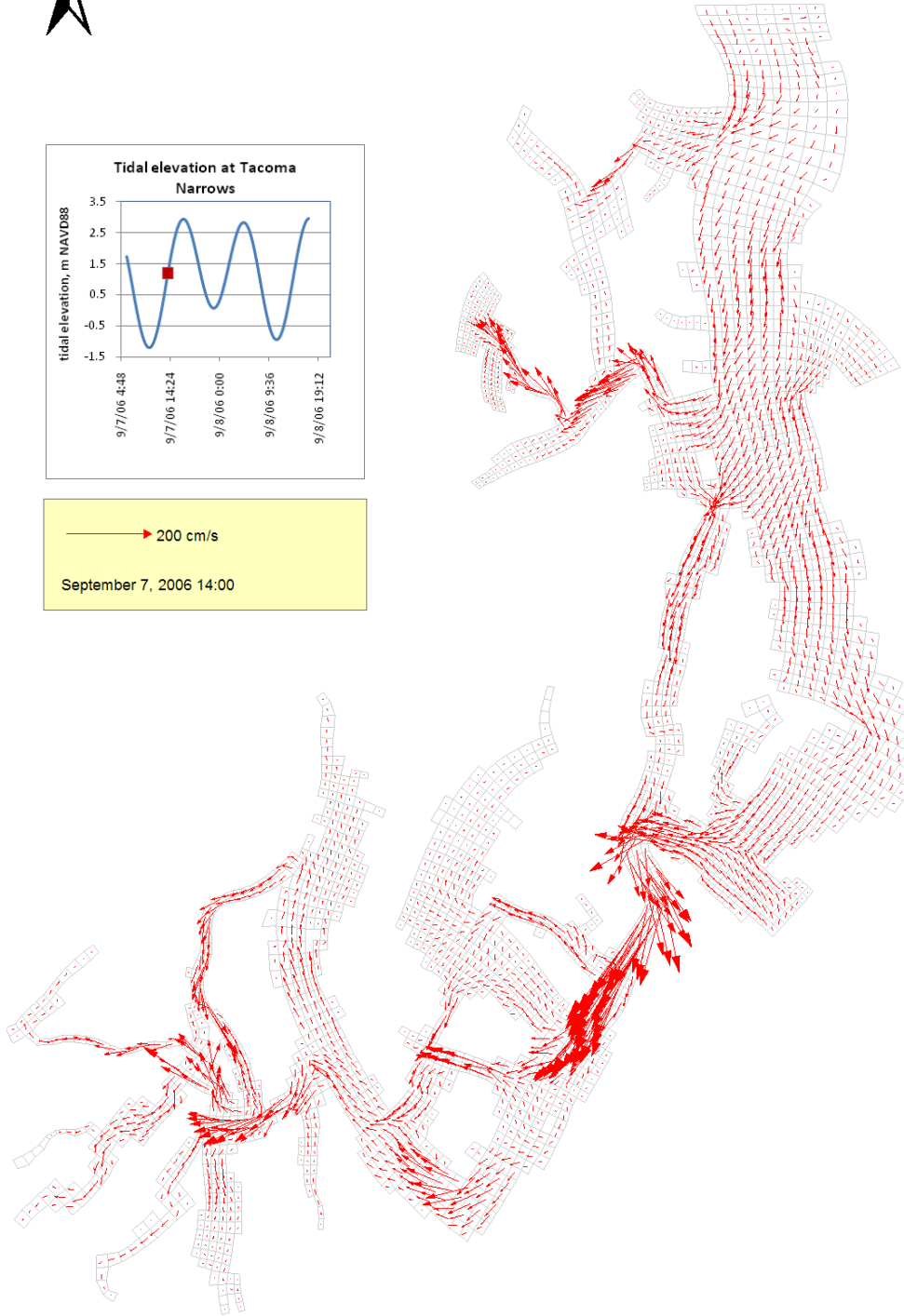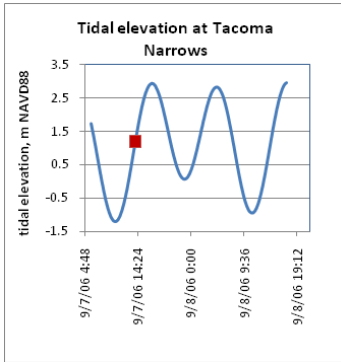
Figure 83. Surface current patterns during a strong flood tide.
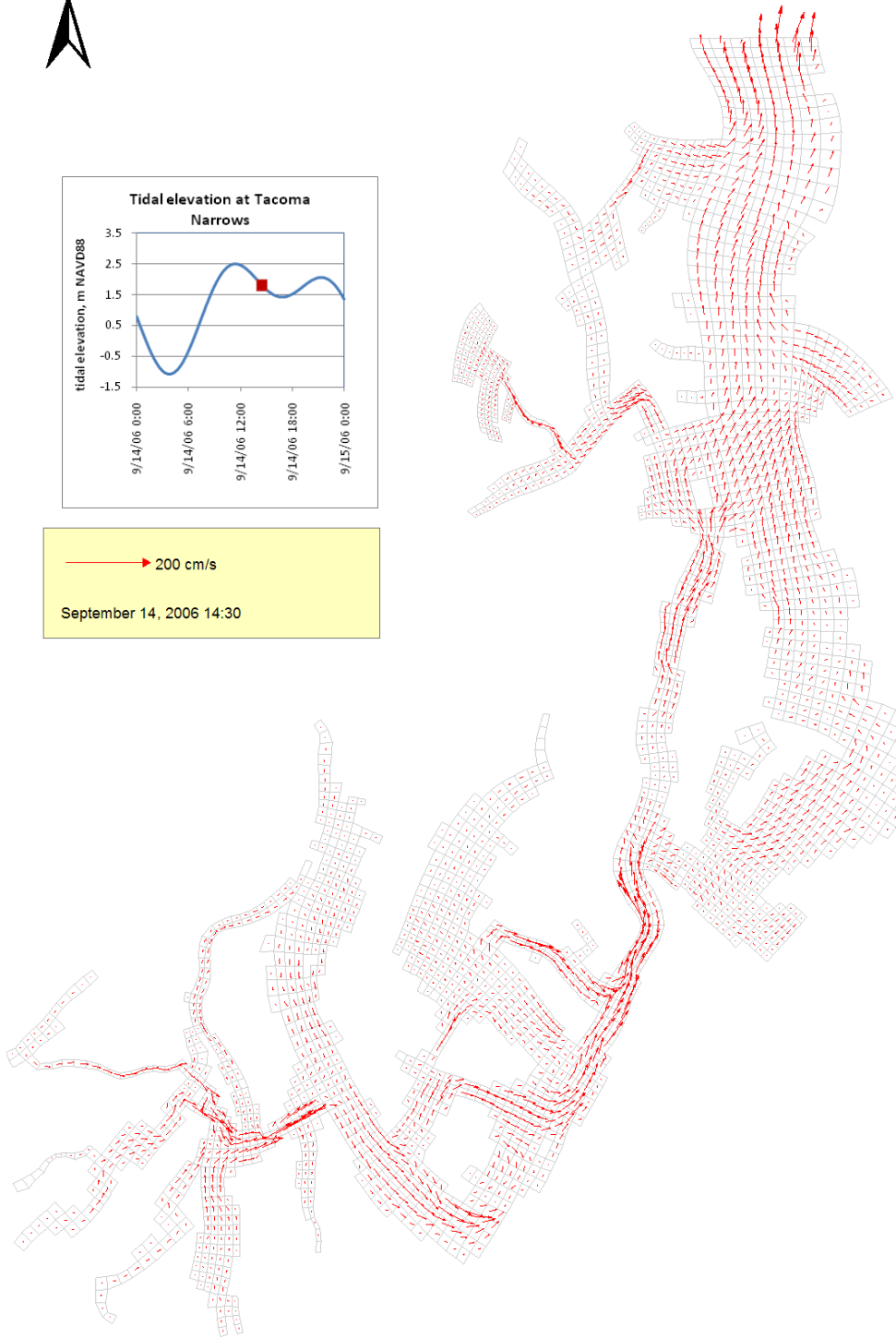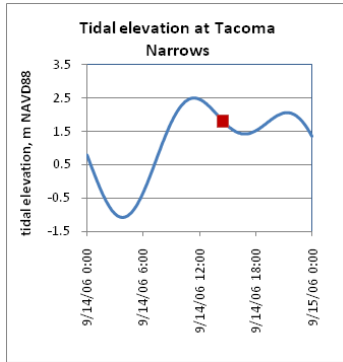
Figure 84. Surface current patterns during a weak ebb tide.
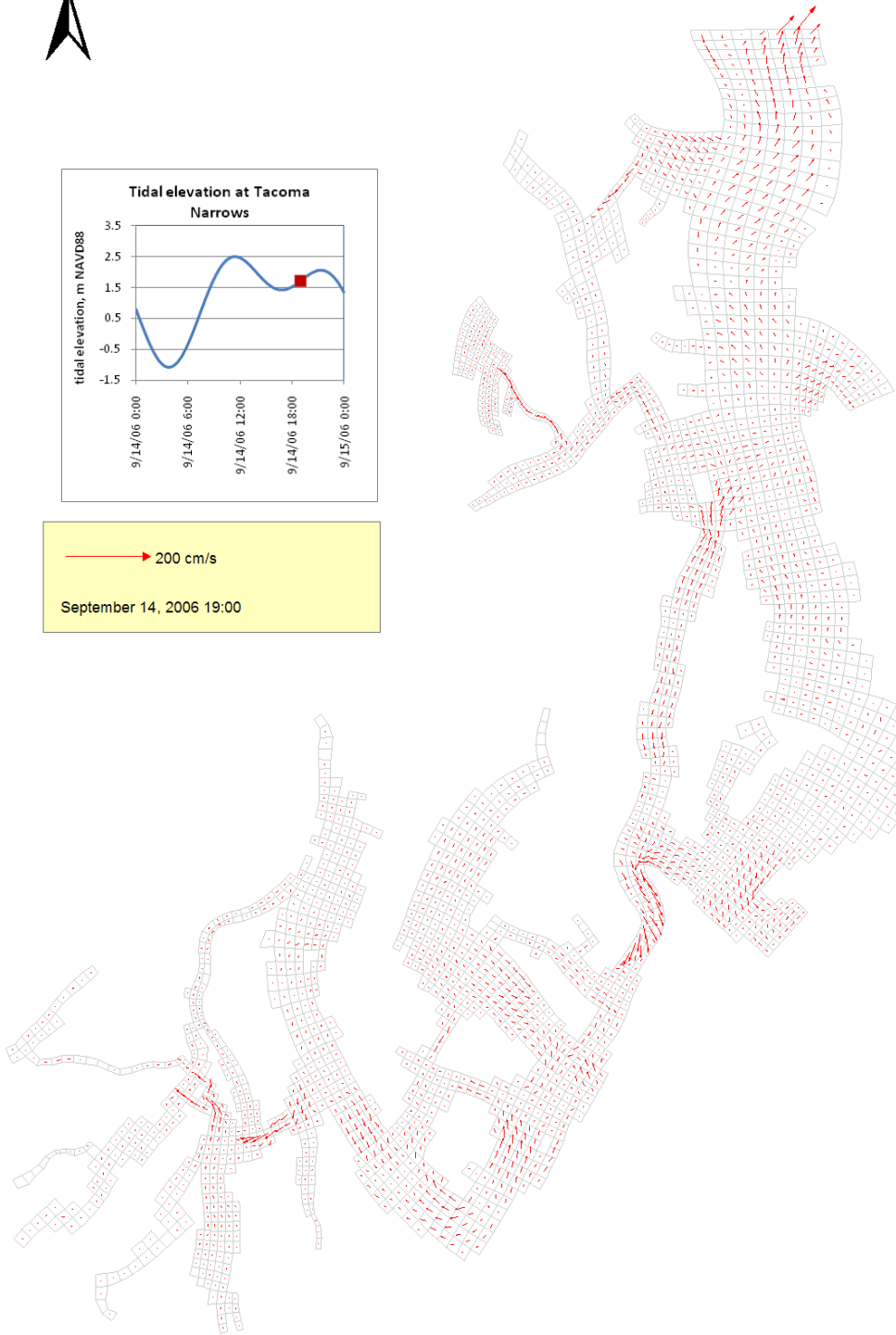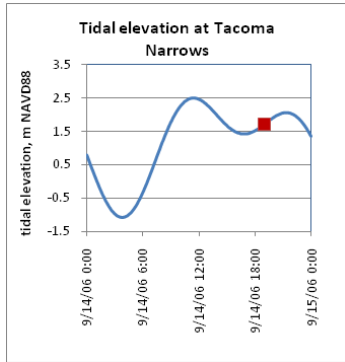
Figure 85. Surface current patterns during a weak flood tide.

Sensitivity Analyses

While only monthly data are available, the northern marine boundary conditions are sufficient for the purposes of this project. We tested the uncertainty in these boundary conditions by adding and subtracting 2°C and 1 psu to the monthly profiles and comparing predicted values within both Central and South Puget Sound. The area influenced by these perturbations was limited to the immediate vicinity of the northern boundary and did not influence the primary area of interest in South Puget Sound.

South Puget Sound Flushing Times

The amount of time water parcels and constituents in the water remain in a given geographical area is fundamental to understanding water quality. However, there is no single agreed-upon method for doing so (Monsen et al., 2002). Flushing time, age, and residence time have been used synonymously to describe how long a water parcel stays in a water body. Different mathematical approaches produce order-of-magnitude differences in the resulting time calculations.

The simplest flushing time estimate, T_{f1}, is simply the volume (V, m^3) divided by the net exchanges (Q, cms):

$$T_{f1} = \frac{V}{Q}$$

The equation can be modified to account for just the intertidal volume and the reflux of water at the boundary of the user-defined volume:

$$T_{f2} = \frac{VT}{(1-b)P}$$

Where V is the total volume, P is the volume of the tidal prism between high tide and low tide, T is the tidal period, and b is the reflux factor that varies from 0.0 to 1.0. The flushing time for South Puget Sound is 4.7 days using a reflux factor of 3% and tidal period of 12.2 hrs (University of Washington, 1971). This approach neglects the freshwater contribution.

However, the effective flushing time of South Puget Sound is longer than the simple T_{f1} or T_{f2} calculations. First, physical processes along the shallow entrance sill just southwest of the Tacoma Narrows impede flow and increase the residence time (Seim and Gregg, 1997). Flood tides transport some of the same water that exited on the previous ebb tide in a process called reflux. Second, estuarine flow leads to two-layer flow that isolates the lower layer and increases flushing time. A third approach to estimate flushing based on a two-layer salt balance (Friebertshauser and Duxbury, 1972) produces longer flushing times of 28 to 174 days (average annual of 56 days) than those derived from simple tidal volume replacement because of estuarine

circulation. Babson et al. (2006) report simple T_{f1} (V/Q) residence time of 19 to 33 days for South Puget Sound. They used a simple two-layer box model to estimate residence time as the ratio of basin volumes to estuarine transport flows.

Another approach is following a tracer concentration in a waterbody treated as a continuously stirred tank reactor (CSTR), where the tracer is instantly mixed throughout the reactor. The concentration of the tracer at the outlet is described as a simple exponential equation:

$$C(t) = C_o e^{-t/T_{f3}}$$

Where C(t) is the concentration at any time t, C_o is the initial concentration, T_{f3} is the flushing time, and t is the time. T_{f3} can be estimated as the slope of a best-fit exponential curve drawn through a time series of tracer concentrations. This approach accounts for not just advection, as estimated by the tidal prism methods, but also dispersion. Flushing time is calculated for an entire water body as one value constant over the water body. Functionally, this approach estimates the time to reduce the initial tracer to 37% (1/e) of the initial tracer concentration. A final approach is simply the time required for a tracer to reach 10% (1-log reduction) or 1% (2-log reduction) of the initial tracer concentration, depending on what time scales are most important.

We evaluated flushing time by filling portions of South Puget Sound with a simulated dye tracer. We first evaluated patterns throughout South Puget Sound by filling the entire region southwest of the Tacoma Narrows (Figure 86). Figure 87 presents the time series of layer-averaged[2] tracer concentration time series at the Tacoma Narrows and 12 other grid cells throughout South Puget Sound (Figure 87). The time to reach 1/e (37%) of the initial tracer concentration ranges from 2 to 260 days.   Figure 88 presents the dye concentration contours at the end of the simulation to illustrate spatial patterns.

We also evaluated flushing time on an inlet-by-inlet basis. To evaluate inlet-specific flushing time and spatial variability within smaller regions, we filled each of five small inlets with dye tracer. Figure 89 presents a snapshot of layer-averaged dye concentration after nearly 36 days to illustrate the spatial patterns within these inlets. Higher concentrations remain after 36 days at the heads of each of the inlets, where exchanges with South Puget Sound are lowest. Given the large variation within an inlet, an inlet-average value must be interpreted carefully.

Because different methods used to quantify flushing time previously produce such highly variable results (4.7 to 174 days), comparing an absolute flushing time for South Puget Sound is not appropriate. However, the model confirms that when estuarine circulation is considered, residence times on the order of several months are reasonable and comparable to the range from previous salt-balance estimates. Also, tracer concentrations at the Tacoma Narrows will be strongly affected by the tidal stage at the beginning of the tracer run. Flushing time will vary seasonally due to changing freshwater contributions that affect net transport and changing tidal prisms.

---

[2] Average of all layers that does not volume-weight varying layer thickness. For illustration purposes.
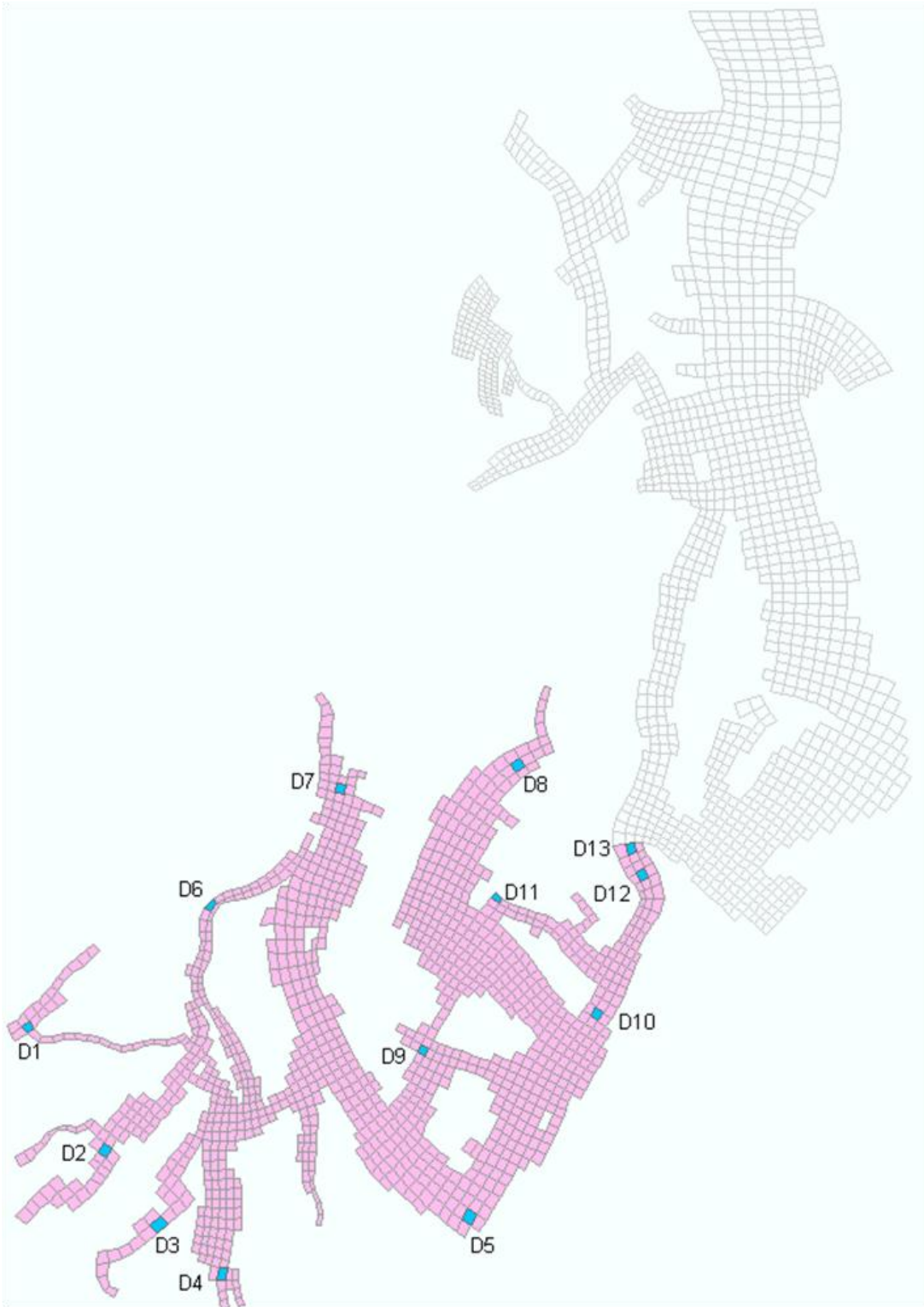
Figure 86. South Puget Sound region with dye added to estimate flushing times.
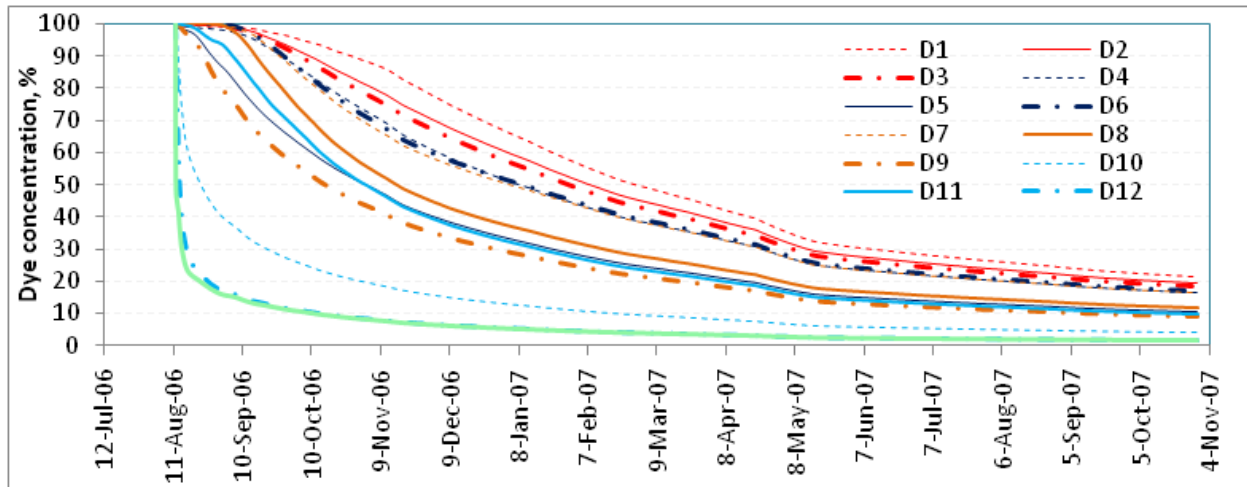
Figure 87. Tracer time series at Tacoma Narrows and 12 other locations shown in previous figure used to estimate flushing times. Layer-averaged tracer concentration does not account for varying layer thickness.
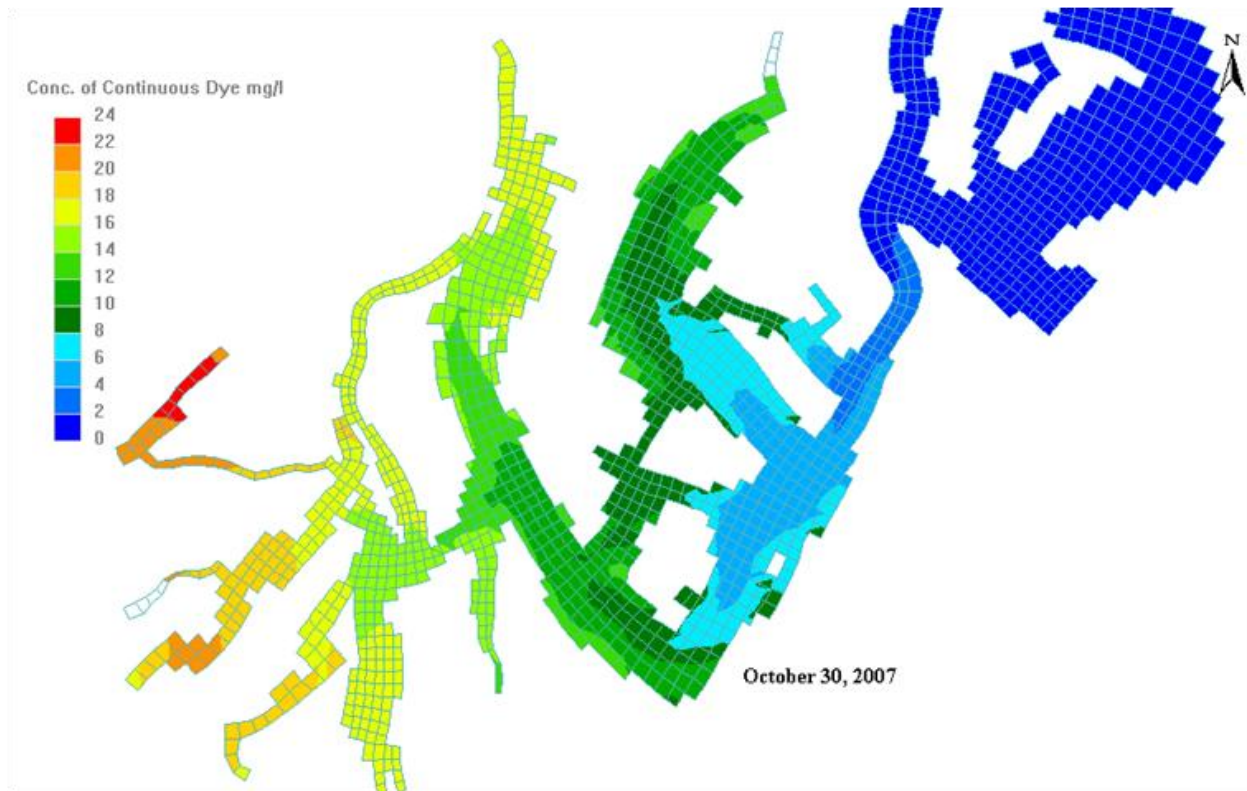

Figure 88. Spatial patterns of dye concentration at the end of the simulation in the previous figure.

Figure 89. Snapshot of layer-averaged dye concentration about a month after dye release throughout each inlet.

Simulated Dye Releases

The next phase of model development involves the calibration of the complete water quality model in GEMSS, with which we will determine whether point and nonpoint sources affect water quality in South Puget Sound. As an interim indicator of areas influenced by rivers and wastewater treatment plants, we simulated dye releases from all river inflows and wastewater facilities with flows >1 mgd. River flows were added to the surface layer while wastewater treatment plant effluent discharges to the near-bottom layer. (All wastewater facilities will be included in the water quality model, including those <1 mgd.)

The model simulated continuous virtual dye releases equivalent to 30 mg/L concentration with neutral buoyancy beginning July 1, 2006. The model uses time-varying daily river flows and wastewater facility discharges. Table 8, however, lists the mean September 2006 flows for rivers >10 cfs and treatment plants > 1 mgd to indicate relative discharge rates. Figures 90 and 91 identify the discharge locations for the rivers and wastewater treatment plants, respectively.

Table 8. Mean September 2006 discharges for all rivers >10 cfs and wastewater treatment plant discharges >1 mgd.

River	Flow rate (cfs)	Treatment plants	Flow rate (cfs)
Puyallup River	1272	West Point	136
Nisqually River	499	South King	86
Lake Washington watershed	395	Simpson Tacoma (process)	28
Green River	340	Chambers Creek	25
Sinclair/Dyes watershed	112	Tacoma Central	22
Deschutes River	61	LOTT	13
Goldsborough Creek	42	Lakota	7.4
Chambers Creek	32	Bremerton	6.4
Burley Creek	20	Midway	6.0
McAllister Creek	19	Tacoma North	5.6
Mill Creek	18	Central Kitsap	5.2
Sherwood Creek	18	Fort Lewis	4.3
Sequalitchew Creek	17	Miller	3.9
Cranberry Creek	17	Redondo	3.3
Kennedy Creek	14	Salmon	2.8
Curley Creek	14	Port Orchard	2.1
Rocky Creek	14	Shelton	2.1
Skookum Creek	12	Gig Harbor	1.1
Coulter Creek	12		
Minter Creek	12		
Olalla	11		
Hylebos	11		
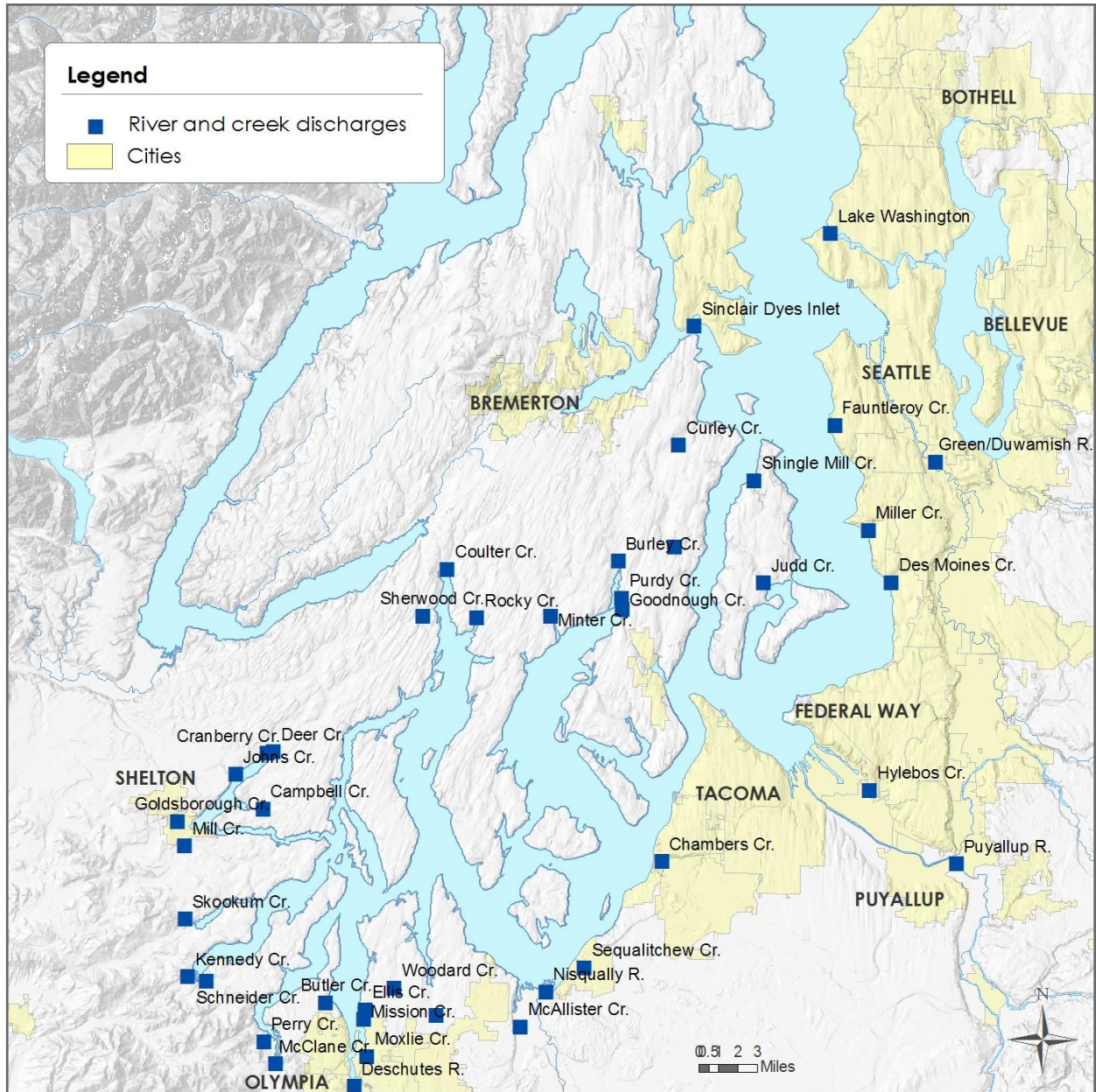
Figure 90. River discharges included in the virtual dye simulation.
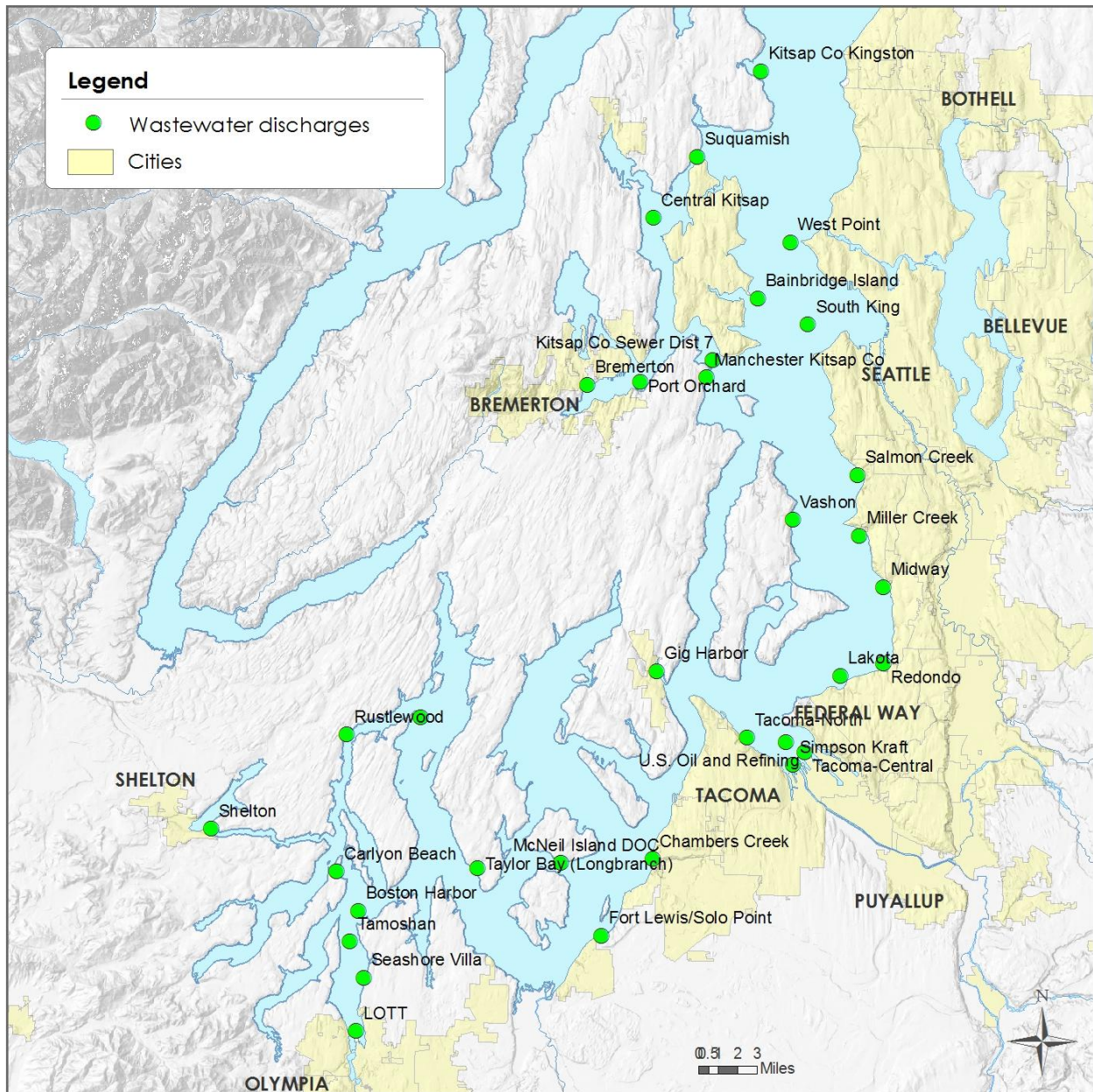
Figure 91. Wastewater discharges to South and Central Puget Sound. Only those listed in Table 8 were included in the virtual dye simulation; all discharges will be simulated in subsequent water quality modeling.

The model simulates virtual tracer concentrations throughout the model domain in four separate runs, one each for rivers and treatment plants in either South or Central Puget Sound, distinguished by the Tacoma Narrows. Maximum dye concentrations can occur near the surface or near the bottom, but results are represented as a water column maximum value from any model layer. Also, the marine flow trajectory reverses with the flood or ebb tide phase and varies with the current velocity.

Because tracer concentrations decrease rapidly away from inflows, the figures in this section summarize model predictions as contours of the minimum dilution factors to illustrate how the

freshwater moves through the marine system. Where predicted concentrations are highest, the dilution factor is lowest, and the dilution factor incorporates order of magnitude changes in dye concentration. A dilution factor of 10 means the maximum tracer concentration is $1/10^{th}$ or 10% of the initial inflow tracer, and a dilution factor of 100 corresponds to a maximum tracer concentration of $1/100^{th}$ or 1% of the initial value.

We used the Puget Sound box model (Babson et al., 2006; Sackmann, 2009) to evaluate how long dye released into South or Central Puget Sound would continue to build up to a pseudo-steady-state condition. While flushing times for South Sound are on the order of a month, box model simulations indicated that the dye continues to build up for several months. We selected September 2007 for output comparison to represent a critical condition for two reasons. First, the model run begins July 1, 2006, and the dye would not reach pseudo-steady state by the September 2006 critical period. Second, although the buildup reaches pseudo-steady state in the winter months, this is not a time of year when low dissolved oxygen levels occur. Therefore, we continued the dye releases through October 2007 and investigated the levels in September 2007.

Figure 92 summarizes tracer releases from South Puget Sound rivers. Lowest dilution levels correspond to the highest predicted tracer concentrations nearest to the river inflows. Maximum concentrations occur near the water surface close to the river inflows, but river tracers extend throughout South Puget Sound. At least some tracer exits through Tacoma Narrows with a dilution level on the order of 100:1 and that water tends to travel north up Colvos Passage.

Tracer from South Puget Sound wastewater treatment plants also is highest and the dilution levels lowest closest to the inflows (Figure 93). Lowest dilution levels, which reflect highest tracer concentrations, occur in Budd Inlet and Hammersley Inlet/Oakland Bay, where wastewater discharges to quiescent waters. Tracers from the Chambers Creek and Fort Lewis wastewater discharges produce more rapid dilution even those facilities have higher flow rates, likely due to the higher water exchanges. Beyond the immediate vicinity of the wastewater treatment plant effluents, maximum concentration and minimum dilution occur within the top several model layers due in part to the overall shallow water at the discharges and fewer model layers. Wastewater effluent buoyancy may also contribute.
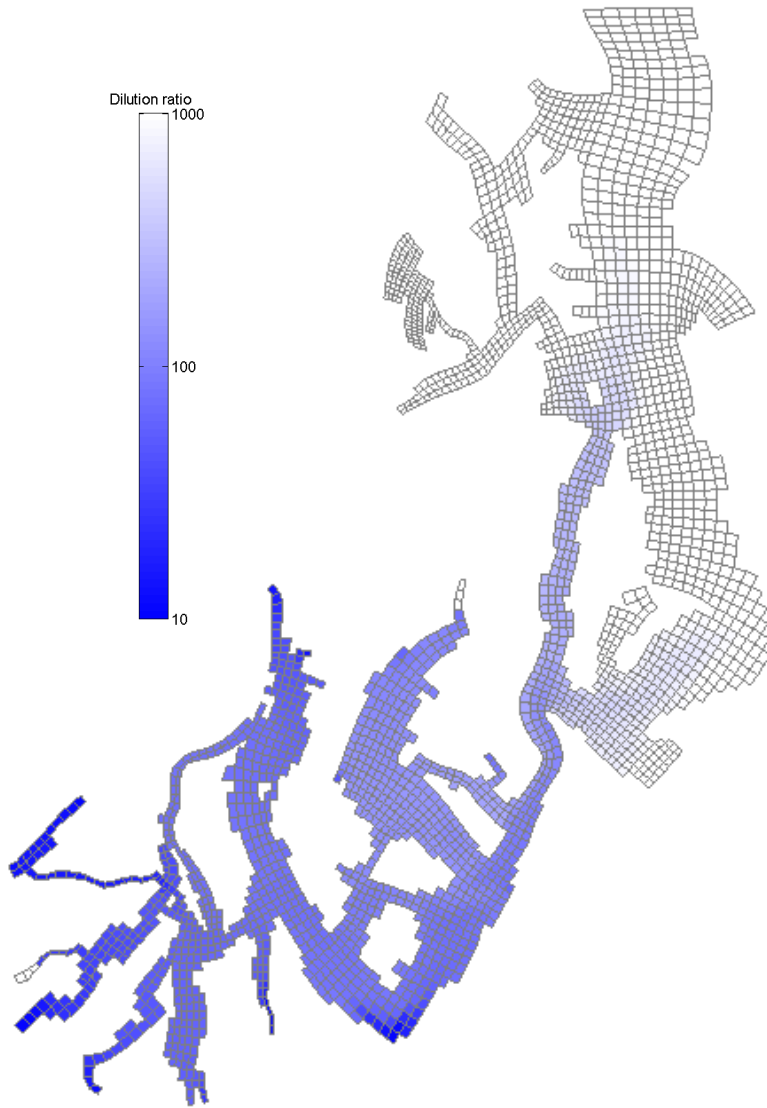
Figure 92. Dilution factors (10 to 1000 scale) calculated from maximum water column dye concentrations for South Puget Sound river tracer simulations (September 2007).
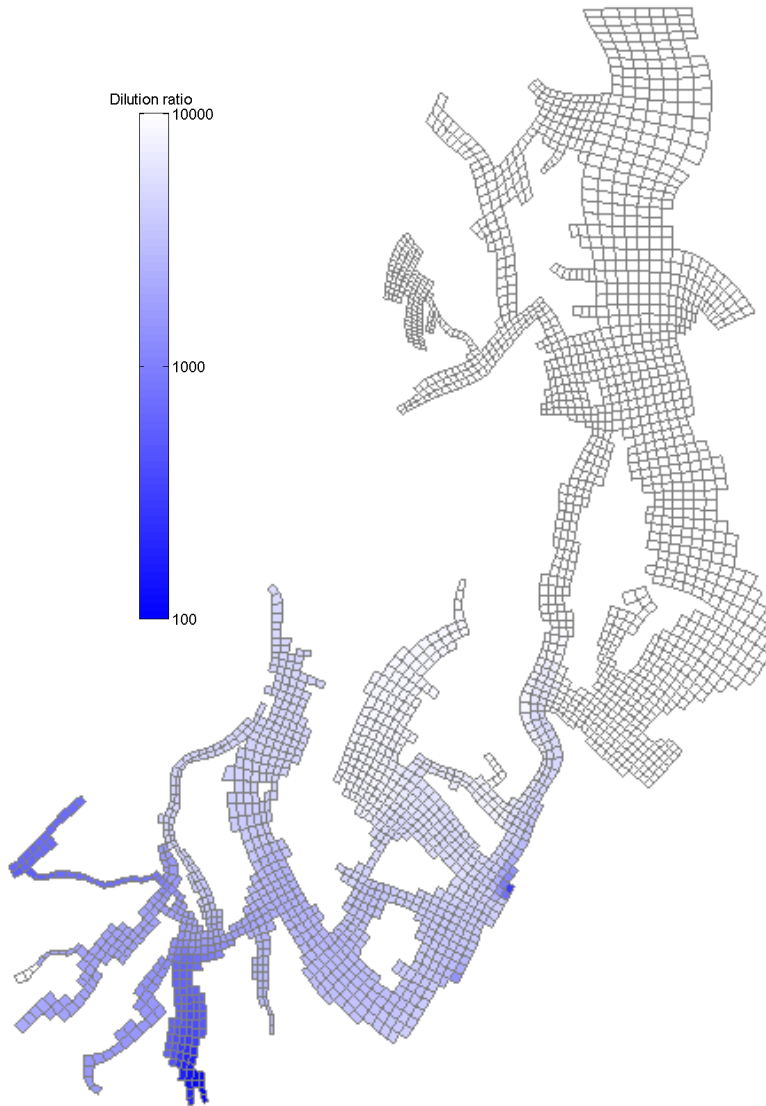
Figure 93. Dilution factors (scale 100 to 10,000) calculated from maximum water column dye concentrations for South Puget Sound wastewater discharge tracer simulations (September 2007).

Next, virtual tracer was added to rivers discharging to Central Puget Sound (Figure 94). Lowest dilution (highest tracer concentration) occurs in Commencement Bay and Elliott Bay, where the Puyallup River and Lake Washington watersheds produce high inflow volumes. On flood tides, at least some Central Puget Sound river tracer enters South Puget Sound. Lowest dilution occurs in the surface waters of Central Puget Sound, and the tracer that enters South Puget Sound tends to remain in the surface layers with uniform dilution levels.
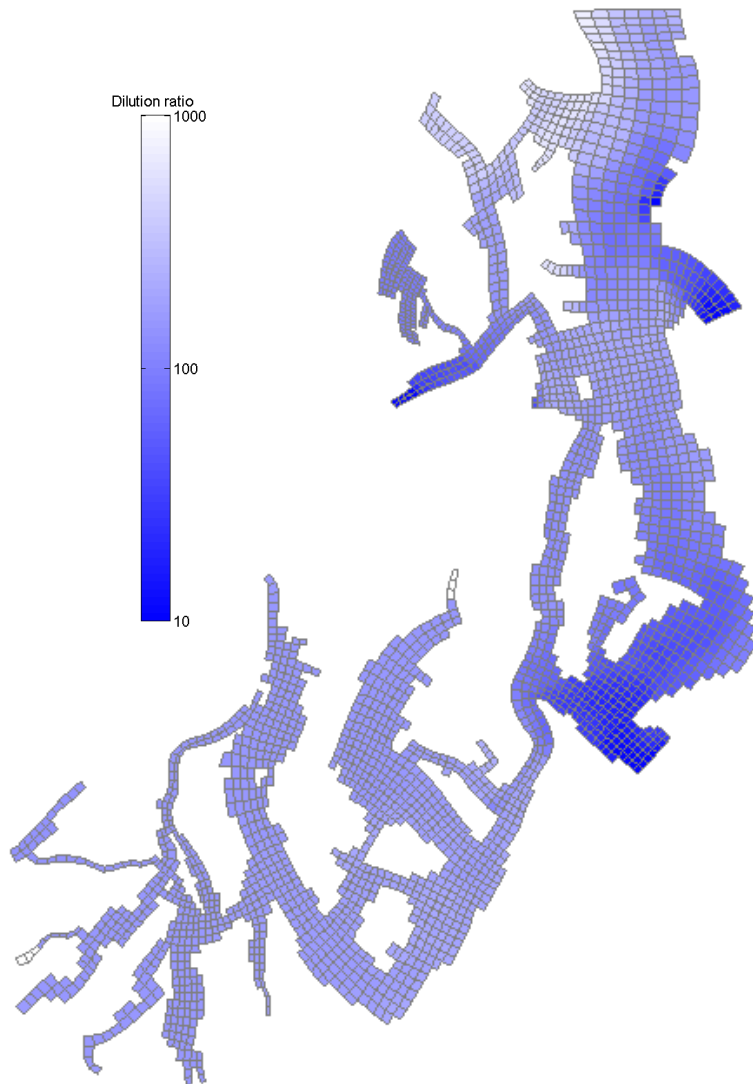
Figure 94. Dilution factors (10 to 1000 scale) calculated from maximum water column dye concentrations for Central Puget Sound river tracer simulations (September 2007).

Wastewater discharges to Central Puget Sound produce the highest concentrations and lowest dilution nearest the discharges in near the population centers of Seattle, Tacoma, and Bremerton (Figure 95). Nearest the wastewater discharges, maximum concentrations and minimum dilution occur in deeper model layers, consistent with near-bottom effluent discharges. However, some dye reaches surface layers within Central Puget Sound. At least some tracer from the Central Puget Sound wastewater discharges enters South Puget Sound on flood tides. Dye concentrations produced in South Puget Sound by Central Puget Sound sources are relatively uniform and reach maximum levels in the lower water column.
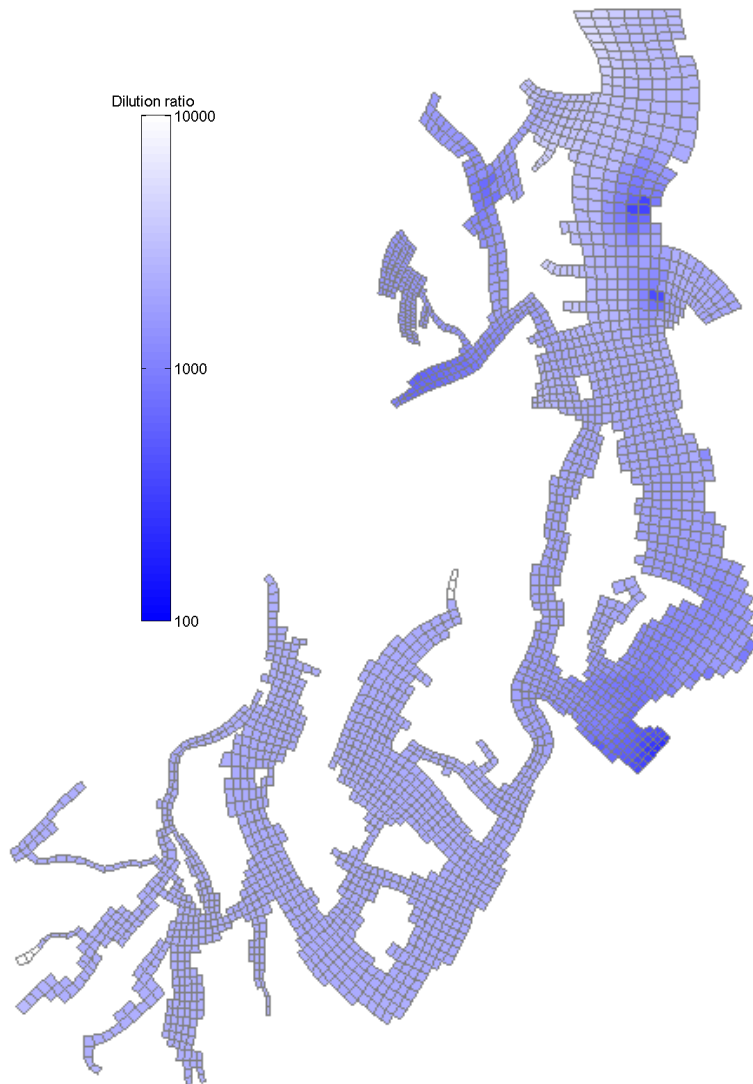
Figure 95. Dilution factors (100 to 10,000 scale) calculated from maximum water column dye concentrations for Central Puget Sound wastewater discharge tracer simulations (September 2007).

For these initial tracer simulations, all wastewater was added to a single near-bottom model grid cell with zero salinity. Each discharge would be instantly mixed throughout a single grid cell, the finest scale that can be resolved with this farfield model. In the case of the largest wastewater discharge to the model domain (West Point), the plume is trapped in the lower water column and does not rise to the surface. This finding is consistent with detailed nearfield modeling conducted with specialized plume models that indicates the plume likely would trap low in the water column (Bruce Nairn, personal communication). Plume trapping characteristics will be evaluated during water quality modeling to ensure the model describes the fate and transport of wastewater discharges.

The purpose of the tracer simulations was to determine whether Central Puget Sound sources have the potential to influence South Puget Sound water quality. Because at least some of the

simulated tracer released from Central Puget Sound rivers and treatment plants enters South Puget Sound during the critical period for low dissolved oxygen levels, we cannot rule out the influence of the Central Puget Sound sources.

Given the intricacies of nutrient transport and transformation within the marine environment, these results do not verify that Central Puget Sound nutrients influence South Puget Sound dissolved oxygen levels. This question must be addressed with the detailed water quality model currently under development. The water quality model will take into account where in the water column nutrients occur and whether or not the nutrients from human sources spur algae growth to the point that the dissolved oxygen water quality standards are violated.

Conclusions

The South and Central Puget Sound circulation model was calibrated to water surface elevations and temperature and salinity data throughout the model domain in 2006 and was confirmed using 2007 water surface elevations, salinity/temperature data, and current velocities. The circulation model performs well and provides the basis for the upcoming water quality model development.

Overall the model predicted water surface elevations well with a RMSE of <16 cm (<5% of the tidal range) throughout the model domain. Hammersley Inlet/Oakland Bay had a RMSE of 50 cm (10% of the tidal range) due to subtle shape complexities that could not be represented well enough by the model grid to describe this fine-scale area. However, the effects were limited in geographic area, and a separate water quality model is available should it be needed.

In addition to comparing the water surface elevations, we transformed the predicted elevations into tidal constituents represented by magnitudes and phases in the frequency domain. The model captures the magnitude and phasing of the five major tidal constituents well. Oakland Bay had the highest errors in the tidal constituents.

The complex shape and circulation patterns produce highly variable temperature and salinity patterns in the model domain, particularly in the surface layers that are influenced by both the meteorological and river boundary conditions. The model reproduces the spatial and temporal patterns in both the surface and near-bottom layers.

The model replicates salinity and temperature throughout the model domain well, although some sharp gradients could not be represented. For the calibration period, salinity results produced a RMSE of 0.6 psu near the surface and 0.4 psu near the bottom compared with field observations at 22 key stations. Temperature calibration produced a RMSE of 0.9°C near the surface and 0.5°C near the bottom. For the 2007 confirmation period, the overall RMSE was 0.6 psu and 0.8°C, with slightly higher errors in the surface compared with the bottom.

Profiles reproduced the seasonal and temporal patterns. Calibration produced RMSEs of 0.4 psu and 0.5°C, while confirmation produced RMSEs of 0.4 psu and 0.7°C. The cooler 2007 surface temperatures were somewhat overpredicted and spring salinities underpredicted compared with data.

Limited boundary condition sensitivity analyses were performed as part of model calibration and confirmation. Additional analyses may be performed as needed.

The model reproduces the cross-sectional averaged instantaneous current velocities recorded at key transects well, including relative magnitudes and phasing. However, several transect aspects were very different from model grid cell orientation, and the direction change likely contributed to differences between the data and model. Bottom-mounted current velocity data confirmed that the model predicts the phasing correctly in Carr, Case, and Budd Inlet. Some fine-scale phenomenon could not be reproduced, such as the east-west variations in Budd Inlet, likely due to the resolution of the model. However, these do not limit the applicability of the model.

Surface current velocities predicted by the model for strong and weak ebb- and flood-tide conditions well, including the relative magnitude and direction, compared with Tide Prints (McGary and Lincoln, 1977). Known features, such as quiescent waters and fast-moving passages, are reproduced by the model.

We applied the model to estimate flushing time for portions of South Puget Sound. Flushing time varied with location within South Puget Sound and is strongly influenced by the method used to calculate it. Flushing time is fastest near the Tacoma Narrows and decreases with distance away. However, flushing time for individual inlets relative to the rest of South Puget Sound is shorter.

We simulated the circulation of virtual dye released from rivers and wastewater treatment plants within South and Central Puget Sound. Based on predicted dilution levels derived from water column maximum dye concentrations, water from these sources exchanges through the Tacoma Narrows. We cannot rule out the influence of Central Puget Sound sources on South Puget Sound water quality, but the results are not sufficient to rule in an influence either given the complexity of nutrient transport and transformation within marine environments. The water quality model is needed to quantify the link between sources and water quality impairments.

Recommendations

We recommend that water quality model development proceed as follows:

1. The circulation model provides the basis for water quality model development. No further calibration or confirmation is necessary. The few areas that were difficult to describe with the circulation model are limited in spatial extent and do not limit model applicability to the overall objective.

2. We recommend model development proceed with the northern boundary established at the Edmonds location. An earlier phase of model development used sites near Alki Point as the northern boundary conditions. However, diluted Central Puget Sound sources reach South Puget Sound and must be considered in the water quality model.

While not necessary for the current effort, we recommend that future detailed model applications in other regions of Puget Sound consider the following:

- Continuous monitoring for temperature and salinity profiles at the model boundary would eliminate any questions of short-term phenomena such as upwelling that could affect water masses entering the model domain. Future Puget Sound-wide networks should consider potential model boundaries in the sampling design.

- Verifying water surface elevations against measured data that includes the effect of wind is very useful. In future modeling where no nearby station provides in situ data, short-term installations of pressure transducers in key locations could verify that wind is parameterized appropriately.

- Particularly in systems where wind plays a strong role, such as Hood Canal, a more extensive network of meteorological stations would be helpful. Our initial study design included the installation of meteorological stations to record wind and other variables near the marine waters. However, the data were not of sufficient quality to use and we relied on National Weather Service stations in South and Central Puget Sound to drive the model.

- Complex local mixing processes around Tacoma Narrows and Hope Island may be improved by site-specific studies. We considered using a finer grid cell in these areas. However, given the long computer runtime, a more detailed model grid would produce runtimes that would not be suitable to water quality scenario simulations.

Next Steps

The next step is to develop the water quality components of the model. We will use project data to develop nutrient and related loads at the northern boundary, river inflows, and wastewater discharges. We will continue to use 2006 as the calibration year and 2007 as the confirmation time period. The monitoring program increased in detail in 2007, but 2007 was an unusually wet and mild summer with higher dissolved oxygen levels than in 2006.

All river and wastewater discharges will be represented as a time series of nutrient loads, including the small wastewater plants that were not included in the initial tracer study.

References

Albertson, S.L., K. Erickson, J.A. Newton, G. Pelletier, R.A. Reynolds, and M.L. Roberts, 2002a. Summary of South Puget Sound Water Quality Study, Washington State Department of Ecology Publication No. 02-03-020. www.ecy.wa.gov/biblio/0203020.html.

Albertson, S.L., K. Erickson, J.A. Newton, G. Pelletier, R.A. Reynolds, and M.L. Roberts, 2002b. South Puget Sound Water Quality Study, Phase 1. Washington State Department of Ecology Publication No. 02-03-021. www.ecy.wa.gov/biblio/0203021.html.

Albertson, S.L., J.K. Bos, G. Pelletier, and M.L. Roberts, 2007a. Circulation and Residual Flow in the South Basin of Puget Sound, and its Effects on Near Bottom Dissolved Oxygen, GBPSRC, March 2007. Vancouver, BC.

Albertson, S., J. Bos, K. Erickson, C. Maloy, G. Pelletier, and M.L. Roberts, 2007b. Quality Assurance Project Plan: South Puget Sound Water Quality Study Phase 2: Dissolved Oxygen. Washington State Department of Ecology Publication No. 07-03-101. www.ecy.wa.gov/biblio/00703101.html.

Aura Nova Consultants, Brown and Caldwell, Evans-Hamilton, J. E. Edinger and Associates, Washington State Department of Ecology, and the University of Washington Department of Oceanography, 1998. Budd Inlet Scientific Study Final Report, prepared for the LOTT Partnership, Olympia, WA.

Babson, A.L., M. Kawase, and P. MacCready. 2006. Seasonal and interannual variability in the circulation of Puget Sound, Washington: A box model study. Atmosphere-Ocean 44(1):29-45.

Bos, J.K., R.A. Reynolds, J. Newton, and S.L. Albertson, 2001. Assessing sensitivity to eutrophication of the southern Puget Sound basin: Spatial and seasonal perspectives. Proceedings of Puget Sound Research Conference, Seattle, WA.

Cole, T.M. and E.M. Buchak, 1995. CE-QUAL-W2: A Two-Dimensional, Laterally Averaged, Hydrodynamic and Water Quality Model, Version 2.0: Users Manual, Instruction Report EL-95-1, US Army Engineer Waterways Experiment Station, Vicksburg, MS.

Collias, E., N. McGary, and C. Barnes, 1974. Atlas of Physical and Chemical Properties of Puget Sound and its Approaches, University of Washington Press, Seattle, WA. 235 pp.

Edinger, J.E. and E.M. Buchak, 1980. Numerical Hydrodynamics of Estuaries in. Estuarine and Wetland Processes with Emphasis on Modeling.

Edinger J.E., and E.M. Buchak, 1995. Numerical Intermediate and Far Field Dilution Modeling. Journal of Water, Air and Soil Pollution 83: 147-160, 1995.

Edwards, K.A., M. Kawase, and C.P. Sarason, 2007. Circulation in Carr Inlet, Puget Sound, During Spring 2003, Estuaries and Coasts Vol. 30, No. 6, p. 945–958 December 2007.

Finlayson, D. P., 2003. Combined bathymetry and topography of the Puget Lowland, Washington State. University of Washington, Seattle, WA. www.ocean.washington.edu/data/pugetsound.

Finlayson, D.P., 2004. Puget Sound Tide Model (PSTides). david.p.finlayson.googlepages.com/pugetsoundtides.

Finlayson, D.P., 2005. Coastal Geomorphology in Puget Sound. Shoreline and Coastal Planners Group, Padilla Bay National Estuarine Research Reserve, Mount Vernon, WA. June 23, 2005.

Friebertshauser, M.A. and A.C. Duxbury. 1972. A water budget study of Puget Sound and its subregions. Limnology and Oceanography 17(2) 237-247.

Hicks, S.D. 2006. Understanding Tides. U.S. Department of Commerce, National Oceanographic and Atmospheric Administration, National Ocean Service Publication. Chapter 8, Tidal Harmonic Constituents. Available from tidesandcurrents.noaa.gov/publications/Understanding_Tides_by_Steacy_finalFINAL11_30.pdf.

Kolluru,V.S., E.M. Buchak, and J.E. Edinger, 1998. Integrated Model to Simulate the Transport and Fate of Mine Tailings in Deep Waters. In Proceedings of Tailings and Mine Waste '98. 1998. Balkema, Rotterdam, ISBN 905410922.

Lavelle, J.W., H.O. Mofjeld, E. Lempriere-Doggett, G.A. Cannon, D.J. Pashinski, E.D. Cokelet, L. Lytle, and S. Gill, 1985. A Multiply-Connected Channel Model of Tides and Tidal Currents in Puget Sound, Washington and a Comparison with Updated Observations. NOAA Technical Memorandum ERL PMEL-84.

McGary, N. and J.H. Lincoln, 1977. Tide prints: Surface currents in Puget Sound. Washington Sea Grant Publication Number WSG 77-1.

Mofjeld, H.O., A J. Venturato, V.V. Titov, F.I. González, and J.C. Newman, 2002. Tidal Datum Distributions in Puget Sound, Washington, Based on a Tidal Model. NOAA Technical Memorandum OAR PMEL-122 (PB2003102259). NOAA/Pacific Marine Environmental Laboratory, Seattle, WA. 35 pp.

Monsen, N.E., J.E. Cloern, L.V. Lucas, and S.G. Monismith, 2002. A comment on the use of flushing time, residence time, and age as transport time scales. Limnology and Oceanography 47(5):1545-153.

Roberts, Mindy, 2009. Puget Sound Dissolved Oxygen Modeling Quarterly Progress Report #2 (January through March 2009). Washington State Department of Ecology (no publication number). http://www.ecy.wa.gov/programs/wq/PugetSound/PS-DOModelingQrtlyRpt2/psdom-qr2.html.

Roberts, M., J. Bos, and S. Albertson, 2008a. South Puget Sound Dissolved Oxygen Study – Interim Data Report. December 2008. Publication 08-03-037. www.ecy.wa.gov/biblio/0803037.html.

Roberts, M., A. Ahmed, and G. Pelletier, 2008b. Deschutes River, Capitol Lake, and Budd Inlet Temperature Fecal Coliform Bacteria, Dissolved Oxygen, pH, and Fine Sediment Total Maximum Daily Load Water Quality Study Findings. Washington State Department of Ecology draft publication.

Sackmann, Brandon. 2009. Quality Assurance Project Plan: Puget Sound Dissolved Oxygen Modeling Study: Large-scale Model Development. Washington State Department of Ecology Publication No. 09-03-103. www.ecy.wa.gov/biblio/0903103.html.

Seim, H E. and M.C. Gregg, 1997. The importance of aspiration and channel curvature in producing strong vertical mixing over a sill. Journal of Geophysical Research, Vol. 102, No. C2. pp 3451–3472.

Thomson, R.E., 1981. Oceanography of the British Columbia Coast. Canadian Special Publication of Fisheries and Aquatic Sciences 56. 291 pp.

University of Washington, 1971. Puget Sound and Approaches Seasonal Variations of Oceanographic Parameters in its Near-surface Waters. Department of Oceanography. Washington Sea Grant Report Contract No. RD-NE4.

URS Company, 1986. Southern Puget Sound Water Quality Assessment Study: Circulation and Flushing in South Puget Sound. Prepared for the Washington State Department of Ecology, Olympia, WA. Publication No. 86-e36. www.ecy.wa.gov/biblio/86e36.html.

Appendices

Appendix A. Model Grid Development

(See separate file from Anise Ahmed)

Appendix B. Glossary, Acronyms, and Abbreviations

ADCP - Acoustic Doppler Current Profiler, a device that measures three-dimensional water velocity as a function of depth from near-bottom to near-surface.

Advection – The transfer of a property such as heat, cold, or salinity, by the horizontal movement of fluid.

Baroclinic – The component of movement that varies with depth as a result of density stratification.

Barotropic - The uniform (depth-averaged) component of water movements that results from changes in water surface elevation due to tides.

Boundary conditions (BCs) – External inputs to a model, or a set of mathematical conditions to be satisfied along the edges or physical boundaries of the region in which the solution is sought.

Curvilinear grid – A uniform model grid composed of shoreline fitting trapezoidal elements.

DO – Dissolved oxygen. The amount of oxygen gas (O_2) dissolved in a volume of water (e.g., mg/l).

Estuarine flow – Water circulation that results from the combined effect of tides and density differences causing net transport seaward at the surface and landward at depth. When the flow pattern is reversed (e.g., landward at the surface) it is said to be inverse.

Forced or forcing – Information used as input to models.

Freshets – High flows resulting from either rain or melting snow.

Geometric mean: A mathematical expression of the central tendency (an average) of multiple sample values. A geometric mean, unlike an arithmetic mean, tends to dampen the effect of very high or low values, which might bias the mean if a straight average (arithmetic mean) were calculated. This is helpful when analyzing bacteria concentrations, because levels may vary anywhere from 10 to 10,000 fold over a given period. The calculation is performed by either: (1) taking the nth root of a product of n factors, or (2) taking the antilogarithm of the arithmetic mean of the logarithms of the individual values.

Initial conditions (ICs) – the starting values for the model at all depths and locations for all state variables (e.g., temperature, salinity, velocity).

Isopycnals – Surfaces or lines of constant density.

N2 – Lunar diurnal tidal constituent

K1 – Principal lunar semidiurnal tidal constituent

Mean tides – The arithmetic mean of mean high water and mean low water. This level is not necessarily mean sea level because of nonlinear tidal constituents.

Mixed tide - Tidal regime exhibiting a mixture of diurnal (daily) and semi-diurnal (~12-h) tides often characterized by a lower high and a higher high tide.

MHW – Mean High Water – the mean of all high tides.

MLLW – Mean Lower Low Water – the mean of only the lower low tides (does not include the higher low tides).

N2 – Larger lunar elliptic semidiurnal tidal constituent

NAVD88 – North American Vertical Datum of 1988.

NOAA – National Oceanographic and Atmospheric Administration

NOS – National Ocean Survey

Nonpoint source – Pollution that enters any waters from any dispersed activities including atmospheric deposition, surface water runoff from agricultural lands, urban areas, forest lands, subsurface or underground sources, or discharges from boats or vessels not otherwise regulated under the National Pollution Discharge Elimination System Program. Generally, any unconfined and diffuse source of contamination. Legally, any source of water pollution that does not meet the legal definition of "point source" in Section 502(14) of the Clean Water Act.

O1 – Lunar diurnal tidal constituent

ORCA – Oceanic Remote Chemical-optical Analyzer (monitoring buoy)

Point Source – Sources of pollution that discharges at a specific location from pipes, outfalls, and conveyance channels to surface water. Examples of point sources include municipal wastewater treatment plants, municipal stormwater systems, industrial waste treatment facilities, and construction sites that clear more than 5 acres of land.

POM – Princeton Ocean Model.

PRISM – Puget Sound Regional Synthesis Model.

Pycnocline – Depth at which the maximum change in density occurs.

Reflux – The amount of outflow from an area that returns when the tide changes. Reflux increases the flushing time of an estuary.

Residence time – The average time it takes for a substance (salinity, water) to move through a known volume.

Residual flow – Refers to the net flow after the tidal exchange (barotropic flow) is removed due to density differences.

RMSE – Root mean square error is defined as the square-root of the sum of the squared differences between the observed data and model results divided by the sample size.

S2 – Principal solar semidiurnal tidal constituent

Thalweg – the deepest along-channel path down an estuary.

TMDL – A Total Maximum Daily Load (TMDL) is a value of the maximum amount of a pollutant that a body of water can receive while still meeting water quality standards; alternatively TMDL is an allocation of that pollutant deemed acceptable to the subject receiving waters.

UTM – Universal Trans-Mercator.

UW – University of Washington.

Watershed – A drainage area or basin in which all land and water areas drain or flow toward a central collector such as a stream, river, or lake at a lower elevation.

Acronyms and Abbreviations

Following are acronyms and abbreviations used frequently in this report.

Ecology	Washington State Department of Ecology
EPA	U.S. Environmental Protection Agency
USGS	U.S. Geological Survey
WWTP	Wastewater treatment plant

Units of Measurement

°C	degrees centigrade
cfs	cubic feet per second
cms	cubic meters per second, a unit of flow.
ft	feet
g	gram, a unit of mass
kg	kilograms, a unit of mass equal to 1,000 grams.
kg/d	kilograms per day
km	kilometer, a unit of length equal to 1,000 meters.
m	meter

mg   million gallons
mgd   million gallons per day
mg/L   milligrams per liter (parts per million)
mL   milliliters
psu   practical salinity units